Functional Characterisation of Plant Cytosolic Thioredoxins

Submitted by

Fleur Catherine Dolman

This thesis is submitted in fulfilment of the requirements for the degree of Doctor of Philosophy

Discipline of Plant and Food Science
School of Agriculture, Food and Wine
Faculty of Sciences
University of Adelaide, Waite Campus
Australia

March 2010

Table of Contents

Abstract

Thioredoxins are small, ubiquitous, disulfide oxidoreductase proteins characterised by a conserved dicysteine active site. Within the cell, they are believed to maintain the redox environment and participate in a broad range of biochemical processes. Plant thioredoxins are a diverse multigene family, primarily classified according to the system by which they are reduced and their subcellular localization. Thioredoxins located in the cytoplasm (type -*h*) are usually dependent on NADPH for reduction by NADPH-thioredoxin reductase. There are four cytosolic thioredoxins in grass species, with subclass 4 believed to be the most ancient. The highly conserved nature of thioredoxin-*h*4, in plant species as diverse as angiosperms and gymnosperms, implies a conservation of gene function. Discovery of thioredoxin-*h*4 function in barley (*Hordeum vulgare*) was the core focus of the research presented in this thesis.

The characterisation of thioredoxin-*h*4 was approached from both, genetic, and protein biochemistry perspectives. To commence the research, the transcript profile of barley thioreodoxin-*h*4 (*HvTrx-h4*) was examined in barley reproductive tissues. As a direct consequence of findings, anther and stigma tissues were used in protein interaction studies employing a mono-cystenic active-site HvTrx-*h*4 affinity chromatography technique. *HvTrx-h4* was mutated, recombinantly expressed, purified and immobilised in order to isolate and identify proteins with which it interacted. Identification of HvTrx-*h*4 protein targets sought to reveal the pathways in which thioredoxin-*h*4 is involved.

To further characterise the expression of *HvTrx-h4*, the promoter and 5′ untranslated regions of genomic sequence were isolated and used to drive expression of green fluorescent protein in transgenically modified barley. This enabled examination of the temporal and spatial regulation of *HvTrx-h4* under normal growth conditions, as well as in response to abiotic stress and plant hormone treatments. Through these studies it was discovered that *HvTrx-h4* is likely to be the subject of post-transcriptional modifications. Subsequent investigations revealed HvTrx-*h*4 is also regulated at the post-translational level through glutathionylation.

Previous studies have ascribed a role for thioredoxins in plant oxidative stress defence. The question of whether modulation of HvTrx-*h*4 expression could be manipulated to alter plant oxidative stress tolerance was considered. To investigate, transgenic tobacco plants (*Nicotiana tabacum*) containing altered amounts of thioredoxin-*h*4 protein were subjected to various stresses; abiotic, biotic and chemical, in nature. Tobacco constitutively over-

expressing thioredoxin-*h*4 displayed increased tolerance to ultraviolet light B, heat and methyl viologen treatment.

Knowledge acquired by this study and presented in this thesis, suggest a role for barley thioredoxin-*h*4 in the oxidative stress response. Furthermore, the description of both post-transcriptional and post-translational regulation of HvTrx-*h*4 constitutes the first report of this level of regulation for a plant cytosolic thioredoxin.

Abbreviations

A	Absorbance
ABA	Abscisic acid
ACPFG	Australian Centre for Plant Functional Genomics
AGRF	Australian Genome Research Facility
Amp	Ampicillin
AOX	Alternative oxidase
APS	Ammonium persulphate
APX	Ascorbate peroxidase
BLAST	Basic local alignment search tool
bp	Base pair(s)
BSA	Bovine Serium Albumin
cv	Cultivar
C-terminal	Carboxy terminal
cDNA	Complementary DNA
CDSP32	Chloroplastic drought-induced stress protein
Da	Dalton(s)
DMSO	Dimethylsulphoxise
DNA	Deoxyribonucleic acid
DNase	Deoxyribonulclease
dNTP	Deoxynucleotide triphosphate
DTT	Dithiothreitol
EDTA	Ethylenediamine tetra-acetic acid
ER	Endoplasmic reticulum
EtBr	Ethidium bromide
FTR	Ferredoxin-thioredoxin reductase
g	Gram(s)
GUS	β-glucuronidase
GPX	Glutathione peroxidase
GRX	Glutaredoxin
h	Hour(s)
H_2O_2	Hydrogen peroxide
$HO^{\bullet}$	Hydroxyl radical
HPLC	High performance liquid chromatography
IPTG	Isopropylthio-ß-o-galactopyranoside
JA	Jasmonic acid
Kb	Kilobase(s)
kDa	KiloDalton(s)
LB	Lauria Broth
M	Molar
MAPK	Mitogen-activated protein kinase
mBBr	Monobromobiamane
min	Minute(s)
mL	Millilitre(s)
mm	Millimetre(s)
mM	Millimolar
mg	Milligram(s)
mRNA	Messenger ribonucleic acid
MS	Murashige & Skoog
mV	millivolt(s)
MV	Methyl viologen (paraquot)
N-terminal	Amino terminal
NADPH	Nicotinamide adenine dinucleotide phosphate
NTR	NADPH-thioredoxin reductase
ng	Nanogram(s)
Ni-NTA	Nickel-nitrilotriacetic acid

nm	Nanometre(s)
$^1O_2$	Singlet oxygen
$O_2^{\bullet-}$	Superoxide
OD	Optical density
PBS	Phosphate buffered saline
PCD	Programmed cell death
PCR	Polymerase chain reaction
Q-PCR	Quantitative PCR
RBDA	Rose Bengal diacetate
RNA	Ribonucleic acid
ROS	Reactive oxygen specie(s)
rpm	Revolutions per minute
RT-PCR	Reverse transcriptase PCR
s	Second(s)
SDS	Sodium dodecyl sulphate
SDS-PAGE	SDS-polyacrylamide gel electrophoresis
SI	Self-incompatibility
SOD	Superoxide dismutase
TBS	Tris buffered saline
TEMED	Tetramethylethylenediamine
Trx-*f*	Chloroplastic type-*f* thioredoxin
Trx-*h*	Cytoplasmic type-*h* thioredoxin
Trx-*m*	Chloroplastic type-*m* thioredoxin
Trx-*o*	Mitochondrial type-*o* thioredoxin
Tm	Melting temperature
Trx	Thioredoxin
UTR	Untranslated region
UVB	Ultraviolet light B
V	Volt(s)
v/v	Volume per volume
w/v	Weight per volume
^oC	Degrees Celsius
g	Units of relative centrifugal force
λ	wavelength
Ω	Ohm
µl	Microlitre(s)
µg	Microgram(s)
µM	Micromole(s)

Statement of Authorship

This work contains no material that has been accepted for the award of any other degree or diploma in any university or other tertiary institute and to the best of my knowledge and belief, contains no material previously published or written by another person, except where due reference being made in the text.

I give consent to this copy of my thesis, when deposited in the University Library, being made available for loan and photocopying, subject to the provisions of the Copyright Act 1968.

I also give permission for the digital version of my thesis to be made available on the web, via the University's digital research repository, the Library catalogue, the Australasian Digital Theses Program (ADTP) and also through web search engines, unless permission has been granted by the University to restrict access for a period of time.

Fleur Dolman

March 2010

Acknowledgements

I would like to thank all the people that have helped and supported me throughout my PhD research and thesis preparation.

Thanks must go to my supervisors Dr Ute Baumann, Dr Juan Juttner and Dr Alfio Comis for their guidance and assistance. Thank you to the Australian Centre for Plant Functional Genomics, the University of Adelaide and the associated staff members, both research and administrative, for providing funding, support and superb facilities in which to conduct my research and professional development. Thanks also to Professor Peter Langridge for providing a laboratory environment in which I enjoyed working. I am also grateful for receiving an Australian Postgraduate Award.

I extend my gratitude to Neil Shirley for his willingness to share his QPCR expertise, the Barley Transformation Team for generating my transgenic barley lines and Dr John Patterson and Kris Ford for their assistance with proteomics 'issues' and analysis. Thanks also to Alexandra Smart for creating the ABA stress series and sharing her data with me.

Many thanks to my colleagues and friends at ACPFG, who helped me in so many different ways and made my PhD a more enjoyable experience.

Finally, I would like to express my sincere gratitude to my family and friends, especially Mum, Dad, Breanna and The Coles', for their unwavering support, patience and understanding. Last but by no means least; thanks must go to Marty for his enduring support and encouragement and for always being there with love and perspective.

1 Literature Review

Thioredoxins

Thioredoxins are globular redox active proteins with a molecular mass of approximately 12-16 kDa (Baumann and Juttner, 2002). Thioredoxins are ubiquitous, thought to be present in almost all living cells (Buchanan and Balmer, 2005). The first thioredoxin was isolated from *Escherichia coli* (*E. coli*) in 1964 by Laurent et al. Since then, it has become evident that thioredoxins have a multifunctional nature. They are involved in a broad spectrum of physiologically significant cellular reactions, primarily playing an important role in maintenance and regulation of the cellular redox environment (Gromer et al., 2004).

1.1 Thioredoxin Super-Family

Identification of new thioredoxins and thioredoxin-related molecules is still occurring in plants, animals and other organisms. Collectively, they are referred to as the thioredoxin super-family and include chloroplastic, cytosolic, mitochondrial, nuclear and endoplasmic reticulum localised thioredoxins. In addition, the thioredoxin super-family encompasses thioredoxin-related proteins such as glutaredoxins, peroxiredoxins, nucleoredoxins and thioredoxin-related transmembrane protein (Aslund and Beckwith, 1999; Carvalho et al., 2006; Meyer et al., 2008).

Thioredoxins are characterised by a redox active site including two neighbouring cysteine's in the conserved motif WCGPC (Trp-Cys-Gly-Pro-Cys) or occasionally WCPPC, which can undergo a reversible redox change (Serrato and Cejudo, 2003). The glycine and proline residues may also influence redox potential and are involved in maintaining the conformation of the active site (Eklund et al., 1991; Holmgren, 1989). This active-site sequence is commonly referred to as the thioredoxin-motif (Figure 1.1A) (Buchanan et al., 1994; Jacquot et al., 1997; Meyer et al., 1999). Three dimensional models of *E. coli* thioredoxins revealed

that the conserved amino acids Pro_{40} and Pro_{76} are at structurally important positions (Eklund et al., 1991).

Usually, to be biologically active a thioredoxin must be in a reduced state. When thioredoxin is in an oxidised state, the cysteines of the active site form a redox modulating disulfide bridge, which is in turn reduced by the respective thioredoxin reductase (Baumann and Juttner, 2002; Gromer et al., 2004). In their reduced form, thioredoxins are extremely efficient protein disulfide oxido-reductases (Gromer et al., 2004; Schurmann and Jacquot, 2000). Oxidoreductase proteins are involved in the formation, breakage or isomerisation of disulfide bonds. Reduced thioredoxins are able to reduce disulfide bonds in target proteins (Figure 1.2) because of their low redox potential, such as –270 mV for the *E. coli* thioredoxin (Haberlein et al., 1995). The reduction of disulfide bonds in target proteins usually results in the activation or deactivation of the target molecule and consequently, the associated pathway (Gromer et al., 2004). Thioredoxins have been found to serve as electron donors in a variety of cellular redox reactions (Holmgren, 1985).

1.2 Thioredoxin Structure

Thioredoxins have a characteristic protein structure comprised of five beta strand sheets, which form a hydrophobic core surrounded by four externalised alpha helices (Figure 1.1B) (Jacquot et al., 1997; Schurmann and Jacquot, 2000). The most highly conserved stretch of sequence is the active site (WCGPC) and is located on a surface loop of the molecule forming the link between the second beta strand and the second alpha helix. This structure is common to most, if not all, protein disulfide oxidoreductases (Coudevylle et al., 2005).

Interestingly, there is only approximately 30% amino acid identity between vertebrate thioredoxins and those found in bacteria and plants. This identity is mainly in the amino (N) terminus of the protein where the active site is located. However, despite minimal primary sequence identity, known tertiary structures of thioredoxins display significant similarities (Coudevylle et al., 2005; Jacquot et al., 1997; Maeda et al., 2008; Mittard et al., 1997).

A) B)

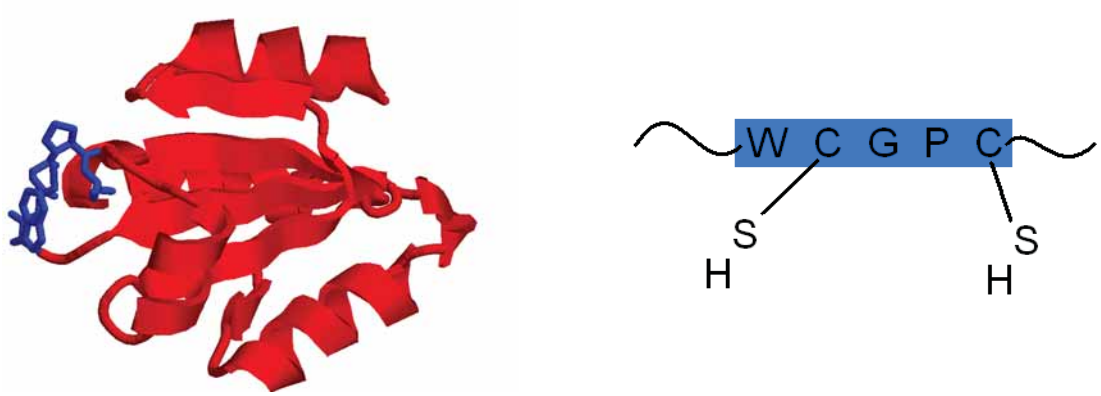

Figure 1.1: **Thioredoxin structure and active site:** A) Model of a spinach thioredoxin showing the globular structure. Generated by Rasmol 2.7. The active-site (thioredoxin motif) is highlighted in blue. The highly conserved structure includes 5 β-sheets & 4 α-helices. B) The thioredoxin active-site consists of two cysteines (C) which can undergo a reversible redox change. This conserved thioredoxin motif consists of the amino acids tryptophan (W), cysteine (C), glycine (G), proline (P) and cysteine (C) respectively. Occasionally, thioredoxins contain the alternative motif WCPPC.

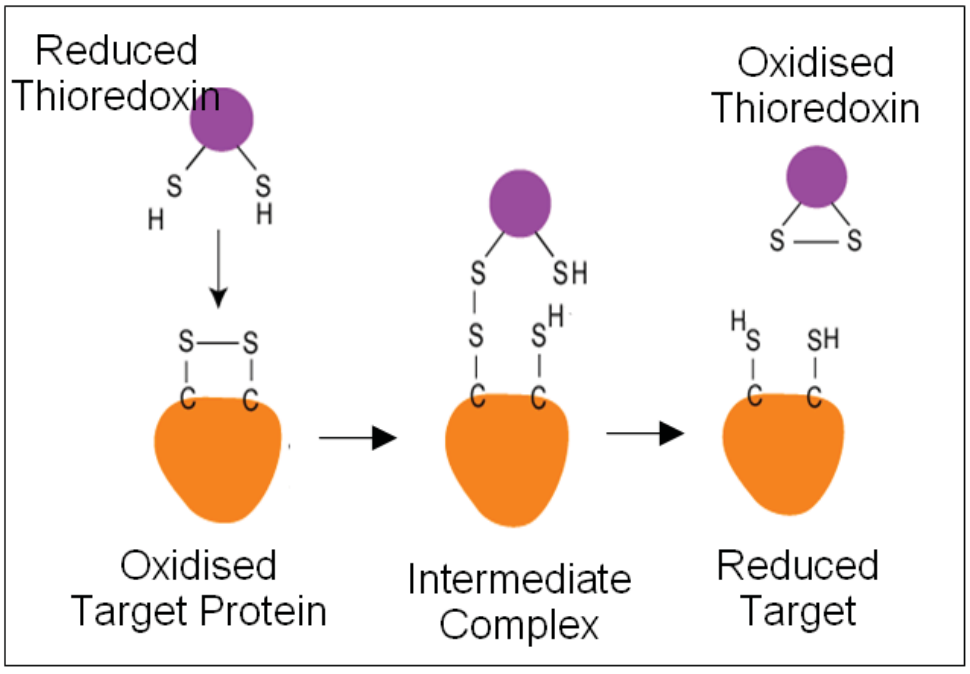

Figure 1.2: **Thioredoxin mechanism of action.** The first nucleophile associated with the thioredoxin active-site attacks a sulfur atom of the target protein, leading to the formation of a short lived mixed disulfide intermediate complex. The second nucleophile then acts to resolve the bond, leaving the originally oxidised target protein in a reduced state.

1.3 Thioredoxin Functions

Thioredoxin was discovered during studies into the formation of deoxyribonucleotides. When required by a cell, deoxyribonucleotides are formed from ribonucleotides by the reduction of a hydroxyl group. This reaction is performed by ribonucleotide reductase and requires reducing equivalents which were found to be provided by thioredoxin (Holmgren, 1989; Laurent et al., 1964).

Thioredoxins' main function is believed to be modulating the activity of proteins (reviewed by Holmgren, 1989). Hence, thioredoxins are involved in a range of biochemical processes and pathways (Baumann and Juttner, 2002; Gromer et al., 2004). These include the regulation of enzymes by activation or deactivation (Arner and Holmgren, 2000; Holmgren, 1989; Zhang and Portis, 1999), the modulation of transcription and translation factors (Balmer and Buchanan, 2002; Hirota et al., 1999; Schenk et al., 1994; Sun and Oberley, 1996), as hydrogen donors (Holmgren, 1989) and responding to oxidative stress (Balmer and Buchanan, 2002; Chae et al., 1994; Koharyova and Kollarova, 2008; Rouhier et al., 2008). Most but not all roles depend upon the capacity of thioredoxins to effectively reduce disulfide bonds in target proteins (Baumann and Juttner, 2002).

Thioredoxin is an important element of the intracellular redox environment, redox-regulating many biochemical pathways and participating in the tight control of cellular functions (Gromer et al., 2004; Schurmann and Jacquot, 2000). Despite the generally reducing cytosolic environment, oxidised species must also exist (Gromer et al., 2004). Indeed, studies by Gitler et al. (2002) have shown that under typical conditions in immortalised human keratinocyte cells, approximately 11% of the cellular thioredoxin is present in the oxidised state.

It has been suggested that thioredoxin plays a role in aspects of hormone action and cytokine function. The study by Gasdaska et al. (1995) demonstrate that the redox properties of thioredoxin are involved in autocrine stimulation. In this study, recombinant human thioredoxin was found to stimulate the proliferation of human tumour cell lines. Significantly, there was a positive correlation between the ability of cell lines to proliferate, presumably due to the autocrine production of growth factors by the cells and the stimulation of proliferation by thioredoxin. The results suggest that thioredoxin acts by a redox mechanism to increase the cell proliferation response to growth factor(s) produced by the cell (Gasdaska et al., 1995). In support, additional studies suggest that the thioredoxin system can act as an autocrine growth-factor, synergizing with interleukin 1 and 2 (Biguet et al., 1994; Wakasugi et al., 1990). Thioredoxin is also believed to act as a reducing agent for several transcription factors,

including the glucocorticoid receptor. Thioredoxin mediated reduction of the glucocorticoid receptor enhances the receptor's ability to bind the hormone (Grippo et al., 1985). Interestingly, thioredoxin dependent reduction of another transcription factor, nuclear factor kappa B (NF-κB), promotes DNA binding (Matthews et al., 1992).

Although essential for most thioredoxin functions, the reducing activity of thioredoxin is not always required. For example, the bacteriophage T7 uses *E. coli* thioredoxin as an essential subunit of the T7 DNA polymerase, but the reducing activity of thioredoxin is not required for polymerase activity (Huber et al., 1986).

Thioredoxins play essential roles in cell systems and may be necessary for cell/organism survival. This has been demonstrated by thioredoxin gene disruption experiments in mice, which resulted in embryonic lethality in homozygous knockout animals (Matsui et al., 1996; Nonn et al., 2003). These, along with many other studies, clearly illustrate the importance of thioredoxin. The large and diverse range of functions and actions of the thioredoxin system have been extensively reviewed by Gromer et al. (2004) and Schürmann et al. (2000). More recently Zeller et al. (2006) has reviewed bacterial thioredoxins.

Plant thioredoxin systems have not been studied as extensively as those in mammals. A comprehensive collection of genomic and biochemical data of the thioredoxins for one plant species has not been obtained to date. Fortunately, plant thioredoxin research is growing and a greater understanding of plant thioredoxin systems is occurring.

1.4 Plants – Two Main Thioredoxin Systems

Unlike animals and bacteria, plants contain a large number of thioredoxin genes (Hisabori et al., 2007; Meyer et al., 2008). Plants have the most complex thioredoxin profile of any type of organism studied, comprising six distinct and often multigenic classes. More than 20 thioredoxin genes have been identified in Arabidopsis thaliana, classified into six main families (Meyer et al., 2008). Thioredoxins-*f*, -*m*, -*x*, -*y* and CDSP32 (an atypical thioredoxin form) are localised to the chloroplast (Cain et al., 2009; Collin et al., 2003). Thioredoxins-*o* are mitochondrial proteins whilst the –*h* members are predominantly cytosolic (Shahpiri et al., 2009). Very recently, Alkhalfioui et al. (2008) identified two novel thioredoxin isoforms in legume (*Medicago truncatula)* and designated them as thioredoxins-*s* in reference to their functional association with symbiosis. Although believed to have evolved from thioredoxins-*m*, thioredoxins-*s* have an atypical catalytic site, an N-terminal extension containing a putative signal peptide, and do not have the common disulfide reductase ability in insulin-based

activity experiments. Also, each thioredoxin-*s* is targeted to the endoplasmic reticulum, as established by green fluorescent protein (GFP) fusion studies (Alkhalfioui et al., 2008).

Although thioredoxins are classified into many different families, two main thioredoxin systems occur, based on the electron donor and the enzyme that catalyses thioredoxin reduction. In the first system, the disulfide bridge formed when thioredoxin is oxidised can be reduced to a dithiol by electrons from NADPH. In the second system, the electrons come from ferredoxin. Reduction is facilitated *via* a corresponding thioredoxin reductase enzyme (Holmgren, 1989). The system utilised typically correlates with the thioredoxin's intracellular location. The chloroplastic thioredoxins of plants and eukaryotic algae and the thioredoxins of oxygenic photosynthetic prokaryotes are reduced *via* the ferredoxin-dependent thioredoxin system. In contrast, thioredoxins in non-photosynthetic tissue and the cytosol and mitochondria of photosynthetic cells are reduced *via* the NADPH-dependent thioredoxin system (Balmer and Buchanan, 2002; Schurmann and Jacquot, 2000).

1.4.1 The Ferredoxin-Dependent Thioredoxin System

The ferredoxin-dependent thioredoxin system is composed of ferredoxin, the novel iron-sulfur enzyme ferredoxin-thioredoxin reductase (FTR) and four nuclear encoded thioredoxins, *-m, -f, -x* and *-y* (Schurmann and Buchanan, 2008). Experimental evidence suggests that thioredoxins-*f* and *-m* represent the major chloroplast forms whilst *-x* and *-y* are of lower abundance (Buchanan and Balmer, 2005). Thioredoxins-*m* and *-f* have been designated in reference to the enzymes with which they were initially found to interact: NADP-malate dehydrogenase and fructose-1,6-bisphosphatase, respectively (Jacquot et al., 1976; Jacquot et al., 1978; Schurmann et al., 1976). Significant progress has been made in understanding this system with respect to function and especially to structure. The crystal structure of each component protein is now known (Schurmann and Jacquot, 2000).

The ferredoxin-dependent thioredoxin system has been found only in photosynthetic eukaryotes and cyanobacteria, and was recently reviewed by Schurmann and Buchanan (2008). In plants it is located in the chloroplast and regulates the redox state of enzymes involved in several biochemical processes (Buchanan, 1991; Scheibe and Anderson, 1981). Chloroplastic thioredoxins are reduced by way of light with ferredoxin being reduced photochemically from water *via* the photosynthetic electron transport system of illuminated thylakoid membranes (Figure 1.3A). Through the reduced ferredoxin, electrons are transferred from photosystem I to FTR. Next, FTR reduces the thioredoxin which in turn alters the redox status of its target protein. In this way, a strict light-sensitive control of both the assimilatory

and dissimilatory pathways is conferred (Balmer and Buchanan, 2002; Baumann and Juttner, 2002; Schurmann and Jacquot, 2000). By interacting with and therefore regulating the activity of target enzymes, thioredoxins-*m* and -*f* play an essential role in the control of photosynthetic carbon assimilation (Buchanan, 1991; Lemaire et al., 2007).

Thioredoxin-*f* types are highly conserved and slightly larger than other thioredoxin types because of additional amino acids at the N-terminus. The C-terminal part of the sequence resembles classical animal thioredoxin as it contains a third, strictly conserved cysteine. This third cysteine is exposed on the surface ~ 9.7°A away from the accessible cysteine of the active-site dithiol (Buchanan and Balmer, 2005).

1.4.2 The NADPH-Dependent Thioredoxin System

Plant cells, like bacterial and animal cells, contain a thioredoxin system dependent on NADPH for its reduction (Florencio et al., 1988; Suske et al., 1979). This system has been identified in all organisms except cyanobacteria, functioning primarily in the cytosol (Banze and Follmann, 2000; Florencio et al., 1988; Laloi et al., 2001; Suske et al., 1979). The reduction of thioredoxin by NADPH (Figure 1.3B) is catalysed by the flavin enzyme, NADPH-thioredoxin reductase (NTR) (Arner and Holmgren, 2000; Holmgren, 1989). In plants, cytosolic thioredoxins regulated by this system have been designated -*h* in reference to their initial discovery in heterotrophic, non-photosynthetic tissue (Johnson et al., 1987). More recently, the -*h* representatives have expanded to included those found in several cell compartments including the cytosol, nucleus, endoplasmic reticulum and mitochondria (Buchanan and Balmer, 2005). It has also been suggested that members of this class may be translocated to organelles. For example, a study by Gelhaye et al. (2004) showed that cytosolic thioredoxin members could also be present in the mitochondria. This phenomenon has also been investigated in an animal system by Hirota et al. (1999), who showed that ultraviolet light B irradiation of mammalian cells induced translocation of a human thioredoxin, regulating nuclear factor kappa B (NF-κB), from the cytoplasm to the nucleus.

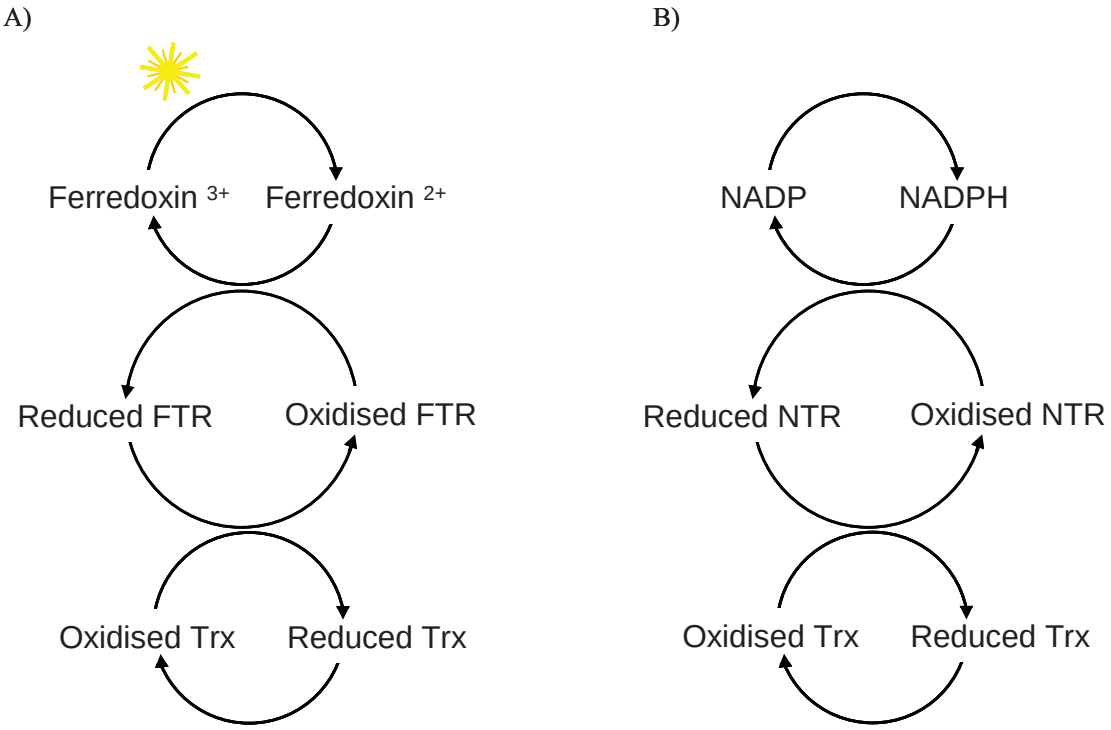

Figure 1.3: **Depiction of the two thioredoxin systems in plants.** A) The ferredoxin-dependent thioredoxin system. In the light, ferredoxin is photochemically reduced *via* the photosynthetic electron transport system. Electrons can then be transferred to ferredoxin-thioredoxin reductase (FTR), which reduces the thioredoxin (Trx). B) The NADPH-dependent thioredoxin system. NADPH provides reducing equivalents and Trx reduction is catalysed by NADPH-thioredoxin reductase (NTR). Figure adapted from Baumann and Juttner (2002).

1.5 Mitochondrial Thioredoxins in Plants

In plants, the presence of thioredoxin in the mitochondria was first reported by Marcus et al. (1991) who isolated thioredoxin-*h* from mitochondrial cell fractions derived from the endosperm of germinating castor beans. Mitochondrial thioredoxin proteins were later isolated by Konrad et al. (1996) after detection of thioredoxin and thioredoxin reductase activities in spinach, soybean, and potato plant mitochondrial extracts. Further work by Banze et al. (2000) identified a mitochondrial specific protein utilizing NADPH and plant thioredoxins as substrates.

Laloi et al. (2001) were the first to characterize a complete plant thioredoxin system located in mitochondria (thioredoxin-*o*). From the *A. thaliana* genome, they identified a gene encoding a thioredoxin with a potential mitochondrial transit peptide, *AtTrx-o1*. In addition, they identified a gene encoding a thioredoxin reductase, also with a typical N-terminal mitochondrial target signal, *AtNTRA*. According to Laloi et al. (2001) AtTrx-*o*1 defined a previously uncharacterized type of thioredoxin by its sequence and the position and number of introns in the gene. In contrast, *AtNTRA* is highly similar to a previously characterized cytosolic NADPH-dependent thioredoxin reductase, *AtNTRB* (Buchanan, 1991), except that it has a putative pre-sequence for import into the mitochondria.

Western blot analysis of *A. thaliana* subcellular and submitochondrial fractions and *in vitro* import experiments showed that AtTrx-*o*1 and AtNTRA were targeted to the mitochondrial matrix through their cleavable N-terminal signal and were cleaved after import. In addition, AtTrx-*o*1 efficiently reduced insulin in the presence of DTT and was reduced efficiently by AtNTRA and NADPH, in activity assays. Therefore, AtTrx-*o*1 and the NADPH-dependent AtNTRA are believed to form a functional plant mitochondrial thioredoxin system (Laloi et al., 2001).

To identify mitochondrial proteins that interact with thioredoxins, Balmer et al. (2004) employed a proteomic approach. Soluble mitochondrial proteins from photosynthetic and heterotrophic tissues were supplied as a source of ‘bait’ proteins and subsequently, fifty potential thioredoxin-linked proteins were identified. These proteins were annotated as being involved in twelve different processes: photorespiration, citric acid cycle and associated reactions, lipid metabolism, electron transport, ATP synthesis/transformation, membrane transport, translation, protein assembly/folding, nitrogen metabolism, sulfur metabolism, hormone synthesis and stress-related reactions (Balmer et al., 2004). However, it is important to note that a mitochondrial thioredoxin was not involved in this protein interaction

experiment. Instead, chloroplastic (-*m*) and cytosolic thioredoxins were the prey proteins, with the source of target proteins (bait) obtained from mitochondrial pea, spinach and potato extracts. In addition, the thioredoxin reductase used to confirm the results was cytosolic and from *A. thaliana* (Balmer et al., 2004). Hence, there is no direct evidence linking thioredoxin-*o* to these proteins and their associated functions.

A study by Gelhaye et al. (2004) using Western blot analyses with mitochondrial protein extracts demonstrated that a poplar (*Populus tremula*) thioredoxin-*h* (PtTrx-*h*2) is targeted to plant mitochondria. Recombinant PtTrx-*h*2 protein was also shown to be reduced efficiently by the mitochondrial thioredoxin reductase AtNTRA. In addition, it was shown that PtTrx-*h*2 could reduce alternative oxidase homodimers (Gelhaye et al., 2004). Alternative oxidase is found in plant mitochondria but not in the mitochondria of other organisms (Baumann and Juttner, 2002).

Very recently, Marti et al. (2009) reported on a thioredoxin-*o* in pea (*Pisum sativum*) (*PsTrx-o1*), which differed from the *AtTrx-o1* by the absence of introns in the genomic sequence. GFP-tagging of PcTrx-o1 revealed that it is located in the nuclei as well as mitochondria. Furthermore, protein interaction studies found that PcTrx-*o*1 is able to regulate mitochondrial alternative oxidase and interact with several other mitochondrial proteins (Marti et al., 2009).

1.6 Cytosolic Thioredoxins in Plants

The cytosolic thioredoxin class represents the largest and most divergent group of plant thioredoxins. In contrast to the situation in animals, few of the putative functions ascribed to thioredoxins in plants have been verified, particularly for the -*h* class (Baumann and Juttner, 2002). The temporal and spatial regulation of cytosolic thioredoxin expression is also largely unknown. Currently, the field is lacking a comprehensive set of genomic and biochemical data for all cytosolic thioredoxins within one plant species.

A number of thioredoxin-*h* cDNA sequences have been isolated from both non-photosynthetic and photosynthetic tissues. All deduced protein sequences share a high degree of similarity although the active-site motif WCGPC is modified to WCPPC in several members (Schurmann and Jacquot, 2000). The NMR solution structure of oxidized thioredoxin-*h* from the photosynthetic green alga *Chlamydomonas reinhardti* and a thioredoxin-*h*1 from poplar are available (Coudevylle et al., 2005; Mittard et al., 1997). The crystal structure of two barley (*Hordeum vulgare*) thioredoxin-*h* isoforms, in the partially reduced state (HvTrx-*h*1) and the oxidized state (HvTrx-*h*2), have also been determined

recently. This study, for the first time, enabled a comparison of the 3D structure of two thioredoxin-*h* isoforms from the same plant species (Maeda et al., 2008).

Analysis of intron positions suggests that there is a common ancestor for plant and green algal thioredoxin-*h* genes (Sahrawy et al., 1996). Typically, plant thioredoxin-*h* sequences are slightly larger than the *E. coli* thioredoxin, representing the prototype prokaryotic thioredoxin, mostly because of N- and/or C-terminal extensions. Primary structure analyses indicate that plant thioredoxin-*h* is more closely related to human thioredoxin than to the *E. coli* type (Schurmann and Jacquot, 2000).

All thioredoxins-*h* characterized to date have sequence characteristics that are distinctive for their class. Most are in the N-terminal region. An example is a tryptophan residue in the N-terminus that increases the extinction coefficient at 290 nm (Lemaire et al., 2000; Stein et al., 1995). Also, cytosolic thioredoxins do not require a signal peptide for cellular localisation and therefore, the N-terminal sequence is significantly shorter compared to thioredoxins in other classes (*Dr Juan Juttner, pers. comm*.).

1.7 Functions of Cytosolic Thioredoxins in Plants

Determining thioredoxin functions in plants is more difficult than in animals. This is because plants contain approximately four to five times as many thioredoxins than animals (Baumann and Juttner, 2002). Plant thioredoxin protein interactions have been extensively studied, demonstrating and suggesting likely functions. An extensive review of established and potential target proteins of plant thioredoxins has recently been published by Montrichard et al. (2009). A number of functions have been proposed for the cytosolic thioredoxin system. However, these have not been as commonly supported by *in vitro* studies as for thioredoxins-*m* and -*f*. In plants, thioredoxin-*h* appears to be involved in multiple functions.

1.7.1 A Messenger: The Companion Cell – Sieve Element Complex

Plant thioredoxins-*h* may participate in modulating redox-dependent signalling cascades, as demonstrated in mammalian cells (Mestres-Ortega and Meyer, 1999). Thiol redox control by the thioredoxin-*h* system is considered as a regulatory mechanism in several signal transduction pathways in plants. Primarily based on the finding that thioredoxin-*h* is one of the most abundant proteins in the phloem sap of rice (*Oryza sativa*), it has been suggested that it may act as signal messenger (Ishiwatari et al., 1995; Ishiwatari et al., 2000). Thioredoxin-*h* has been detected not only in the phloem sap of monocots such as rice and wheat, but also in dicots such as *Ricinus* and *Cucurbita* (Schobert et al., 1998). Interestingly, glutaredoxin, a

similar redox regulator, has also been identified in the sieve tube exudates of four dicotyledonous species (Szederkenyi et al., 1997). These findings allude to redox systems and thioredoxins being integral for the function of sieve tube complexes. Mature sieve tubes have no cellular organelles yet require a functional plasma membrane (Sjolund, 1997). Since they lack both ribosomes and nuclei they are believed to be incapable of protein synthesis (Parthasarathy, 1975). Therefore, phloem proteins are thought to be synthesised in neighbouring companion cells and subsequently transported into the sieve elements *via* plasmodesmata (Fisher et al., 1992). In support of this idea, microinjection studies with mesophyll cells from rice, *Cucurbita* and *Ricinus* have revealed that recombinant thioredoxin-*h* has the capacity to mediate its own cell-to-cell transport through plasmodesmata (Balachandran et al., 1997; Ishiwatari et al., 1998).

To determine the structural motifs required for cell-to-cell transport, Ishiwatari et al. (1998) generated two thioredoxin-*h* mutants altered in charged residues predicted to project from the protein surface. This was achieved by the deletion of five amino acids at the N-terminal or substitution of four amino acids for alanine at the C-terminus. Both mutants were incapable of plasmodesmatal movement. These results imply that surface charge topology is important for the binding and/or transport of thioredoxins through plasmodesmata (Ishiwatari et al., 1998). These findings indicate that thioredoxin-*h* is mobile in plants and may act as a signal. This is further supported by the identification of a receptor kinase as a target for thioredoxin-*h* in *Brassica* (Bower et al., 1996). The phosphorylation of this receptor kinase, which is inhibited by thioredoxin-*h*, is a signal for a self-incompatibility reaction (Cabrillac et al., 2001) which will be discussed below.

Ishiwatari et al. (1995) suggested that thioredoxin-*h* may also help repair damaged (oxidised) proteins in sieve tubes. Compared with normal cells, replacement of damaged proteins in sieve tubes with re-synthesised protein would be less efficient as the proteins would require transportation. Therefore, by reducing oxidised proteins, thioredoxin-*h* may be important in overcoming such inherent difficulties (Ishiwatari et al., 1995). However, as yet no evidence has emerged to support this proposal.

1.7.2 Self-incompatibility

A role for thioredoxins in the self-incompatibility (SI) response of plants was first reported by Bower et al. (1996) and further investigated by Mazzurco et al. (2001). In self-incompatible *Brassica*, the SI system prevents self-pollination or pollination between two plants carrying the same S allele (Mazzurco et al., 2001) (Reviewed by Cock, 2000). A number of genes at

the S locus have been characterised (Casselman et al., 2000) including the S locus receptor kinase (SRK) gene which encodes the female determinant of SI (Takasaki et al., 2000). Mutations in the SRK gene abolish self-incompatibility (Goring et al., 1993; Nassrallah et al., 1994). Bower et al. (1996) identified two thioredoxins-*h*, THL-1 and THL-2, which specifically interacted with the kinase domain of SRK. Using a yeast two-hybrid system, Mazzurco et al. (2001) identified a cysteine (Cys_{465}) in the N-terminus of the SRK that is required for interaction with THL-1 and -2. Deletion or substitution of this cysteine resulted in a loss of interaction. The necessity of a particular cysteine is consistent with the ability of thioredoxins to reduce disulfide bonds and suggests that Cys_{465} is involved in a disulfide bond. In support of this idea, further mutational studies demonstrated that the interaction is dependent upon a functional thioredoxin active site, because mutagenesis of the cysteines in the active site of THL-1 abolished the interactions with SRK (Mazzurco et al., 2001).

Mazzurco et al. (2001) suggested that THL-1 and -2 act as negative regulators of SRK in the absence of a stimulus. This hypothesis was investigated by Cabrillac et al. (2001). They first showed that SI in *Brassica oleracea* involves the phosphorylation of SRK, which occurred *in vivo* within 1 hour of self-pollination. A protein present in stigma extract was able to act as an inhibitor, preventing auto-phosphorylation of SRK. According to Cabrillac et al. (2001), *in vitro* studies indicated that the inhibitor was thioredoxin THL-1, as depletion of thioredoxin from stigma extract abolished this inhibitory effect. The SRK–thioredoxin inhibition was found to be released in a S-locus-haplotype specific manner by the addition of pollen coat proteins after self-pollination. These findings support a model in which THL-1 and -2 interact in a reversible manner with SRK in stigmas, preventing spontaneous activation of the SI signalling pathway. A resin thiobond was used to deplete the stigma extract of thioredoxin. Many non-thioredoxin proteins contain a thioredoxin-like motif and these would have also been removed from the stigma extract. Therefore, it can not be concluded, based on this information alone, that thioredoxin was responsible for the inhibitory effect of SRK phosphorylation.

To further investigate the biological roles of THL-1 and -2 in pollen-pistil interactions, Haffani et al. (2004) used the stigma-specific SLR1 promoter to drive antisense suppression of THL-1 and -2 mRNA in *Brassica napus* cv Westar. Although this cultivar is usually compatible, a low level constitutive rejection was observed in the transgenic plants, against all *B. napus* pollen tested. In addition, pollen rejection exhibited the same characteristics as a typical *Brassica* self-incompatibility response, as revealed by fluorescence microscopy

observations. Therefore, it can be concluded that THL-1 and -2 are indeed required for full pollen compatibility in *B. napus* cv Westar (Haffani et al., 2004).

An interesting finding of Cabrillac et al. (2001) was that a functional, reduced active site is required for thioredoxin-mediated inhibition of SRK phosphorylation. However, SRK inhibition appears to involve direct binding of the inhibitor. How thioredoxin might form an inhibitory complex with SRK through the active site remains as yet unexplained (Baumann and Juttner, 2002).

1.7.3 Seed Germination

Evidence indicates that in cereals, seed germination is accompanied by a substantial change in the redox state of proteins. Embryo and starchy endosperm proteins present mainly in an oxidised form in dry seed are converted to a reduced or sulfhydryl state following imbibition. In cereals, cytosolic thioredoxins are widely distributed in most organs and developmental stages. However, expression analysis of two wheat thioredoxin-*h* genes, TaTrx-*h*A and TaTrx -*h*B, showed high accumulation in mature seeds (Serrato et al., 2001). This result may indicate that synthesis and accumulation of these proteins occurs during formation of the seed (Serrato et al., 2001). Consequently, it has been suggested that plant cytosolic thioredoxins act as a reducing system participating in the mobilization of protein reserves during seed germination. In support of this hypothesis, Lozano et al. (1996) demonstrated that during germination, thioredoxin-*h* is converted to a partially reduced state.

When reduced, thioredoxin may act as a signal early in seed germination to mobilise reserves in three ways. Firstly, thioredoxin-*h* may directly reduce seed storage proteins, thereby enhancing their solubility and susceptibility to proteolysis. Studies by Lozano et al. (1996) and Yano et al. (2001) suggest that germination of plant seeds involves the reduction of seed storage proteins. Among the known target proteins of thioredoxin-*h* in seeds are the storage proteins, hordeins in barley (Yano et al., 2001) and glutenins and gliadins in wheat (Marx et al., 2003). These proteins are insolubilised in disulfide-bound complexes during maturation and drying. Upon germination, they are reduced to the sulfhydryl state. It has been shown that gliadins and glutenins, the major wheat storage proteins, are reduced by thioredoxin-*h in vitro* (Kobrehel et al., 1992; Wong et al., 1995).

The second proposed role is the reduction and inactivation of disulfide proteins that inhibit specific amylases and proteases. Therefore, they make it possible for stored starch and proteins to be broken down. Jiao et al. (1993) demonstrated that thioredoxin-*h* reduces and

inactivates inhibitors of hydrolytic enzymes including the α-amylase/subtilisin inhibitor of barley. In addition, thioredoxin-*h* can also reduce thiocalsin, a seed-specific serine protease which, following reduction, is activated by calcium (Besse et al., 1996). Reduced thiocalsin was able to cleave thioredoxin reduced gliadins and glutenins. A third role involves thioredoxins reducing, hence activating, individual enzymes required for germination (Wong et al., 2004).

Studies with transgenic wheat and barley grain have supported the proposed role of thioredoxin-*h* in seed germination. Wong et al. (2002) showed that over-expression of thioredoxin-*h* in barley endosperm accelerated germination, the associated release of starch-hydrolysing enzymes and the reduction of storage and other proteins. Furthermore, transgenic wheat with suppressed thioredoxin-*h* expression showed the opposite effect. Germination was inhibited, which led to protection against pre-harvest sprouting (Guo et al., 2007).

Evidence for thioredoxin mediated regulation of seed enzymes has also been supplied by Cho et al. (1999). Barley transgenic lines over-expressing wheat thioredoxin-*h* in seed displayed a fourfold increase in the activity of pullanase, an enzyme that specifically cleaves α-1, 6 linkages in starch (Cho et al., 1999). However, immunolocalisation studies by Serrato et al. (2003) describe the presence of thioredoxin-*h* at high levels in the nucleus of scutellum and aleurone cells but only at very low levels in the endosperm. Cho et al. (1999) and Wong et al. (2002) drove thioredoxin-*h* expression with an endosperm specific promoter, resulting in abnormally high levels of thioredoxin-*h* in the endosperm. Hence, the functions of thioredoxin-*h* identified by Cho et al. (1999) may not occur naturally, despite its ability in the conditions provided.

The finding by Serrato et al. (2003) that thioredoxin-*h* was predominantly localised in the nucleus of scutellum and aleurone cells suggests another role for thioredoxin-*h*. Perhaps its function in seed germination is as a transcriptional regulator. This hypothesis is supported by studies in mammalian systems which allude to thioredoxin-*h* being a transcriptional regulator, for example, by reducing the transcription factor NF-κB (Matthews et al., 1992).

A study by Alkhalfioui et al. (2007) investigated whether thioredoxin linked redox changes in germinating seeds were restricted to cereals alone. Using a legume (*M. truncatula*), the redox state of proteins interacting with thioredoxin-*h* were assessed in germinating seeds, using the thiol-specific probe monobromobiamane (mBBr). Approximately half of the proteins that were oxidised or partly reduced in dry seeds became more reduced upon germination. The

mBBr gel staining patterns were similar for proteins reduced *in vivo* during germination or *in vitro* by thioredoxin-*h*. These data suggests that thioredoxin-*h* functions in the germination of seeds of dicotyledons as well as moncotyledons (Alkhalfioui et al 2007).

The diverse roles proposed for thioredoxin types -*h* in cereal seeds has very recently been reviewed by Shahpiri et al. (2009) and Zahid et al. (2008). The reviews focus on function, regulation, interaction and structure data in barley (Shahpiri et al., 2009) and wheat (Zahid et al., 2008).

1.7.4 Pathogen Defence

Laloi et al. (2004) showed that the *A. thaliana* thioredoxin-*h*5 gene (*AtTrx-h5*) is up-regulated during incompatible interactions with the bacterial pathogen *Pseudomonas syringae*, suggesting a role for thioredoxin in pathogen recognition or defence. In support of this idea, Rivas et al. (2004) revealed a role for a Cf-9-interacting thioredoxin (CITRX) in regulating pathogen defence in tomato. Tomato Cf-9 resistance protein is required for defence against the fungal pathogen *Cladosporium fulvum*, which carries the corresponding avr9 gene. Although the exact mechanism is unclear, virus-induced gene silencing of CITRX resulted in an accelerated Cf-9/Avr9-triggered hypersensitive response with enhanced pathogen-induced accumulation of reactive oxygen species, alteration of calcium-dependent protein kinase activity and induction of defence-related genes in both tomato and tobacco (*Nicotiana benthamiana*) (Rivas et al., 2004). Silencing of CITRX also conferred increased resistance to a race of *C. fulvum* that was otherwise virulent on Cf-9 tomato. This study showed that CITRX acts as a negative regulator of the cell death and defence responses mediated by Cf-9 (Rivas et al., 2004). This was the first study to implicate thioredoxin activity in the regulation of plant disease resistance. However, it remains to be shown if this function of CITRX actually requires its redox activity/ ability.

A study on fungal infection (Victoria blight) of oats (*Avena sativa*) by Sweat and Wolpert (2007) also demonstrated an involvement of *AtTrx-h5* in pathogen defence. They found that a dominant gene conferring sensitivity to the fungus *Cochliobolus victoriae* encoded AtTrx-*h*5. As demonstrated using *AtTrx-h5* knockout mutants and chimeric proteins, the response to *C. victoriae* was quite specific to AtTrx-*h*5. The closely related *AtTrx-h3* could not fully compensate for the loss of *AtTrx-h5*. They also showed that AtTrx-*h*5, but not AtTrx-*h*3, is highly induced in sensitive *A. thaliana* following fungal treatment. Interestingly, only the first of the 2 active-site cysteine residues was required, suggesting that AtTrx-*h*5 function in the Victorin pathway involves an atypical mechanism of action (Sweat and Wolpert, 2007).

Tada et al. (2008) also reported a role for *A. thaliana* cytosolic thioredoxins during plant pathogen challenge. It was demonstrated that upon pathogen challenge, salicylic acid induced AtTrx-*h*5 to catalyse the release of NPR1 (non-expressor of pathogen-related genes 1) monomer, by reduction of disulfide bonds. NPR1 is a master regulator of salicylic acid-mediated defence genes. Mutations in either NPR1 or AtTrx-*h*5 impaired NPR1-mediated disease resistance against *P. syringae*. Interestingly, both AtTrx-*h*3 and AtTrx-*h*5 were required for full induction of the pathogenesis-related (PR) genes (Tada et al., 2008).

1.7.5 Oxidative Stress Protection

Oxidative stress occurs when the rate of reactive oxygen species (ROS) generation exceeds the detoxification abilities of the cell (Shulaev and Oliver, 2006). Thioredoxins-*h* may provide cellular protection against oxidative stress. In contrast to bacteria, yeast and mammals, where it has clearly been shown that cytosolic thioredoxins are involved in response to oxidative stress (Carmel-Harel and Storz, 2000; Nordberg and Arner, 2001), the functions of thioredoxin-*h* in response to oxidative stress in plants needs to be confirmed and investigations are ongoing.

The disruption of the two thioredoxin genes in *S. cerevisiae* leads to phenotypes including the inability to use methionine sulfoxide or sulfate as a source of sulfur, modified cell cycle parameters and reduced hydrogen peroxide (H_2O_2) tolerance (Muller, 1991). A functional complementation study by Mouaheb et al. (1998) using these thioredoxin-deficient yeast mutants, suggests that cytosolic *A. thaliana* thioredoxins are involved in different cellular processes, such as protection against H_2O_2, an oxidative stress molecule. Transformation with *AtTrx-h2* or *AtTrx-h3* complemented aspects of the *S. cerevisiae* mutant phenotype, depending on the expressed thioredoxin. Both *AtTrx-h2* and *AtTrx-h3* induced methionine sulfoxide assimilation and restored a normal cell cycle. In addition, *AtTrx-h2* also conferred growth on sulfate whilst *AtTrx-h3* restored H_2O_2 tolerance (Mouaheb et al., 1998).

An involvement of thioredoxin-*h* in the response to oxidative stress was further supported by the identification of a cytosolic peroxiredoxin as an *in vivo* target of AtTrx-*h*3 in yeast (Verdoucq et al., 1999). Peroxiredoxins are abundant low-efficiency peroxidases and have been identified in bacteria, yeast, animals and higher plants as a common anti-oxidative stress protein (Dietz, 2003; Rouhier and Jacquot, 2002). Yamazaki et al. (2004) also identified a monomeric type II peroxiredoxin as a target of *A. thaliana* thioredoxins-*h*. This was the first study indicating a direct interaction between the type II peroxiredoxin and a cytosolic thioredoxin in higher plants. Furthermore, it was recently reported that a thioredoxin-*h*, type I

peroxiredoxin and NTR co-localise in the nuclei of seed cells suffering oxidative stress (Pulido et al., 2009). In addition to their role in anti-oxidative stress systems, plant peroxidoxins and thioredoxins-*h* could be involved in modulating redox-dependent signalling cascades, as demonstrated in mammalian cells (Dietz, 2003).

Traverso et al. (2007) reported induction of a pea (*Pisum sativum*) thioredoxin, PsTrx-h1, by oxidative stress. Furthermore, functional complementation experiments in a trx1Δ trx2Δ double mutant yeast demonstrated that *PsTrx-h1* is involved in redox-imbalance control. Traverso et al. (2007) suggested this was achieved through interaction with peroxiredoxins. In contrast, they found that expression of *PsTrx-h2* in the yeast mutant resulted in hypersensitivity to hydrogen peroxide. These contrasting results were consistent with differential gene expression and protein accumulation data for the two isoforms, which indicated specific functions for pea thioredoxins-*h* and an involvement in oxidative stress (Traverso et al., 2007). The link between plant thioredoxins-*h* and oxidative stress is discussed further in section 1.13.1.1.

1.8 Specificity of Cytosolic Thioredoxins

The large number of plant cytosolic thioredoxins raises questions about their functional specificity and possible redundancies. Initially functional redundancy was thought to be highly likely, considering that *in vitro* protein interaction experiments identified similar thioredoxin protein targets, even when thioredoxins from different groups were used as 'bait' (Balmer et al., 2004; Yamazaki et al., 2004). For example, a cytosolic thioredoxin was reported to interact with chloroplastic proteins (Yamazaki et al., 2004). Although *in vitro* specificity for protein targets (interacting proteins) appears to be low, other data suggests that the specificity of thioredoxins-*h* is probably linked to tissue and sub-cellular localizations, temporal expression and/or the reduction pathway involved. Furthermore, yeast complementation studies with five *A. thaliana* thioredoxin-*h* isoforms provided *in vivo* evidence for different target specificities (Mouaheb et al., 1998).

A study by Reichheld et al. (2002) found that several thioredoxins-*h* differ by their level of expression, as well as the plant organ or cell-type in which they are expressed. These data were obtained by Northern analysis, semi-quantitative RT-PCR and transgenic promoter-GUS fusion experiments. Together, the results provided evidence of distinct expression patterns for the eight *AtTrx-h* members studied. In addition, it was found that *AtTrx-h5* expression was induced following challenge with a *P. syringae* protein elicitor, whilst *AtTrx-h3* was not (Reichheld et al., 2002). Later it was also shown that *AtTrx-h5* expression is induced by biotic

and abiotic stresses, unlike *AtTrx-h3*, which is constitutively expressed (Laloi et al., 2004). Also, *AtTrx-h3* was unable to fully compensate for the functional loss of *AtTrx-h5* in *A. thaliana* knockout mutants, despite being the most closely related *A. thaliana* thioredoxin.

In pea, PsTrx-*h*1 and -*h*2 are differentially expressed (Traverso et al., 2007). PsTrx-*h*1 protein was abundant in flowers and vascular tissue, whilst *PsTrx-h2* gene expression was barely detected. Furthermore, as previously discussed in section 1.7.5, contrasting functions for these pea thioredoxins are likely, considering their differing capacities to functionally complement a yeast trx1Δ trx2Δ double mutant (Traverso et al., 2007). Likewise, a study of thioredoxin-*h* expression in barley seed tissues suggests that thioredoxins-*h* are differentially regulated but may also have some common roles. In aleurone layers, transcripts (mRNA) of *HvTrx-h1* and -*h2* were present but only HvTrx-*h*1 protein was detected.

Together, these reports suggest that individual members of the multigenic family of plant cytosolic thioredoxins are likely to have specific and non-redundant functions. The temporal and spatial expression profile of each thioredoxin-*h* gene may influence its specific role. Therefore, comparison of profiles for all thioredoxins-*h* within a single plant species may reveal or point to specific functions.

Knockouts of individual thioredoxin genes have been suggested as a way of providing insight into the degree of redundancy within a thioredoxin class. However, to date, almost all such attempts have provided no recognisable phenotype. For example, Laloi et al. (2004) reported that regulation of *AtTrx-h5* is unique among the *A. thaliana* thioredoxin-*h* family. However, an *A. thaliana* knockout mutant for *AtTrx-h5* did not display an altered phenotype under the stress conditions that triggered expression of the gene (Dos Santos and Rey, 2006). The lack of a phenotype has been attributed to compensation by other members of the thioredoxin-*h* family (Laloi et al., 2004; Meyer et al., 2005). Therefore, perhaps single transgenic plants containing knockouts of multiple thioredoxins-*h* would be more informative.

1.9 Cytosolic Thioredoxins in Grasses

Initial phylogenetic analysis of grass thioredoxins-*h* indicated that there were 4 distinct subclasses that evolved prior to the divergence of monocotyledonous and dicotyledonous plants (Juttner, 2003). More recently, a tomato thioredoxin-*h* with unique features was identified (Rivas et al., 2004) and a barley homologue has been cloned by Dr Juan Juttner (*unpublished, ACPFG, University of Adelaide*). It is probable that this thioredoxin-*h* forms a fifth subclass but further investigation is required for confirmation. Therefore, grass thioredoxin-*h* sequences likely form five distinct subclasses designated 1–5 (Figure 1.4), which are conserved across grass species (*Dr Juan Juttner, pers. comm.*). The presence of distinct subclasses and the high level of sequence similarity within subclass members suggest some level of functional conservation within individual subclasses across grass species.

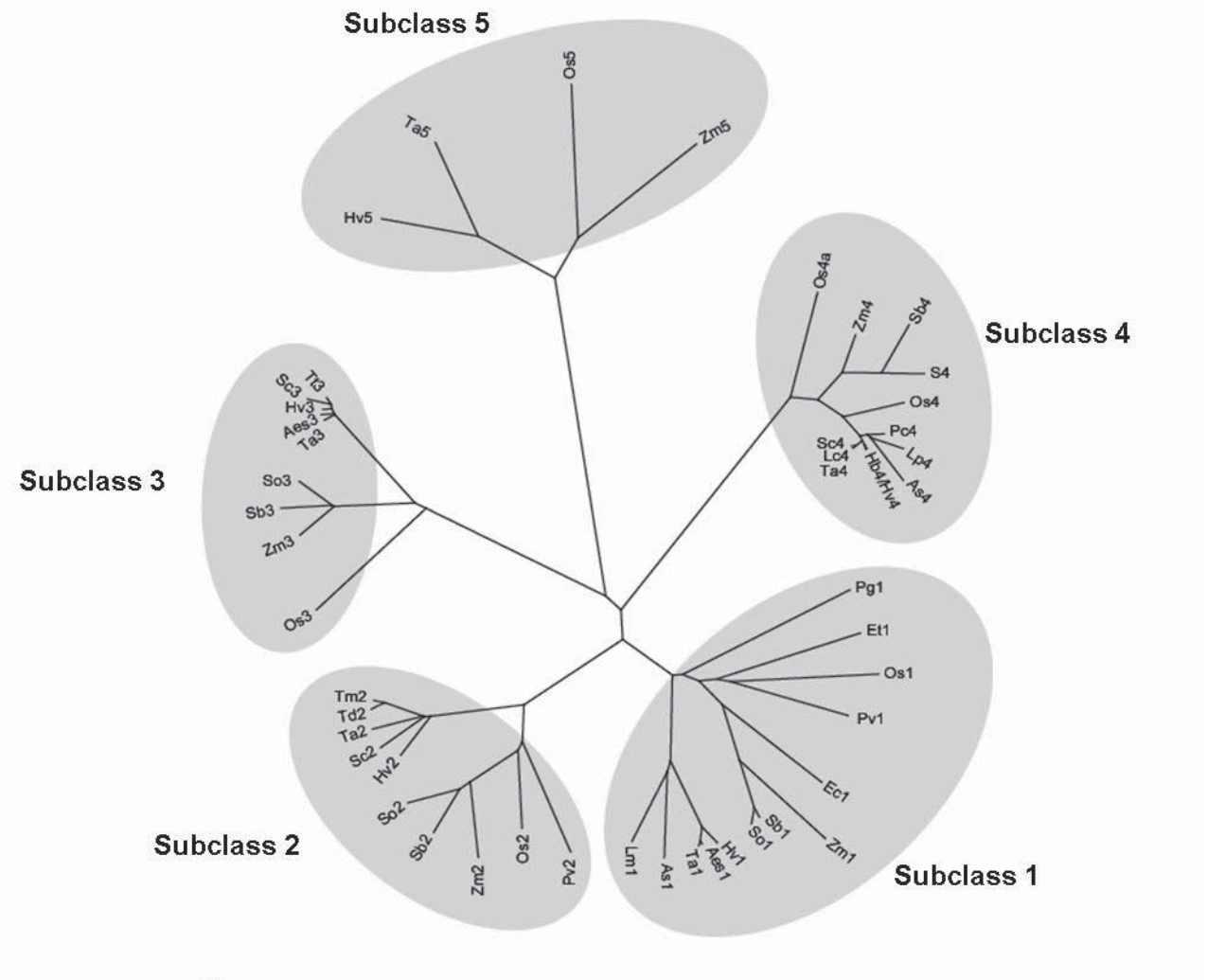

Figure 1.4: **Phylogenetic tree of grass thioredoxins-*h*.** Grass thioredoxin-*h* sequences form five distinct subgroups. Subclass 4 appears to share the greatest sequence similarity with ancient plant forms (biophytes and ferns). Species and Accession numbers: *Aegilops speltoides* Aes1 (BQ840991), Aes3 (BF292230); *Avena sativa* As1 (CN818445), As4 (CN821300); *Eleusine coracana* Ec1 (CX264712); *Eragrostis tef* Et1 (DN482993); *Hordeum bulbosum* Hb4 (AF159385); *Hordeum vulgare* Hv1 (AY245454), Hv2 (AY245455), Hv3 (BG418853), Hv4 (BE437654), Hv5 (CA001861); *Leymus chinensis* Lc4 (AAO16555); *Lolium multiflorum* Lm1 (AU250179); *Lolium perenne* Lp4 (AF159387); *Oryza sativa* Os1 (D26547), Os2 (CK072119), Os3 (CB627372), Os4 (CK007234), Os4a (CF991431), Os5 (NP_913796); *Panicum virgatum* Pv1 (DN151405), Pv2 (DN142385); *Pennisetum glaucum* Pg1 (CD725295); *Phalaris coerulescens* Pc4 (AF159388); *Saccharum officinarum* So1 (CA297726), So2 (CA237255), So3 (CA285731), So4 (CA226963); *Secale cereale* Sc2 (BE586970), Sc3 (BE637204), Sc4 (AF159386); *Sorghum bicolour* Sb1 (AW923038), Sb2 (AW924685), Sb3 (AW678266), Sb4 (CN128867); *Triticum aestivum* Ta1 (CV763567), Ta2 (X69915), Ta3 (BE402773), Ta4 (CK163487), Ta5 (BJ266273); *Triticum durum* Td2 (AJ001903); *Triticum monococcum* Tm2 (BG608088); *Triticum turgidum* Tt3 (AJ611750); *Zea mays* Zm1 (AI770787), Zm2 (BE510268), Zm3 (AW566291), Zm4 (BM269264), Zm5 (CD446146). Figure adapted from one supplied by Dr Juan Juttner (*unpublished*).

1.9.1 Grass Cytosolic Thioredoxin Subclasses 1 – 5

Subclass 1 members all share high protein sequence identity (70-83%), between grass species. Significantly, they all have almost identical N-terminal sequences (Juttner, 2003). A mutational study involving the removal of five of these N-terminal amino acids was found to abolish the ability of the thioredoxin to transport itself across plasmodesmata (Ishiwatari et al., 1998). The thioredoxins identified in rice sieve elements are members of this subclass (Ishiwatari et al., 1995).

Subclass 2 members are also highly conserved, having 71-83% amino acid identity. Most of the sequence differences are located in the N-terminal region of the predicted proteins. A unique feature of this subclass is that the N-terminus is predominantly hydrophobic with a high proportion of alanine and threonine residues (Juttner, 2003). Subclass 2 thioredoxins-*h* from maize and sorghum are currently the only grass thioredoxins known to contain the less common thioredoxin motif, WCPPC (Juttner, 2003).

Subclass 3 members are highly conserved, having 72-90% identity between predicted proteins. These thioredoxins are similar in structure to subclass 2 thioredoxins-*h* in the N-terminus, in that they are predominantly hydrophobic (10 of the first 15 residues). Subclass 3 members have the longest protein sequences of all grass thioredoxins-*h*. All subclass 3 members contain a KDEL endoplasmic reticulum retention signal near the C-terminus, suggesting that these thioredoxins-*h* may reside in the endoplasmic reticulum (Juttner, 2003).

Thioredoxins-*h* forming the fourth subclass are the most highly conserved of all subclasses, with the proteins from the different grass species having at least 86% amino acid identity with each other. Members of this subclass can readily be distinguished from other grass thioredoxins-*h* by the presence of a conserved cysteine at position 4 in the mature protein, as well as three conserved phenylalanines towards the carboxyl end (Juttner, 2003).

Interestingly, phylogenetic analysis indicates that grass thioredoxin subclass 4 is the most closely related to vertebrate out-group sequences (*Dr Juan Juttner, pers. comm.*). Subclass 4 thioredoxins-*h* share the greatest sequence similarity with ancient plant forms (biophytes and ferns) (Juttner, 2003). The high sequence similarity of thioredoxins-*h*4 in plant species as diverse as angiosperms and gymnosperms implies a stricter conservation of gene function. Furthermore, these relationships could suggest that subclass 4 represents a more ancient subclass whose origin predates the appearance of the angiosperms at least 200 million years

ago (Juttner, 2003). *A. thaliana* thioredoxin-*h*9 and poplar (*P. tremula/tremuloides*) thioredoxin-*h*4 are members of subclass 4 (Koh et al., 2008).

A fifth grass thioredoxin subclass has been proposed, involved in pathogen and transcription factor interactions. However, it has recently been questioned whether this thioredoxin really does reside in the cytosol. Further investigations, including immunolocalisation experiments, are in progress (*Dr Juan Juttner, pers. comm.*).

Thioredoxins and Oxidative Stress

1.10 Oxidative Stress and Reactive Oxygen Species

The appearance of oxygen in the atmosphere enabled respiratory metabolism and efficient energy generation systems. However, it also led to the formation of oxidative stress in the form of reactive oxygen species (ROS) in cells (Temple et al., 2005). ROS are partially reduced or excited forms of atmospheric oxygen and are continuously and unavoidably produced in cells during aerobic metabolism. ROS include superoxide ($O_2^{\bullet -}$), hydrogen peroxide (H_2O_2), hydroxyl radicals ($HO^{\bullet}$), and singlet oxygen ($^1O_2$) and all are by-products of normal biological, metabolic, redox reactions (Arora et al., 2002; Kotchoni and Gachomo, 2006; Moller et al., 2007). The hydroxyl radical is the most reactive of all the common ROS (Moller et al., 2007). ROS have the potential to be both beneficial and harmful to cellular metabolism, depending upon their concentration (Kotchoni and Gachomo, 2006).

To date, ROS have been associated with aging and modifications of cellular and molecular components in animal and plant cells (Kotchoni and Gachomo, 2006; Moller et al., 2007). A common feature among the different ROS types is their capacity to affect many important cellular functions, because biological molecules are susceptible to attack by ROS. Unless efficiently metabolized ROS can rapidly oxidize and damage nucleic acids, modify polyunsaturated fatty acids and carbohydrates, oxidise proteins, inactivate enzymes and cause lipid peroxidation of membranes (Apel and Hirt, 2004; Arora et al., 2002; Foyer and Noctor, 2005a; Moller et al., 2007; Temple et al., 2005). Clearly, ROS can react with a large variety of biomolecules, resulting in cellular dysfunction and irreversible damage, which ultimately leads to cell death or the appearance of necrotic lesions (Foyer and Noctor, 2005b; Girotti, 2001; Pitzschke et al., 2006). In contrast, ROS can influence the expression of a number of genes and participate in signal transduction pathways (Dalton et al., 1999; Moller et al., 2007). For example, it has been shown that ROS can modulate the activity of specific transcription factors, thereby directly affecting gene expression (Pitzschke et al., 2006). This suggests that cells have evolved strategies to use ROS to control biological programs.

1.11 Reactive Oxygen Species in Plants

ROS are produced in plants as products of mainstream enzymatic reactions (Moller et al., 2007) and they are also regularly produced during the aerobic phase of photosynthesis and photorespiration (Asada and Takahashi, 1987; Kotchoni and Gachomo, 2006; Mittler, 2002). In plant tissues, the photosynthetic electron transport system is the major source of active

oxygen (Asada, 1994). During electron transfer reactions, ground state oxygen is converted to more reactive ROS forms by sequential reduction to $O_2^{\bullet -}$, H_2O_2 and $HO^{\bullet}$, as presented in Figure 1.5 (Klotz, 2002). The electron transport chain also has the potential to generate $^1O_2$ (Arora et al., 2002; Moller et al., 2007). Consequently, ROS production in plants is unavoidable in an oxygen atmosphere. Hypoxia and anoxia are special cases where most of the ROS production occurs during the reoxygenation phase (Blokhina et al., 2003).

In plants, the conversion of $O_2^{\bullet -}$ into H_2O_2 can be facilitated by superoxide dismutase (SOD). H_2O_2 then gives rise to $HO^{\bullet}$ through the Fenton reaction, which is catalysed mainly by free transition metal ions (Moller et al., 2007). Each ROS has very different properties (Moller et al., 2007). The relatively stable H_2O_2 molecule is usually in low millimolar to micromolar concentrations in plant tissues, depending on the compartment (Cheeseman, 2006; Halliwell and Gutteridge, 2002; Puntarulo et al., 1988). In contrast, $O_2^{\bullet -}$ and $HO^{\bullet}$ have very short half-lives and are present at very low concentrations; too low to have been measured accurately (Moller et al., 2007). The ROS discussed have differing reactivities. $O_2^{\bullet -}$ mainly reacts with protein Fe-S centres whilst $^1O_2$ is particularly reactive with conjugated double bonds. $HO^{\bullet}$ reacts rapidly with all types of cellular components. Therefore, each ROS leaves a unique footprint in the cell, in the form of different oxidatively modified components (Moller et al., 2007).

Figure 1.5: **Reactive oxygen species (ROS) cascade.** Beginning with ground state triplet oxygen (dioxygen), various ROS are generated, primarily through energy transfer in the form of electrons ⊖ and protons ⊕. Figure adapted from Apel and Hirt (2004).

1.11.1 Production sites of ROS in plant cells

In plants, ROS are continuously produced as by-products of various metabolic pathways, which are localised in different cellular compartments (Foyer et al., 1994). Sources of ROS production in plants include chloroplasts, mitochondria, peroxisomes and cell-wall-bound peroxidase (Apel and Hirt, 2004; Davletova et al., 2005; Mittler, 2002). Plants and animals differ in their major sources of ROS production; chloroplasts and mitochondria respectively.

In green plants, the chloroplasts and peroxisomes are the main ROS producers through photorespiration (Foyer and Noctor, 2003). Chloroplasts produce $^1O_2$ at photosystem II and $O_2^{\bullet-}$ at photosystem I (Asada, 2006) and photosystem II (Pospisil et al., 2004) as by-products of photosynthesis (Moller et al., 2007). Some ROS generated by the electron transport chain escape and can be detected in various other cell compartments (Banerjee et al., 2003).

Most of the oxygen turnover in an aerobic organism is used in the mitochondria for substrate metabolism and production of ATP (Kotchoni and Gachomo, 2006). An estimated 1–5% of oxygen consumption, of isolated mitochondria, results in ROS production (Moller and Kristensen, 2004). Mitochondria produce $O_2^{\bullet-}$ at complexes I and III in the electron transport chain, also as a by-product (Moller et al., 2007). In plants grown in darkness, mitochondria become the main ROS producers (Maxwell et al., 1999; Moller and Kristensen, 2004).

In the green tissues of plants, the relative contribution of mitochondria to ROS production appears to be very low (Purvis, 1997). The presence of alternative oxidase (AOX) in plant mitochondria, which catalyses the reduction of O_2 by ubiquinone, may explain this low ROS level. The AOX competes for electrons and could therefore help to reduce the production of ROS (Pitzschke et al., 2006). This hypothesis is supported by findings that transgenic cultured tobacco cells over-expressing AOX resulted in reduced ROS production. Conversely, antisense lines with reduced levels of AOX accumulation displayed ROS levels five times higher than control cells (Maxwell et al., 1999). Also, Wagner et al. (1995) found that H_2O_2 induces the synthesis of AOX.

The peroxisomes produce $O_2^{\bullet-}$ and H_2O_2 in several key metabolic reactions including the photorespiratory glycolate oxidase reaction, fatty acid β-oxidation, the enzymatic reaction of flavin oxidases and the disproportionation of $O_2^{\bullet-}$ radicals (del Rio et al., 2006; Foyer and Noctor, 2003). Additionally, the plasma membrane NADPH-oxidase produces $O_2^{\bullet-}$ on the outer surface, which participates in several physiological processes following pathogen recognition (Torres and Dangl, 2005).

1.11.2 ROS Signalling in Plants

Rapid progress has been made in defining ROS as a major signal in diverse biological processes in plants (Pitzschke et al., 2006). For example, in higher plants ROS have a key role in the signal transduction network of stress-inducible genes (Bartels, 2001; Davletova et al., 2005; Miller et al., 2008; Mittler et al., 2004). Evidence also indicates that ROS can function as signalling molecules during regulation of plant development. Furthermore, it is likely that plants purposefully generate ROS as signalling molecules to control processes such as pathogen defence, programmed cell death and stomata behaviour (Apel and Hirt, 2004; Foyer and Noctor, 2005a; Gechev et al., 2006).

ROS are ideally suited to act as signalling molecules as they are small and can diffuse over short distances. Among the different ROS, only H_2O_2 can cross plant membranes and therefore directly function in cell-to-cell signalling (Pitzschke et al., 2006). Pathways of ROS signalling are made possible by homeostatic regulation through antioxidant redox buffering. Because antioxidants continuously process ROS, they determine the lifetime and the specificity of the ROS signal (Foyer and Noctor, 2005a). To date, the signalling processes involved in oxidative stress responses are not as well understood in plants as in bacteria, yeast and mammals.

Foyer and Noctor (2009) very recently published a comprehensive review entitled ‘Redox Regulation in Photosynthetic Organisms: Signalling, Acclimation, and Practical Implications’, which is highly recommended for further reading.

1.12 Antioxidant Systems in Plants

A stable and balanced cellular redox environment is of vital importance to all organisms (Kotchoni and Gachomo, 2006). High concentration of ROS can cause extensive cell damage or death. Consequently, the levels of ROS must be tightly regulated (Kotchoni and Gachomo, 2006; Mittler et al., 2004; Neill et al., 2002). Antioxidant systems are responsible for this regulation, determining the extent to which ROS accumulate, to maintain proteins and other cellular components in an active state for metabolism (Foyer and Noctor, 2005a).

The response of a plant to ROS depends on the specific ROS, its concentration, site of production and interactions with other stress molecules. The developmental stage and prehistory of the plant cell, such as previous stress encounters, is also influential (Apel and Hirt, 2004; Gechev et al., 2006). This explains why complex arrays of non-enzymatic and enzymatic detoxification mechanisms in plants have evolved.

Like most aerobic organisms, plants have developed sophisticated strategies to cope with the toxic effects of ROS. The first line of antioxidant defence is to prevent the formation of ROS by controlling reactions that lead to their generation (Netto, 2001; Pitzschke et al., 2006). For example, metal chelators can prevent ROS formation by suppressing ROS generating reactions. Suppression of the metal-catalysed Haber-Weiss-type reaction reduces the production of the very reactive $HO^{\bullet}$ (Netto, 2001). There are no scavengers of $HO^{\bullet}$ known, so it seems the only way to avoid oxidative damage by this radical is to control the reactions that lead to its generation (Pitzschke et al., 2006).

The second line of antioxidant defence is composed of antioxidant enzymes and low molecular weight compounds. In circumstances where ROS formation can not be prevented, antioxidant components attempt to scavenge and decompose these to avoid damage to the plant (Netto, 2001).

The cellular arsenal for ROS scavenging includes the low molecular weight antioxidants such as ascorbate, glutathione, flavonoids, carotenoids, polyphenols and alkaloids. Plants also make tocopherols (vitamin E) that act as important liposoluble redox buffers. Of these, ascorbate and glutathione are the major cellular redox buffers, interacting with numerous cellular components (Foyer and Noctor, 2005a; Pitzschke et al., 2006). Like all other aerobic organisms, plants maintain most cytoplasmic thiols in the reduced state. This is mainly achieved through the low thiol-disulfide redox potential imposed by millimolar amounts of glutathione (Foyer and Noctor, 2005a). Specifically, glutathione acts as a disulphide reductant to protect thiol groups on enzymes, regenerate ascorbate and react with $^1O_2$ and $HO^{\bullet}$ (Arora et al., 2002). Unlike many animal cells, plant cells also synthesise high concentrations of ascorbate (vitamin C). This extra hydrophilic redox buffer helps provide robust protection against oxidative stress (Foyer and Noctor, 2005a). Ascorbate is present at high concentrations in chloroplasts, the cytosol, vacuole and the apoplastic space of leaf cells in high concentrations (Foyer et al., 1991; Polle et al., 1990). It is a very important antioxidant in plants, playing a fundamental role in the removal of H_2O_2 (Foyer and Noctor, 2003). Redox homeostasis is regulated by large amounts of these antioxidants to absorb and buffer reductants and oxidants (Foyer and Noctor, 2005a). Their importance has been demonstrated in studies of mutants with decreased ascorbic acid levels (Conklin et al., 1996) or altered glutathione content (Grant and Loake, 2000), which resulted in hypersensitivity to stress.

Enzymatic ROS scavenging mechanisms in plants include SOD, ascorbate peroxidise (APX), glutathione peroxidase and catalase. They quench toxic compounds or regenerate antioxidants

through their reducing power (Pitzschke et al., 2006). Superoxide dismutase, a family of metalloenzymes, catalyses the disproportionation of $O_2^{\bullet-}$ to molecular oxygen and H_2O_2 (Pitzschke et al., 2006; Scandalios, 1993). Importantly, this decreases the risk of $HO^{\bullet}$ formation from $O_2^{\bullet-}$ *via* the metal-catalysed Haber–Weiss-type reaction (Arora et al., 2002).

Glutathione peroxidise, APX and catalase facilitate the detoxification of H_2O_2. Unlike most other organisms, plants have multiple genes encoding SOD and APX isoforms that are targeted to specific cellular locations (Asada and Takahashi, 1987). Three isozymes of SOD, designated Mn-SOD, Cu/Zn-SOD and Fe-SOD, have been reported in various plant species (Arora et al., 2002). Ascorbate peroxidase activity has mainly been reported from chloroplasts and the cytosol (Chen and Asada, 1989) but has also been found in mitochondria (Anderson et al., 1995).

All the antioxidant components described above do not act independently. Their synthesis is very tightly regulated in both time and space (Netto, 2001). Because of these antioxidant systems, plant cells generally cope well with high generation rates of ROS, even singlet oxygen (Foyer and Noctor, 2005a).

Antioxidants also influence plant growth and development by modulating processes from mitosis and cell elongation to senescence and death (de Pinto and De Gara, 2004; Potters et al., 2004; Tokunaga et al., 2005). Data suggests that a balanced amount of ROS is crucial for many different metabolic processes in plants (Bartels, 2001; Davletova et al., 2005; Kotchoni and Gachomo, 2006). However, the most important role for ROS are to confer essential information on the cellular redox state (signalling) and to provide plants with efficient ROS scavenging systems (Arora et al., 2002). They undoubtedly protect plants from destructive oxidative reactions.

1.13 Abiotic and Biotic Stress

Plant responses to environmental stresses have been analysed extensively at biochemical and molecular levels (Kotchoni and Gachomo, 2006; Rizhsky et al., 2004). It has been determined that ROS are required for processes facilitating adaptation to environmental stress conditions (Bartels, 2001; Ramanjulu and Bartels, 2002). Growing evidence suggests ROS-antioxidant interaction acts as a metabolic interface for signals derived from the environment. This interface modulates the appropriate induction of defence or acclimation processes or alternatively, execution of cell death programs (Foyer and Noctor, 2005a; Miller et al., 2008).

In plants, the balance between production and scavenging of ROS may be disturbed by adverse external conditions. A common feature of different stress factors is their potential to increase the production of ROS in plant tissues. Intracellular levels of ROS can rapidly rise when plants are exposed to biotic and abiotic stresses, because they generate more ROS than they can be scavenged (Apel and Hirt, 2004; Foyer and Noctor, 2005b; Gechev et al., 2006; Mittler et al., 2004). Abiotic stress arises from an excess or deficit in the physical or chemical environment. Abiotic factors include drought, water-deficit, salinity, heat shock, heavy metals, high light, ultraviolet radiation, ozone, nutrient deprivation and extreme temperatures (Bartels, 2001). Biotic stress refers to pathogen attack or stress imposed by other organisms (Grant and Loake, 2000).

Production of ROS is not necessarily deleterious. For example, plants have developed systems to increase the generation of ROS in order to kill pathogens (Bolwell, 1999; Grant and Loake, 2000). Reactive oxygen species are also involved in the physiological and biochemical mechanisms of disease resistance in plants. In plant-microbe interactions ROS participate in the plant defence response by acting as signalling agents (Lamb and Dixon, 1997) or by causing reinforcement of cell walls through oxidative cross-linking (Brisson et al., 1994; Brown et al., 1998; McLusky et al., 1999; Mellersh et al., 2002). Importantly, the type and source of ROS generated has been shown to depend on the plant-pathogen combination (Bolwell, 1999).

Plants have evolved diverse ways to thwart pathogens attempting to enter cells. Likewise, plant pathogens have developed various independent and clever mechanisms of penetrating and accessing plant cell contents. Therefore, preventing pathogen penetration during plant infection is firstly reliant upon perception of the pathogen by the plant host cells. Subsequently, activation of networks resulting in production of ROS, secondary metabolites

and pathogenesis related proteins is required. All of these components must work collectively to launch an adequate defence mechanism against the pathogen infection (Bolwell, 1999).

In many plant-pathogen interactions, the activities and levels of the ROS detoxifying enzymes APX and catalase are down-regulated by salicylic acid and nitric oxide (Klessig et al., 2000). In these cases, ROS accumulation and activation of programmed cell death (PCD) occurs since the plant produces more ROS whilst simultaneously decreasing its ROS scavenging capacities. In a study with soybean cells, it was evident that suppression of ROS detoxifying mechanisms is crucial for the onset of PCD (Delledonne et al., 2001). The authors showed that ROS production, without suppression of ROS detoxification, did not result in the induction of PCD (Delledonne et al., 2001). This indicates that coordinated production of ROS and down-regulation of ROS scavenging mechanisms is essential.

The function of ROS during abiotic stresses appears to be opposite to that during pathogen defence. Abiotic stresses induce ROS scavenging enzymes to decrease the concentration of toxic intracellular ROS levels. The differing responses to ROS, between biotic and abiotic stresses, probably result from hormone action and crosstalk between signalling pathways. Alternatively, the different stresses may induce ROS production and/or accumulation in distinct locations and concentrations and these differences are recognised by the plant (Pitzschke et al., 2006).

The conflicting response of a plant to biotic and abiotic stresses must be significant when exposed simultaneously to pathogen attack and abiotic stress. The plants ability to regulate ROS production and scavenging mechanisms in such a situation has been investigated by Mittler et al. (1999). They found that tobacco plants exposed to oxidative stress (high oxygen pressure) showed reduced PCD when subsequently challenged with a bacterial pathogen (Mittler et al., 1999).

The oxidative stress pre-treatment provided increased levels of ROS scavenging enzymes, thus reducing the plants ability to accumulate adequate levels of ROS to induce PCD (Pitzschke et al., 2006). Additionally, plants overproducing catalase show decreased resistance to pathogen infection (Polidoros et al., 2001), wounding (Orozco-Cardenas and Ryan, 1999), and high light treatment (Mullineaux and Karpinski, 2002).

Manipulating ROS levels by genetic engineering has been proposed as a promising way to increase resistance against multiple environmental stresses (Bartels, 2001). However, this

could be complicated because genes related to ROS respond differently to different stress treatments (Foyer et al., 1994).

1.13.1 Thioredoxins as Antioxidants

In mammalian cells, thioredoxin affects many processes connected to redox homeostasis through intracellular signalling pathways, regulation of transcription factors and detoxification mechanisms. These processes include inhibition of apoptosis, modulation of inflammation and control of redox balance (Arner and Holmgren, 2000). Mammalian thioredoxins can reduce H_2O_2 directly (Kang et al., 1998; Spector et al., 1988). In addition, thioredoxins function as $^1O_2$ quenchers and $HO^{\bullet}$ scavengers and act as hydrogen donors for peroxidases (Chae et al., 1994; Das and Das, 2000). Kang et al. (1998) also demonstrated that the mammalian thioredoxin system provides reducing equivalents to peroxiredoxins, which subsequently reduce H_2O_2. Significantly, it has been shown that over-expression of human thioredoxin in mice enhances resistance to oxidative stress and prolongs life (Mitsui et al., 2002). Likewise, a thioredoxin was found to be involved in the oxidative stress protection system of *Drosophila melanogaster*, as a null-mutation of the thioredoxin reduced life-span (Svensson and Larsson, 2007).

In yeast (*S. cerevisiae),* the best-characterised component of ROS sensing is the transcription factor Yap1p, which regulates many key antioxidant genes. Yap1p accumulates in the nucleus of cells following exposure to H_2O_2. Subsequently, the transcription of ~70 genes is altered, including those encoding thireodoxin-2, thioredoxin reductase, cytosolic catalase, cytosolic SOD and those involved in glutathione synthesis and metabolism (Temple et al., 2005). Similarly, the bacterial oxyR factor is activated through protein thiol oxidation (Bauer et al., 1999).

In animals, there is a thioredoxin-linked mechanism for the ROS-activated mitogen-activated protein kinase (MAPK) kinase kinase, ASK1. In unstimulated cells, ASK1 and thioredoxin interact, resulting in an inactive state (Saitoh et al., 1998). Upon oxidative stress, thioredoxin is oxidized which releases ASK1. Consequently, ASK1 homodimers can form to activate the MAPK pathway. Currently it is not known if thioredoxin-mediated MAPK activation also exists in plants (Saitoh et al., 1998).

Zhang et al. (2007) investigated the role of a human mitochondrial thioredoxin, designated Trx2. Trx2 was shown to form a disulfide bond with a peroxiredoxin (Prx3) *in vivo* and *in vitro*. Also, endogenous Trx2 was oxidized in cells treated with a GSH-synthesis inhibitor.

Furthermore, when transfected with an active-site mutant of Trx2 ($Cys_{93}Ser$ conversion) the cells were more sensitive to mitochondrial oxidative stress caused by tert-butylhydroperoxide or TNF-α plus cycloheximide. Conversely, over-expression of *Trx2* provided protection against toxicity. Consequently, the Trx2 system was reported to function in parallel with the glutathione system, to protect cells from oxidative stress (Zhang et al., 2007).

1.13.1.1 Plant Thioredoxins as Antioxidants

Recently, it has emerged that plant thioredoxins participate in the oxidative stress response. As a major supplier of reducing power for ROS detoxification and protein repair, plant thioredoxins are likely to play an essential role in protecting the plant against oxidative damage (Dos Santos and Rey, 2006). The functional involvement of plant thioredoxins in protecting plants from oxidative damage was first established using heterologous complementation in a *S. cerevisiae* strain lacking thioredoxin. Two *A. thaliana* thioredoxin types, -*m* and -*x*, could restore tolerance to oxidative stress induced by either H_2O_2 or an alkyl hydroperoxide. Three of the *A. thaliana* thioredoxins-*m* and one -*x* induced H_2O_2 tolerance, to the same extent as the endogenous yeast thioredoxins (Issakidis-Bourguet et al., 2001).

In another study, *A. thaliana* mutant lines containing a disrupted gene coding for a ferredoxin-thioredoxin reductase (FTR) subunit, had increased sensitivity to oxidative stress as well as a higher amount of 2-cysperoxiredoxin (Keryer et al., 2004). This provides evidence of an antioxidant role for the FTR-thioredoxin system in plants. In addition, most genes encoding chloroplastic thioredoxins are preferentially expressed in leaves in response to variations in light intensity and quality. This could indicate a function in the redox balance related to photosynthetic metabolism (Dos Santos and Rey, 2006). Furthermore, an *A. thaliana* knock-out mutant of novel NADPH-thioredoxin reductase (NTR), with an extended C-terminus containing a putative thioredoxin active site, shows growth inhibition and hypersensitivity to methyl viologen, drought and salt stress (Serrato et al., 2004). This study indicates involvement of the plant NTR-thioredoxin system in oxidative stress responses as well. Additionally, Reichheld et al. (2007) reported that *A. thaliana* plants responded to perturbation of the glutathione pool by buthionine sulfoximine, a specific inhibitor of glutathione biosynthesis, by increasing the amount of AtTrx-*h*3. Also, of note is an investigation of protein repair systems in sugarcane, which indicated involvement of several thioredoxin homologues including thioredoxin-*h* (*Oryza sativa*), thioredoxin-*m* (*Mesembryanthemum crystallinum*), thioredoxin-*f* (*Zea mays*) and thioredoxin reductase (*A. thaliana*) (Netto, 2001).

Recent development of proteomic tools has provided insight into the proteins with which plant thioredoxins interact. Specifically, the labelling of target sulfhydryl groups and an affinity chromatography method using a mutated thioredoxin to trap interacting proteins, have facilitated the identification of many putative target proteins. These studies have assisted prediction of thioredoxin functions, including a possible role for thioredoxin regulation of enzymes known to be involved in oxidative stress responses, including SOD, catalase, peroxidises, peroxiredoxins and glutaredoxins (Balmer et al., 2004; Marchand et al., 2004; Wong et al., 2004; Yamazaki et al., 2004)

The involvement of thioredoxins in oxidative stress tolerance *in planta* has been established using a genetic approach in potato (*Solanum tuberosum*). It was identified that a peroxide-detoxifying enzyme (BASI 2-Cys peroxiredoxin) is a target for a chloroplastic drought-induced stress protein (CDSP32), a thioredoxin. In transgenic plants lacking CDSP32 thioredoxin, methyl viologen treatment caused increased sensitivity and a higher lipid peroxidation level in thylakoids, compared to wild-type plants. Hence, CDSP32 is a critical component in the defence system against lipid peroxidation in photosynthetic membranes, and is likely to be a physiological electron donor to BASI peroxiredoxin (Broin and Rey, 2003). Evidently, CDSP32 is a thioredoxin participating in the defence against oxidative damage.

Further insight into the function of CDSP32 was gained by Rey et al. (2005) who identified three protein targets which participate in protection against oxidative damage; two peroxiredoxins (PrxQ and the BAS1 2-Cys peroxiredoxin) and a B-type methionine sulfoxide reductase. They showed CDSP32 can form heterodimeric complexes with PrxQ and the peroxiredoxin displays CDSP32-dependent peroxidase activity. Furthermore, under photo-oxidative stress induced by methyl viologen, potato plants over-expressing a mutant CDSP32 with an altered active site, exhibited decreased maximal PSII photochemical efficiency and retained much less chlorophyll compared with wild-type plants. Rey et al. (2005) proposed that the increased sensitivity results from the trapping *in planta* of the targets involved in the protection against oxidative damage (Rey et al., 2005). Based on the identity of targets and on the phenotype of transgenic plants, thioredoxins such as CDSP32 appear to be highly specialised in their function.

More evidence for the involvement of plant cytosolic thioredoxins in oxidative stress was reported by Laloi et al. (2004). Expression of the *A. thaliana* thioredoxin-*h*5 gene (*AtTrx-h5*) was shown to be up-regulated under conditions that trigger oxidative stress, such as wounding, abscission and senescence, as well as during incompatible interactions with the

bacterial pathogen *P. syringae*. It was concluded that *AtTrx-h5* was involved in an oxidative stress response (Laloi et al., 2004). However, whether this role includes protection against oxidative stress remains to be determined.

Very recently Park et al. (2009) reported that AtTrx-*h*3 performs dual functions, acting as a disulfide reductase or a molecular chaperone, depending upon its protein conformation. It was shown that AtTrx-*h*3 conferred enhanced tolerance to heat-shock in *A. thaliana*, primarily through the chaperone function. Furthermore, the structural and functional switching was shown to be regulated by redox status as well as heat shock (Park et al., 2009). These findings suggest the preservation of native conformations of cytosolic proteins during oxidative stress events is certainly a potential role for cytosolic thioredoxins *in planta*.

As discussed, evidence indicates that thioredoxins can perform functions related to the control of cell redox homeostasis in higher plants. Thioredoxins may modulate the activity of enzymes by directly scavenging ROS, or they could control the repair of stress-induced DNA damage, as shown in *C. reinhardtii* (Sarkar et al., 2005). Alternatively, they might participate in oxidative stress-linked signalling pathways possibly through the control of glutathione peroxidase and peroxidase redox status, as shown in yeast (Delaunay et al., 2002; Vivancos et al., 2005). It is also possible that the thioredoxin-linked disulfide–dithiol switch may have a key role in controlling transcription and translation in higher plants under oxidative stress conditions (Dos Santos and Rey, 2006).

The increasing evidence for the involvement of plant thioredoxins in antioxidant defence mechanisms indicates that thioredoxins are likely to participate in protecting plants from oxidative damage (Rouhier et al., 2008). They are probably also important in plant acclimation to environmental change, especially if redox interactions are involved in orchestration of abiotic stress responses (Dos Santos and Rey, 2006). For further information, a recent review by Rouhier et al. (2008), which focuses on redox-based antioxidant systems in plants, and includes a comparative biochemical and structural analysis of the major thiol oxidoreductases, is recommended.

1.14 Project Aims

The aim of this research project is to determine the function of grass cytosolic thioredoxins in subclass 4, in particular, the *Hordeum vulgare* member (HvTrx-*h*4). Investigations will focus on HvTrx-*h*4 expression, regulation and response to oxidative stress.

The specific objectives of the work include:

Analysis of *HvTrx-h4* mRNA expression levels in different tissues, at specific developmental stages and under different environmental conditions;

Expression analysis, using transgenic barley containing the *HvTrx-h4* promoter and 5′ untranslated region linked to a reporter gene (green fluorescence protein (GFP) fusion constructs), to provide insight into *HvTrx-h4* gene regulation in barley plants subjected to oxidative stress;

Identification of the proteins that interact with HvTrx-*h*4;

Functional analysis using transgenic tobacco plants in which *Phalaris coerulescens* thioredoxin-*h*4 is over-expressed or the endogenous *Nicotiana tabacum* thioredoxin-*h*4 is silenced.

2 General Materials and Methods

2.1 Plant Material

Hordeum vulgare plant material was obtained from a glasshouse collection maintained at the Waite campus, University of Adelaide, Australia.

2.2 Reagents

All chemicals used were analytical or molecular biology grade.

Chemicals were purchased from Merck Australia, Sigma-Aldrich and/or Biolab.

Solutions were prepared with nanopure water and autoclaved where appropriate.

Bacterial cloning and expression vectors were supplied by Dr Juan Juttner.

2.3 Manufacturers

Biolab, Clayton, VIC, Australia

Invitrogen Life Technologies: Invitrogen Australia Pty Ltd, Mount Waverley, VIC, Australia

Merck Pty Ltd, Kilsyth, VIC, Australia

QIAGEN Pty Ltd, Clifton Hill, VIC, Australia

Sigma-Aldrich (including Sigma-Proligo), Castle Hill, NSW, Australia

2.4 General Molecular Methods

2.4.1 Oligodeoxyribonucleotides

Primers were designed using primer design software Primer 3 ((Rozen and Skaletsky, 2000); http://frodo.wi.mit.edu/cgi-bin/primer3/primer3_www.cgi) and NetPrimer (http://www.premierbiosoft.com/netprimer/netprlaunch/netprlaunch.html). All primers were obtained from Sigma-Proligo, Australia and are listed in Appendix B.

2.4.2 Polymerase Chain Reaction (PCR)

Standard PCR conditions were used to amplify desired regions of genomic or cDNA. PCR reactions typically contained 20 ng DNA, 1 x PCR Reaction Buffer [20 mM Tris-HCl pH 8.4, 50 mM KCl] 1.5 mM $MgCl_2$, 0.2 mM dNTPs, 0.2 μM of each specific primer and 1 unit Platinum Taq DNA Polymerase (Invitrogen). PCR conditions for amplification were as follows: 2 min denaturing at 94^{o}C; 25-35 cycles of 30 s denaturing at 94^{o}C, 30 s annealing at primer Tm and elongation at 72^{o}C for 30 s/500 bp of product; and a final extension for 8 min at 72^{o}C.

2.4.3 First-Strand cDNA Synthesis

First-strand cDNA synthesis in preparation for Q-PCR was carried out using the Omniscript Reverse Transcriptase kit (Qiagen). 1 μg *Hordeum vulgare* cv Golden Promise total RNA, 1 x Buffer RT, 500 ng Oligo-dT primer, 10 units of Superase-In [RNase inhibitor], 0.5 mM of each dNTP and 4 units of Omniscript Reverse Transcriptase were combined in a 20 μl reaction. The reaction mixture was incubated at 37^{o}C for 1 h followed by 93^{o}C for 5 min then rapid cooling on ice.

2.4.4 Reverse Transcriptase - Polymerase Chain Reaction (RT-PCR)

Analysis of gene expression *via* RT-PCR was achieved using the SuperScript III One-Step RT-PCR System with Platinum® *Taq* DNA Polymerase kit (Invitrogen). Gene specific primers (0.2 μM of each primer) and 120 ng of high quality total RNA were used with all steps executed according to the manufacturer's instructions (Invitrogen).

2.4.5 Nucleic Acid Quantification and Quality Assessment: Gel Electrophoresis

The concentration of nucleic acids was determined spectrophotometrically (NanoDrop ND-1000 spectrophotometer) at 260 nm. Nucleic acid fragments were visualised on ethidium bromide-stained (1 μg/ml) 0.8-1.6% agarose gels. Samples were loaded with 1 x loading

buffer [15% (v/v) Ficoll type 4000, 0.25% (v/v) bromophenol blue, 0.25% (v/v) xylene cyanol FF] and electrophoresed in 1 x TAE Buffer [40 mM Trizma base, 1 mM Na_2EDTA, pH to 8 with glacial acetic acid] at 100 volts. Gels were photographed under UV, λ302 nm. DNA fragment sizes were estimated by comparing their mobility to bands of known sizes, in a molecular weight marker (Hyperladder I and II, Bioline, Australia).

2.4.6 Purification of DNA from Agarose Gel

Desired DNA bands were excised from agarose gels under long wavelength UV and purified using the MinElute Gel Extraction Kit according to the manufacturer's instructions (Qiagen).

2.4.7 Restriction Enzyme Digestion

Restriction enzyme digestion was carried out in a 10 µl volume. Each reaction contained 1-10 µg DNA, 5-10 units of restriction enzyme and 1 x complimentary reaction buffer (as determined by the manufacturer). When required, 1 x Purified BSA (Sigma) was also included. The reaction mixture was incubated at 37°C for 1 h.

2.4.8 Preparation of Chemical Competent *Escherichia coli* Cells

Escherichia coli, strain DH5α, cells were streaked onto a Luria broth agar plate [1% (w/v) Bacto-tryptone, 0.5% (w/v) Bacto-yeast extract, 1% (w/v) NaCl, 1.5% (w/v) Agar, pH 7.0] and incubated overnight at 37°C. A single colony was used to inoculate 250 mL of SOB medium [2% (w/v) Bacto-tryptone, 0.5% (w/v) Bacto-yeast extract, 0.1 M NaCl, 2.5 M KCl] in a 2 L flask. Cells were grown to an optical density of 0.6 at 600 nm, at 18°C with vigorous shaking. The flask was chilled on ice for 10 min then the cells were transferred to pre-chilled 250 mL centrifuge bottles. Cells were pelleted by centrifugation at 2,500 rpm for 10 min at 4°C (JA14 rotor, Beckman J2-21) and resuspended in 80 mL TB buffer [10 mM Pipes (1,4-piperazinediethanesulfonic acid), 55 mM $MnCl_2$, 15 mM $CaCl_2$, 250 mM KCl, pH 6.7]. Cells were incubated in an ice bath for 10 min then the centrifugation was repeated. Cells were gently resuspended in 20 mL TB containing 7% (v/v) DMSO and incubated in an ice bath for 10 min. The suspension was aliquoted into microcentrifuge tubes, snap-frozen immediately in liquid nitrogen and stored at -80°C.

2.4.9 Cloning of PCR Products

PCR products to be cloned were either purified directly from the PCR reaction using QIAquick PCR Purification Kit (Qiagen) according to the manufacturer's instructions, or extracted from ethidium bromide stained agarose gels (see 2.4.5). Purified fragments were

ligated into pGEM-T Easy vector using the pGEM-T Easy vector kit (Promega, Australia) in a 10 µl volume using 3 units T4 DNA Ligase and DNA at an approximate ratio of 1_{vector} : 3_{insert} according to the Rapid Ligation Protocol. The reaction proceeded at 4°C overnight or at 25°C for 2 h.

The ligation reaction products were purified by an N-butanol precipitation when required. Briefly, 10 volumes of n-butanol was added to ligation products, vortexed for 5 s and centrifuged at 11,300 *g* for 10 min. The supernatant was discarded, 200 µl of 70% ethanol added and centrifugation repeated. Supernatant was aspirated, plasmid DNA dried under vacuum for 15 min and resuspended in 5 µl sterile nanopure water.

Ligation products were transformed into chemical competent *Escherichia coli* cells by heat shock. Ligation product (10 µl) was mixed with 100 µl of cells and chilled on ice for 20 min, followed by incubation at 42°C for exactly 1 min. The cells were immediately resuspended in 400 µl Luria broth (LB) [1% (w/v) bacto-tryptone, 0.5% (w/v) yeast extract, 1% (w/v) NaCl, pH 7.0] and incubated at 37°C for 1 h with gentle shaking. Aliquots of 50-400 µl of transformed cell culture were spread on selective nutrient agar plates [LB, 1.5% (w/v) agar, 100 µg mL^{-1} ampicillin, 25 µg mL^{-1} iso-propyl-beta-D-thiogalactopyranoside, 40 µg mL^{-1} 5-bromo-4-chloro-3-indolyl-beta-D-galactopyranoside] and incubated at 37°C overnight.

Single colonies were picked at random, replica plated and grown as 2 or 5 mL overnight cultures in LB media supplemented with 100 µg mL^{-1} ampicillin.

2.4.10 Plasmid DNA Extraction

Plasmid DNA preparations from overnight cultures were prepared using the QIAprep Spin Miniprep Protocol (Qiagen) according to the manufacturer's instructions.

2.4.11 Sequencing

Plasmid DNA (200 ng) was prepared for sequencing in both directions using 1.6 µM of the sequencing primers T7 and SP6 with the ABI Prism BigDye Terminator v 3.0 Cycle Sequencing Kit with AmpliTaq DNA polymerase. Thermocycling conditions consisted of 25 cycles of 96°C for 10 s, 50°C for 5 s and 60°C for 4 min. The resulting products were transferred to a microcentrifuge tube, precipitated twice with 75% isopropanol and the pellet was dried at 37°C. Sequencing was carried out by IMVS sequencing facility, Adelaide, Australia.

2.4.12 Nucleotide Sequence Analysis

Sequence analysis and manipulations were performed using the WebAngis and Biomanager software packages operated by the Australian National Genome Information Service (http://www.angis.org.au). For DNA and protein sequence alignments CLUSTALW (Thompson et al., 1994) was used. Vector NTI 9.1 and associated programs (Invitrogen, 2004) were also used for sequence analysis and manipulations. BLAST (Basic Local Alignment Search Tool; (Altschul et al., 1990) analysis was used to search for and compare sequences against a selection of non-redundant databases and was accessed through the National Centre for Biotechnology Information (NCBI) (http://www.ncbi.nlm.nih.gov). The TIGR database was also used to obtain some plant nucleotide sequences (http://compbio.dfci.harvard.edu/tgi/plant.html).

2.5 Genomic DNA Protocols

2.5.1 Genomic DNA Isolation from *Hordeum vulgare*

Approximately 500 mg of young leaf tissue in a 1.5 mL microcentrifuge tube, containing one 5 mm and three 3.5 mm sterilised ball-bearings, was immersed in liquid nitrogen. The material was ground to a fine powder by 2-3 rounds of 30 s vortexing followed by refreezing. The powder was homogenised with 600 µl DNA extraction buffer [1% (w/v) sarcosyl, 100 mM Tris-HCl, 100 mM NaCl, 10 mM Na_2EDTA, pH 8.5] for 2 min by gentle tube inversion. The mixture was extracted with 600 µl phenol/chloroform/isoamyl alcohol (25:24:1 v/v/v) for 5 min, alternating between heavy hand mixing for 30 s and partial phase separation. The two phases were separated by centrifugation at 12,000 x g for 5 min at room temperature. The aqueous phase was collected and the phenol/chloroform/isoamyl alcohol extraction was repeated. DNA was precipitated with 60 µl 3 M sodium acetate (pH 4.8) and 600 µl isopropanol and collected in pellet form following centrifugation at 12,000 x g for 5 min. The DNA pellet was washed for 15 min on an orbital rotor with 1 mL 70% ethanol. The DNA was again collected by centrifugation at 12,000 x g for 5 min, the ethanol was aspirated and the DNA pellet air-dried. DNA was resuspended in 50 µl R40 [40 µg RNAse A in TE buffer [10 mM Tris-HCl, 1 mM EDTA, pH 8.0]] by incubation at 4°C overnight. The DNA concentration was determined spectrophotometrically (NanoDrop ND- 1000 spectrophotometer). All DNA samples were stored at -20^{o}C.

2.5.2 Genomic DNA Isolation from *Nicotiana tabacum*

DNA was isolated from approximately 1 g of *Nicotiana tabacum* leaf material as for *Hordeum vulgare* (see 2.5.1) except for the addition of 100 mM sodium thiosulfate to the DNA extraction buffer.

2.5.3 Southern Analysis

The following southern analysis techniques were based on methods by Southern, 1975.

2.5.3.1 DNA Digestion and Capillary Blotting

DNA to be probed (~15 µg) was digested with restriction enzymes (see 2.4.7) and electrophoresed on 0.8-1.2% agarose gels (see 2.4.5). Fragments were transferred to a charge-modified nylon membrane (Hybond N+, Amersham Biosciences, UK) by overnight capillary blotting with 0.4 M NaOH. The membrane was washed briefly with 2 x SSC [150 mM NaCl, 15 mM tri-sodium citrate (pH 7.0)] and membranes were stored at 4^{o}C in the dark.

2.5.3.2 Oligo-labelling of DNA Probes

Specific DNA probes were generated by standard PCR (see 2.4.2) using the relevant specific primers. The PCR product was visualised on a 1% agarose gel (see 2.4.5) and extracted (see 2.4.6). Labelling reactions containing 50 ng of denatured template DNA, 0.9 µg of each probe specific primer and 9mer random primer mix, 12.5 µl of Oligo-labelling Buffer [60 µM of each dATP, dTTP and dGTP; 150 mM Tris-HCl pH 7.6; 150 mM NaCl; 30 mM $MgCl_2$; 300 µg mL^{-1} acetylted DNase-free BSA], 2 units of Klenow fragment (Boehringer, Mannheim) and 4 µl α^{32}P-dCTP were combined in a final volume of 25 µl with ice-cold nanopure water. The reaction mix was incubated at 37^{o}C for a minimum of 30 min. Radiolabelled DNA was separated from unincorporated nucleotides using a QIAquick nucleotide removal kit (Qiagen) and eluted with 100 µl 10 mM Tris-EDTA (pH 8.5). Labelled probes were denatured at 100^{o}C for 5 min prior to hybridisation to membrane.

2.5.3.3 Hybridisation

Prior to probe addition, the membrane was placed in a glass cylinder bottle (Hybaid) and pre-hybridised in 10 mL of pre-hybridisation buffer [20% 5 x HSB [3 M NaCl, 0.1 M Pipes, 0.025 M Na_2EDTA pH 6.8], 10% Denhardts III [10% (w/v) SDS, 5% (w/v) tetrasodium pyrophosphate, 2% (w/v) gelatine, 2% (w/v) ficoll, 2% (w/v) polyvinyl pyrollidone], 5 mg salmon sperm DNA, to final volume with nanopure water] for 12 -20 h at 65^{o}C, with rotation. Pre-hybridisation buffer was replaced with 10 mL pre-warmed hybridisation solution [20% 5

x HSB, 20% Denhardts III, 2.5% dextran sulfate, 5 mg salmon sperm DNA, to final volume with nanopure water]. Denatured radioactive DNA probe was added and the membrane hybridised overnight at 65°C, with rotation. Following probe hybridisation, membranes were washed at low stringency with pre-warmed 2 x SSC, 0.1% (w/v) SDS at 65°C for 2 x 5 min, followed by high stringency washing with pre-warmed 0.1 x SSC, 0.1% SDS at 65°C for 20 min, with gentle shaking. Hybridisation of labelled probes to DNA was visualised by exposure of washed membranes to X-ray film. Specifically, the membrane was secured in a cassette containing X-ray film (Fuji, Super HR-G30) and intensifying screens and stored at -80°C for 1-7 days, depending upon probe signal intensity. Films were developed using an AGFA CP1000 developing machine (Germany).

2.5.3.4 Removal of Radioactive Probes from Southern Membranes

Southern membranes were stripped of radioactive probes by immersion in stripping solution [0.1% SDS, 2 mM Na_2EDTA pH 8.0] heated to 90°C, followed by incubation at 65°C for 30 min. Stripped membranes were subsequently exposed to X-ray film for 5 days to ensure the probe had been removed.

2.6 RNA Protocols

2.6.1 Small Scale Isolation of Total RNA from Plant Material

Solutions used for RNA extractions were prepared using autoclaved nanopure water and all non-plastic material (such as mortars, pestles, glassware, spatulas) were sterilised by baking in aluminium foil at 180°C overnight. When possible, plasticware was sterilised by autoclaving whilst other plastic material (e.g. electrophoresis tank) was soaked in 0.4 M NaOH for 15 min or sprayed with RNaseZap (Ambion, USA), then rinsed 3 times with autoclaved nanopure water.

Approximately 10-100 mg of plant material in a 1.5 mL microcentrifuge tube, containing one 5 mm and three 3.5 mm sterilised ball bearings, was immersed in liquid nitrogen until frozen. The material was ground to a fine powder by alternating cycles of vortexing and refreezing. RNA was extracted using 1 mL of TriReagent (Gibco BRL, Invitrogen). Samples were vigorously shaken, incubated for 5 min at room temperature and then centrifuged at 12,000 *x g* for 10 min at 4°C. The supernatant was transferred to a fresh 1.5 mL Eppendorf tube containing 200 µl chloroform, incubated for 3 min then centrifuged at 12,000 *x g* for 15 min at 4°C. The RNA, located in the upper aqueous phase was transferred to a sterile 1.5 mL Eppendorf tube, precipitated with 500 µl isopropanol and pelleted by centrifugation at 12,000

x g for 10 min at 4°C. RNA was washed with 75% ethanol for 5 min, air-dried for 20 min at room temperature and resuspended in 30 µl DEPC-treated water *via* a 10 min incubation at 60°C. The RNA concentration was determined spectrophotometrically (NanoDrop ND-1000 spectrophotometer). All RNA samples were stored at -80°C.

2.6.2 Removal of Contaminating DNA

Removal of DNA was performed using the DNA-free kit (Ambion, USA). A maximum of 10 µg of RNA was combined with 1 x DNase Buffer and 2 units rDNase 1 in a 50 µl volume. The mixture was incubated at 37°C for 30 min. DNase Inactivation reagent (0.1 volumes) was then added, followed by incubation at room temperature for 2 min, with flick-mixing every 20-30 s. The mixture was centrifuge at 10,000 *x g* for 1.5 min, the RNA (supernatant) collected and stored at -80°C.

2.6.3 RNA Quality – Gel Electrophoresis

To assess the quality of total RNA isolated, 2 µg aliquots were added to 2 volumes of RNA loading buffer [70% (w/v) deionised formamide, 0.04% (w/v) bromophenol blue, 5% (v/v) glycerol, 0.1 mM EDTA], heat denatured at 65°C for 2 min and chilled on ice for 2 min. Samples were loaded onto 1.2% agarose gels containing ethidium bromide made with fresh 1 x TAE and run in electrophoresis tanks pre-treated with 0.4M NaOH for 1-2 h or RNaseZap to remove RNase.

2.6.4 Northern Analysis

2.6.4.1 Capillary Blotting

Total RNA to be probed (~15 µg) was electrophoresed on 1.2% agarose gels (see 2.6.3). Gels were soaked in 10 x SSC [1.5 M NaCl, 0.15 M tri-sodium citrate (pH 7.0)] for 15 min and RNA was transferred to a charge-modified nylon membrane (Hybond N+, Amersham Biosciences, UK) by capillary blotting overnight with 10 x SSC. The membrane was washed briefly with 2 x SSC and air-dried. Membranes were stored at 4°C (short-term) or -20°C (long term), in the dark.

2.6.4.2 Hybridisation

Membranes were pre-hybridised in 10 mL of hybridisation buffer [50% (v/v) formamide, 5 x SSPE [0.9 M NaCl, 0.05 M sodium phosphate, 5 mM Na_2EDTA pH 7.7], 1 x Denhardt's (Sambrook et al., 1989), 1% (w/v) SDS, 100 µg/mL yeast RNA] overnight at 42°C, with rotation (Hybridisation oven, Hybaid). Hybridisation buffer was replaced immediately prior to

addition of labelled probe. A denatured radioactive DNA probe, prepared as previously described (see 2.5.3.2), was added and the membrane hybridised overnight at 42°C with rotation.

Following probe hybridisation, membranes were washed at low stringency with pre-warmed 1 x SSC, 0.1% SDS at 65°C for 20 min, followed by 20 min washes at increasing stringencies [pre-warmed 0.5 x SSC, 0.1% SDS then 0.2 X SSC, 0.1% SDS then 0.1 x SSC, 0.1% SDS], with gentle shaking. Probe hybridisation was determined by autoradiography as previously described in 2.5.3.3.

2.6.4.3 Removal of Radioactive Probes from Northern Membranes

Northern membranes were stripped of radioactive probes by immersion in stripping solution [0.1% SDS, 2 mM Na_2EDTA pH 8.0] heated to 90°C, followed by incubation at 65°C for 30 min. Stripped membranes were subsequently exposed to X-ray film for 5 days to ensure the probe had been removed.

2.7 Protein Protocols

2.7.1 Protein Quantification: Bradford Assay

Protein concentrations were determined as described by Bradford et al. (1976), using known BSA concentrations as standards.

2.7.2 Separation and Visualisation of Proteins by 1D SDS-PAGE and Coomassie Staining

Protein quantity and purity were visualised by denaturing SDS-PAGE, using the Mini-Protean polyacrylamide gel apparatus system (BioRad, USA) and coomassie staining. To resolve thioredoxin proteins, 12-14% (w/v) polyacrylamide gels were poured between glass plates spaced 1-1.5 mm apart. The resolving gel fraction (~4 mL) was poured, allowed to set and then overlayed with stacking gel solution (~2 mL). The resolving gel solution consisted of 3.5 mL 40% (v/v) acrylamide/Bis 29:1 solution (BioRad), 2.5 mL 1.5 M Tris-HCl buffer (pH 6.8), 100 µl 10% (w/v) SDS, 20 µl TEMED (Sigma) and 3.85 mL sterile nanopure water. Polymerization was initiated with 50 µl 10% (w/v) ammonium persulphate. The stacking gel solution consisted of 500 µl 40% (v/v) acrylamide/Bis 29:1 solution (BioRad), 1.5 mL 0.5 M Tris-HCl buffer (pH 6.8), 50 µl 10% (w/v) SDS, 12 µl TEMED (Sigma) and 3.2 mL sterile nanopure water. Polymerization was initiated with 25 µl 10% (w/v) ammonium persulphate.

Protein samples were heated at ≥ 80°C in 1 x loading-dye [0.4 M Tris (pH 6.8), 10% (w/v) SDS, 30% (w/v) glycerol, 0.6 M DTT and 3-4 grains of bromophenol blue] for 10 min before loading onto the gel. Electrophoresis was executed in running buffer [25 mM Tris (pH 8.3), 250 mM Glycine, 0.1% (w/v) SDS] at 50 mA per gel for approximately 70 min or until the loading-dye-front reached the bottom of the gel.

Proteins separated on polyacrylamide gels were stained with colloidal Coomassie Brilliant Blue R-250 (Sigma). Proteins were fixed in 45% (v/v) methanol/10% (v/v) acetic acid for 30-45 min. Gels were then stained with coomassie solution [45% (v/v) methanol, 10% (v/v) acetic acid, 0.25% (w/v) Coomassie Brilliant Blue R-250] for 1.5-2 h. Destaining of the polyacrylamide gel was achieved with 45% (v/v) methanol/10% (v/v) acetic acid for 2 x 20 min followed by several changes of 10% acetic acid, until the stained protein bands were clearly visible. All incubations were at room temperature with gentle shaking.

An alternative protein separation system, the XCell SureLock protein electrophoresis tank (Invitrogen), was also used. For this system, polyacrylamide gels were poured into 1.5 mm plastic cassettes. All gel components, running buffers and conditions were the same as for the Mini-Protean system previously described. Alternatively, NuPAGE® 4-12% Bis-Tris 1.5 mm, 10 or 15 well pre-cast gels were purchased from Invitrogen. These gels were run in MES buffer instead [2.5 mM MES, 2.5 mM Tris (pH 7.3), 0.005% SDS, 0.05 mM EDTA] and stained with colloidal Coomassie Brilliant Blue G-250 (Sigma).

2.7.3 Electro-Transfer of Proteins to Nitrocellulose Membrane

Proteins were transferred to Nitrobind 0.22 micron nitrocellulose membranes (GE Water and Process Technologies, USA) using a Criterion Wet Blotter (BioRad). Polyacrylamide gels containing the separated protein samples of interest were placed onto nitrocellulose membrane, which was immersed in transfer buffer [25 mM Tris, 150 mM Glycine and 10% (v/v) methanol]. Remaining under transfer buffer and avoiding inclusion of air bubbles, the gel and membrane were sandwiched between filter paper, sponges and the plastic cassette. The cassettes were inserted into the tank which was filled with ice-cold transfer buffer and surrounded by slurry ice. Protein electro-transfer was carried out at 300 mA for 75 min. Immediately following protein transfer, membranes were incubated in blocking solution [5% (w/v) skim milk powder diluted in phosphate buffered saline (PBS) [137 mM NaCl, 2.7 mM KCl, 10 mM Na_2HPO_4, 1.8 mM KH_2PO_4 (pH 7.4)] or tris buffered saline (TBS) [50 mM Tris-HCl (pH 7.5), 150 mM NaCl]].

2.7.4 Antibody Purification and Concentration

2.7.4.1 Freeze Drying

Antibody samples to be freeze dried were dialysed in water at 4^{o}C using dialysis tubing of the appropriate pore size, for ≥ 2 h. Dialysed samples were transferred into a conical flask which was placed in a dry-ice/isopropanol slurry. The flask was continually rotated until the sample froze to the flask walls, forming a thin coating. The opening of the flask was sealed with a single layer of Parafilm 'M' (American National Can, USA) containing a single small hole. The flask was placed in the freeze dryer (Christ, Germany) at -60^{o}C and put under vacuum overnight or until a dry powder was visible. Dried antibody was stored at -20^{o}C and resuspended in the desired buffer when required for use.

2.7.4.2 Protein G Column

To concentrate and purify antibody serum, a Protein G column (Amersham Biosciences, UK) was used according to the manufacturer's instructions. Briefly, 8 mL of Binding Buffer [20 mM sodium phosphate pH 7.0] was syringed through the column, followed by loading of the column with antibody serum. The column was incubated at room temperature for 45 min to allow binding of the antibody and then washed with 7 mL of Binding Buffer. Three mL of 0.1 M Glycine, pH 2.7, was used to elute the antibody, which was immediately neutralised with 0.1 M Tris, pH 9.0, at a ratio of 100 µl mL^{-1} elution.

2.7.4.3 De-salting

To desalt antibody serum, a HiTrap™ Desalting Column (Amersham Biosciences, UK) was used according to the manufacturer's instructions. Briefly, 25 mL of PBS was syringed through the column, followed by the antibody sample. To elute the antibody, 3 mL of PBS was syringed into the column and the elution was collected.

3 Functional Characterisation of Transgenic Tobacco Plants with Altered Thioredoxin-*h*4 Expression

3.1 Introduction

Broadacre crops are greatly affected by environmental conditions and in Australia, abiotic stresses are regularly responsible for large reductions in crop yield and quality (Passioura, 2007). A plants response to an abiotic stress is determined by the particular stress type and is tailored accordingly, in order to protect the plant. Hence, the physiological, biochemical and molecular processes induced by stress events have an element of specificity dependant upon the environmental situation (Miller et al., 2008; Mittler, 2006). As reviewed in Chapter 1, thioredoxins are believed to play a role in protection against oxidative stress and have previously been linked with plant responses to various abiotic stresses such as drought, heat, cold, high-light and ultraviolet light (Kocsy et al., 2004; Laloi et al., 2004; Pagano et al., 2000; Rey et al., 1998). In addition, plant thioredoxin targets identified are known to be involved in antioxidant mechanisms, expression of plant thioredoxin genes are induced by reactive oxygen species (ROS) and functional evidence of plant thioredoxins acting as antioxidants *in vivo*, has been reported (reviewed by Dos Santos and Rey, 2006).

David Olde, a PhD student at the University of Adelaide, generated several transgenic *Nicotiana tabacum* lines with altered thioredoxin expression. The tobacco plants were engineered to constitutively over-express a *Phalaris coerulescens* cytosolic thioredoxin from subclass 4 (*PcTrx-h4*) or to silence expression of the tobacco ortholog *NtTrx-h4*. These plants provided an opportunity to investigate and characterise the potential role of thioredoxin-*h*4 in relation to oxidative stress, using a comparative functional analysis approach. The work presented in this chapter is focussed on the response of the transgenic tobacco plants to oxidative stresses, particularly derived from abiotic stress events, in an attempt to gain insight into the function of plant cytosolic thioredoxin-*h*4.

3.2 Materials and Methods

3.2.1 Construct and Transformation Methods

Transgenic *N. tabacum* (tobacco) seeds were obtained from David Olde who had generated them for his PhD research (*University of Adelaide*). Several lines of transgenic tobacco were transformed to over-express *P. coerulescens* thioredoxin-*h* protein (PcTrx-*h*4). Another set of transgenic tobacco lines were engineered to silence expression of endogenous *N. tabacum* thioredoxin-*h*4 (NtTrx-*h*4). Generation of the transgenic tobacco will be briefly described as it was not part of the work conducted for this thesis. The transgenic tobacco lines contained a construct with *PcTrx-h4* in a sense or antisense orientation behind a constitutive 35S promoter for tobacco (*David Olde*). The 35S promoter was chosen due to its high level of expression in dicots. The construct also contained a kanamycin selection marker (nptII) for ease of *in vitro* selection of transformants. The vector used was pBI121 and *PcTrx-h4* was cloned in place of the GUS gene, in the sense and antisense orientations. The resulting constructs were used to transform *Agrobacterium tumiefaciens* strain AGL1. *N. tabacum* cv Xanthi leaf disc cells were dedifferentiated to callus, which was transformed *via* an *Agrobacterium*-mediated tobacco transformation system and then plants were regenerated (Clemente., 2006). All plants were self-crossed, seed was collected and transformants were analysed. The following generations of seed (T1 and T2) were also collected.

3.2.2 Growth Conditions

Tobacco seedlings and plants were grown in a variety of conditions, depending upon the experiment for which they were to be used. Seedlings germinated on solidified MS Media in Petri dishes were grown under white light (fluorescent tubes, GRO-LUX, 100 µmol m^{-2} sec^{-1}) with a 10-12 h photoperiod at 22-24^{o}C, in a growth-cabinet or growth-room, depending upon the experiment. Soil grown tobacco was germinated in potting mix (coco peat) and transplanted into appropriately sized pots as they grew larger. Soil-grown tobacco was housed in a glasshouse where they were maintained at approximately 24°C during the day (13 h) and 18°C during the night (11 h). Light intensity was mostly as dictated by the season and weather conditions. Average relative humidity was 50% and 80% during the day and night, respectively.

3.2.3 Tobacco Solid MS Media

Solid MS Media included stock solutions that were filter sterilised. 20 x Macronutrient solution [20.6 mM NH_4NO_3; 18.8 mM KNO_3; 2.3 mM $CaCl_2.2H_2O$; 1.5 mM $MgSO_4.7H_2O$; 1.3 mM KH_2PO_4], 1000 x Micronutrient solution [5 μM KI; 100 μM H_3BO_3; 100 μM $MnSO_4.4H_2O$; 30 μM $ZnSO_4.7H_2O$], and Iron solution [100 μM $FeSO_4.7H_2O$; 100 μM Na_2EDTA] were made. MS media solution consisted of 3% sucrose, 1 x Macronutrient solution, 1 x Micronutrient solution, 1 x Iron solution, vitamins [2 mg/L glycine; 0.5 mg/L nicotinic acid; 0.5 mg/L Pyridoxine-HCl; 0.1 mg/L Thiamine-HCl; 100 mg/L Myo Inositol]. MS media solution was filter sterilized and pH adjusted to 5.8 with KOH. To make the solid MS Media, MS Media solution was added to 0.8% agar, which had been autoclaved and cooled to approximately 60^{o}C. Using aseptic technique, the media was poured into Petri dishes of the desired size and allowed to set.

3.2.4 Seed Sterilisation Technique

Approximately 150 seeds were placed in a 1.5 mL eppendorf tube and rinsed with 1 mL of 70% ethanol *via* manual agitation and tube inversion for 1 min, to remove hydrophobicity of the seeds as well as to kill bacteria. Using the same technique, seeds were rinsed twice with sterile nanopure water. Seeds were then sterilised with 1 mL of 0.5% bleach for 10 min, with mixing by a mechanical rotor, to kill fungal spores and viruses. Finally, the seeds were rinsed for 5 times with 1 mL sterile nanopure water for 1 min and were resuspended in 60 μl sterile nanopure water. Using aseptic technique and the suction of a 20-200 μl micropipette, individual seeds were transferred onto solid MS media for germination.

3.2.5 Identification of Homozygous Individuals

Second generation (T_2) transgenic tobacco plants that were homozygous for the introduced DNA (PcTrx-*h*4 transgene) were identified by determining the ratio of seedlings able to germinate and grow in the presence of kanamycin versus seeds unable to grow (Mendelian segregation ratio). The kanamycin resistance gene (nptII) was contained between the left and right borders of the construct (insertion cassette), as was the *PcTrx-h4* gene. Therefore, kanamycin resistance is linked to integration of *PcTrx-h4* into the plant genome and can be used to track inheritance of the transgene. Forty seeds from each T_2 plant were grown on large petri dishes of MS agar containing 150 mg L^{-1} kanamycin, under white light (fluorescent tubes, GRO-LUX, 100 μmol m^{-2} sec^{-1}) with a 12 h photoperiod at 24^{o}C and 12 h darkness at 22^{o}C, in a growth-room for 3-4 weeks.

3.2.6 RNA Expression Analysis of *PcTrx-h4* and *NtTrx-h4* Transcript in Transgenic Tobacco

Extraction of RNA from tobacco and subsequent Northern analysis were carried out as detailed in Section 2.6 of Chapter 2. A 410 bp fragment of *HvTrx-h4* cDNA was amplified from a pQE-70 vector containing *HvTrx-h4* (see 4.2.2) using primers Hv4E70F and Hv4E70R (Appendix B) and was used as a probe to detect transcripts of the introduced *PcTrx-h4* gene. *HvTrx-h4* and *PcTrx-h4* are highly similar in sequence identity, making it possible for an *HvTrx-h4* probe to detect *PcTrx-h4* transcripts. A 710 bp fragment of *NtTrx-h4* cDNA was amplified from a pGEM-T easy vector containing *NtTrx-h4* (*courtesy of David Olde, University of Adelaide*) using vector primers SP6 and T7 (Appendix B) and was used as a probe to detect the endogenous *NtTrx-h4* transcripts.

3.2.7 Pollen-Development Assessment for Transgenic Tobacco

To assess the viability of pollen from the transgenic tobacco plants, pollen physiology was observed at 10 x and 40 x magnification (Leica Microscopie Systemes, Switzerland). The pollen was derived from green anthers collected from tobacco flowers that had just opened with the edges starting to turn pink in colour. Anthers were dissected open and the pollen was placed on a glass slide and stained with filtered aceto-orcein solution.

3.2.8 Protein Extraction Methods

A variety of techniques were used to extract proteins from tobacco plant tissues. The protein extraction method chosen was dependent upon the plant material and the future analysis to which extracted material was subjected.

3.2.8.1 For Western Analysis of Transgenic Tobacco to Confirm Over-expression of Thioredoxin-h4: Phenol Extraction, Methanol/Ammonium Acetate Precipitation

Fresh leaf material was ground to a fine powder under liquid nitrogen and suspended in 500 µl of ice-cold extraction buffer [50 mM Tris pH 8.5; 5 mM EDTA; 100 mM KCL; 1% DTT; 30% (w/v) sucrose); 1 tablet of 'complete mini' protease inhibitor cocktail (Roche) per 100 mL], in a 2 mL eppendorf tube. Ice-cold tris-buffered phenol (pH 8.0) (500 µl) was added to each sample followed by vortexing at 4^{o}C for 15 min and then centrifugation at 6000 *x g* for 3 min at 4^{o}C. The organic phase was collected. To the remaining insoluble material, 250 µl of ice-cold extraction buffer and 250 µl of phenol was added, vortexed for 5 min, the phases separated by centrifugation at 6000 x g for 3 min at 4^{o}C and the organic layer was isolated. The two organic phases collected were combined, 5 volumes of 100 mM ammonium acetate

in methanol was added and the proteins were precipitated at -20°C overnight. Proteins were pelleted by centrifugation at 16,000 *x g* for 30 min at 4°C, and incubated with ice-cold acetone/0.2% DTT at -20°C for 1 h, twice. The protein pellet was air-dried at room temperature and resuspended in 100 µl of SDS loading buffer [0.4 M Tris (pH 6.8), 10% (w/v) SDS, 30% (w/v) glycerol, 0.6 M DTT and 3-4 grains of bromophenol blue].

3.2.8.2 For Carbonylation Western Analyses

Healthy, freshly harvested, young leaves (2 cm^2) were placed in 2 mL eppendorf tubes and tubes were filled with freshly made, cold, extraction buffer [50 mM Tris-HCl pH 7.5; 1 mM EDTA] containing plant protease inhibitor cocktail. Samples were vortexed vigorously at 4°C for 15 min and then centrifuged at 4,000 *x g* for 10 min at 4°C. The cytosolic fraction was harvested by centrifugation of the supernatant at 100,000 *x g* for 30 min at 4°C. Supernatant was collected and protein concentration was determined by a Bradford assay (see 2.7.1).

3.2.8.3 For PNGase F Treatment: TCA/Acetone/Phenol/SDS Extraction with Methanol/ Ammonium Acetate Precipitation

Leaf tissue was ground to a fine powder under liquid nitrogen using a mortar and pestle and transferred to a 2 mL eppendorf tube, which was subsequently filled with 10% TCA/acetone. Samples were mixed by vortexing and then sedimented *via* centrifugation at 16,000 *x g* for 3 min at 4°C unless otherwise stated. The resulting pellet was washed with 80% methanol containing 0.1 M ammonium acetate (w/v), then with 80% acetone and air-dried at room temperature to remove all residual acetone. To each pellet, 0.6 mL of Phenol/SDS Buffer per 0.1 g of starting tissue was added, mixed, incubated for 5 min at room temperature, and sedimented. The supernatant (upper phenol phase) was collected and mixed with 100% methanol containing 0.1 M ammonium acetate. Samples were incubated at -20°C overnight, or -80°C for 30 min, to precipitate proteins. Proteins were collected by centrifugation at 16,000 *x g* for 5 min at 4°C, washed with methanol, air-dried, washed with 80% acetone and air-dried again. The resulting "clean" proteins were resuspended in 20 mM ammonium bicarbonate (pH 8.0).

3.2.9 Western Analyses

Protein quantification, separation and transfer to nitrocellulose membrane was performed as detailed in Section 2.7 of Chapter 2.

3.2.9.1 For Antibody Specificity Test

The specificity of antibody, raised in rabbit against PcTrx-*h*4, was tested using recombinant purified barley thioredoxins-*h*1 to -*h*4 (as described in Chapter 4). A membrane, containing a sample of each recombinant HvTrx-*h*4 protein, was blocked with 4% skim milk powder in TBS at room temperature overnight, with gentle shaking. The membrane was washed in TBS for 7 min, 3 times and then incubated with primary antibody, raised against *P. coerulescens* thioredoxin-*h*4 (PcTrx-*h*4) in rabbit, at room temp overnight with gentle shaking. The membrane was again washed 3 times in TBS for 7 min prior to incubation with secondary antibody, Sigma anti-rabbit alkaline phosphatase conjugated [1:10,000 in TBS] for 2 h at room temperature. The membrane was washed a further 3 times in TBS for 7 min per wash. Antibodies were detected with nitroblue tetrazolium/bromochloro indolyl phosphate (NBT/BCIP). The surface of the membrane was completely covered with the NBT/BCIP substrate (Sigma), which resulted in development of a purple colour. Once bands had almost reached the desired intensity, after approximately 2 min, the reaction was stopped with a continuous flow of RO water.

3.2.9.2 Thioredoxin-h4 Detection in Unstressed Tobacco

A nitrocellulose membrane, containing proteins derived from healthy transgenic tobacco leaves (see 3.2.8.1), was probed using polyclonal antibodies raised against PcTrx-*h*4 in rabbit. Secondary antibody conjugated to alkaline phosphatase (Sigma) was detected by NBT/BCIP. Briefly, the membrane was blocked with 5% (w/v) BSA in TBS overnight at 4^{o}C then at 37^{o}C for 1 h with gentle shaking. The membrane was washed 3 x 5 min in 0.1% (w/v) BSA in TBS, with gentle shaking. The first wash was performed at 37^{o}C and the remaining washes were at room temperature. Next, the membrane was incubated with rabbit anti-PcTrx-*h*4 antibody [700 µl serum in 50 mL TBS containing 1% (w/v) BSA and 0.05% (v/v) Tween-20] for 2 h at room temperature with gentle shaking. The membrane was washed again as previously but always at room temperature. Secondary antibody, anti-rabbit alkaline phosphatase conjugated (Sigma) [1:10,000 in TBS containing 1% (w/v) BSA and 0.05% (v/v) Tween-20], was used to detect primary antibody by incubation of the membrane for 1.75 h at room temperature with gentle shaking. Excess secondary antibody was removed from the membrane by washing twice, for 5 min at room temperature, with TBS containing 0.1% (w/v) BSA, and then twice

more with TBS only. Antibodies were detected as in 3.2.9.1 but with Western Blue Stabilized Substrate for Alkaline Phosphatase (Promega).

3.2.9.3 N-linked Glycosylation Assessment of Thioredoxin-h4

A nitrocellulose membrane, containing proteins derived from transgenic tobacco leaves (see 3.2.8.3) and treated with PNGase F enzyme, was probed using polyclonal antibodies raised against PcTrx-*h*4 in rabbit as described in 3.2.9.2 with slight variations. Excess secondary antibody was removed from the membrane by washing twice, for 5 min at room temperature, with TBS containing 0.1% (w/v) BSA, and then twice more with TBS only for 10 min per wash. The membrane was rinsed with RO water and the antibodies were detected as described in 3.2.9.1.

3.2.10 Stress Treatments

For all stress treatments, dose curves were performed to determine optimal stress conditions. Transgenic and wild-type control plants were stressed simultaneously with at least two discrete homozygous transgenic lines tested.

3.2.10.1 Ultraviolet Light B (UVB) Stress

Ultraviolet light B (UVB: λ302 nm) stress experiments were conducted on transgenic and wild-type tobacco plants grown on solidified MS media in petri dishes [10 h photoperiod in a growth room or growth cabinet with 24^{o}C day and 22^{o}C night temperatures] and in pots of soil (glasshouse conditions). To induce UVB stress, 3-8 week old tobacco seedlings were placed in an enclosed Perspex box and exposed to 0.2-1.2 Wm^{-2} of for 1-48 h, as dictated by the experimental design. Lids were removed from Petri dishes to expose the seedlings growing on solidified MS media. All other growth conditions remained unchanged during irradiation. For media grown tobacco, at least 2 plates containing approximately 20 (small petri dish) or 40 (large petri dish) seedlings each, were subject to UVB treatment. A third plate was untreated to serve as a control.

3.2.10.2 Heat Stress

To elicit heat stress, 7 week old soil-grown tobacco plants were watered to soil saturation and placed at 42^{o}C in an oven at approximately 1 pm for 24 h. No light was present during the heat treatment.

3.2.10.3 Water Deficit Stress

Two tobacco lines over-expressing thioredoxin-*h*4, two tobacco thioredoxin-*h*4 knockdown lines and wild-type tobacco plants were subjected to water deficit stress. Six plants per line were grown in individual pots of soil to the height of 30 cm (approximately 2 months old). Water deficit stress for tobacco was achieved by withholding water in a controlled manner. Soil volumetric water content (VWC) was determined with a soil moisture meter (TDR 100 Spectrum Technologies, Illinois, USA). The measuring probes were inserted 11 cm into the soil at approximately 4 pm every 1-2 days. Water was added to the pots that were drying at a faster rate than others in order to attain a uniform decrease in volumetric water content (VWC) in the soil. The VWC of the soil during water deficit stress was recorded throughout the experiment. Relative leaf water content (RLWC) was determined by the standard method (Barr and Weatherley, 1962). Six leaf samples per plant were taken after 32 days of with-holding water and weighed (FW). Leaves were then rehydrated in water, surface dried and weighed again (TW). Next, the leaves were dried at 80^{o}C for 48 h and then 37^{o}C for 12 h. Dry leaf weights were recorded (DW) and the RLWC was calculated as a percentage using the formula: RLWC (%) = [(FW-DW)/(TW-DW)] x 100. Water withholding continued for 3 pots per line and the time until plant death was recorded. The remaining three pots were rewatered and monitored closely to assess plant recovery speed and extent.

3.2.10.4 Botrytis Cinerea Fungal Challenge

Tobacco plants were challenged with infection by the necrotrophic fungus *Botrytis cinerea*. Eight-day-old *B. cinerea* cultures on potato dextrose agar (PDA) were supplied by Dr Ian Dry (CSIRO, Plant Industry, Adelaide). Excess PDA was removed from plugs that were 0.5 or 1 cm^2 in size and contained a uniform covering of *B. cinerea*. These plugs were firmly placed on attached tobacco leaves from fully grown plants; the 3rd or 4th newest leaf on each plant. Leaves were covered in clear plastic bags which contained some moisture to increase humidity, which assisted with fungal infection. After 3 days of infection, the culture plugs were removed and the leaves assessed for degree of infection.

3.2.11 Free Radical Challenge

For free radical inducing treatments, the chemicals methyl viologen (MV) (also known as paraquot; Sigma), Rose Bengal diacetate (RBDA) and hydrogen peroxide (H_2O_2) were applied (liquid droplets) to attached leaves of approximately 2-month-old soil grown tobacco. The oxidative stress responses of untransformed and transgenic tobacco plants, over-expressing PcTrx-*h*4 or with NtTrx-*h*4 knocked down, were compared and contrasted. Dose-

response experiments using a series of concentrations were performed for each chemical to determine the dose required for leaf damage to be visible on the untransformed control plant. MV (10 µl) in 0.1% (v/v) Tween-20, at concentrations ranging from 1 to 200 µM, was applied to healthy leaves about 15 cm in length, approximately 1 h before nightfall. Initially, RBDA was diluted in 0.01% Tween-20 and 15 µl droplets were pippetted onto the 3rd youngest leaf, being approximately 3.5 cm in length, of each plant. However, the RBDA appeared to precipitate out of solution and dry on the leaves as a white crystal powder. Therefore, as recommended by the manufacturers, DMSO was used as a solvent instead. A 5 mM stock in water was diluted to final concentrations (0 – 1 mM) using DMSO and each leaf was treated with 5 µl droplets. Freshly made H_2O_2 was diluted with water to concentrations of 0 – 1.5 M and 10 µl droplets were pipetted onto healthy attached leaves, approximately 12 cm in length, to be absorbed. Treated leaves were monitored at 30 mins after treatment, then hourly for 12 hours and then twice daily until necrotic lesions developed, or for up to 1 week. The extent of the oxidative damage was assessed by examining the necrotic area of the leaf.

3.2.12 Detection of Carbonylated Proteins

Two approaches were used to detect carbonylated proteins by immunodetection of 2,4-dinitrophenylhydrazone (DNP); a method based on that reported by Job et al. (2005) and a kit based approach using the OxyBlot^{TM} Protein Oxidation Detection Kit (Chemicon, USA). Proteins were extracted from leaf tissue derived from UVB and heat stressed tobacco plants over-expressing PcTrx-*h*4 (see 3.2.8.2). Wild-type and unstressed transgenic tobacco plants were also examined, to serve as controls.

3.2.12.1 Protein Derivatization

A 200 µg aliquot of each protein sample was combined with 4 volumes of 10 mM 2,4-dinitrophenylhydrazine (DNPH) in 2 M HCl. Samples were gently mixed at room temperature for 30 min. Proteins were precipitated with 5 volumes of ice-cold buffer P [20% TCA/80% acetone (v/v), 1 mM DTT] and collected by centrifugation at 15,000 *x g* for 15 min at 4^{o}C. Precipitated protein was washed with 1 mL of ice-cold acetone containing 1 mM DTT at 4^{o}C 3 times, for 5 min per wash and protein re-pelleted by centrifugation at 15,000 *x g* for 5 min. A final wash was performed with 1 mL of ice-cold 1:1 (v/v) ethanol:ethyl acetate. Proteins were re-solubilised in 45 µl of loading buffer [7 M urea, 2 M thiourea, CHAPS, 1% SDS, 20 mM DTT, trace of bromophenol blue] by incubation at 37^{o}C for 1 h.

3.2.12.2 Immunodetection of DNPH

DNPH derivatised samples were separated by electrophoresis (duplicate gels, 20 µl sample per well) and stained with Coomassie blue (see 2.7.2) or transferred to nitrocellulose membrane (see 2.7.3). The membrane was blocked overnight with 50 mL TBS, pH 7.6, containing 5% skim-milk powder (w/v), by incubation at 4^{o}C with gentle agitation. The carbonylated proteins were immunodetected using a mouse anti-DNP antibody (Sigma). Primary antibody (20 µl) was added to the blocking solution and membrane incubation continued for 22 h. Next, the membrane was washed in TBS for 10 min and then 3 times for 20 min, prior to incubation with secondary antibody, anti-mouse alkaline phosphatase conjugated (Sigma) [1:10,000 in TBS] for 2 h at room temperature. The membrane was again washed, 4 times in TBS for 15 min per wash. Antibody was detected with NBT/BCIP substrate (Sigma) as described in 3.2.9.1.

3.2.12.3 OxyBlot^{TM} Protein Oxidation Detection Kit

Proteins were extracted as recommended by the kit manufacturer (Chemicon, USA). Protein derivatization and immunodetection was performed according to the manufacturer's instructions (Chemicon, USA).

3.2.13 Detection of Hydrogen Peroxide in Tobacco Leaves

Hydrogen peroxide was detected *in situ* as described by Wang et al. (2006). Briefly, the fourth youngest leaf of 3-month old tobacco plants was harvested. Leafstalks were immediately placed in 0.1% 3,3-Diaminobenzidine (DAB), pH 3.8 (Sigma) and incubated at room temperature, in the dark, for 2 h to allow stain uptake. Leaves were irradiated with 1.2 Wm^{-2} of UVB (λ302 nm) for 2 h. Chlorophyll was cleared by boiling leaves in 95% ethanol.

3.2.14 Detection of Superoxide in Tobacco Leaves

$O_2^{\cdot -}$ was detected *in situ* as described by Doke and Ohashi (1988) with some modifications, Briefly, the fourth youngest leaf of 3-month old tobacco plants was harvested. Leaves were irradiated with 1.2 Wm^{-2} of UVB (λ302 nm) for 2 h. Following vacuum infiltration of 0.05 M sodium phosphate, pH7.5 containing 0.1% nitroblue tetrazolium (NBT), the leaves were incubated at room temperature for 20 min under white light. The reaction was stopped and chlorophyll was cleared from the leaves by boiling in 95% ethanol.

3.2.15 Protein Unfolding Assessment: Tunicamycin Treatment

Large, healthy leaves of the same approximate age, on 2-month-old, soil grown, tobacco were treated with 10 µl drops of tunicamycin at concentrations of 0, 50 and 100 µg μl^{-1}. Treated leaves were observed for the development of necrosis.

3.2.16 N-linked Glycosylation Assessment: Peptide-N-glycosidase F (PNGase F) Treatment of Thioredoxin-*h*4

Extracted protein samples (see 3.2.8.3) derived from transgenic tobacco over-expressing PcTrx-*h*4 were diluted with 20 mM ammonium bicarbonate (pH 8.0) to obtain 50 µg of protein in exactly 50 µl. To each protein sample, 5 µl of 0.2% SDS containing 100 mM 2-mercaptoethanol was added. Samples were incubated in boiling water for 10 min then cooled on ice before addition of 5 µl of 15% TritonX. Samples were well mixed gently by hand (inversion) prior to the addition of 10 µl PNGase F enzyme (Sigma, proteomic grade), which was prepared according to manufacturer's instructions (Sigma). Samples were mixed by inversion and incubated at 37^{o}C for 30 min, 1 h or 2 h, depending upon the experimental design being tested. Finally, samples were placed in boiling water for 5 min, ready for separation by electrophoresis and Western analysis (see 3.2.9.3). Control samples were treated in the same manner with the exception that no PNGase F enzyme was added.

3.3 Results

3.3.1 Transgenic Tobacco Plants with Altered Levels of Thioredoxin-*h*4 Expression

Several lines of transgenic tobacco over-expressed *P. coerulescens* thioredoxin-*h*4 (*PcTrx-h4*). Also, a transgenic tobacco line was engineered to silence expression of the endogenous *N. tabacum* thioredoxin-*h*4 (*NtTrx-h4*).

3.3.1.1 Identification of Homozygous Transgenic Nicotiana tabacum cv Xanthi

The zygocity status of transgenic tobacco expressing the *PcTrx-h4* gene in sense or antisense was examined. Seed (T_2) collected from 3 to 5 individual progeny plants of the original lines was grown on solidified MS media containing kanamycin. Since the kanamycin resistance gene was also included in the insertion cassette, kanamycin resistance should be linked to integration of *PcTrx-h4* into the plant genome. Hence, the ability of the transgenic plants to grow in the presence of kanamycin can be used to track inheritance of the *PcTrx-h4* transgene. Furthermore, by employing Gregor Mendel's 'Law of Segregation', it was possible to identify the transgenic tobacco lines homozygous for *PcTrx-h4*.

The number of germinated seeds that were able, or unable, to continue growth for at least 3 weeks in the presence of 150 mg mL^{-1} kanamycin was determined. Four homozygous lines identified, 2 lines over-expressing *PcTrx-h4* and 2 knock-down lines, are shown in Table 3-1. The resulting Mendelian segregation ratios of 'seed germination followed by seedling development' against 'seed germination only', revealing lines homozygous for the transgene, is also included in Table 3-1. Seeds that did not germinate were considered non-viable because despite the presence of kanamycin, all viable seeds should be able to germinate by utilizing their seed energy reserves. A ratio of $_{\text{seedling devemopment}}3{:}1_{\text{no seedling development}}$ indicated that the parent plant was heterozygous for the transgene. When a parent plant is homozygous for the transgene, it is expected that all progeny can grow in the presence of kanamycin (unless affected by an unrelated phenomenon), as all would inherit a copy of the kanamycin resistance gene. The 'seedling development' against 'no seedling development' ratios displayed in Table 3-1 are all greater than 3:1, with the lowest being 38:1, and clearly indicate that these transgenic tobacco lines are homozygous for the transgene. Seed from the homozygous lines identified were used for subsequent experiments and following generations (seed) were derived from self-fertilized individuals, all of which should also be homozygous for the transgene.

Table 3-1: **Transgenic tobacco lines identified as homozygous for sense (PcTrx-*h*4 over-expression) or antisense (NtTrx-*h*4 knock-down) transgenes.** Seeds were germinated on solidified MS media containing kanamycin and seedling growth was observed for 3 weeks. The Mendelian Segregation Ratio of 'seed germination and seedling development' against 'seed germination but no seedling development' was used to identify homozygous lines.

Plant Line	Plate Replicate	Growth	No Growth	Ratio
Sense (OE 1)	a	35	2	**55:1**
	b	37	-	
	c	36	-	
	Average	36	0.66	
Sense (OE 2)	a	34	-	**109:1**
	b	37	-	
	c	37	1	
	Average	36	0.33	
Antisense (KO 1)	a	37	-	**38:1**
	b	39	2	
	c	Fungal Contamination		
	Average	38	1	
Antisense (KO 2)	a	36	1	**111:1**
	b	37	-	
	c	37	-	
	Average	36.67	0.33	

3.3.1.2 Altered Thioredoxin-h4 Transcript and Protein Expression in Transgenic Nicotiana tabacum cv Xanthi

Epigenetic gene silencing is frequently observed in transgenic plants, whereby transgenes become silenced in subsequent generations (Fagard and Vaucheret, 2000). Therefore, to confirm that the homozygous transgenic tobacco lines, to be used in subsequent experiments, were over-expressing or not expressing thioredoxin-*h*4, Northern and Western analyses were performed. As expected, transcript of the introduced transgene *PcTrx-h4* was detected in all transgenic lines but was absent in the wild-type tobacco (Figure 3.1A). No endogenous *NtTrx-h4* transcript was detected in the antisense knockout transgenic tobacco lines (Figure 3.1B). Secondly, Western analysis was performed on the same transgenic tobacco lines using an antibody specific to PcTrx-*h*4. PcTrx-*h*4 was detected in the transgenic tobacco lines expressing the sense *PcTrx-h4* transgene (Figure 3.2). Therefore, it was confirmed that these two tobacco lines were over-expressing thioredoxin-*h*4 protein. Figure 3.3 demonstrates specificity of the anti-PcTrx-*h*4 antibody, using the highly similar barley cytosolic thioredoxin proteins (described in Chapter 4). The antibody was able to discriminate between the four barley thioredoxins-*h* and bound specifically to subclass 4 (Figure 3.3).

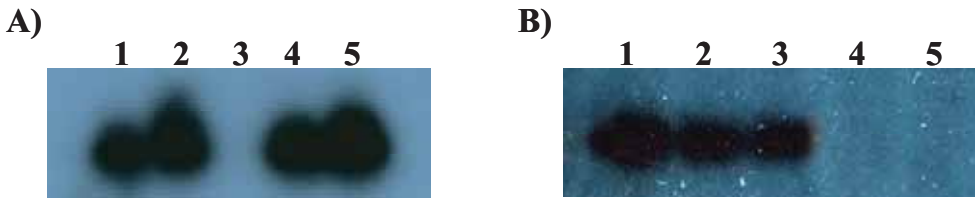

Figure 3.1: **Northern analysis shows altered levels of *thioredoxin-h4* expression in transgenic tobacco.** A) Autoradiograph showing expression of *P. coerulescens thioredoxin-h4* transgene in transgenic (1, 2, 4, 5) but not wild-type (3) tobacco lines. B) Autoradiograph showing expression of endogenous *N. tabacum thioredoxin-h4* in wild-type (3) and sense transgenic lines (1, 2) but none in antisense transgenic lines (4, 5).

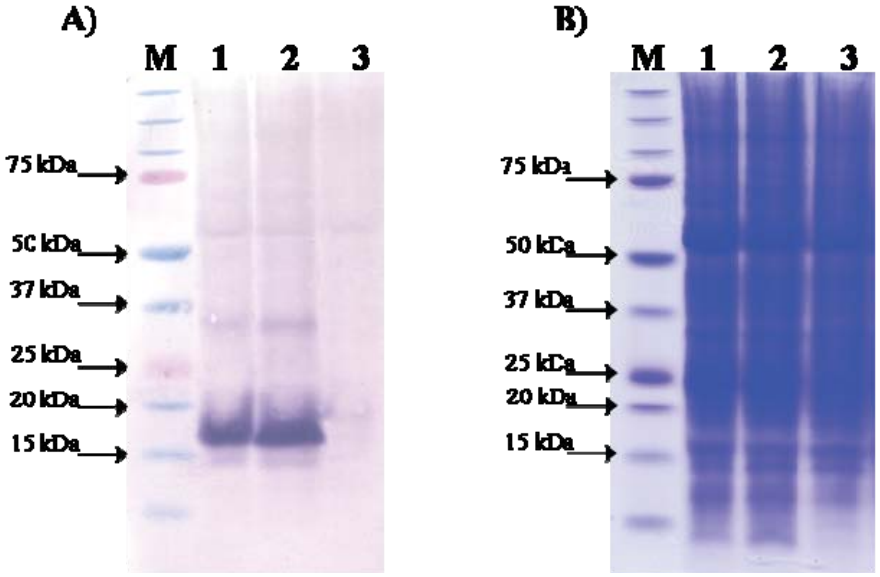

Figure 3.2: **Western analysis detects *Phalaris coerulescens* thioredoxin-*h*4 protein in transgenic tobacco lines constitutively expressing *PcTrx-h4*.** Protein was extracted from tobacco leaves, separated by SDS-PAGE and probed with an antibody specific to PcTrx-*h*4. A) Nitrocellulose membrane showing detection of anti-PcTrx-*h*4 antibody at the predicted size/location of PcTrx-*h*4, in transgenic tobacco expressing the sense *PcTrx-h4* transgene (1,2) and wild-type tobacco (3). B) Coomassie stained denaturing polyacrylamide gel showing total protein loaded per sample. Protein size was inferred from alignment with BioRad Dual Colour Marker (M).

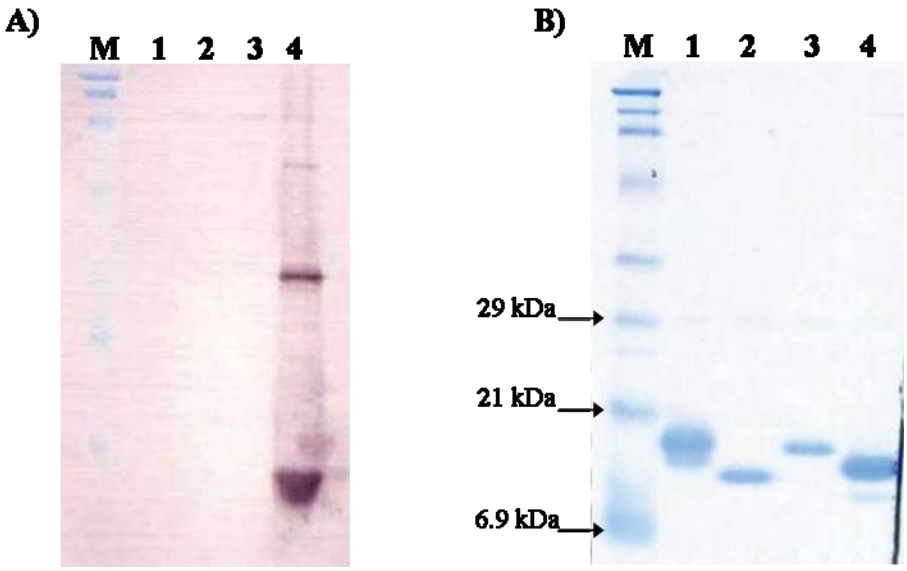

Figure 3.3: **Western analysis shows anti-PcTrx-*h*4 antibody with binding specificity for cytosolic thioredoxin, sub-class 4 protein.** Thioredoxin proteins were expressed in *E.coli* and purified as described in Chapter 4. A) Nitrocellulose membrane showing thioredoxin-*h*4 specific binding of polyclonal antibody raised against PcTrx-*h*4 homolog in rabbit. B) Coomassie stained denaturing polyacrylamide gel showing total protein loaded per sample. Lane 1: recombinant HvTrx-*h*1; lane 2: recombinant HvTrx-*h*2; lane 3: recombinant HvTrx-*h*3; lane 4: recombinant HvTrx-*h*4. Protein sizes were inferred from alignment with BioRad Broad Range Marker (M).

3.3.1.3 Phenotype of Transgenic Tobacco Plants and T2 Pollen

The transgenic tobacco plants were examined throughout development for differences in phenotype (visible), compared to each other and wild-type tobacco plants. On close inspection, no obvious phenotypic differences in transgenic tobacco plants were seen when the plants were grown in a favourable environmental condition. Transgenic tobacco plants were grown in soil and on solidified MS media, in glasshouse, growth room and growth cabinet conditions and at no stage were phenotypic differences observed.

Thioredoxin-h4 is highly conserved across angiosperms and consequently, one hypothesis is that it may be involved in a key process in reproductive tissues (Juttner, 2003) (discussed further in Chapter 5). Furthermore, quantitative polymerase chain reaction data showed barley thioredoxin-*h*4 transcript expression was relatively high in anther tissues (Chapter 5). Therefore, the effect on anthers of silencing *thioredoxin-h4* was of interest. It was considered that the absence of thioredoxin-*h*4 may result in developmental changes during pollen biogenesis. Accordingly, the morphology of pollen in the *thioredoxin-h*4 knock-down transgenic tobacco lines was examined under magnification. The pollen morphology was estimated to be approximately 95% normal in appearance. The majority of the pollen was large, plump and taut. Approximately 5% were shrivelled, smaller and stained a lighter shade of pink, which indicates they were likely to be non-viable. From these observations, correlated with that for the wild-type pollen which was also examined, it was concluded that the absence of thioredoxin-*h*4 did not impact the pollen biogenesis in tobacco. Seed germination was also considered to be the same for all tobacco lines, both transgenic and wild-type, based solely on observations made during preparations for other experiments.

3.3.2 Stress Tolerance in Transgenic Tobacco

As highlighted in Chapter 1, plant cytosolic thioredoxins have previously been linked with oxidative stress protection roles and most recently, abiotic stress protection. Accordingly, it was hypothesised that altering thioredoxin-*h*4 protein levels in tobacco might alter the plants ability to respond to, and cope with, environmental stresses. The *PcTrx-h4* sense and anti-sense transgenic tobacco plants generated (section 3.3.1) were subjected to a range of oxidative stress inducing events. The stress-response of these plants was then examined to determine whether over-expression, or reduced/no expression, of thioredoxin-*h*4 affected the stress tolerance capacity of the tobacco.

For all stress challenges, dose-response experiments were conducted to determine the amount of stress required until an altered phenotype in wild-type tobacco became apparent. The plants were then assessed for their ability to recover and continue to grow once the stress had been removed. To accurately assess the effect of altering thioredoxin-*h*4 expression in relation to oxidative stress, it was important to ensure that a stress response was being assessed and not a death response. For the experiments described in this chapter, a 'stress response' was deemed to have occurred only if the plant was able to recover from the stress event and not if the stress treatment directly resulted in eventual plant death. Following stress treatments, tobacco responses were monitored, compared and contrasted against that of wild-type tobacco, with the aim being to elucidate the role of thioredoxin-*h*4 in stress responses.

3.3.2.1 Water Deficit Stress

In southern Australia, drought is a common cause of plant oxidative stress. Different types of drought exist, primarily dictated by latitude and a combination of climatic factors including, water deficit, heat stress, vapour pressure deficit, salinity and soil-type (Fischer and Turner, 1978; Izanloo et al., 2008). In Australia, water deficit is one of the major drought components (Izanloo et al., 2008). With this in mind, the water deficit tolerance of transgenic tobacco over-expressing *PcTrx-h4* was assessed. The plants (6 per line) were grown in pots and the rate of soil drying was controlled as described in 3.2.10.3. Briefly, after watering the soil to saturation the volumetric water content (VWC) was monitored with a soil moisture meter and water was added when required, in order to achieve a uniform drying rate (Table 3-2, Figure 3.4). No differences in the rate of water use by plants, as determined by speed of soil drying, were apparent between wild-type and transgenic tobacco lines (Table 3-2, Figure 3.4). After 19 days the soil ceased to dry further, within detectable limits by the probe, and the soil VWC remained constant up to 32 days of water withholding. No differences in tolerance to water deficit were evident between transgenic and wild-type plants. All plants wilted at the same rate and to the same extent as determined by visual inspection (Figure 3.5). This conclusion was supported by calculating the relative water content (RWC) of leaves from each line (Figure 3.6) as described in 3.2.10.3. After 32 days of water withholding, 3 of the plants per line were rewatered. All lines recovered at the same rate upon rewatering, as determined visually. The remaining 3 plants per line, which were not rewatered, all reached death at approximately the same time, with no differences in time-to-death distinguishable between the wild-type and transgenic plants.

Table 3-2: **Percentage of volumetric water content (VWC) in soil during water deficit stress.** The soil VWC was measured for 6 plants growing in individual pots for 4 tobacco lines over-expressing *PcTrx-h4* (OE1-4) and wild-type tobacco (WT). The average value per line is displayed. Water was added to pots drying at a faster rate than others, in order to attain a uniform decrease in soil VWC.

# Days After Water Cessation	Volumetric Water Content in Soil (%)				
	WT	OE1	OE2	OE3	OE4
1	16.00	12.17	6.67	17.33	18.00
2	13.33	10.83	6.00	14.50	14.33
5	8.00	8.33	4.67	10.67	8.83
6	7.17	6.83	3.67	8.00	6.17
8	5.33	5.00	3.83	7.50	5.67
9	4.17	4.33	3.17	5.33	4.00
10	3.67	4.00	3.17	4.67	4.00
12	3.17	3.17	3.00	4.00	3.33
13	3.00	3.33	2.83	3.50	3.17
15	3.00	3.00	2.67	3.17	3.00
16	3.00	3.00	3.00	3.00	3.00
19	2.67	2.83	2.33	2.83	2.67

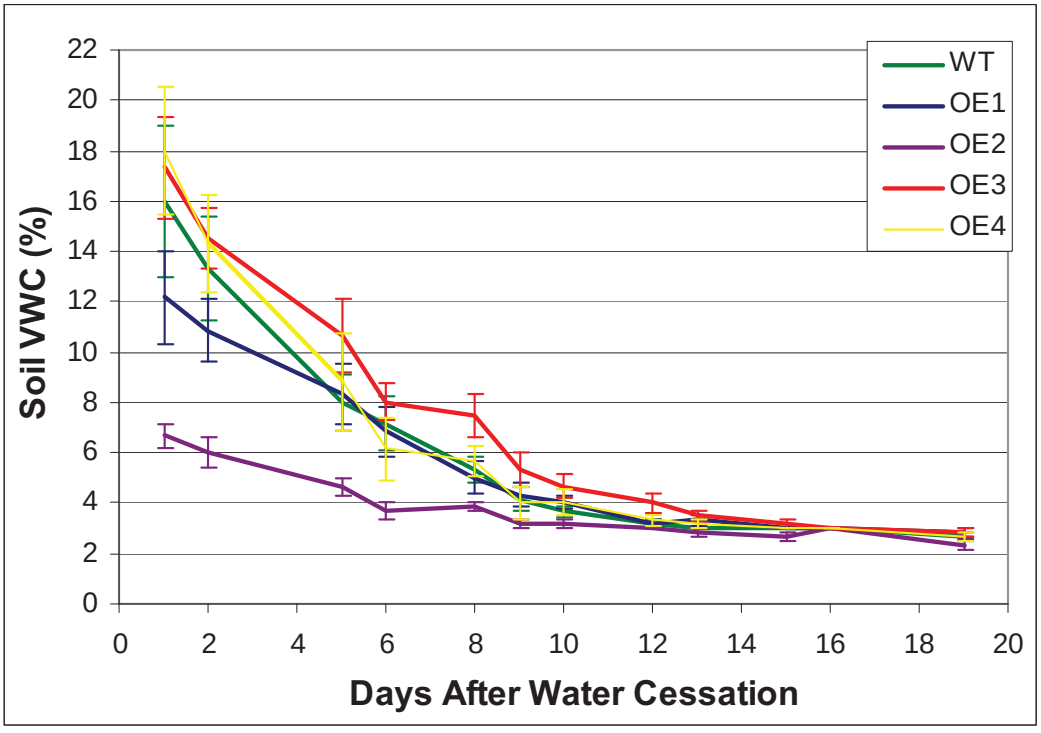

Figure 3.4: **Graphical representation of Table 3.2 - volumetric water content (VWC) in soil during water deficit stress**. VWC (%) and associated standard error were derived from 6 pots per tobacco line, either over-expressing PcTrx-*h*4 (OE1- 4) or wild-type (WT).

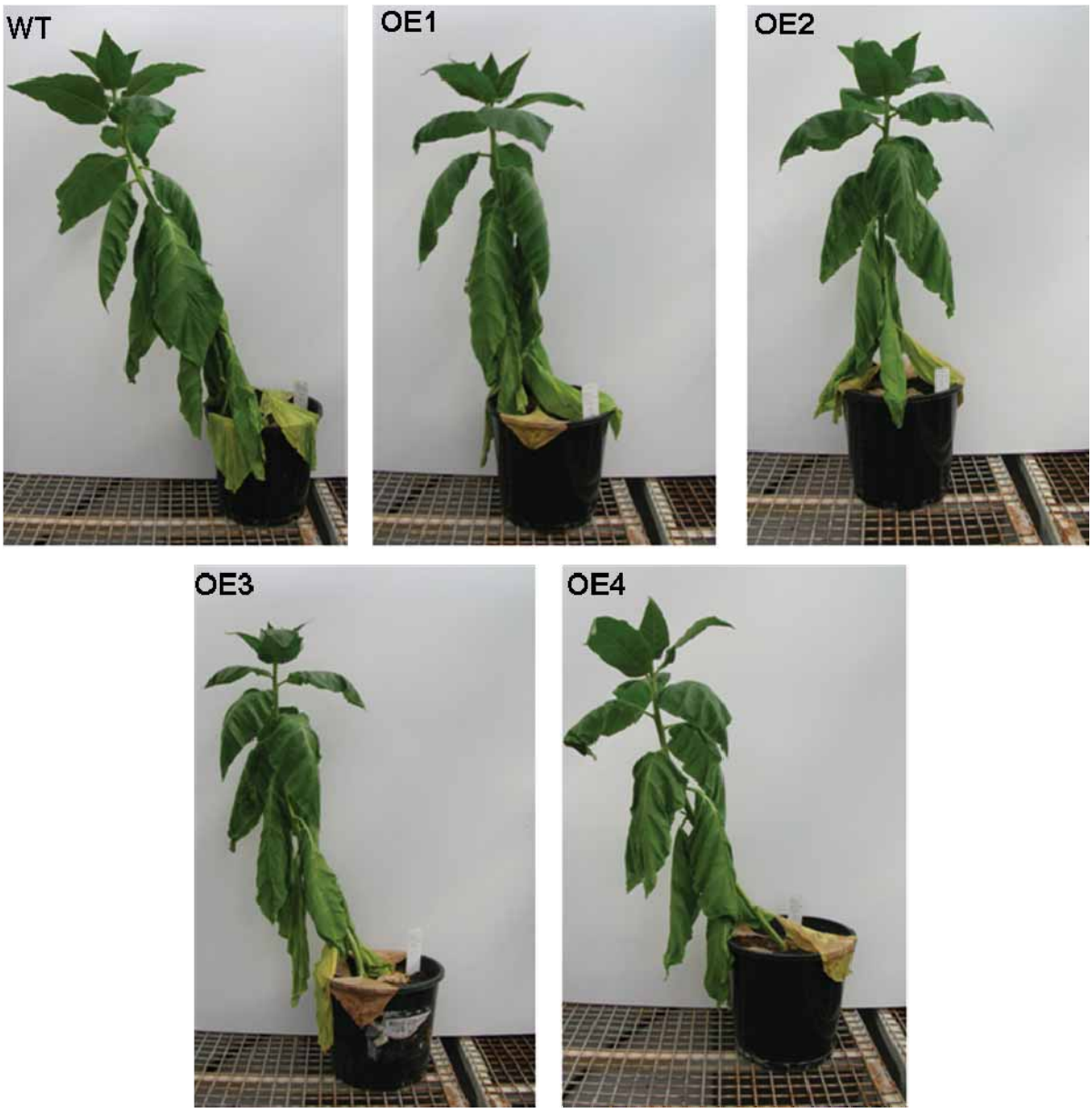

Figure 3.5: **Over-expression of *PcTrx-h4* does not confer tolerance to water deficit stress in tobacco.** Wild-type (WT) and 4 discrete transgenic tobacco lines over-expressing *PcTrx-h4* (OE1-4) were subjected to controlled water deficit stress. Six 2-month-old tobacco plants per line were stressed and photographs were taken 32 days after cessation of watering. One representative plant per line is shown.

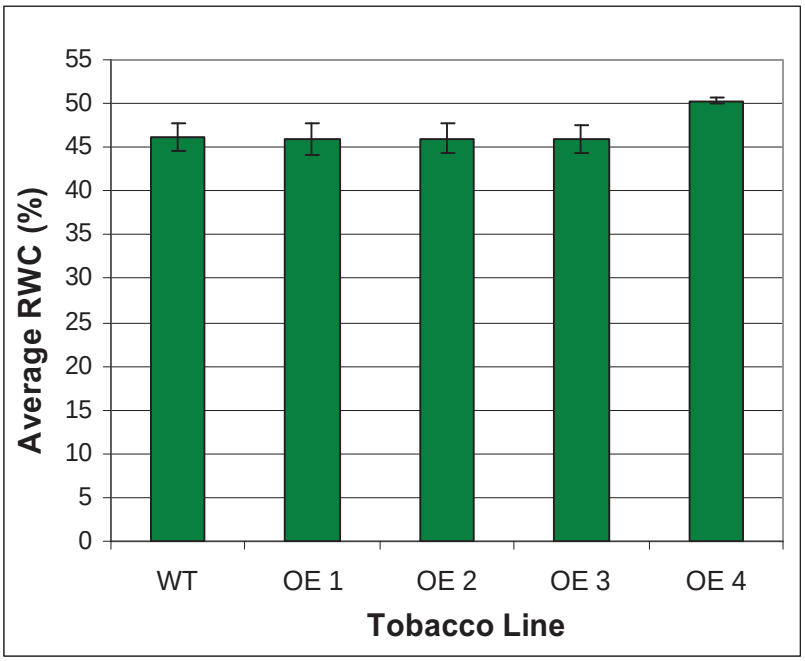

Figure 3.6: **Over-expression of *PcTrx-h4* does not confer tolerance to water deficit stress in tobacco.** For each tobacco line the relative water content (RWC) of leaves, was calculated after 32 days of withholding water. RWC (%) and associated standard error were derived from six 2-month-old tobacco plants, per line.

3.3.2.2 Heat Stress

Another common component of drought stress in Australia is heat (Passioura, 1996). Large rises in air temperature often due to hot dry winds in southern Australia, means that a plants physiological and biochemical response to heat is essential for plant protection and survival of crops (Passioura, 1996). To determine whether thioredoxin-*h*4 played a role in a plants response or tolerance to heat, the wild-type and transgenic tobacco plants were subjected to 42^{o}C for 24 h. The NtTrx-*h*4 knock-down transgenic tobacco (*not shown*) exhibited the same phenotype as the wild-type tobacco (Figure 3.7), having wilted leaves. In stark contrast, the tobacco lines over-expressing PcTrx-*h*4 were only slightly wilted (Figure 3.7), indicating that the presence of PcTrx-*h*4 in abnormally high levels imparted tolerance for heat, in these tobacco plants.

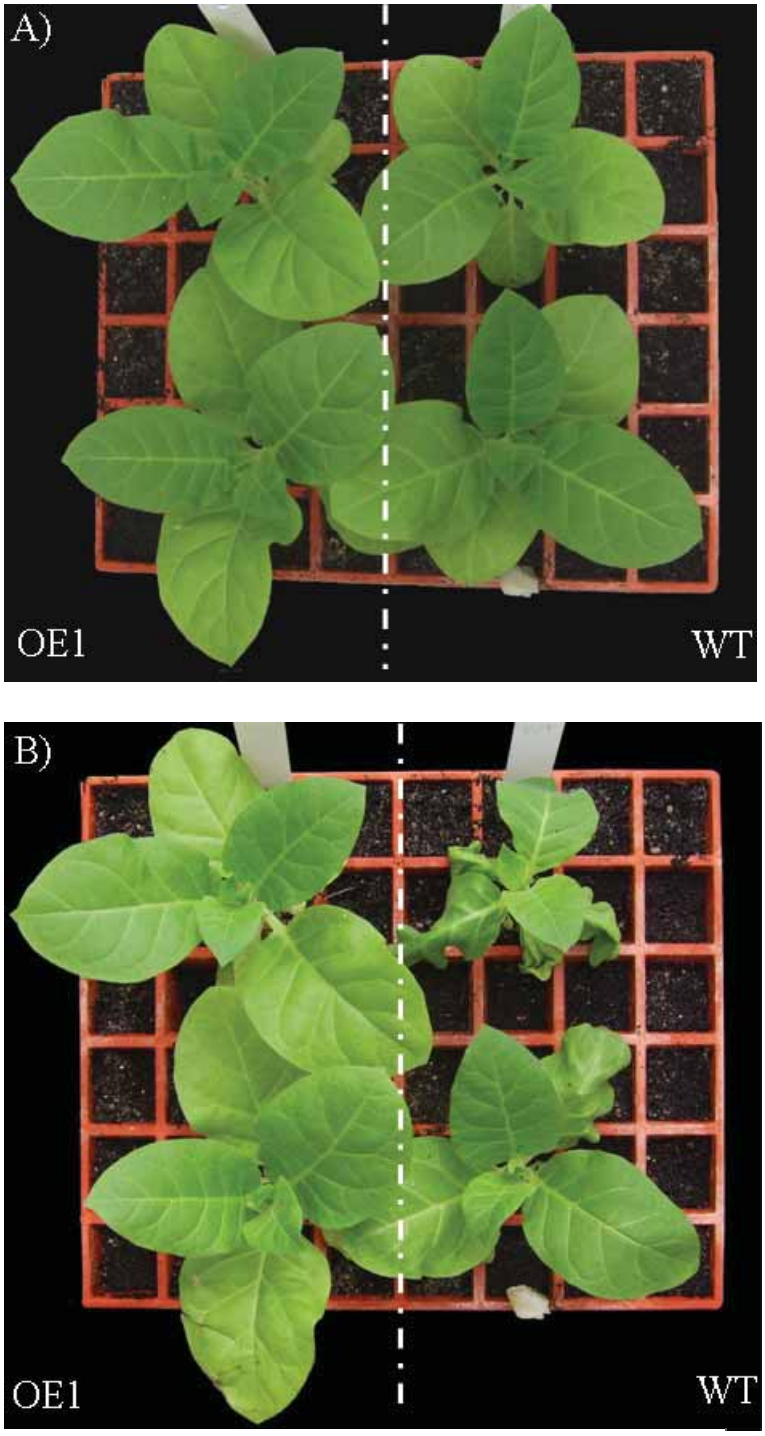

Figure 3.7: **Tobacco over-expressing *PcTrx-h4* (OE1) displays increased tolerance to heat stress compared with wild-type tobacco (WT).** Seven-week-old tobacco plants were placed at 42^{o}C for 24 h. A) Tobacco plants before heat stress. B) Tobacco plants immediately after heat stress.

3.3.2.3 Ultraviolet Light B Irradiation

A common environmental stress that field grown plants must cope with, particularly in Australia, is UVB (Miller et al., 2008; Ulm and Nagy, 2005). To see if thioredoxin-*h*4 plays a role in a plants response or tolerance to UVB, the wild-type and transgenic tobacco plants were grown in several mediums and subjected to a range of UVB (λ302nm) doses, as dictated by the corresponding dose-curve results (*not shown*). Approximately ninety 6-week-old seedlings (grown on MS media) were irradiated with 0.6 Wm^{-2} of UVB for 24 h. Seedlings grown in shallow plates or trays of soil for 3 weeks were exposed to 0.6 Wm^{-2} of UVB for 40 h. Potted 6-week-old tobacco plants were exposed to 0.8 Wm^{-2} of UVB for 24 and 48 h. For each experiment and each tobacco line, multiple unstressed plants grown in the corresponding medium served as controls. This allowed assessment of growth retardation resulting from UBV stress.

Tobacco plants were initially grown on media so that kanamycin could be included to ensure transgenic plants were being examined. However, it was decided that soil grown plants would allow assessment of the UVB response of larger plants and also, the inclusion of kanamycin was a redundant control as the lines had been identified as homozygous for the transgene. Interestingly, it was clear that the tobacco lines grew faster when in soil compared to when on solid MS media. Also, the soil grown tobacco seedlings were much hardier and able to tolerate more UVB irradiation. Therefore, they required greater doses of UVB irradiation before a stress-response could be visually detected. The increased robustness of the soil grown tobacco may be because a small amount of UV can penetrate into the glasshouse, where the soil grown plants were housed, whilst the media-grown plants had no prior UV exposure.

Tobacco lines over-expressing *PcTrx-h4* displayed increased tolerance to UVB irradiation, whether grown on solidified MS media, in shallow plates of soil or individual pots (Figure 3.8). The stress symptoms that were visible on wild-type plants, such as leaf yellowing, chlorosis, necrosis and rolling, were not observed for the constitutively expressed PcTrx-h4 plants (Figure 3.8). Instead, the leaves remained taut, full in shape and green (Figure 3.8). In addition, the wild-type plants ceased to grow for a period of time, depending upon the stress severity, and recovered slowly whilst the tobacco over-expressing *PcTrx-h4* continued to grow, faster than the wild-type plants, although slower than the corresponding unstressed transgenic control plants. An exception to this observation was following treatment of 6-week-old tobacco grown in pots of soil which were exposed to 0.8 Wm^{-2} of UVB for 48 h

(Figure 3.8D). This length of exposure induced severe stress and was too long as the plants took an extremely long time to recover (several weeks) and continue growing. In fact, for both wild-type and transgenic plants, only new leaves grew from the meristems whilst the stressed leaves died and fell off the plant. Therefore, we consider observations from this experiment to be indicative of a death response rather than a stress response (Figure 3.8D).

Regardless of the growth or UVB stress conditions used, the *NtTrx-h4* silenced transgenic tobacco behaved akin to the wild-type tobacco (*not shown*). This indicates that the absence of NtTrx-*h*4 did not result in the plants becoming hypersensitive to UVB.

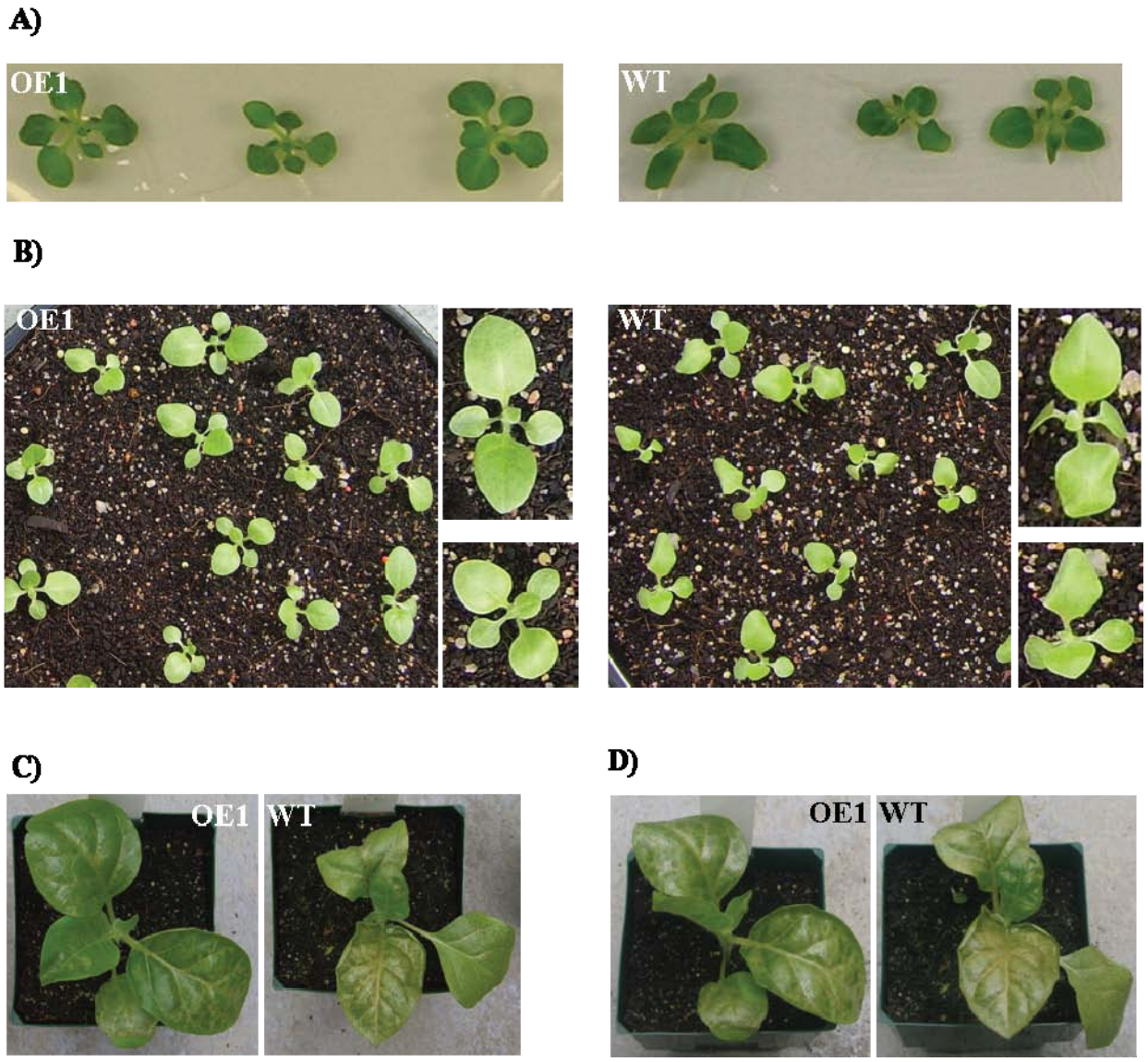

Figure 3.8: **Tobacco over-expressing *PcTrx-h4* (OE1) displays increased tolerance to UVB (λ 302 nm) compared with wild-type tobacco (WT).** A) 6-week-old tobacco seedlings grown on MS agar plates were exposed to 0.6 Wm^{-2} of UVB for 24 h. B) 3-week-old tobacco plants grown in plates of soil were exposed to 0.6 Wm^{-2} of UVB for 40 h. C) and D) 6-week-old tobacco plants grown in pots of soil were exposed to 0.8 Wm^{-2} of UVB for 48 h. Photographs shown for A), B) and C) were taken immediately after UVB irradiation. Photographs shown for D) were taken after 16 h of recovery.

3.3.2.3.1 Biochemical Confirmation of Tobacco Stress Phenotypes Following UVB Irradiation and Heat Stress

The comparative stress-response phenotypes observed between tobacco lines indicates *PcTrx-h4* over-expression confers increased tolerance to UVB and heat, in tobacco. To further investigate this result quantification of the degree of plant stress caused by UVB and heat, as well as discovery of the forms of protein damage, was endeavoured to assess the oxidative stress response(s) at a biochemical level. Unstressed, UVB irradiated and heat stressed samples were harvested from wild-type and transgenic tobacco over-expressing *PcTrx-h4*, from several individual experiments. These samples were used in three different assays, described below, focussed upon malondialdehyde (MDA) production, fatty acid oxidation and protein carbonylation.

Reactive oxygen species cause peroxidation of polyunsaturated fatty acids which produces malondialdehyde (MDA) (Hartley et al., 1999). MDA is a commonly measured end product of lipid peroxidation and a thiobarbituric acid (TBA)-based assay is widely accepted and has been extensively used in plants, including tobacco (Roxas et al., 2000; Shulaev and Oliver, 2006). Reaction of MDA with TBA can be measured spectrophotometrically at 532 nm and the concentration of MDA calculated using its extinction coefficient of 155 $mM^{-1}cm^{-1}$ (Dhindsa et al., 1981; Heath and Packer, 1968; Hideg et al., 2003). Another sensitive assay to quantify oxidative damage is the ferrous oxidation-xylenol orange (FOX) assay which quantifies lipid hydroperoxides in plant extracts. The FOX assay provides an indication of initial fatty acid oxidation, which is an early membrane-associated stress event in plant tissue (DeLong et al., 2002). The MDA (TBA-based) and FOX (version II) assays were employed to quantify and compare oxidative damage in the tobacco leaf samples. However, despite much effort with both of these assays, the results were arbitrary and not reproducible. Consequently conclusions could not be made.

Protein carbonylation is an irreversible oxidative process where carbonyl groups are introduced into proteins, which inhibits or alters their activity and increases their susceptibility to proteolytic attack (Johansson et al., 2004). It was hypothesised that PcTrx-*h*4 was able to protect target proteins from carbonylation and consequently, increased the stress tolerance of the plant. Protein carbonylation is a widely used marker of protein oxidation and the carbonyl groups can be detected immunologically (Johansson et al., 2004; Levin, 1990; Shulaev and Oliver, 2006). To achieve this, the carbonyl groups in the protein side chains are derivatised to 2,4-dinitrophenylhydrazone (DNP) by reaction with 2,4-dinitrophenylhydrazine

(DNPH). The DNP-derivatised protein samples are separated by electrophoresis and subjected to Western analysis using primary antibodies, specific to the DNP moieties (Johansson et al., 2004; Levine et al., 1994). This experiment was performed many times with varying protein extraction and immunoblot conditions, as dictated by previous studies (Keller et al., 1993; Levin, 1990; Levine et al., 1994; Reznick, 1994; Wang et al., 2006). It was found that the method used for protein extraction and resolubilisation, following DNPH treatment, affected protein separation and resolution. The outcome of the most successful method of protein extraction and separation is shown in Figure 3.9A. Despite employing Bradford assays to quantify protein concentrations, protein loading was uneven (Figure 3.9A). Further complication appeared to be related to the primary antibody (anti-DNP, Sigma), as demonstrated by the lack of specificity (Figure 3.9B) and extended development times in excess of 12 min. In an attempt to resolve these issues, a commonly used kit (OxyBlot™ Protein Oxidation Detection Kit, Chemicon, USA) was employed for the carbonylation analysis, which contained a ready-made positive control and primary antibody. Again, a comparative carbonylation analysis of unstressed against UV and Heat stressed, wild-type and transgenic (*PcTrx-h4* over-expressed) tobacco, was attempted. For these experiments, again DNPH treatment seemed to interfere with the protein separation, as indicated by the lack of resolution of discrete protein bands for these treated samples. Consequently, antibody binding streaks down each gel well were also seen, including for the positive control. However, the antibody detection of the positive control was successful, indicating the immunodetection aspect of the experiment was correct (*data not shown*). Laboratory-cast as well as pre-cast (Invitrogen) polyacrylamide gels (4-15% bis-tris and glycine-tris based) all yielded the same result. Thus, unfortunately, no conclusions could be made regarding the carbonylation status of the control and oxidatively stressed tobacco samples.

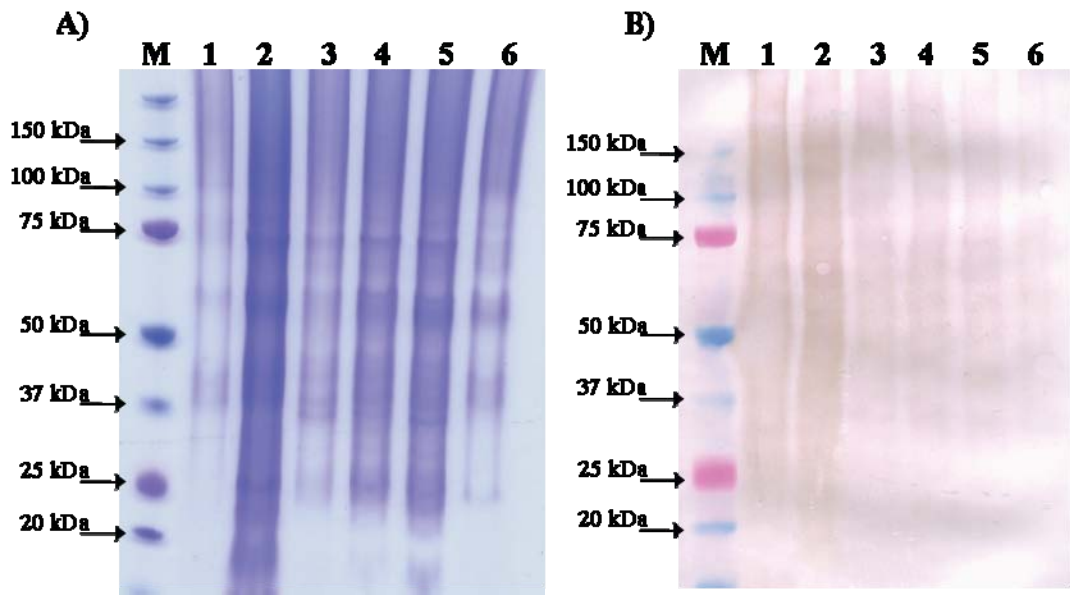

Figure 3.9: **Western analysis to determine extent of protein damage in the form of carbonylation.** Protein was extracted from UVB irradiated (1,2), heat stressed (3,4) and unstressed (5,6) tobacco leaves, derived from wild-type (1,3,5) and transgenic tobacco over-expressing *PcTrx-h4* (2,4,6). Protein extracts were derivatised with 10 mM 2,4-dinitrophenylhydrazine, separated by SDS-PAGE and probed with an antibody specific to 2,4-dinitrophenylhydrazone (DNP). A) Coomassie stained denaturing polyacrylamide gel shows amount, quality and resolution of protein. B) Nitrocellulose membrane shows (lack of) detection of anti-DNP antibody. Protein sizes can be inferred from alignment with BioRad Dual Colour Marker (M).

3.3.2.4 Fungal Challenge with Botrytis Cinerea

Abiotic stresses, such as excessive UVB irradiation and heat, generate reactive oxygen species (ROS) which can serve as signalling molecules but are also damaging to plant cells. Similarly, biotic stresses elicit a burst in ROS (Foyer and Noctor, 2009). Therefore, it was considered that if the transgenic tobacco over-expressing PcTrx-*h*4 had increased tolerance to UVB and heat, it may also be more tolerant to a biotic stress such as fungal infection. To test this hypothesis, the transgenic and control tobacco plants were challenged with the necrotrophic fungus *Botrytis cinerea*, courtesy of Ian Dry (CSIRO). When the *B. cinerea* was at its most active/optimum infection stage, 8-days old (*Dr Ian Dry, pers. comm.*), it was applied to the tobacco leaves. First it was established that the *B. cinerea* culture supplied was indeed able to infect the *N. tabacum* cv Xanthii (Figure 3.10). The experiment was performed 3 times using either the 3rd or the 4th newest leaf on each plant with 0.5 or 1 cm^2 plugs of potato dextrose agar (PDA) upon which a uniform culture of *B. cinerea* was present. After 3 days of infection, the plugs of culture were removed and the leaves assessed for degree of infection. Not only were untransformed control plants used but also control PDA-only plugs were applied to all plants to ensure any necrosis seen was not due to the agar. Not all leaves were always successfully infected but this result was independent to the tobacco plant line, PcTrx-*h*4 over-expressed or control. To assist with infection in subsequent experiments, some leaves were also mildly wounded to provide entry points for the necrotrophic fungus. All of these sites were successfully infected as determined by the area of necrosis that developed and expanded over time (Figure 3.10). Importantly, this necrosis did not develop to the same extent on wounded leaves that were treated with PDA only (Figure 3.10).

No differences in the ability nor the severity of *B. cinerea* infection were observed between transgenic and control tobacco plants. All lines appeared to be infected at the same rate and to the same extent (*data not shown*). Hence, it was concluded that over-expression of *PcTrx-h4* did not confer tolerance to *B. cinerea* infection. Also, absence of endogenous NtTrx-*h*4 did not result in faster or more extensive *B. cinerea* infection, meaning that these plants were not hypersensitive.

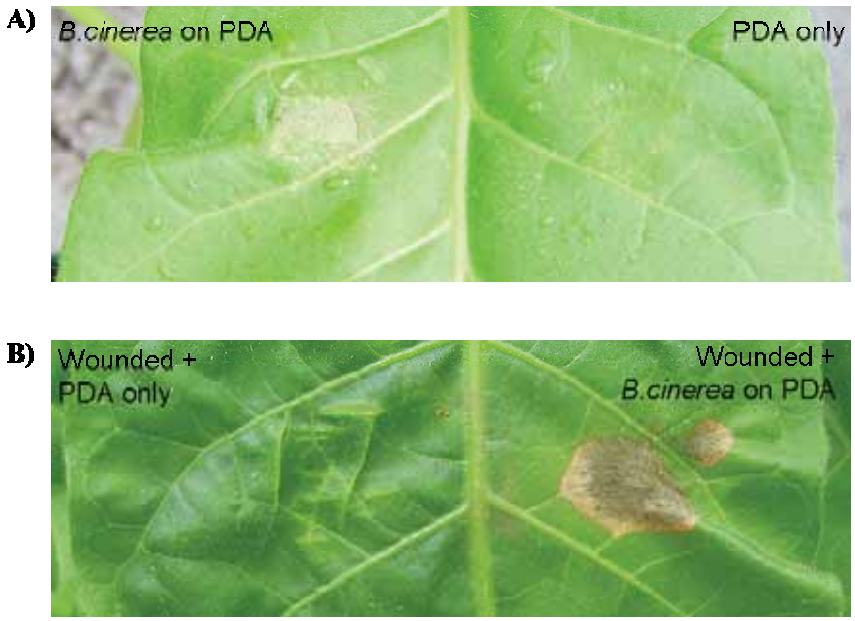

Figure 3.10: ***Botrytis cinerea*** **successfully infects tobacco, to the same extent in transgenic and control plants.** *B. cinerea* cultures were supplied on PDA and used to infected tobacco leaves. Plugs (0.5 and 1 cm^2) of 8-day-old cultures were applied to normal (A) and mildly wounded (B) tobacco leaves of the 3rd or 4th youngest full leaf. Photographs were taken 3 days after infection and are representative of the phenotype seen on both transgenic (*PcTrx-h4* over-expressed or *NtTrx-h4* knocked-down) and control tobacco plants.

3.1.1 Response of Transgenic Tobacco to Specific Reactive Oxygen Species (ROS)

It was questioned whether PcTrx-*h*4 was providing tolerance to UVB irradiation and heat exposure by minimising the effect of ROS, which are generated in large quantities by these oxidative stress inducing conditions (Hidema and Kumagai, 2006; Miller et al., 2008; Wahid et al., 2007). To answer this question, 3 different ROS-generating chemical compounds were topically applied to leaves, from untransformed and transgenic tobacco over-expressing *PcTrx-h4*, and the tolerances were compared. At least 3 leaves per plant, and 3 plants per line, were treated. Specifically, responses to hydrogen peroxide (H_2O_2), Rose Bengal diacetate (RBDA) and methyl viologen (MV), also known as paraquat, were investigated as each initially generates a different suite of ROS (Hartel et al., 1992; Shimizu et al., 2006).

An H_2O_2 dose-response experiment on wild-type control plants determined that a high concentration of H_2O_2 (1 to 1.5 M) was required before visible necrosis developed at the application site. Perhaps the requirement of such high H_2O_2 concentrations is related to the rapidly degrading nature of H_2O_2, which may result in a significantly lower concentration of H_2O_2 entering the plant tissue. However, no differences in the degree of H_2O_2 tolerance were observed when comparing treated leaves containing PcTrx-*h*4 over-expressed against the wild-type control (Figure 3.11).

Rose Bengal diacetate is a cell-permeable molecule capable of generating singlet oxygen, from triplet oxygen, when exposed to light. For initial experiments, RBDA was prepared in a background of 0.01% Tween-20. However, upon topical application to the tobacco leaves, a white powder crystallised and no leaf damage was observed. Hence, it was concluded that a 0.01% Tween-20 background solution for 0 – 1 mM RBDA was not appropriate as the RBDA did not fully dissolve and/or was precipitating. Instead, DMSO was successfully used as recommended by another manufacturer (Invitrogen) to address the precipitation issues. All leaves from each transgenic line responded to RBDA treatments in the same way and to the same extent as the wild-type control leaves. However, a small amount of leaf necrosis at the application sites of the DMSO control was also detected. At a 100 μM RBDA concentration, the area of necrosis was not distinguishable from that of the DMSO control (Figure 3.12). Consequently, if only a slight change in tolerance to RBDA was conferred by over-expression of *PcTrx-h4*, this would not have been detected.

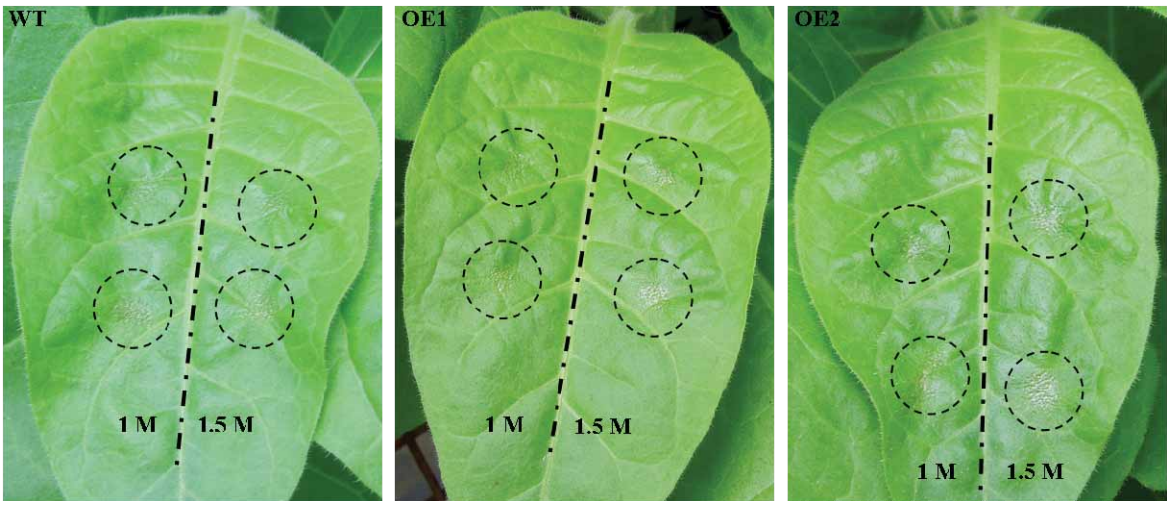

Figure 3.11: **Over-expression of *PcTrx-h4* does not alter response to H_2O_2.** Two discrete tobacco lines over-expressing *PcTrx-h4* (OE1-2) and wild-type tobacco (WT) are equally as tolerant to topical application of H_2O_2. Healthy leaves, approximately 12 cm in length, of the same age, attached to 2-month-old soil grown tobacco plants, were treated with 10 µl droplets of H_2O_2: Concentrations of 1 M left of main vein and 1.5 M right of main vein. Photographs were taken 24 hours after treatment.

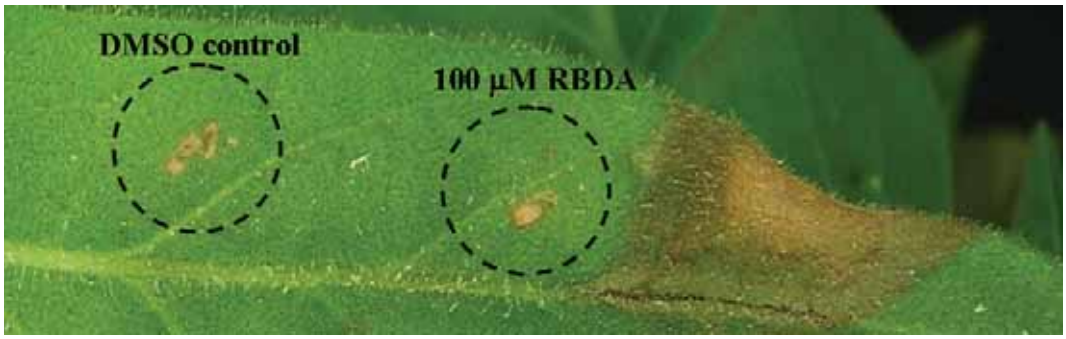

Figure 3.12: **DMSO induces leaf necrosis undistinguishable to that induced by 100 µM RBDA.** Healthy leaves, approximately 3.5 cm in length, attached to 2-month-old soil grown tobacco plants, were treated with 5 µl drops of RBDA. Areas of application for the DMSO and 100 µM RBDA are circled, left and right respectively. A RBDA concentration of 1 mM resulted in obvious leaf necrosis (not circled). No difference in response to RBDA treatment was observed, between wild-type and transgenic (*PcTrx-h4* over-expressed) tobacco plants. Photographs were taken 24 hours after treatment.

Methyl viologen is readily reduced to a stable but oxygen-sensitive mono-cation radical. It rapidly reacts with molecular oxygen, generating a superoxide radical and subsequently, hydrogen peroxide. The secondary reaction between these two species produces a hydroxyl radical (Morimyo, 1988). The enhancement of superoxide formation by MV means that the ROS profile is different to that elicited by RBDA and H_2O_2 alone. A dose-response experiment on wild-type control plants determined that 60 μM (in a background of 0.1% Tween-20) was a high enough MV concentration to result in leaf necrosis at the application site. As shown in Figure 3.13, the transgenic tobacco lines over-expressing PcTrx-*h*4 were more tolerant to MV treatment compared to the wild-type tobacco plants. The smaller, patchy necrotic lesions observed (Figure 3.13) did not develop further during the 7 day observation period.

In summary, PcTrx-*h*4 did not confer a detectable change in tolerance to H_2O_2 nor RBDA, but did increase tolerance to MV. Therefore, it was concluded that tolerance to ROS due to *PcTrx-h4* over-expression had a degree of specificity; only for the suite of ROS induced by MV.

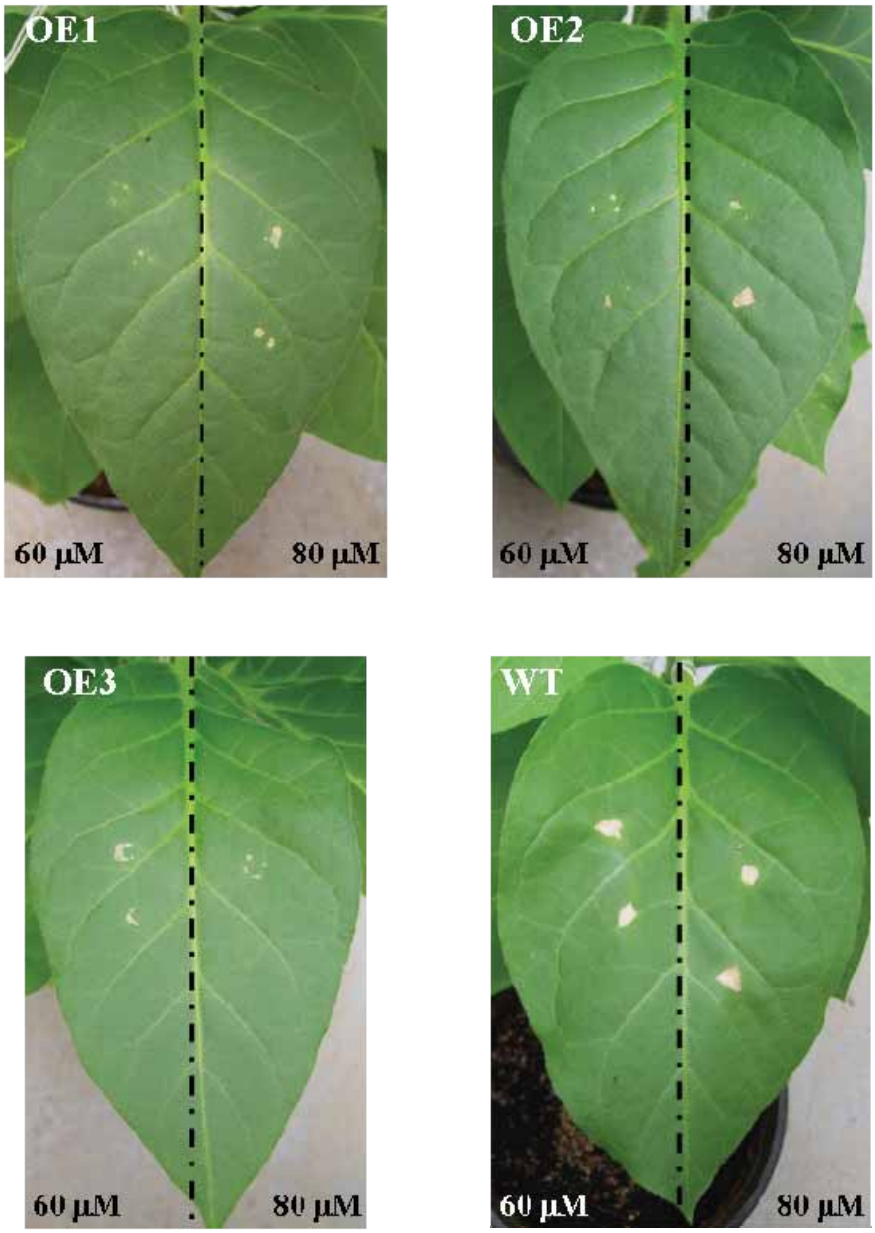

Figure 3.13: **Three discrete tobacco lines over-expressing *PcTrx-h4* (OE1-3) display increased tolerance to MV compared with wild-type tobacco (WT).** Methyl viologen droplets (10 µl) were applied to healthy leaves, approximately 15 cm in length, of the same age, attached to 2-month-old tobacco plants: Concentrations of 60 µM left of main vein and 80 µM right of main vein. Photographs were taken 48 hours after treatment

3.3.4 Accumulation of Reactive Oxygen Species in Transgenic Tobacco

Over-expression of *PcTrx-h4* resulted in increased tolerance to UVB, heat and MV. All 3 of these stresses generate the reactive oxygen species (ROS) superoxide (O_2^-) and H_2O_2, amongst other free radicals. Therefore, it was speculated that PcTrx-*h*4 may be participating in scavenging of ROS, either directly or indirectly. To investigate this theory, the accumulation of H_2O_2 and superoxide in tobacco leaves was investigated. Wild-type and transgenic tobacco leaves over-expressing *PcTrx-h4* were irradiated with UVB (1.2 Wm^{-2} (λ 302 nm) for 2 h) and stained with 3,3-Diaminobenzidine (DAB) or nitroblue tetrazolium (NBT), which are specific to H_2O_2 and O_2^- respectively.

Upon comparing the stained leaves, it was discovered that H_2O_2 accumulated to the same extent in both the wild-type and transgenic tobacco leaves (Figure 3.14A). Superoxide was also present at the same levels (Figure 3.14B). This result suggests that PcTrx-*h*4 does not participate in the scavenging of ROS and is consistent with the unaltered tolerance to H_2O_2 and RBDA in the transgenic tobacco plants. Hence, the increased tolerance to UVB irradiation, heat stress and MV treatment must occur *via* an alternative mechanism.

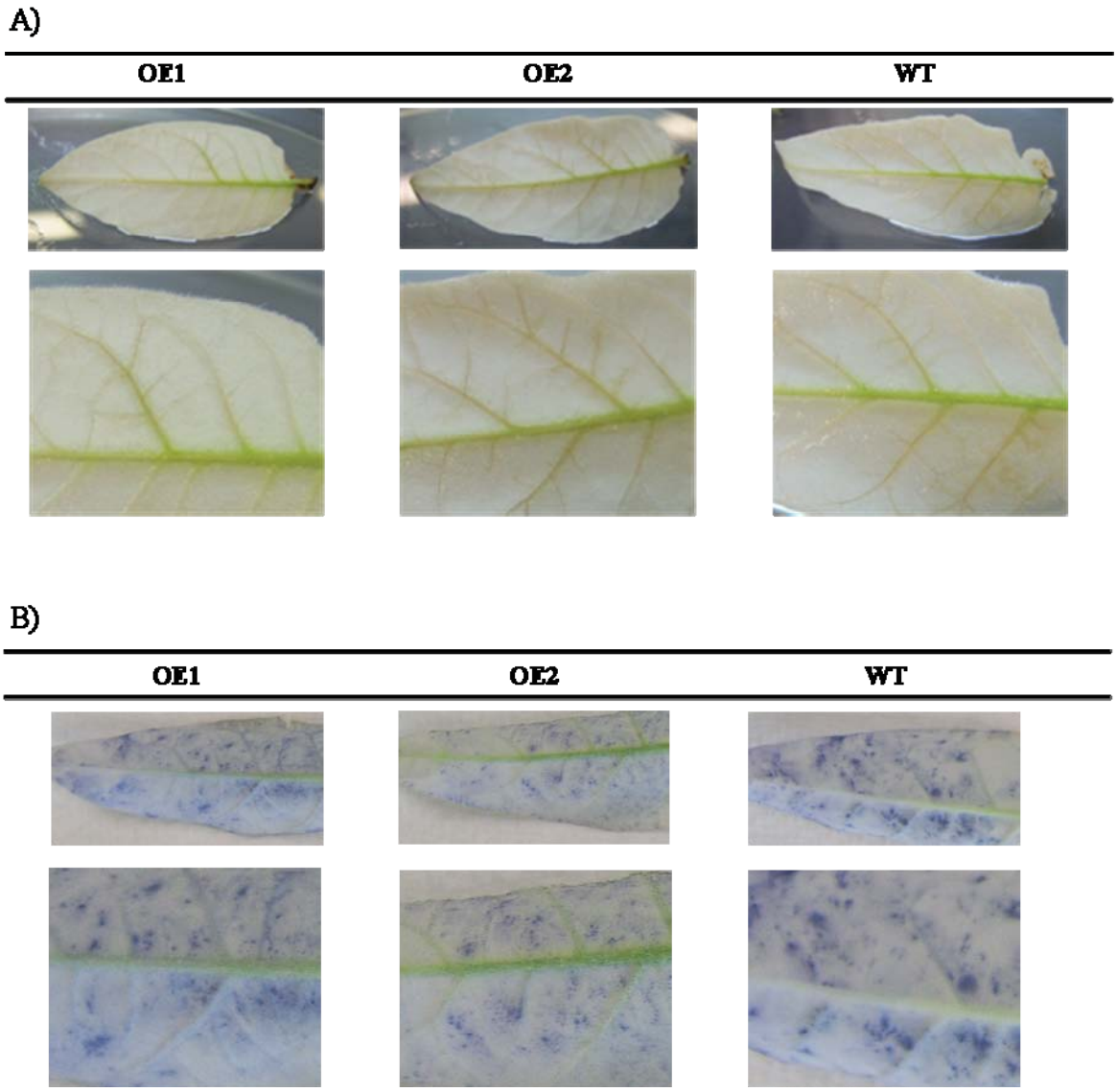

Figure 3.14: **Tobacco over-expressing *PcTrx-h4* (OE1-2) accumulates H_2O_2 (A) and superoxide (B) to the same degree as wild-type tobacco (WT), when exposed to UVB.** The fourth youngest leaves, from 3-month-old tobacco plants grown in soil, were infiltrated with DAB reagent (A) or NBT (B), then exposed to 1.2 Wm^{-2} UVB (λ 302 nm) for 2 h. To aid visualization of the stain, chlorophyll was removed from each leaf by boiling in 100% ethanol.

3.3.5 Thioredoxin-*h*4 is Potentially N-linked Glycosylated

Resulting from barley thioredoxin-*h*4 sequence analysis (reported in Chapters 4 and 5) and discussions centred upon possible thioredoxin-*h*4 function(s), the protein sequence of PcTrx-*h*4 was examined more closely for motifs that might allude to how thioredoxin-*h*4 interacts with its target proteins (in addition to the conserved active site, WCPCG). Within the protein sequence of PcTrx-*h*4 a potential N-linked glycosylation motif (NFS) was identified; located adjacent to the thioredoxin active-site motif (WCGPC) (Figure 3.15) (*courtesy of Dr John Patterson, ACPFG, University of Melbourne*). Upon alignment with orthologous sequences it was discovered to be highly conserved (Figure 3.15).

N-linked glycosylation is known to play a key role in protein folding (Malhotra and Kaufman, 2007). Tunicamycin is an antibiotic that inhibits the synthesis of N-linked glycoproteins, making it a strong inhibitor of N-linked glycosylation. Therefore, when cells are treated with tunicamycin, protein folding is disturbed (Iwata and Koizumi, 2005). This property of tunicamycin along with the transgenic tobacco over-expressing PcTrx-*h*4 provided an opportunity to test if the NFS motif was functional, and establish if thioredoxin-*h*4 is N-linked glycosylated. The aim was to treat the transgenic tobacco with tunicamycin and see if the oxidative stress tolerance conferred by PcTrx-*h*4 was subsequently removed, indicating that PcTrx-*h*4 protein folding, hence function, was disrupted. To begin, tunicamycin (0, 50 and 100 μg μl^{-1} was topically applied (10 μl) to both transgenic and wild-type tobacco leaves (*performed by Dr Juan Juttner*). Unexpectedly, the transgenic tobacco displayed increased tolerance to tunicamycin (Figure 3.16). Necrotic regions developed to a greater extent on wild-type leaves, compared to the transgenic leaves constitutively over-expressing PcTrx-*h*4 (Figure 3.16). Consequently, an alternative hypothesis to explain the increased stress tolerance of the transgenic tobacco was considered. One possible explanation is that PcTrx-*h*4 may protect target proteins by preventing or decreasing protein unfolding, which is known to increase in the presence of ROS, which are in high abundance in oxidatively stressed plants (Apel and Hirt, 2004; Martinez-Sanchez et al., 2005). Alternatively, it could be reasoned that PcTrx-*h*4 might assist in protein re-folding processes. Also remaining for further investigation is whether or not PcTrx-*h*4 is itself N-linked glycosylated

```
Hv4 MGGCVGKGR-GIVEEKLDFKGGNVHVITTKEDWDQKIEEANKDGKIVVANFSASWCGPCR
Pc4 MGGCVGKDR-GIVEDKLDFKGGNVHVITTKEDWDQKIAEANKDGKIVVANFSASWCGPCR
Lp4 MGGCVGKDR-SIVEDKLDFKGGNVHVITTKEDWDQKVAEANKDGKIVVANFSASWCGPCR
Ta4 MGGCVGKGR-SIVEEKLDFKGGNVHVITTKEDWDQKIEEANKDGKIVVANFSASWCGPCR
Sc4 MGGCVGKGR-SIVEEKLDFKGGNVHVITTKEDWDQKIEEANKDGKIVVANFSASWCGPCR
Lc4 MGGCVGKGR-SIVEEKLDFKGGNVHVITTKEDWDQKIEEANKDGKIVVANFSASWCGPCR
Hb4 MGGCVGKGR-GIVEEKLDFKGGNVHVITTKEDWDQKIEEANKDGKIVVANFSASWCGPCR
Os4 MGGCVGKGRRHIEEDKLDFKGGNVHVITSKEDWDRKIEEANKDGKIVVANFSASWCGPCR
Zm4 MGGCAGKVRRDDEEK-LDFKGGNVHIITSNEGWDQKIAEANRDGKTVVANFSASWCGPCR
```

Figure 3.15: **Identification of a potential N-glycosylation motif (NFS) in orthologous thioredoxin-*h*4 amino acid sequences.** Amino acid sequences were aligned using ClustalW multiple alignment software and a conserved NFS motif (highlighted in pink) was found adjacent to the active site motif WCGPC (highlighted in green). Sequence are from the following species: *Hordeum vulgare* (Hv4), *Phalaris coerulescens* [AF159388] (Pc4), *Lolium perenne* [AF159387] (Lp4), *Triticum aestivum* [AF438359] (Ta4), *Secale cereale* [AF159386] (Sc4), *Leymus chinensis* [TA69309_45] (Lc4), *Hordeum bulbosum* [AF159385] (Hb4), *Oryza sativa* [AF435817] (Os4) and *Zea mays* [AF435816] (Zm4).

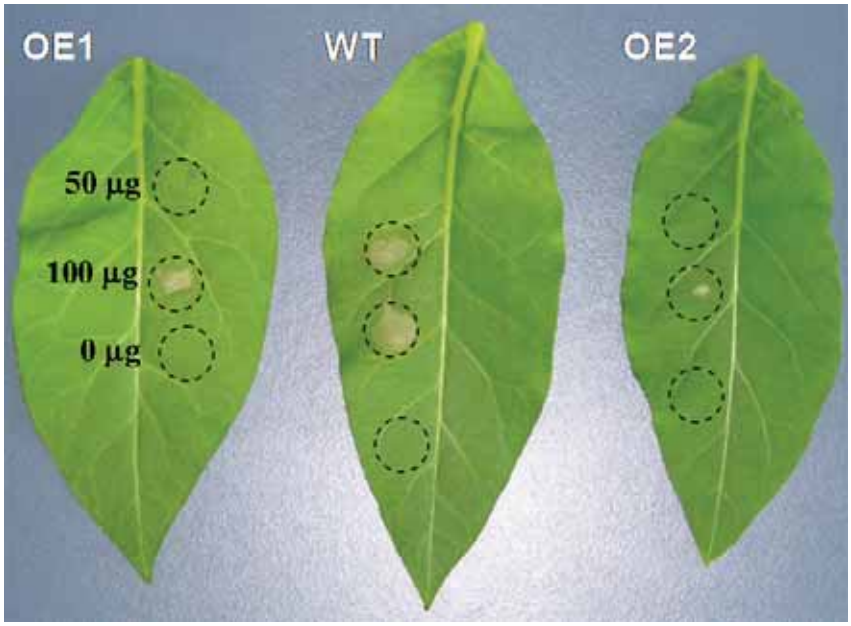

Figure 3.16: **Over-expression of *PcTrx-h4* confers increased tolerance to tunicamycin.** Large, healthy leaves of the same age on 2-month-old attached tobacco leaves were treated with 10 µl drops of tunicamycin at concentrations of 50 and 100 µg μl^{-1}. Two discrete transgenic tobacco lines over-expressing *PcTrx-h4* (OE1-2) displayed increased tolerance to tunicamycin treatment, as determined by the size of necrotic lesions developing, compared to the wild-type control tobacco (WT). Application sites are circled. Photographs were taken 48 h after treatment. (*Courtesy of Juan Juttner, ACPFG, University of Adelaide*).

To continue investigation of the glycosylation status of PcTrx-*h*4, protein extracts from the transgenic tobacco were treated with the enzyme Peptide-N-glycosidase F (PNGase F), which is commonly used to deglycosylate proteins. PNGase F releases asparagine-linked oligosaccharides from glycoproteins and glycopeptides by hydrolyzing the amide of the asparagine side chain (Iwata and Koizumi, 2005). Treated protein extracts could then be resolved by electrophoresis and probed with a PcTrx-*h*4 specific antibody. A shift in protein size, when comparing untreated against treated samples, was expected if the PcTrx-*h*4 was deglycosylated by PNGase F

The experiment was performed multiple times and as seen in lane 1 of Figure 3.17A, proteins were successfully extracted and separated by electrophoresis. However, the PNGase F treatment protocol appeared to contribute to protein degradation. To locate the source of contention, a step-wise analysis of the protocol was performed. The process prior to addition of PNGase F (addition of 0.2% SDS containing 100 mM 2-mercaptoethanol, 10 min boiling, ice cooled, addition of 15% TritonX) appeared to reduce the amount of protein visible on the gel (Figure 3.17A, lane 2), despite the protein source being the same as for untreated protein (Figure 3.17A, lane 1). Similarly, the entire treatment, minus PNGase F enzyme addition, caused protein degradation (Figure 3.17A, lane 3). The protein separation profiles, however, remained unaltered by these treatments. The complete treatment resulted in an alteration of the protein banding profile, which indicated that PNGase F was effectively deglyosylating proteins (Figure 3.17A, lane 4). Interestingly, protein degradation appeared to be less than seen in the control sample, without PNGaseF added (Figure 3.17A, lane 3).

As evident in Figure 3.17B, antibody quality problems were encountered. Specifically, the antibody sensitivity was insufficient for adequate detection of PcTrcx-*h*4 in the protein samples. It was previously demonstrated that this antibody was capable of detecting PcTrx-*h*4, in transgenic tobacco samples over-expressing *PcTrx-h4* (see Figure 3.2) and the positive control was also detected (Figure 3.17B, lane 5). Therefore, it was concluded that not enough protein was loaded onto the gel in the PNGase F experiment, to see PcTrx-*h*4 detection by the antibody. Unfortunately, the amount of protein that could be loaded was limited by the treatment protocol and the maximum capacity of the wells in the polyacrylamide gel being used. If the protein concentration was increased, the PNGaseF enzyme treatment failed. The protein concentration issues may have been further compounded by the protein degradation (*see above*), and hence further reducing the quantity of PcTrx-*h*4 available for detection. In summary, although a highly conserved NFS motif was identified, the hypothesis that thioredoxin-*h*4 is N-linked glycosylated was not verified or disproven experimentally.

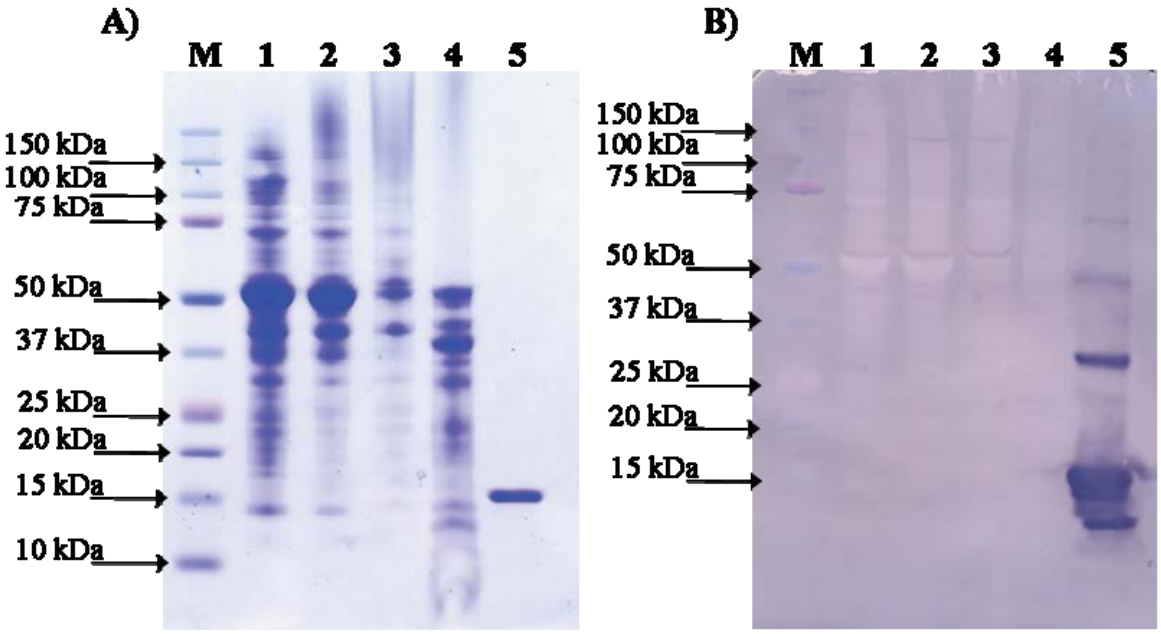

Figure 3.17: **Western analysis reveals antibody strength is insufficient to detect PcTrx-*h*4 in PNGase F treated tobacco protein samples.** The PNGase F treatment protocol results in an altered separation profile but also protein degradation. Protein was extracted from tobacco leaves over-expressing PcTrx-*h*4 and treated with PNGase F. A) Coomassie stained denaturing polyacrylamide gel showing quality of total protein loaded per sample. B) Nitrocellulose membrane showing binding of antibody specific to thioredoxin-*h*4. Samples analysed were: untreated protein (1), protein treatment ceased immediately prior to PNGase F addition (2), protein subjected to full treatment except PNGaseF addition (3), Complete treatment (4), Positive control (purified recombinant HvTrx-*h*4) (5). Protein sizes were inferred from alignment with BioRad Dual Colour Marker (M).

3.4 Discussion

3.4.1 Thioredoxin-*h*4 and Oxidative Stress Tolerance

Thioredoxins are able to supply reducing power to target proteins, thereby protecting these proteins and subsequently the entire plant against oxidative damage (Dos Santos and Rey, 2006). Oxidative stress has been linked with thioredoxins in different ways, including its involvement in ROS signalling, changes in expression and through the processes in which its protein targets operate (see Chapter 1). Whilst not all thioredoxins are involved in oxidative stress related pathways, the findings presented in this chapter indicate that thioredoxin-*h*4 can function in an oxidative stress protection capacity. Specifically, over-expression of PcTrx-*h*4 in tobacco conferred increased tolerance to UVB, heat and methyl viologen. Mammalian thioredoxins have previously been linked with cellular responses to UV irradiation. For example, thioredoxin expression is induced by UV irradiation (Nishinaka et al., 2001). Also, Yokomizo et al. (1995) found that human cells engineered to have reduced levels of thioredoxin were more sensitive to UV radiation. Furthermore, thioredoxin expression was shown to increase in response to UVB irradiation in human melanocytes (Funasaka and Ichihashi, 1997). Very recently Buechner et al. (2008) demonstrated that thioredoxin-1 prevented UVB induced expression of collagen type Iα1, in human skin cells. Nonetheless, this is the first reported case of a plant thioredoxin conferring UVB tolerance. No previous studies examining a plant thioredoxin in relation to UVB have been reported, to our knowledge. A similar study to the one reported in this chapter, focussed on an *Arabidopsis thaliana* thioredoxin-*h*, AtTrx-*h*5, which was found to be strongly activated by irradiation with UVC (Laloi et al., 2004). It was hypothesised that a salicylic acid based signalling pathway was involved as salicylic acid accumulates after exposure to UVC as well as during pathogen infection, which also up-regulated AtTrx-*h*5 (Laloi et al., 2004). However, AtTrx-*h*5 is not an ortholog of PcTrx-*h*4 and PcTrx-*h*4 did not confer tolerance to pathogen attack, so conclusions cannot be inferred (Appendix A).

Very recently, heat tolerance was seen in transgenic *A. thaliana* plants over-expressing a thioredoxin-*h*, AtTrx-*h*3 (Park et al., 2009). The transgenic and wild-type plants were incubated at 40^{o}C for 3 days and their tolerance compared. In the same study, it was discovered that AtTrx-*h*3 has two functions, acting as a disulfide reductase and as a molecular chaperone. The heat tolerance was attributed to its chaperone function. Interestingly, it was concluded that AtTrx-*h*3 protein expression was not induced by the heat treatment but that the heat shock regulated its function through a post-translational modification. Considering this

study, investigation into the possibility of PcTrx-*h*4 also having a chaperone function may be warranted. However, it is important to note that AtTrx-*h*9 is the ortholog of PcTrx-*h*4, not AtTrx-*h*3 (Appendix A).

Earlier studies have also linked thioredoxins-*h* with heat tolerance. A study was conducted with two maize cultivars differing in their thermal tolerance, being either highly chilling-tolerant or highly chilling-sensitive. A heat treatment at 42^{o}C for 1 day resulted in a decrease of ZmTrx-*h* protein in the chilling-tolerant plants whilst it increased in the chilling-sensitive variety (Kocsy et al., 2004). A poplar (*Populus euphratica*) thioredoxin-*h* was also up-regulated by heat stress (Ferreira et al., 2006). A treatment consisting of a gradual increase in temperature, up to 42^{o}C but with a 37^{o}C maximum overnight, for 4 days, induced accumulation of thioredoxin-*h*. The specific subclass of ZmTrx-*h* that was detected in the Western analysis was not reported but the antibody was said to be specific to the -*h* class, not detecting thioredoxins-*f* or -*m*. Similarly, the subclass of the *P. euphratica* thioredoxin-*h* was not reported. Regardless, it was considered that the ZmTrx-*h* might be connected to redox signalling systems as it was concluded there was an association between thioredoxin-*h* and glutathione levels in the plants, which were altered following abiotic stress (Kocsy et al., 2004). For the *P. euphratica* thiordoxin-*h*, Ferreira et al. (2006) simply stated that the increase might be related to the role of the thioredoxin-*h* in the oxidative stress response.

The data outlined in this chapter shows that PcTrx-*h*4 over-expression did not confer tolerance to water-deficit stress. This is interesting because water-deficit is a key component of the major abiotic stress, drought, in which excessive UVB and heat are also commonly involved (Izanloo et al., 2008). The lack of tolerance to water-deficit stress was initially surprising as Q-PCR results obtained by Alexandra Smart (*PhD Student, ACPFG, University of Adelaide*), using tissue from barley plants that had been subjected to a cyclic water deficit regime, revealed an increase in HvTrx-*h*4 transcript after the third 'drought' event (*unpublished data*). Thus, it was considered that a cyclic water-deficit regime for the transgenic tobacco may yield different results to the single prolonged event. However, the transgenic tobacco plants were constitutively over-expressing PcTrx-*h*4 and therefore, if PcTrx-*h*4 played a role in water-deficit tolerance it could be expected to be effective immediately. Its expression would not need to be induced by successive drought events.

Thioredoxin has been connected to water-deficit tolerance previously. Expression of a potato chloroplastic drought-induced stress protein (CDSP32), which is comprised of two thioredoxin modules, was increased following water withholding for 10 to 12 days (Rey et al.,

1998). Rey et al. (1998) proposed that tolerance was due to CDSP32 assisting with preservation of the thiol:disulfide redox potential of chloroplastic proteins during water deficit(Rey et al., 1998). Following further studies, it was speculated that CDSP32 might supply electrons to a thioredoxin-dependent protein involved in ROS scavenging, or regenerate inactivated proteins (Broin et al., 2000). More recent studies lead to the theory that CDSP32 played a role in defence against lipid peroxidation in photosynthetic membranes and was probably an electron donor to a peroxide-detoxifying enzyme (peroxiredoxin BAS1), thereby facilitating water-deficit tolerance (Broin and Rey, 2003). Furthermore, a study investigating protein expression changes in wheat grains identified many thioredoxin-*h* targets to be differentially regulated following drought stress (Hajheidari et al., 2007). However, despite these previous studies linking thioredoxins to drought responses, our results did not provide evidence of *PcTrx-h4* involvement in a role resulting in provision of water-deficit tolerance.

During examinations of CDSP32 expression, MV treatments were performed on potato plants. Broin et al. (2000) found that CDSP32 transcript abundance greatly increased in response to MV application. Interestingly, the correlating protein also increased but to a lower extent than the transcript. In addition, MV has been shown to increase the level of lipid peroxidation in plants that lacked CDSP32, when compared to the wild-type potato (Broin and Rey, 2003).

Methyl viologen treatment was also found to up-regulate expression of a thioredoxin-*h* gene in rice (*Oryza sativa*) seedlings. Northern analysis revealed the induction occurred within 4 h and continued for at least 12 h (Tsukamoto et al., 2005). The MV tolerance observed in our tobacco plants over-expressing *PcTrx-h4* correlates well with the MV induction of CDSP32 and the rice thioredoxin-*h* transcript. However, a study with *Rhodobacter sphaeroides*, which are facultative phototrophic bacteria, found that TrxA (transcript and protein) was up-regulated in response to MV. Yet inconsistently, it was also reported that a mutant *R. sphaeroides* strain with decreased TrxA levels was more resistant to MV than the wild type strain (Li et al., 2003b). The same mutant strain was more sensitive to H_2O_2 (Li et al., 2003b). Points of further complication are the findings that, whilst expression of the TrxA orthologs in *Bacillus subtilise* and *Oenococcusoeni* are induced by H_2O_2, the *E. coli* TrxA ortholog is not affected by H_2O_2 or MV (Guzzo et al., 2000; Prieto-Alamo et al., 2000; Scharf et al., 1998). Despite this, deletion of TrxA in *E. coli* was found to increase sensitivity to H_2O_2 (Ritz et al., 2000).

R. capsulatus has an additional thioredoxin, TrxC, that is absent in *R. sphaeroides*. This TrxC was removed to create a mutant *R. capsulatus* strain which was then grown in the presence of oxidative stress inducing compounds. Growth of the TrxC deficient strain was found to be inhibited by H_2O_2 to a greater extent than the wild-type strain. It was also more sensitive to MV (Li et al., 2003a).

Thioredoxins have similarly been connected to oxidative stress protection in plants, through their response to H_2O_2 treatments. For example, Mouaheb et al. (1998) demonstrated that *A. thaliana* thioredoxins (AtTrx-*h*3 and -*h*4) could restore tolerance to H_2O_2 in mutant yeast (*Saccharomyces cerevisiae*) that were thioredoxin deficient and thus initially H_2O_2 hypersensitive. None of the other thioredoxins-*h* tested (AtTrx-*h*1, -*h*2 and -*h*5) were able to confer H_2O_2 tolerance (Mouaheb et al., 1998).

Functional complementation studies using the same thioredoxin deficient yeast strain have also indicated that the pea (*Pisum sativum*) thioredoxins-*h* have oxidative stress protection roles. PsTrx-*h*1 was able to confer H_2O_2 tolerance to the mutant yeast and it was speculated that PsTrx-*h*1 achieved this through interaction with peroxiredoxin/s (Traverso et al., 2007). Peroxiredoxins reduce H_2O_2 and can be subsequently reactivated by thioredoxins (Wood et al., 2003). In contrast, PsTrx-*h*2 increased H_2O_2 hypersensitivity of the yeast mutant, so it may not function in a protective capacity but could still be involved in oxidative stress processes (Traverso et al., 2007).

In agreement with the results presented in this chapter, individual thioredoxins have previously displayed differential regulation in response to MV and H_2O_2. In view of these studies, it appears that the degree of tolerance to MV or H_2O_2, attributed to thioredoxin, is variable and probably dependent upon the specific thioredoxin investigated. Considering the varied findings within the literature, researchers must be conscious of the need to comprehensively characterise the behaviour of thioredoxins on a case by case basis.

The lack of *Botrytis cinerea* tolerance in the transgenic tobacco over-expressing PcTrx-*h*4 correlates with the lack of tolerance to H_2O_2 and also with the analogous H_2O_2 accumulation levels observed for UVB stressed wild-type and transgenic tobacco plants. Hydrogen peroxide is a key trigger for programmed cell death, which is required for *B. cinerea* to infect the host tissue (Williamson et al., 2007). Hence, if tolerance to H_2O_2 was evident, *B. cinerea* tolerance would have been expected. As previously mentioned, transcript of AtTrx-*h*5 increased significantly in response to an incompatible reaction with a pathogen, *Pseudomonas syringae* (Laloi et al., 2004). It was hypothesised that the AtTrx-*h*5 was participating in defence

mechanisms involving the oxidative burst which results from pathogen attack, such as that occurring during *B. cinerea* infection. It is possible that the transcript of the endogenous NtTrx-*h*4 did increase following *B. cinerea* infection, similar to AtTrx-*h*5s response. Regardless, constitutive expression of PcTrx-*h*4 in the tobacco did not increase tolerance to the fungal attack and importantly, AtTrx-*h*5 and PcTrx-*h*4 are not orthologs (Appendix A), so conclusions cannot be inferred.

3.1.1 Mechanism of Tolerance

The lack of tolerance to water deficit, H_2O_2, Rose Bengal diacetate and a necrotrophic fungus, suggests that the tolerance to UVB and MV is not acquired through a general, broad-range oxidative stress tolerance process. Instead, tolerance must be arising through a more specific mechanism. Although some thioredoxins are able to directly reduce H_2O_2, quench singlet oxygen and scavenge hydroxyl radicals (Das and Das, 2000; Spector et al., 1988) PcTrx-*h*4 does not appear to be involved in ROS scavenging mechanisms, neither directly nor indirectly through provision of redox power to other scavenging enzymes. Not only does the lack of tolerance to H_2O_2 and Rose Bengal diacetate support this theory, but also the fact that superoxide and H_2O_2 accumulation, in response to UVB irradiation, was the same between wild-type and tobacco plants over-expressing *PcTrx-h4*.

It is commonly proposed that thioredoxins may modulate the activity of other enzymes that scavenge ROS. This theory is supported by the numerous proteins that thioredoxins are thought to interact with, which participate in ROS scavenging processes. For example, some of the thioredoxin-*h* targets identified in plants include peroxiredoxin, superoxide dismutase (SOD), peroxidases and GSH-dehydroascorbate reductase (Maeda et al., 2004; Marx et al., 2003; Wong et al., 2004; Yamazaki et al., 2004). However, not all of these target proteins have been confirmed as true thioredoxin-*h* interactors and the validity of the interactions is questionable. For example, the SOD identified to interact with a barley cytosolic thioredoxin was believed to be chloroplastic and therefore, the physiological importance of the interaction could be considered ambiguous (Maeda et al., 2004). Despite previous results, our results indicate PcTrx-*h*4 does not confer tolerance through enhancement of ROS scavenging, neither directly nor indirectly.

A rice thioredoxin-*h* (OsTrx-*h*), which is transcriptionally induced by MV, contains a 28 bp motif in its promoter region. This motif is conserved across two other antioxidant defence genes; SOD and a glutaredoxin (GRX). It was shown to act as a cis-element in response to oxidative stress and was named accordingly; coordinate regulatory element for antioxidant

defence (CORE) (Tsukamoto et al., 2005). Importantly, the expression of SOD, GRX and OsTrx-*h* were all co-ordinately induced by MV. Tsukamoto et al. (2005) therefore hypothesised that multiple genes were involved and controlled by a common regulatory mechanism, involving the novel CORE motif, in response to MV. Considering this, the possibility of the PcTrx-*h*4 promoter containing a similar CORE motif is of great interest. If the CORE motif is present, an indication of the mechanism of MV tolerance conferred by PcTrx-*h*4 over-expression would in part be provided. This is especially significant when considering that increased tolerance for MV but not H_2O_2 was conferred by PcTrx-*h*4 over-expression, just as the OsTrx-*h* gene responded to MV but not H_2O_2 (Tsukamoto et al., 2005).

Chapter 5 of this thesis contains information about the barley thioredoxin-*h*4 (*HvTrx-h4*) promoter which was isolated for analysis. HvTrx-*h*4 is an ortholog of PcTrx-*h*4, sharing 96% amino acid identity (Appendix A). The *HvTrx-h4* promoter sequence was analysed for the CORE motif identified in rice but was not found. Furthermore, the rice thioredoxin-*h* containing the CORE, did not align closely with the *HvTrx-h4* promoter, nor did the *AtTrx-h9* promoter sequence (orthologous to *HvTrx-h4*) (Appendix A). Therefore, the rice thioredoxin-*h* is likely to be a member of a different subclass. In addition, Tsukamoto et al. (2005) were unable to identify the CORE motif in the *A. thaliana* genome and homologous promoter sequences of cytosolic SOD, thioredoxins and GRX from other plants. Subsequently, they concluded that the CORE motif is not conserved in other plant species, although they speculated that other plants probably do contain functionally similar cis-elements, but with different sequences (Tsukamoto et al., 2005). In summary, the MV-responsive rice thioredoxin-*h* CORE is unlikely to be present in the *PcTrx-h4* promoter but perhaps a functionally similar motif exists.

It remains possible that thioredoxins may confer oxidative stress tolerance by alternate means. Given tobacco plants over-expressing *PcTrx-h4* displayed increased tolerance to tunicamycin, the involvement of PcTrx-*h*4 in protein folding or unfolding processes is worth considering. PcTrx-*h*4 may have conferred tunicamycin tolerance by protecting proteins from irreversible damage, unfolding or by assisting with refolding of damaged proteins. Thioredoxins have previously been implicated in protein folding, as reviewed by Berndt et al. (2008). In plants, some thioredoxin protein targets identified, including HSP 60/70 and chaperones, are involved in protein assembly and folding processes (Balmer et al., 2004; Yamazaki et al., 2004). In addition, it is well established that thioredoxins can reduce oxidised proteins, thereby renewing their functional ability, which is particularly important for maintaining cellular processes and redox balance (Meyer et al., 2008). Hence, an excess of PcTrx-*h*4 may

result in more proteins remaining functional, including those that are involved in protein folding or prevention of protein unfolding. To investigate this hypothesis further, protein aliquots derived from wild-type and transgenic tobacco over-expressing *PcTrx-h4* could be treated with tunicamycin, followed by labelling of the newly generated sulfhydryl (SH) groups with the thiol-specific probe, monobromobiamane. Subsequent separation of the treated and untreated protein samples, using polyacrylamide gels, would enable a comparison of protein shifts (treated compared to untreated) and visual quantification of extent of modified proteins (wild-type compared to transgenic). Hence, the degree of protein protection offered by PcTrx-*h*4 could be established.

If PcTrx-*h*4 is itself N-linked glycosylated, tunicamycin should inhibit its function. However, because PcTrx-*h*4 is constitutively expressed in relative high abundance in the transgenic tobacco plants, perhaps some PcTrx-*h*4 remains unaffected by the tunicamycin (if assuming it is indeed a subject of glycosylation). If enough PcTrx-*h*4 was to remain functional it is reasonable to expect that necrotic regions would not develop in response to tunicamycin treatment of the transgenic tobacco leaves. If this is occurring, the tunicamycin tolerance would be considered 'artificial' and not related to PcTrx-*h*4 function. To our knowledge, glycosylation of a thioredoxin has not been reported previously. Nonetheless, it is feasible that the NFS motif identified in PcTrx-*h*4 and orthologs is indeed functional.

Heat, UVB and MV tolerance conferred by PcTrx-*h*4 may be 'synthetic' and result from an artificially induced PcTrx-*h*4 function, especially considering hypersensitivity was not seen for transgenic tobacco in which NtTrx-*h*4 expression was silenced. If thioredoxin-*h*4 really does assist plants to cope with stress, it could be argued that its absence would make the plants more vulnerable. However, thioredoxin-*h*4 is just one member of the large super-family of thioredoxins (Meyer et al., 2008). For example, it has been predicted that there are more than 40 thioredoxin genes in the *A. thaliana* genome (Meyer et al., 2005). Consequently, functional redundancy and compensation by other thioredoxins is highly likely. If this is indeed the case then removal of NtTrx-*h*4 may have little or no effect on the plants stress tolerance capacity. In support, an *A. thaliana* T-DNA insertion mutant that inactivates AtTrx-*h*5 is not hypersensitive to oxidative stresses, including UV irradiation, despite AtTrx-*h*5 gene expression being induced in the control plants. The absence of this phenotype was attributed to compensation by other thioredoxin-*h* members (Laloi et al., 2004). Meyer et al., (2005) also argued that a high diversity of functional specialization and/or a high level of redundancy probably exists within the thioredoxin super-family. To study functional redundancy within

thioredoxin families is a difficult task which would require careful, systematic analysis of a suite of mutant plants lacking multiple thioredoxins.

To address the issue of an artificial function potentially occurring, resulting in increased stress tolerance, transcript and protein expression analysis of the endogenous NtTrx-*h*4 could be employed. Considering the *HvTrx-h4* post-transcriptional and post-translational results obtained and described in Chapter 5, transcript analysis is not recommended. Instead, Western analysis of NtTrx-*h*4 protein expression is likely to be more informative. This technique relies upon development of a specific antibody with suitable strength and specificity to allow visible detection and evaluation of NtTrx-*h*4 protein abundance. Unfortunately this in itself is not trivial and currently such an antibody is not available.

3.1.1 Conclusion

Over-expression of *PcTrx-h4* in tobacco confers tolerance to specific stresses, specifically UVB, heat and MV. Evidence suggests the tolerance mechanism does not involve scavenging of ROS. Suppression of thioredoxin-*h*4 expression in tobacco did not result in plant hypersensitivity to any of the oxidative stress inducing treatments investigated. Hence, the stress tolerance conferred by PcTrx-*h*4 may be artificial due to the unnaturally high PcTrx-*h*4 protein levels. Alternatively, other thioredoxin-*h* members may be compensating for the loss of *NtTrx-h4*. If so, the stress tolerances discovered allude to specific stress responses in which PcTrx-*h*4 is endogenously involved. PcTrx-*h*4 also provides tolerance to topical application of tunicamycin which may suggest a connection to protein folding processes. Finally, thioredoxin-*h*4 may be glycosylated, as indicated by the presence of a highly conserved NFS motif within the protein sequence.

4 Identification of Proteins Interacting with *Hordeum vulgare* Thioredoxin-*h*4

4.1 Introduction

Phylogenetic analysis suggests that of all the grass cytosolic thioredoxins, subclass 4 represents the most ancient subclass. It is thought that subclass 4 predates the evolution of the angiosperms which occurred at least 200 million years ago (Juttner, 2003). The highly conserved nature of thioredoxins-*h*4, in plant species as diverse as angiosperms and gymnosperms, implies a conservation of gene function. To gain insight into function, one strategy is to identify the proteins interacting with thioredoxin-*h*4. Subsequently, this may reveal the key cellular pathway/s in which thioredoxin-*h*4 is involved. Considering the findings outlined in Chapter 3 it is possible that thioredoxin-*h*4 interacts with and regulates proteins essential for protection against oxidative stress. To date, no cereal thioredoxin-*h*4 protein targets have been identified.

One approach that can be employed to isolate proteins interacting with thioredoxin is monocysteinic affinity chromatography (Verdoucq et al., 1999). The technique exploits the mechanism by which thioredoxin reduces a specific disulfide bond in target proteins. Thioredoxin reduction of a target disulfide involves the formation of a short-lived and unstable heterodisulfide bond connecting the thioredoxin to the target protein prior to full reduction of the targeted disulfide, as previously described in Chapter 1 (Figure 1.2). Mutation of the buried cysteine in the thioredoxin active site (WCGPC) anchors the ordinarily transient heterodisulfide, thus covalently linking the target protein to thioredoxin. Importantly, this bond can be resolved by dithiothreitol (DTT), enabling collection of the trapped proteins (Brandes et al., 1996). Depending upon the source of proteins to which thioredoxin is exposed, interactions occurring in whole tissues, or even individual cellular compartments, can be captured and identified using the monocysteinic affinity

chromatography technique. This strategy was first applied to generate covalent complexes between thioredoxin-*f* and phosphoribulokinase (Brandes et al., 1996). Since then, it has been used to isolate thioredoxin target proteins from a diverse range of plant tissues and specific organelles.

Studies by Verdoucq et al. (1999) successfully used a mutant *Arabidopsis thaliana* thioredoxin-*h*3, containing a cysteine to serine substitution in the active site, to isolate a peroxisomal membrane protein in yeast. Motohashi et al. (2001) exploited the thioredoxin mechanism of action in the same way, but added an extra component to the monocysteinic affinity chromatography technique. They immobilised the thioredoxin to a resin that was specifically activated for protein binding by cyanogen bromide. Through this modified technique, four chloroplast *m*-type thioredoxin target proteins were identified in the stroma lysate of spinach chloroplasts (Motohashi et al., 2001). Using the same method, Balmer et al. (2003) identified proteins interacting with thioredoxins-*m* and thioredoxin-*f*. Fifteen of the potential protein targets were categorised into 10 different chloroplast processes, some of which had not been previously associated with thioredoxins. Proteins believed to participate in chloroplast-nucleus signalling, protein assembly/folding and degradation, oxidative regulation, and biosynthesis of vitamins, tetrapyrrole and isoprenoid were all deemed to be interacting with thioredoxin.

Possible target proteins of cytosolic thioredoxins in higher plants have also been investigated using the immobilised affinity chromatography technique. Yamazaki et al. (2004) isolated proteins interacting with thioredoxin-*h* in the cell lysate of dark-grown *A. thaliana* whole tissues. The proteins identified were grouped into four main classes based on the pathways in which they were thought to be involved; anti-oxidative stress system, protein folding and degradation, protein biosynthesis, and metabolic enzymes.

The immobilised affinity chromatography technique has been applied in a study with a potato (*Solanum tuberosum*) chloroplastic drought-induced stress protein (CDSP32), to gain further insight into its function (Rey et al., 2005). CDSP32 contains typical features of thioredoxins in the C-terminal region, facilitating the application of immobilised affinity chromatography. CDSP32 was found to interact with 3 plastidic proteins involved in photosynthetic processes and 3 that participate in protection against oxidative damage.

The work presented in this chapter utilises the monocysteinic thioredoxin-immobilised affinity chromatography technique and was undertaken to gain further insight into the function of barley thioredoxin-*h*4 (HvTrx-*h*4). The buried (2^{nd}) cysteine in the active site of

HvTrx-*h*4 was mutated to serine and the resulting, purified protein was immobilised to cyanogen bromide-activated resin, thereby primed to stably bind proteins interacting with HvTrx-*h*4.

Findings presented in chapter 3 indicate that barley HvTrx-*h*4 may participate in the pant oxidative stress response or protein folding pathways. The identification of target proteins involved in such pathways would give weight to this hypothesis. Conversely, alternative functions may be revealed.

4.2 Materials and Methods

4.2.1 Site-Directed Mutagenesis and Incorporation of Restriction Sites

To remove the disulfide resolving property from the thioredoxin-h4 active site, in order to trap proteins interacting with thioredoxin-*h*4, a mutated version of HvTrx-*h*4 was expressed. A two-stage PCR based site-directed mutagenesis reaction was performed to introduce a nucleotide change (G to C) at position 176 (from coding start) in *Hordeum vulgare* thioredoxin-*h*4 cDNA. This altered the second active-site cysteine residue, at position 58, to a serine residue. At the same time, restriction sites were attached to the each end of the sequence to facilitate insertion of the PCR product into an expression vector, in the desired coding frame.

The site-directed mutagenesis process required four specific primers (Table 4-1) and three separate standard polymerase chain reactions (PCR) of 25 µl with 30 cycles (see 2.4.2) and is shown schematically in Figure 4.1. The high fidelity proofreading enzyme, ProofStart DNA Polymerase (Qiagen), was used in the PCRs to maintain sequence accuracy. Firstly, primers Hv4E70F and Hv4MutR were used to generate a 195 bp fragment whilst primers Hv4MutF with Hv4E70R generated a 242 bp fragment. The fragments were resolved on a 2.4% (w/v) agarose gel and solubilised from the gel as described in sections 2.4.5-6.

To obtain the complete, mutated sequence of HvTrx-*h*4 a third PCR was initiated without primers, containing 0.5 µl of each extracted fragment. This caused the complementary ends of the two cDNA fragments to anneal to each other and act as polymerase initiation sites. After the fifth cycle of amplification, primers Hv4E70F and Hv4E70R were added and the thermocycling was continued a further 25 times. The amplified fragment was resolved and viewed on a 1.6% (w/v) agarose gel and the desired band of 410 bp was solubilised from the gel as described in section 2.4.5-6.

To introduce restriction sites to each end of the wild-type *HvTrx-h4* sequence, to facilitate insertion into an expression vector, primers Hv4E70F and Hv4E70R were used in a standard PCR (see 2.4.2). The product was resolved on a 1.6% (w/v) agarose gel and the desired band of 410 bp was extracted from the gel as described in sections 2.4.5-6.

The resulting mutated and wild-type *HvTrx-h4* sequences were ligated independently into vector pGEM T-easy and transformed into chemically competent *Escherichia coli*, strain DH5α (see 2.4.9). Plasmids from individual colonies were extracted (see 2.4.10) and

sequenced (see 2.4.11) to verify sequence accuracy and presence, or absence, of introduced mutation and restriction sites.

Table 4-1: **Primers used for site-directed mutagenesis and incorporation of restriction sites.** The restriction sites are underlined and the site-specific nucleotide mutation is highlighted in red.

Primer	Nucleotide Sequence	Modification
Hv4E70F	5'-TAAGCATGCGCGGGGGCTGTGTGGGCAAG-3'	SphI (GCATGC) Restriction site
Hv4MutF	5'-GGTGTGGGCCATCCCGTGTCATTGCAC-3'	G to C Base change
Hv4MutR	5'-GTGCAATGACACGGCATGGCCCACACC-3'	G to C Base change
Hv4E70R	5'-TAAAGATCTACTGCCATCACCAAGAGC-3'	BglII (AGATCT) Restriction site

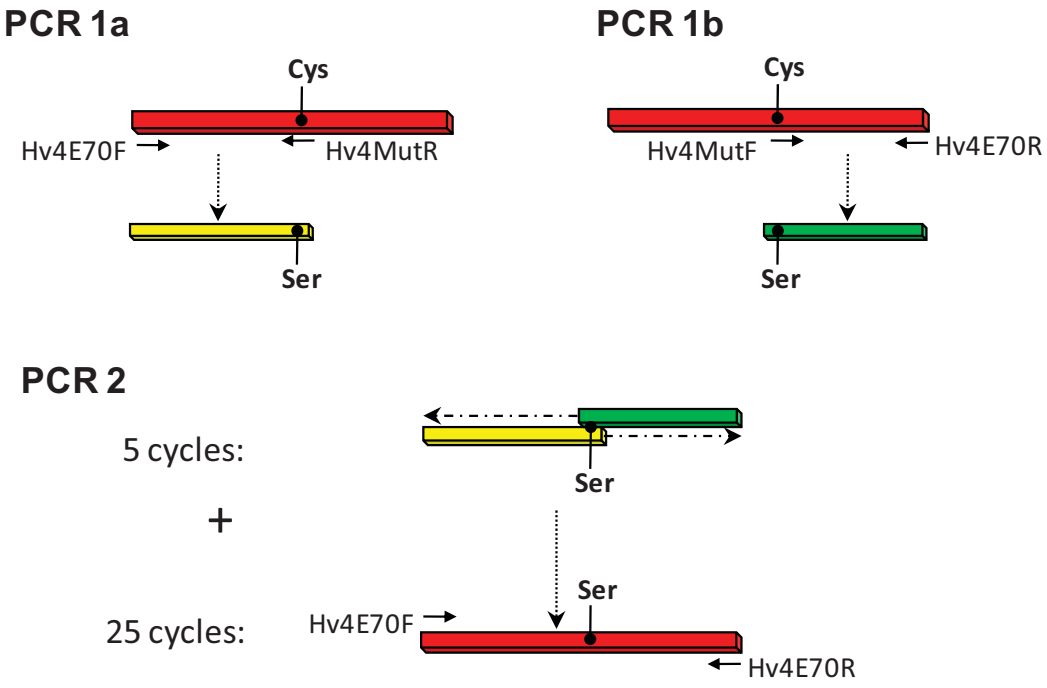

Figure 4.1: **Diagrammatic representation of the site-directed mutagenesis technique.** PCRs 1a and 1b result in *HvTrx-h4* fragments containing the $Cys_{58}Ser$ mutation at the 3' and 5' ends respectively. These two products are combined in PCR 2 and the complementary ends act as polymerase initiation sites. After 5 cycles, primers Hv4E70F and Hv4E70R are added to the reaction mixture resulting in amplification of the full *HvTrx-h4* sequence, which now contains a serine in the place of cysteine at position 58.

4.2.2 Insertion of Wild-type and Mutant *HvTrx-h4* into a Protein Expression Vector

Mutant and wild-type *HvTrx-h4* sequences were restricted from their pGEM-Teasy vectors with enzymes SphI and BglII, in buffer M (Roche), in a 50 µl final volume (see 2.4.7). Fragments were resolved by a 1.6% agarose gel (see 2.4.5) and purified (see 2.4.6). The protein expression vector pQE-70 (Figure 4.2), which introduces a tag of 6 consecutive histidine residues (6xHis tag) to the C-terminus of the protein, was also linerised with SphI and BglII (see 2.4.7). Cut *HvTrx-h4* fragments were independently ligated into the linerised vector and transformed into *E. coli*, strain M15 (see 2.4.9). Individual colonies resulting were cultured in 5 mL Luria broth overnight (see 2.4.9). For long-term storage, 600 µl was mixed with 400 µl 50% sterile glycerol, snap frozen and stored at -80^{o}C. Plasmids were extracted from the remaining cell culture (see 2.4.10) and sequenced (see 2.4.11) to identify those containing the mutant *HvTrx-h4*:pQE-70 or wild-type *HvTrx-h4*:pQE-70 construct.

Figure 4.2: **pQE-70 vector used to express HvTrx-*h*4 wild-type and mutant recombinant proteins in *Escherichia coli* strain M15.** Mutant and wild-type *HvTrx-h4* sequences were inserted into pQE-70 using SphI and BglII restriction sites, resulting in the attachment of a 6xHistidine tag to the C-terminus. PT5: T5 promoter; lac O: lac operator; RBS: ribosome binding site; ATG: start codon; 6xHis: 6xHis tag sequence; MCS: multiple cloning site with restriction sites indicated; Col E1: Col E1 origin of replication; Ampicillin: ampicillin antibiotic resistance gene. pQE-70 diagram from 'The QIA*expressionist*™' handbook, pg 34 (Qiagen).

4.2.3 Protein Expression

Wild-type and mutant forms of *HvTrx-h4* in the pQE-70 protein expression construct were expressed in *E. coli*, strain M15, as His-tagged proteins. Cells were grown to an OD_{600} of 0.6, at 37^{o}C with gentle shaking in Luria broth supplemented with 1 mg mL^{-1} ampicillin and 25 µg mL^{-1} kanamycin. Cultures were induced by 1 mM IPTG for 3.5 h. Cells were harvested by centrifugation at 4,000 *x g* for 10 min and frozen at -20^{o}C until use.

4.2.4 Purification of 6xHis-Tagged Protein from *E. coli* Cultures

Proteins expressed with a 6-His tag in *E. coli* were purified using unbound nickel-nitrilotriacetic acid (Ni-NTA) metal-affinity chromatography matrices (nickel resin) (Qiagen, Australia). Frozen cell pellets were resuspended in 4 mL lysis buffer [50 mM NaH_2PO_4, 300 mM NaCl, 10 mM Imidazole, pH 8.0] supplemented with 25 µg mL^{-1} RNAse, 25 µg mL^{-1} DNAase and 0.5 mg mL^{-1} lysozyme. Cell suspension was chilled on ice for 15 mins, sonicated to lyse cells and centrifuged at 4,000 *x g* for 10 min at 4^{o}C. Per 4 mL supernatant (cleared lysate), 1 mL pre-equilibrated nickel resin (Qiagen, Australia) was added [resin washed 3 times with lysis buffer, sedimented by centrifugation at ≤ 600 *x g* and resuspended 1_{resin}:$1_{lysis\ buffer}$]. Resin-lysate suspension was gently mixed by inversion using a suspension mixer rotor (Ratek, Vic) for 30 min at 4^{o}C, then resin was collected by centrifugation at ≤ 600 *x g* for 1 min at 4^{o}C. A sample of supernatant (flow through) was collected for analysis. The resin containing his-tag bound thioredoxin protein was washed 3 times with wash buffer 1 [50 mM NaH_2PO_4, 300 mM NaCl, pH 8.0] containing 20 mM Imidazole, 3 times with wash buffer 2 [50 mM NaH_2PO_4, 300 mM NaCl, pH 6.0] and 3 times with wash buffer 3 [100 mM KH_2PO_4, pH 6.0]. Purified protein was eluted from the resin using elution buffer [100 mM KH_2PO_4, 2 mM EDTA, pH 3.0] with 1 min of gentle mixing by inversion and incubation for 4 min at room temperature, followed by centrifuge at 600 *x g* for 1 min. Supernatant was collected and pH immediately adjusted with titration buffer [100 mM KH_2PO_4, 2 mM EDTA, pH 10.0] at a ratio of 12.5 µl per 100 µl of elution supernatant. Elution and titration was repeated a second time and the fractions pooled.

4.2.5 Western Analysis: Immunodetection of Histidine-Tagged Proteins.

Detection of poly-histidine tagged recombinant proteins was achieved through immunoblotting. Purified mutant and wild-type recombinant proteins were resolved by SDS-PAGE (see 2.7.2), transferred to nitrocellulose membrane (see 2.7.3) and probed with monoclonal anti-polyhistidine clone His1 antibody (Sigma), which was conjugated to alkaline phosphatase. Briefly, the membrane was blocked with 5% skim milk powder in TBS

overnight at 4°C, washed 3 x 10 min in TBS then incubated with anti-polyhistidine antibody [1:1000 dilution in TBS] for 1.75 h at room temperature, with gentle shaking. The membrane was again washed 3 x 10 min in TBS and antibodies were detected colourmetrically by incubation with nitroblue tetrazolium/bromochloro indolyl phosphate (NBT/BCIP) development solution (Sigma). Once bands had almost reached the desired intensity, the reaction was stopped with running RO water.

4.2.6 Silver Staining of 1D SDS-Polyacrylamide Gels

Polyacrylamide gels were silver stained based on the method described by Blum et al. (1987). Briefly, the gel was fixed in 50% methanol-12% acetic acid overnight and then rinsed 3 times in 95% ethanol for 20 min. The gel was incubated in formaldehyde fixing solution [40% methanol, 0.5% formaldehyde (37% (v/v) solution)] for 30 min, equilibrated in water with three 5 min rinses, followed by incubation with 0.02% sodium thiosulfate for 1 min. The gel was rinsed three times with water for 1 min, incubated with 0.1% silver nitrate for 10 min and again rinsed three times with water for 1 min. Stain development was induced by the addition of thiosulfate developing solution [3% sodium carbonate, 0.1% formaldehyde (37% (v/v) solution), 4 ng mL^{-1} sodium thiosulfate] and the reaction stopped with 50% methanol-12% acetic acid. A final wash in 50% methanol for 30 min removed acetic acid. Gentle shaking of the gel occurred for all incubation and rinse steps.

4.2.7 Ruthenium II Barthophenanthroline Disulphate (RuBP) Staining of 1D SDS-Polyacrylamide Gels

Polyacrylamide gels were stained in RuBP based on the method described by Lamanda et al. (2004). Briefly, the gel was fixed in 30% ethanol-10% acetic acid for 15 h and then rinsed in 20% ethanol 4 x 30 min. The gel was incubated in 1 μM RuBPs (Sigma: Tris(bathophenanthrolinedisulfonate)ruthenium(II) sodium salt) solution for 6 h, equilibrated in water with two 10 min rinses, followed by destaining in 40% ethanol-10% acetic acid for 15 h. A final incubation in water for 10 min was performed and the gel was scanned using Typhoon 8600 [excitation at 532 nm, emission filter 610BP30] (Molecular Dynamics, USA). Gentle shaking of the gel occurred for all incubation and rinse steps.

4.2.8 Protein Concentration and/or Buffer Exchange

Amicon Ultra-4 centrifugal filter units were used for buffer exchange and concentration of protein solutions with centrifugation ≤ 4,000 *x g*, as directed by the manufacturer (Millipore, Australia).

4.2.9 Reduction of Recombinant HvTrx-*h*4 Proteins

To obtain monomer conformations of the mutant and wild-type recombinant HvTrx-*h*4 proteins, samples of interest were incubated with 10 mM DTT for 10 min at 65^{o}C.

4.2.9.1 Thioredoxin Activity Assay: Thioredoxin Catalysed Reduction of Insulin by Dithiothreitol (DTT)

The thioredoxin catalysis of insulin reduction was measured spectrophotomerically with POLARstar OPTIMA microplate reader (BMG Labtech, Australia) at 650 nm, 25^{o}C, every 30 sec for 60 minutes. As reduction proceeds a white precipitate forms, chiefly from the free β-chain of insulin which is released. Hence, there is a quantitative relationship between the rate of insulin disulfide reduction and the rate of precipitation (Holmgren, 1979). The assay consisted of 100 mM potassium phosphate, 2 mM EDTA pH 7.0 containing 0.85 mg insulin and varying concentrations of barley thioredoxin-*h*4 recombinant protein. The reaction was initiated by the addition of DTT to the reaction well at 0.35 mM final concentration.

4.2.10 Trapping of Proteins Interacting with HvTrx-*h*4

Trapping of proteins interacting with thioredoxin-*h*4 was based on the method described by Yamazaki et al. (2004). Several key variations of the protocol described below were implemented, as indicated in the results section 4.3.5.

4.2.10.1 Coupling of Recombinant HvTrx-h4 Protein to Sepharose

CNBr activated Sepharose 4B resin (Amersham Biosciences, USA) was swelled in 1 mM HCl. Using a sintered glass filter funnel, the resin was washed with 1 mM HCl, then coupling buffer [0.1 M NH_4HCO_3, 0.5 M NaCl, pH 8.3] and resuspended in coupling buffer. Mutant and wild-type recombinant HvTrx-*h*4 proteins in coupling buffer background (see 4.2.8), were incubated with the resin at 4^{o}C overnight with gentle mixing by inversion using a suspension mixer rotor (Ratek, Vic). The resin-bound thioredoxin complex was washed with coupling buffer 5 times for 2 min, to remove unbound protein. Centrifugation was performed at 200 *x g* for 1 min to sediment the resin complex. Remaining active groups on the resin were blocked by incubation with 0.1 M Tris-HCl pH 8.0 for 15 h at 4^{o}C with gentle mixing by inversion followed by two 2 min washes with coupling buffer. Any proteins already trapped to the resin-bound HvTrx-*h*4 were reduced by incubation in coupling buffer containing 10 mM DTT for 10 min at room temperature. The resin complex was again washed twice in coupling buffer. Finally, a series of 10 washes with buffers alternating between Buffer A [0.1

M $NaCH_3CO_2$, 0.5 M NaCl, pH 4.0] and coupling buffer were performed. The resin-bound thioredoxin complex was kept in coupling buffer until addition of plant protein extract.

4.2.10.2 Preparation of Plant Protein Extract

Approximately 300 mg of *H. vulgare* anthers and stigmas, at approximately 1 day pre-anthesis maturity stage, were collected using forceps, snap frozen and ground to a fine powder under liquid nitrogen. The tissue was resuspended in 10 mL of PBS (pH 7.5) containing protease inhibitors [10 μM Bestatin-HCl, 100 μM Leupeptin, 10 μM E64, 1 μM Pepstatin A, 10 mM 1,10 phenanthroline] (Sigma). The slurry was centrifuged at 7,000 *x g* for 30 min at 4°C (Avanti J-E, Beckmann Coulter, USA) to pellet the cellular debris. The supernatant was transferred by needle and syringe to Quick-Seal tubes (#342414; Ultra-Clear) and centrifuged at 100,000 *x g* in an Optima L-80 XP ultracentrifuge, using SW 55Ti or SW32 Ti rotors (Beckmann Coulter, USA), for 1 hour at 4°C. The resulting supernatant was concentrated as described in 4.2.8.

4.2.10.3 Collection of Immobilised Proteins Bound to HvTrx-h4

The thioredoxin-resin complex was gently mixed with the plant protein extract for 1 h at room temperature to allow protein interactions to occur. Resin-complexes were washed with Buffer B [20 mM NH_4HCO_3, 0.1% (w/v) SDS, pH 7.5] for 2 min, with sedimentation by centrifugation at 200 *x g* for 1 min, to remove non-specifically bound proteins. They were then washed with Buffer C [20 mM NH_4HCO_3, 0.2 M NaCl, pH 7.5] until the absorbance of the washed solution at 280nm was close to zero and steady (~7 times). Two final washes with Buffer D [20 mM NH_4HCO_3, pH 7.5] were performed to remove NaCl. The interacting proteins were eluted by suspending the resin in Elution Buffer [0.1M NH_4HCO_3, pH 8.5] containing freshly added 20 mM 2-mercaptoethanol, and gently mixing for 1 h at room temperature, followed by centrifugation at 200 *x g* for 1 min. The supernatant was collected, stored at 4°C and the elution repeated.

4.2.11 In-Gel Tryptic Cleavage of Proteins

Gel sections containing proteins of interest were excised from a RuBP stained polyacrylamide gel. Proteins were in-gel digested with sequencing grade modified trypsin (Promega, U.S.A.) as described by Natera et al. (2008) with some modifications. Gel slices were washed three times for 5 min with 100 mM NH_4HCO_3 and dehydrated by centrifugation under vacuum. The proteins were reduced by incubation in 10 mM DTT in 100 mM NH_4HCO_3 at 56 °C for 1 h, then alkylated with 55 mM iodoacetamide in 100 mM NH_4HCO_3 by incubation at room temperature for 45 min. Following dehydration with acetonitrile and centrifugation under vaccuum, the gel slices were rehydrated on ice in buffered trypsin [12.5 ng trypsin per 1 µl 100 mM NH_4HCO_3] for 30 min. Excess buffered trypsin solution was replaced with 100 mM NH_4HCO_3 and the proteins continued to be digested overnight at room temperature. For all following incubations, supernatants were collected. Peptides were extracted by incubation of the gel pieces at room temperature with shaking for 15 min, twice with 50% acetonitrile in 5% formic acid (v/v) and twice with 100% acetonitrile. Rehydration of the gel pieces was achieved by incubation in 100 mM NH_4HCO_3 in between each of the acetonitrile treatments. All supernatants were pooled and the final volume was reduced to 10–20 µl under a vacuum. The resulting sample solution was reconstituted in 0.1% (v/v) formic acid to 60 µl and filtered through a 0.20 µM Minisart RC4 single use syringe filter (Sartorius, Germany) prior to LC-MS/MS analysis.

4.2.12 In-Solution Tryptic Cleavage of Proteins

In-solution digests were carried out as described by Natera et al. (2008). Protein pellets were resuspended in 8 M urea before being reduced and alkylated as described for the in-gel digest (see 4.2.11). Urea concentration was reduced to <1 M with 100 mM NH_4HCO_3 before overnight trypsin digestion at 37°C. The pH was adjusted to 3 with 100% formic acid and the tryptic peptides were passed over a C18 SepPak column (Waters, U.S.A.) and concentrated under vacuum to a final volume of 100 µl. To the concentrated tryptic peptides Buffer A [25 mM ammonium formate in 5% (v/v) acetonitrile] was added and they were separated on a PolySulfoethyl Aspartamide SCX column® [4.6 mm × 200 mm, 5 µM, 300 Å-1] (PolyLC Inc., U.S.A.) attached to an Agilent 1100 series HPLC system (Agilent Technologies, U.S.A.) with the following separation gradient: Buffer A for 10 min then up to 100% Buffer B [500 mM ammonium formate in 25% (v/v) acetonitrile] over 30 min; 100% Buffer B for an additional 30 min, then back to 100% Buffer A over 10 min, at a flow rate of 0.7 mL min^{-1}. Fractions were collected every 30 sec and reduced to 10–20 µL under a vacuum. Each fraction was resuspended in 60 µl of 0.1% formic acid and analysed by LC-MS/MS.

4.2.13 Mass Spectrometry

MS and MS/MS data was acquired using a nanospray source on a QStar XL hybrid quadrupole-TOF LC-MS/MS (Applied Biosystems/MDS Sciex, U.S.A.) using the AnalystQS software (Applied Biosystems/MDS Sciex) operating in a data-dependent acquisition mode. This software was also used to process the spectra prior to database searching.

4.2.14 Data Analysis and Informatics

Protein identification was achieved by comparing the MS/MS spectra against the green plants subset of the NCBI non-redundant (nr) protein database. Mascot software (Perkins et al., 1999) (Matrix Science, U.K.) run on an in-house server was also used for database searches. The parameters used for initial Mascot searches were as follows: Database - NCBInr (2503385 sequences; 849188404 residues); Taxonomy - Viridiplantae (179913 sequences); Enzyme - trypsin; Fixed modifications - carbamidomethyl; Variable modifications - oxidized methionine; Peptide mass tolerance - ±0.25 Da; Mass values - monoisotopic; Maximum missed cleavages - up to 1 missed cleavage site; Fragment mass tolerance - ±0.15 Da.

4.3 Results

4.3.1 Generation and Purification of Wild-type and Mutant Recombinant Barley Thioredoxin-*h*4 Proteins

Mutation of the second cysteine in the thioredoxin-*h*4 active site (WCGPC) to a serine was achieved through site-directed mutagenesis. Specifically designed primers (Table 4-1) successfully introduced a single base mutation at the cDNA level, changing the codon TGC to TCC, resulting in the desired amino acid change in the expressed protein (Figure 4.3). PCR primers were also used to introduce restriction sites to the start (SphI) and end (BglII) of both the mutated and wild-type thioredoxin-h4 cDNA sequences. These restriction sites enabled ligation of the sequences, in the correct frame, into the expression vector pQE-70. The resulting constructs were independently transformed into *E. coli* strain M15 and protein expression was induced. The resulting histidine-tagged wild-type and mutant recombinant thioredoxin-*h*4 proteins were purified using unbound nickel-nitrilotriacetic acid (Ni-NTA) metal-affinity chromatography matrices. The native, purified proteins, approximately 14 kDa in size, were visualised on 12% polyacrylamide, biscine-tris, Coomassie blue stained gels (Figure 4.4).

```
  1 atgggggctgtgtgggcaagggtcgtggcattgtggaagaaaagcttga 50
  1 M  G  G  C4 V  G  K  G  R  G  I  V  E  E  K  L  D  17

 51 tttcaaaggtggaaatgtgcatgtcataacaaccaaagaggactgggacc 100
 18  F  K  G  G  N  V  H  V  I  T  T  K  E  D  W  D  Q 34

101 agaagattgaagaagcaaacaaggatgggaaaattgttgtagcaaacttc 150
 35   K  I  E  E  A  N  K  D  G  K  I  V  V  A  N  F   50

151 agtgcttcgtggtgtgggccatgccgtgtcattgcacctgtttatgctga 200
 51 S  A  S  W  C55 G  P  C58 R  V  I  A  P  V  Y  A  E  67

201 gatgtccaagacttatcctcaactcatgttcttgacaattgatgttgatg 250
 68  M  S  K  T  Y  P  Q  L  M  F  L  T  I  D  V  D  D 84

251 acctaatggatttcagctcaacatgggacatccgcgcaaccccgacgttc 300
 85   L  M  D  F  S  S  T  W  D  I  R  A  T  P  T  F   100

301 ttcttcctcaaaaacggccagcagatcgacaagctcgtcggcgccaacaa 350
101 F  F  L  K  N  G  Q  Q  I  D  K  L  V  G  A  N  K  117

351 acccgagctggagaagaaagtgcaagctcttggtgatggcagttga 396
118  P  E  L  E  K  K  V  Q  A  L  G  D  G  S  *   131
```

Figure 4.3: ***Hordeum vulgare thioredoxin-h4* cDNA (black) and amino acid (brown) sequences.** The active site, including mutation target-site, is highlighted red. The TGC codon was changed to TCC using site-directed mutagenesis and is highlighted blue. The additional amino terminal cysteine, unique to cytosolic thioredoxin class 4, is highlighted green.

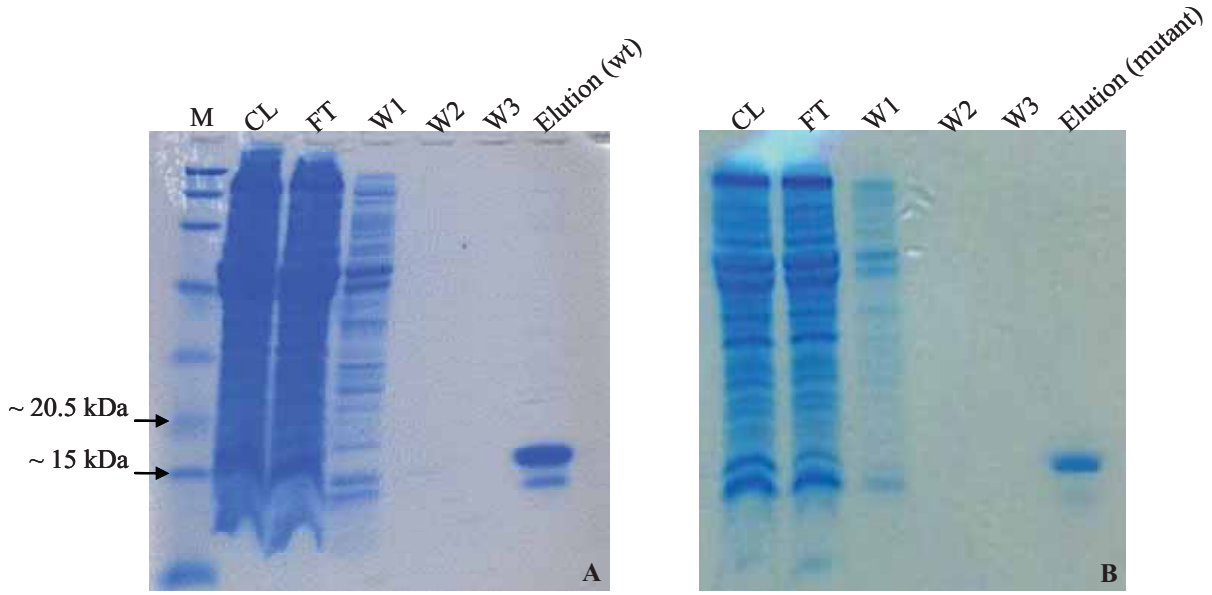

Figure 4.4: **Purification of wild-type (A) and mutant (B) thioredoxin-*h*4 recombinant proteins.** Recombinant thioredoxin-*h*4 proteins were expressed in *E. coli* and purified using Ni-NTA matrices. BroadRange Marker (M); cleared lysate (CL); flow-through following protein binding to matrix (FL); 1st wash solution (W1); 2nd wash solution (W2); 3rd wash solution (W3); eluted, purified thioredoxin-*h*4 recombinant protein (Elution).

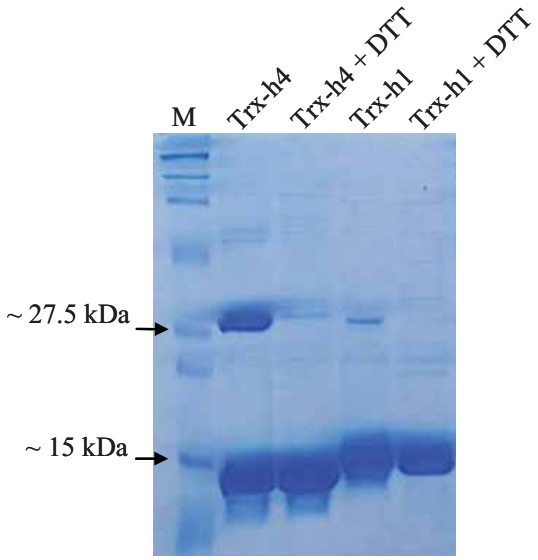

Figure 4.5: **Thioredoxin-*h*4 protein dimers are more prevalent than thioredoxin-*h*1 protein dimers.** Recombinant thioredoxin-*h*1 and -*h*4 proteins, purified by the same process and stored in the same conditions, were visualised before and after treatment with 10 mM DTT. Reduction with DTT results in a decrease in the dimer form. BroadRange Marker (M); Recombinant HvTrx-*h*4 (lane 1); Recombinant HvTrx-*h*4 treated with DTT (lane 2); Recombinant HvTrx-*h*1 (lane 3); Recombinant HvTrx-*h*1 treated with DTT (lane 4)

4.3.2 Dimerisation of Recombinant Barley Thioredoxin-*h*4 Protein

A second, higher molecular weight protein band in the purified recombinant thioredoxin-*h*4 protein samples was observed on Coomassie stained polyacrylamide gels (Figure 4.5 and Figure 4.7). This band was present in both the wild-type and mutant forms following storage at -20^{o}C and became more intense when the sample was repeatedly frozen and thawed. The additional protein band of approximately 28 kDa matches the predicted size of a recombinant thioredoxin-*h*4 homodimer. To test the supposition that the 28 kDa protein is a thioredoxin-*h*4 homodimer, the purified protein samples were treated with 10 mM DTT. Consistent with the upper band comprising dimerised HvTrx-*h*4, there was a decrease in concentration of the 28 kDa protein corresponding to an increase in the 14 kDa HvTrx-*h*4 monomer following DTT treatment (Figure 4.5). The concentration of DTT required to successfully reduce the majority of the dimers present was determined using a DTT concentration gradient treatment (Figure 4.6).

It was observed that dimer formation did not occur to the same extent in purified samples of recombinant thioredoxins, -*h*1 -*h*2 and -*h*3. The relative abundance of homodimer present in purified samples of HvTrx-*h*4 and HvTrx-*h*1 is given in Figure 4.5. The result shown for thioredoxin-*h*1 (Figure 4.5) was found to be representative of thioredoxins-*h*2 and -*h*3 (*data not shown*). All thioredoxins were expressed, purified and stored in the same manner. It is speculated that the extra, unique cysteine present in the amino terminus (Cys_4) of thioredoxin-*h*4 is, at least in part, facilitating its homodimerisation.

For use in the trapping of interacting proteins, it is essential that both wild-type and mutant HvTrx-*h*4 recombinant proteins are in the active form. Reduction of the dimer results in an increased binding capacity of the thioredoxin protein (Buchanan and Balmer, 2005). Consequently, the purified, native samples were treated with 10 mM DTT immediately prior to their use in protein trapping experiments, to obtain a higher proportion of the protein in the active, monomer conformation (Figure 4.7).

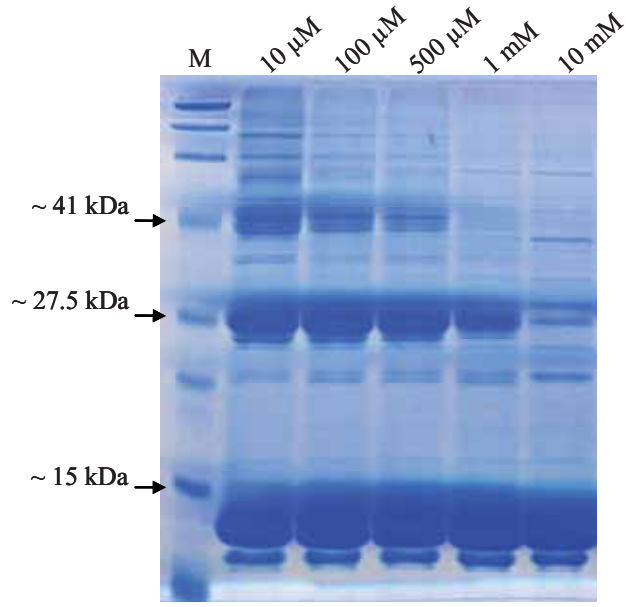

Figure 4.6: **Determination of DTT concentration required to reduce thioredoxin-*h* dimers.** Recombinant thioredoxin-*h* protein was treated with 10 µM to 10 mM DTT for 10 min at 65°C. Broad Range Marker (M); 10 µM DTT (lane 1); 100 µM DTT (lane 2); 500 µM (lane 3); 1 mM (lane 4); 10 mM DTT (lane 5)

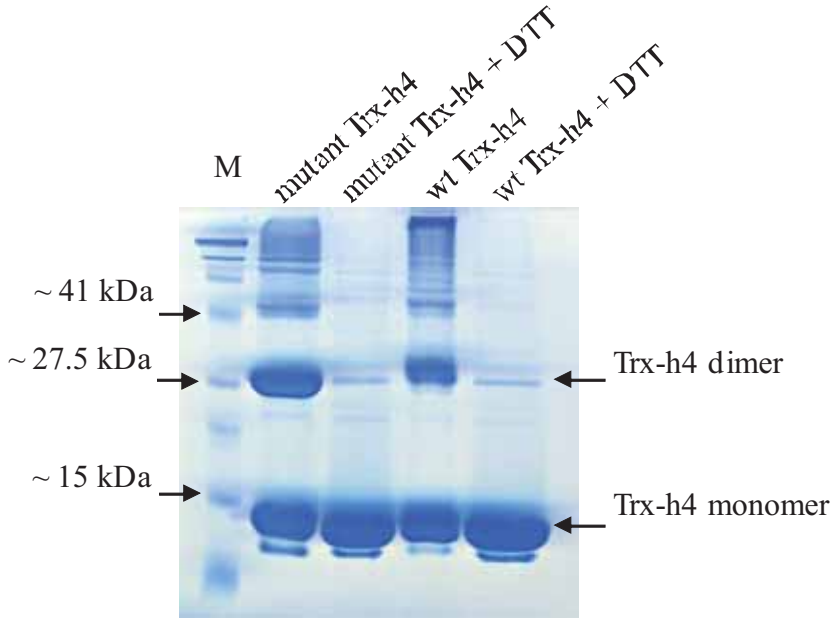

Figure 4.7: **Acquisition of thioredoxin-*h*4 protein in the active conformation (monomer).** Mutant and wild-type recombinant proteins were treated with 10 mM DTT, at 65°C for 10 min, to obtain a higher proportion of the protein in monomer form. Broad Range Marker (M); Mutant recombinant HvTrx-*h*4 (lane 1); Mutant recombinant HvTrx-*h*4 treated with DTT (lane 2); Wild-type recombinant HvTrx-*h*4 (lane 3); Wild-type recombinant HvTrx-*h*4 treated with DTT (lane 4)

4.3.3 Additional Low Molecular Weight Protein in Purified Thioredoxin-*h*4 Samples

Despite rigorous purification, a lower band of approximately 13 kDa resolving just under the HvTrx-*h*4 monomer was always obtained (Figure 4.6 and Figure 4.7). The lower molecular weight band was purified from both wild-type and mutant thioredoxin-*h*4 protein preparations, as seen in Figure 4.7. The lower protein band is not seen following expression and purification of other recombinant proteins, including thioredoxins-*h*1 (Figure 4.5), -*h*2 and -*h*3 (*data not shown*), using the same expression vector, *E. coli* strain and procedures. Three possibilities for the presence of the lower molecular weight band in HvTrx-*h*4 recombinant samples exist; it is a contaminant, a truncated form of HvTrx-*h*4 or a post-translationally modified form of HvTrx-*h*4.

Investigations were firstly conducted using a monoclonal anti-polyHistidine antibody (Sigma). The protein bands were transferred to a nitrocellulose membrane and both the higher and lower molecular weight were detected by the anti-polyHistidine antibody (Figure 4.8A). This result indicates the lower molecular weight protein contains a polyhistidine sequence, as it is also being purified by the Ni-NTA matrices. Next, the hypothesis that the smaller protein is a modified form of HvTrx-*h*4 was investigated using Western hybridisation with a polyclonal antibody raised against thioredoxin-*h*4. Both the higher and lower molecular weight bands were detected by the thioredoxin-*h*4 specific antibody (Figure 4.8B), which indicates each band contains HvTrx-*h*4 protein.

To determine whether the HvTrx-*h*4 protein present in the lower molecular weight band was a truncated form, the proteins were excised and subjected to N-terminal Edman degradation sequencing. Protein in solution, not separated by SDS-PAGE, was also sent for analysis. Unfortunately, the sequencing was unsuccessful due to contamination with the full-length thioredoxin-*h*4 protein. Complete separation of the differing proteins was endeavoured but never successful. However, if the smaller protein is a truncated form of HvTrx-*h*4, the anti-polyHistidine Western analysis result indicates the N-terminus is lost, considering the his-tag is located at the C-terminus of the protein (Figure 4.2).

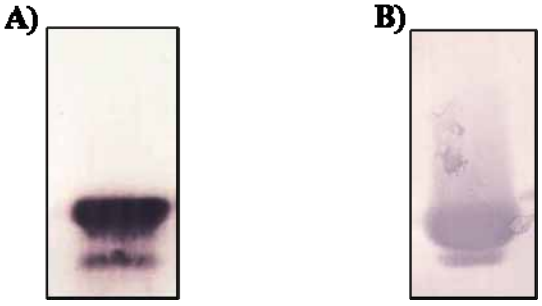

Figure 4.8: **Immunodetection of his-tagged and thioredoxin-*h*4 proteins.** Purified (his-tag) recombinant proteins were resolved by SDS-PAGE, transferred to nitrocellulose and probed with specific antibodies. A) Immunodetection of proteins containing multiple, successive histidines. The membrane was probed with monoclonal anti-polyhistidine clone His1 antibody (Sigma). Both upper and lower molecular weight bands were detected in the purified HvTrx-*h*4 sample. B) Immunodetection of thioredoxin-*h*4 proteins. The membrane was probed with a thioredoxin-*h*4 specific antibody. Both upper and lower molecular weight bands were detected in the purified HvTrx-*h*4 sample.

4.3.4 Thioredoxin-*h*4 Activity Assays: Reduction of Disulphides in Insulin.

Thioredoxin is able to catalyze the non-specific reduction of insulin disulfides by the reducing agent dithiothreitol (DTT) (Holmgren, 1979). To ensure the HvTrx-*h*4 recombinant proteins were active and able to participate in redox reactions despite the additional histidine-tag attached, the ability of recombinant thioredoxin-*h*4, in the wild-type form, to reduce insulin disulfides following reduction by DTT was evaluated. As seen in Figure 4.9, recombinant HvTrx-*h*4 protein is able to reduce disulfides in insulin after the addition of DTT. This confirms the protein is active and that the histidine-tag does not interfere with thioredoxin-*h*4 function. In addition, the rate of insulin reduction increased as a function of thioredoxin concentration (Figure 4.9).

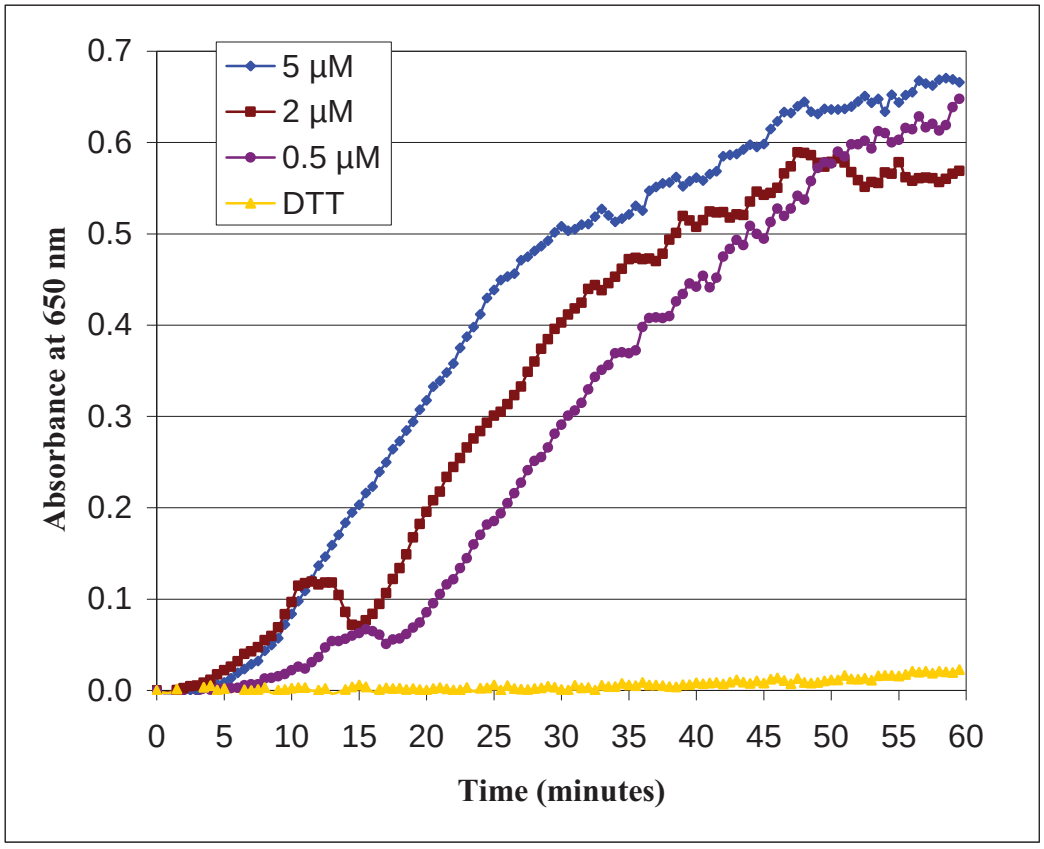

Figure 4.9: **The reduction of insulin by recombinant barley thioredoxin-*h*4 protein.** Insulin reduction by different concentrations of HvTrx-*h*4 (0.5, 2 and 5 µM) was measured spectrophotomerically at 650 nm and recorded every 30 seconds for 60 minutes. Reduction of insulin by DTT in the absence of HvTrx-*h*4 served as a control. Data courtesy of Juan Juttner, ACPFG, University of Adelaide *(unpublished)*.

4.3.5 Isolation of Proteins Interacting with Barley Thioredoxin-*h*4

Figure 4.10 illustrates the theory underpinning the CNBr activated resin affinity chromatography experiment attempted. Several variations to the method described in 4.2.10 were attempted. Initial experiments used a different set of buffers to those described (4.2.10) and half the amount of CNBr-activated resin was used. A quarter of the amount of HvTrx-*h*4 was incubated with the resin and the coupling buffer contained 100 mM sodium carbonate instead of 100 mM ammonium bicarbonate. The thioredoxin:resin coupling was allowed to proceed for 2 h. In addition, wash buffers B and C contained 20 mM Tris-HCl instead of 20 mM ammonium bicarbonate. Also, there were no wash buffer D steps. Elution was performed with 20 mM Tris-HCl, 200 mM NaCl and 10 mM DTT at pH 7.5, compared to 100 mM ammonium bicarbonate pH 8.5 containing 20 mM 2-mercaptoethanol as described in 4.2.10. Young, green leaf tissue supplied the source of target proteins. Unfortunately, no proteins potentially interacting with HvTrx-*h*4 were isolated with this affinity chromatography procedure. Only protein bands corresponding to Rubisco sub-units were visible on the Coomassie stained polyacrylamide gels.

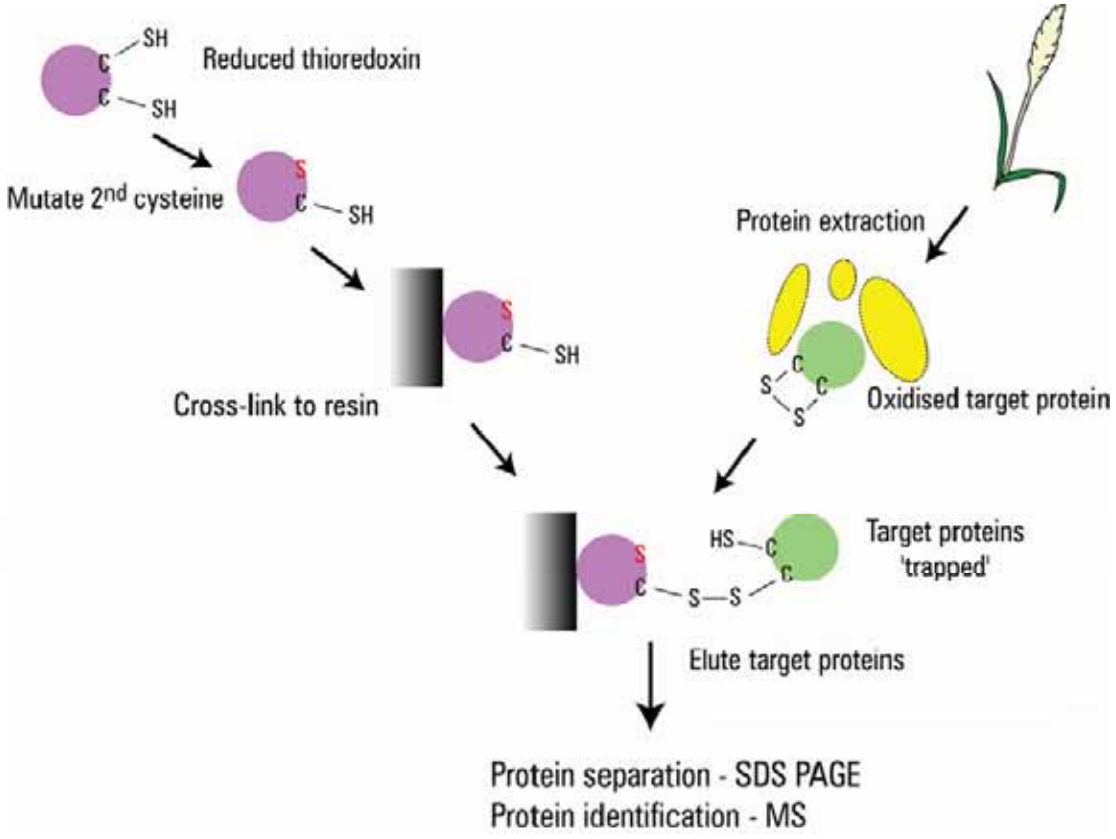

Figure 4.10: **Diagrammatic representation of the technique used to isolate proteins interacting with thioredoxin-*h*4.** Method based on that by Yamazaki et al. (2004) with thioredoxin-*h*4 protein directly immobilised to resin.

It was speculated that leaves were not an ideal tissue to use as the high quantity of Rubisco in this tissue appeared to saturated the eluted proteins, thereby 'swamping out' other possible interacting proteins. Therefore, alternative non-green tissues were considered. It was decided that barley anthers and stigmas would be suitable, collected at the 5 to 1 day(s) pre-anthesis stages of development, considering QPCR data obtained showed relatively high levels of HvTrx-*h*4 expression in these tissues at these stages (see Chapter 5). The first version of the protocol was again attempted with the anthers and stigmas providing the source of target proteins.

Figure 4.11A presents the Coomassie stained polyacrylamide gel showing the absence of interacting proteins in the mutant HvTrx-*h*4 bait sample elution. To visualise protein bands present in lower concentrations, SDS-PAGE was repeated and silver staining was performed as it has increased protein staining sensitivity. This resulted in the appearance of several discrete protein bands potentially containing proteins interacting with HvTrx-*h*4 (Figure 4.11B). However, despite the absence of Rubisco and the presence of protein bands, the affinity chromatography was again deemed unsuccessful. This was because the same protein bands were visible in both the wild-type and mutant HvTrx-*h*4 bait samples (Figure 4.11B). Although there appeared to possibly be some proteins bands unique to the mutant HvTrx-*h*4, they were at such a low concentration that unfortunately, identification by mass spectrometry was unsuccessful. Consequently, the experimental protocol was reviewed and modifications made, resulting in the method described in 4.2.10.

The modified protocol (4.2.10) incorporated additional resin and thioredoxin protein with the aim of increasing the quantity of resin:thioredoxin complexes forming, and thereby increasing the quantity of each protein type trapped and eluted, which would allow for easier visualisation and subsequent identification. The buffer modifications attempted to reduce the washing stringency to prevent unintentional removal of proteins interacting with the mutant thioredoxin, which may have been occurring previously whilst also attempting to remove non-specific interactions. A final wash in 20 mM ammonium bicarbonate was added to remove salts and further remove potentially remaining non-specific interactions. Barley anthers and stigmas collected at the 5 to 1 day(s) pre-anthesis stages of development again supplied the source of target proteins. In addition, a resin-only control sample was introduced to verify that the resin was being sufficiently blocked by 100 mM Tris-HCl (pH 8) as recommended by the resin manufacturers.

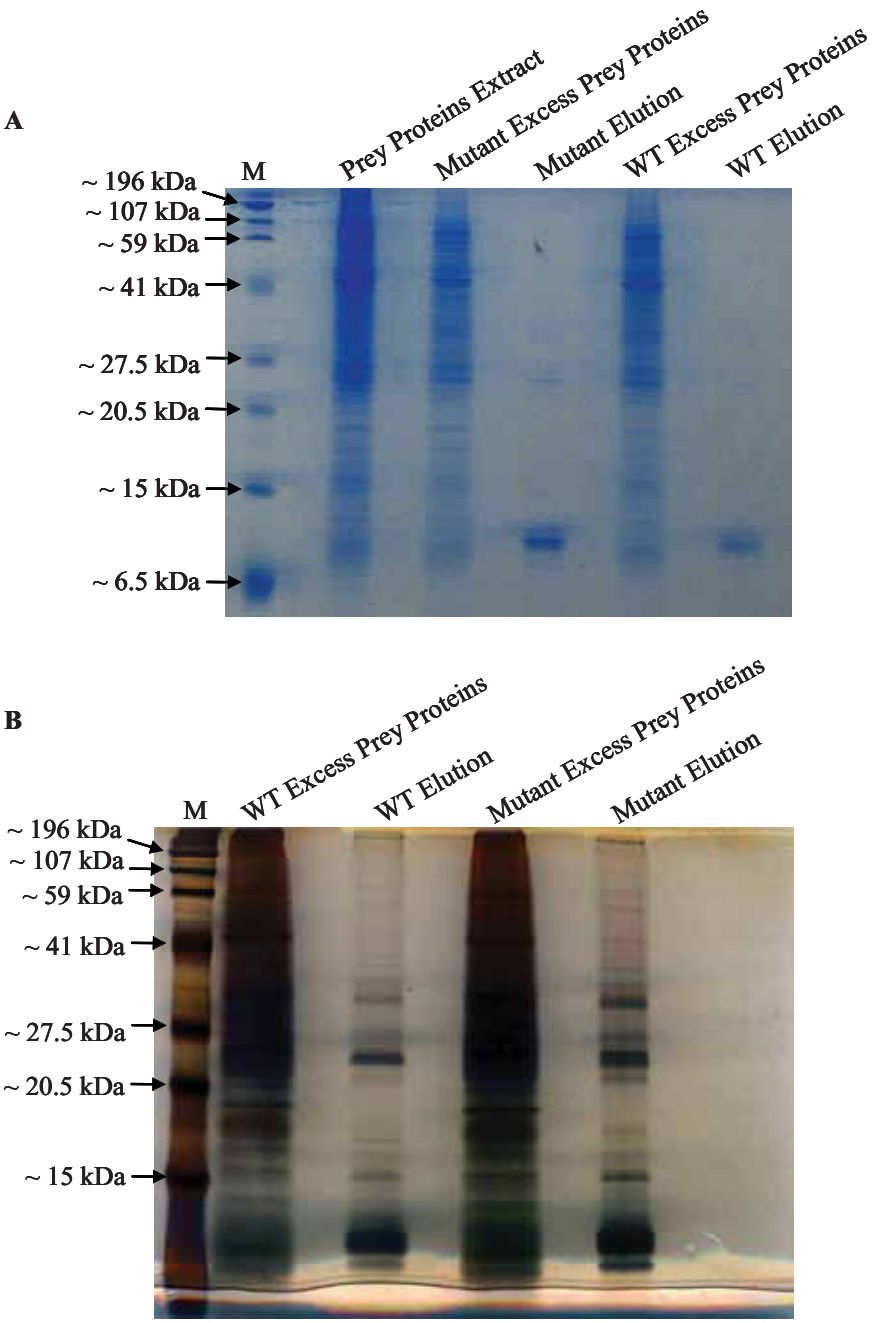

Figure 4.11: **Visualisation of proteins potentially interacting with thioredoxin-*h*4.** Proteins trapped to mutant and wild-type thioredoxin-*h*4 protein:resin bait complexes were released (elutions), resolved by SDS-PAGE [12%] and stained with Coomassie brilliant blue **(A)** or sodium thiosulfate/silver nitrate **(B)**. Initial anther/stigma extract of prey proteins, and excess prey proteins recovered immediately following incubation with bait complexes, are also shown. Invitrogen BenchMark Protein Ladder (M).

Figure 4.12 shows the proteins successfully trapped and eluted following the modified method. Proteins were separated by SDS-PAGE on a 12% polyacrylamide large format gel and visualised by staining with Ruthenium II Barthophenanthroline Disulphate (RuBP). Each well held 150 µl of sample which equated to approximately 12 µg of proteins interacting with wild-type HvTrx-*h*4, 18 µg of proteins interacting with mutant HvTrx-*h*4 and 4 µg of proteins eluted from the resin-only control sample. Interestingly, quite a lower concentration of proteins was eluted from the resin-only control sample compared to the mutant and wild-type thioredoxin-*h*4 samples. Thirty one gel sections of bands containing proteins of interest were excised (Figure 4.12), the proteins digested with trypsin and identified by mass spectrometry. Table 4-2 contains a list of the identified proteins in each band per sample. A portion of the elution collected for each sample was directly analysed by mass spectrometry and the resulting proteins identified are listed in Table 4-3.

As expected, HvTrx-*h*4 was present in both the wild-type and mutant samples but not the resin-only control sample, for both gel and liquid elution samples (Tables 4-2 and 4-3). It is likely that the elution process dislodged a small proportion of the bound recombinant thioredoxin-*h*4 proteins from the resin. Alternatively, endogenous thioredoxins-*h* present in the bait protein source may have formed dimers with the resin bound recombinant thioredoxins-*h*4, which were subsequently eluted. Dimerisation of subclass 4 cytosolic thioredoxins was previously observed (Figure 4.5).

All proteins trapped by mutant recombinant HvTrx-*h*4, except for tubulin and elongation factor-1β, were also trapped by the wild-type recombinant HvTrx-*h*4 (Tables 4-2 and 4-3). This may indicate the majority of the isolated proteins were not interacting with HvTrx-*h*4 exclusively through its active site. Tubulin and elongation factor-1β were also found in the resin-only control.

Proteins identified exclusively in the HvTrx-*h*4 wild-type and mutant samples were *H. vulgare* homologues of: profilin 2/4, a 14-3-3A like protein, a 14-3-3b and a protein similar to a Group V allergen precursor. Although a pollen allergen precursor was identified only in the mutant thioredoxin-*h*4 sample of the liquid digests (Table 4-3), it was also found in gel band slices of wild-type and control samples (Table 4-2). In addition, the 14-3-3 proteins were identified in gel slices (14-3-3b) and liquid fractions (14-3-3A like) and are perhaps in fact the same protein. Similarly, a profilin was identified from both gel and liquid but assigned as profilin 3 and profilin 2/4 respectively, but profilin 3 was also found in the resin-only control. The remainder of the isolated proteins were also present in the resin-only control samples

(Tables 4-2 and 4-3). Hence, the majority of proteins appear to be interacting with the resin and not HvTrx-*h*4, mutant or wild-type.

Results from both protein trapping methods indicate unsuitable washing steps were performed and that there are problems with the non-specific binding of proteins to the resin. The wash steps were too rigorous, removing the proteins isolated by HvTrx-*h*4. Yet the results also indicate that the wash steps were not stringent enough, considering the large number of bands common to all samples including the control (Figure 4.12,Tables 4-2 and 4-3). Consequently, to attempt to achieve a suitable washing stringency, a third adaptation of the method was made using 20 mM Tris-HCl based washes but fewer of them. The coupling buffer remained the same (100 mM ammonium bicarbonate) but the wash steps were executed as alternate washes with 20 mM Tris-HCl / 200 mM NaCl and 20 mM Tris-HCl / 0.1% (w/v) SDS. The final desalting wash was omitted. To combat the problem of unspecific binding of proteins to the resin, the blocking step was modified to occur for 6 h longer with 200 mM Tris-HCl. In addition, an extra control was introduced consisting of the mutant thioredoxin-*h*4 protein bound to the resin and then the cysteines inhibited with iodoacetamide. Unfortunately, this method was also unsuccessful as no proteins were ever recovered in any of the elutions, for any of the four samples, despite several attempts made.

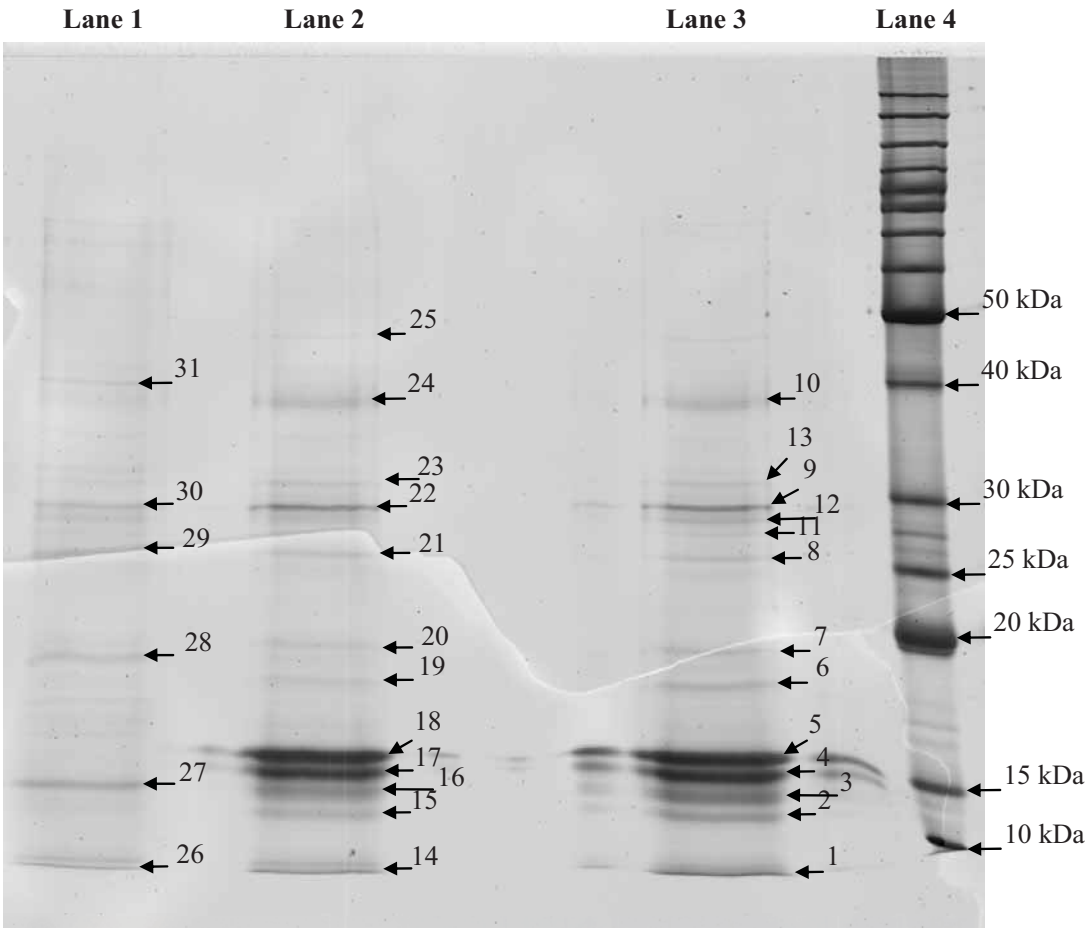

Figure 4.12: **Visualisation of proteins potentially interacting with thioredoxin-*h*4.** Proteins trapped to wild-type (lane 2) and mutant (lane 3) thioredoxin-*h*4 proteins, or resin-only control (lane 1), were released and separated by SDS-PAGE [12%]. Bands were numbered (1-31) and excised for further analysis. BenchMark Protein Ladder (lane 4)

Table 4-2: **Identification of proteins in bands labelled in Figure 4.12.** Following separation of proteins by SDS-PAGE, bands were excised and proteins digested. Samples were analysed by mass spectrometry and the Mascot software was employed to identify the peptides. Elution from the 'resin only' sample served as a control.

Identified Protein	Accession #	Band # & Sample Origin		
		Mutant	Wild-type	Resin only
Thioredoxin h-like protein [Hordeum vulgare]	gi|24637225	2, 4, 5	15, 17, 18	×
Similar to Peroxiredoxin, complete: UP|Q7F529	TC146841	6	19	×
Hv14-3-3b [Hordeum vulgare]	gi|1070354	13	23	×
Profilin 3 [Phleum pratense]	gi|2415700	3	16	27
Similar to AT3g52500/F22O6_120, partial (7%): UP|Q93ZE7 BLAST: match to Bet v I allergen [Zea mays]	TC146785 gi|54111527	7	20	28
Homologue to Dehydroascorbate reductase, complete: UP|Q84UH6	TC139245	8	21	29
Cytosolic triosephosphate isomerase [Hordeum vulgare] complete: GB|AAB41052.1|	TC131409	8	21	29
Pollen allergen precursor [Hordeum vulgare]	gi|1808987	9, 11, 12	22	30
14-3-3 protein homologue [Hordeum vulgare]	gi|22607	9, 12	22	30
Homologue to Fructose 1,6-bisphosphate aldolase, complete: UP|Q6QWQ3	TC146546	10	24	31
Similar to Pollen allergen KBG 41 precursor (Poa p 9): UP|MP92_POAPR (P22285)	TC143169	10	24	31
Homologue to Adenosine kinase-like protein (Fragment), partial (91%): UP|Q84P58	TC131518	10	24	31
No proteins identified in bands analysed	-	1	14, 25	26

Table 4-3: **Identification of proteins in liquid elution fractions.** Following the interacting-proteins trapping procedure, eluted proteins were digested and samples were analysed by mass spectrometry. The Mascot software was employed to identify the peptides. Elution from the 'resin only' sample served as a control.

Identified Protein	Accession #	Sample Origin		
		Mutant	Wild-type	Resin only
Pollen allergen precursor [Hordeum vulgare]	gi|1808987	✓	×	×
Thioredoxin h-like protein, complete: UP|Q8GZR4	TC147156	✓	✓	×
Similar to Group V allergen precursor, partial (91%): UP|O81341	TC133595	✓	✓	×
Homologue to Profilin 2/4 complete: UP|PRO2_PHLPR (Pollen allergen Phl p 11/12)	TC139883	✓	✓	×
14-3-3-like protein A, complete: UP|143A_HORVU	TC139070	✓	✓	×
Similar to Peroxiredoxin, complete: UP|Q7F529	TC146841	✓	✓	✓
Homologue to Dehydroascorbate reductase, complete: UP|Q84UH6	TC139245	✓	✓	✓
Unknown Protein	TC147240	✓	✓	✓
Homologue to Elongation factor 1-beta, complete: UP|EF1D_WHEAT	TC138855	✓	×	✓
Tubulin alpha-2 chain, complete: UP|TBA2_HORVU	TC131375	✓	×	✓
Homologue to Fructose 1,6-bisphosphate aldolase, complete: UP|Q6QWQ3	TC146546	×	✓	✓
Similar to Pollen allergen KBG 41 precursor (Poa p 9): UP|MP92_POAPR	TC142638	×	✓	×

4.4 Discussion

4.4.1 Homodimerisation of Recombinant Barley Thioredoxin-*h*4 Protein

Members of subclass 4 can readily be distinguished from other grass thioredoxins-*h* in part by the presence of a conserved cysteine at position 4 in the mature protein (Juttner, 2003). It is speculated this unique cysteine is facilitating homodimerisation of the recombinant HvTrx-*h*4 which is seen in Figure 4.5. Non-active site thiols in mammalian thioredoxins have been found to form a disulfide bridge between two thioredoxin molecules (Weichsel et al., 1996). Dimerisation of thioredoxins in plants has also been reported previously. A spinach thioredoxin-*f* containing a conserved surface exposed cysteine at position 73, C-terminal to the active site motif, was found to form covalent homodimers (Del Val et al., 1999; Kamo et al., 1989). The spinach thioredoxin-*f* dimer was more abundant in samples that were repeatedly frozen, which was also observed for recombinant HvTrx-*h*4 in this study. In further investigations a mutational variant of thioredoxin-*f*, where Cys_{73} was replaced with a serine, alanine or glycine, prevented the formation of covalent homodimers (Del Val et al., 1999). This demonstrated that the dimer forms through a disulfide linkage involving Cys_{73} (Del Val et al., 1999). Perhaps Cys_4 in HvTrx-*h*4 is also involved in the formation of disulfide bonds, leading to HvTrx-*h*4 homodimers.

Interestingly, the dimer formation of the spinach thioredoxin-*f* could be reversed by incubation with reduced glutathione. Del Val et al. (1999) speculated that *in vivo*, reduced glutathione in the chloroplast might prevent the formation of dimers. It is plausible that this phenomenon may also occur for HvTrx-*h*4 in the cytoplasm, given the glutathionylation data obtained and outlined in Chapter 5.

A recent study by Koh et al. (2008), centred on a poplar thioredoxin-*h* (PtTrx-*h*4) that contains an N-terminal cysteine, further supports the proposed linkage of dimerisation with Cys_4. PtTrx-*h*4 and HvTrx-*h*4 have high sequence similarity (61% identity) and the extra cysteine is at amino acid position 4 in both proteins (Appendix A), suggesting that they are orthologous sequences. Koh et al. (2008) found that reducible dimers were present in wild-type PtTrx-*h*4 as well as Cys_{58}Ser and Cys_{61}Ser mutant forms, containing substitutions of the first or second cysteine in the active site motif, respectively. Koh et al.'s (2008) Cys_{61}Ser mutant corresponds to the mutant HvTrx-*h*4 (Cys_{58}Ser) in this study and they appear to behave the same way with respect to dimerisation. Koh et al.'s (2008) Cys_{61}Ser mutant dimers were in high abundance and disappeared under reducing conditions, which indicates the presence of intermolecular disulfide bonds (Koh et al., 2008). Significantly, only monomers

were observed for the Cys_4Ser PtTrx-*h*4 mutant in the absence of DTT. Considering the study by Koh et al. (2008), it is highly likely that the presence of the extra amino-terminal cysteine in HvTrx-*h*4 is indeed responsible for the formation of homodimers. Moreover, the presence of dimers in both wild-type and mutant HvTrx-*h*4 forms (Figure 4.7) coupled with the PtTrx-*h*4 structure showing the 2nd active site cysteine is buried within the protein (Koh et al., 2008), it is likely that the dimers occur *via* a Cys_4 and the first cysteine in the active site motive (Cys_{55}) and/or two Cys_4 residues.

4.4.2 Modified Form of Recombinant Barley Thioredoxin-*h*4 Protein

Two protein bands, slightly smaller than the predicted size of the recombinant thioredoxin-*h*4 protein, were seen on Coomassie stained polyacrylamide gels (Figures 4.4- 4.7). Both bands were detected by a barley thioredoxin-*h*4 specific antibody (Figure 4.8B) which indicates each band contains HvTrx-*h*4 protein. A commercial antibody raised against a recombinant polyHistidine tagged fusion protein also detected both protein bands (Figure 4.8A). This antibody specifically recognises native and denatured, reduced forms of polyhistidine tagged fusion proteins such as those expressed using the pQE vectors (Qiagen). Therefore, I am confident the antibody is detecting the polyhistidine tail attached to the C-terminus of recombinant thioredoxin-*h*4. These two observations together suggest that a modified form of recombinant HvTrx-*h*4 may be present. Recombinant HvTrx-*h*4 was cloned to contain polyhisitidines at the carboxy-terminus of the protein. Therefore, if the smaller protein band is a truncated form of HvTrx-*h*4, the truncation must be at the amino-terminus of the protein for it to be detected by the anti-polyhistidine antibody.

Truncation of thioredoxins has been previously reported in the literature. A human cytosolic 10 kDa truncated thioredoxin (Trx80) was discovered, lacking the last 20-24 amino acids at the C-terminus (Silberstein et al., 1989). Macrophages have been reported to cleave the 12 kDa full-length thioredoxin to yield the truncated form (Newman et al., 1994). In contrast to the full length thioredoxin, Trx80 is a potent mitogenic cytokine (Pekkari et al., 2003). Trx80 is also commonly seen as a dimer and lacks reductase activity, unlike the full-length thioredoxin (Pekkari et al., 2003). The Trx80 dimer forms *via* non-covalent interactions (Pekkari et al., 2003) which is in contrast to the HvTrx-*h*4 dimerisation hypothesis (see 4.4.1), where it is speculated that intermolecular disulphide bonds are involved. However, perhaps the truncated version of HvTrx-*h*4 behaves and functions differently to the full-length form, just as Trx80 does. One key difference between the putative truncated HvTrx-*h*4 and Trx80 is

the location of truncation, N-terminal and C-terminal respectively, and perhaps this is significant, if it also occurs *in planta*.

Laloi et al. (2001) reported on an *A. thaliana* thioredoxin, AtTrx-*o*1, which is targeted to the mitochondrial matrix *via* its cleavable N-terminal signal. When aligned with HvTrx-*h*4 it is clear that despite the truncation of AtTrx-*o*1 following import, none of the 'true' thioredoxin protein is removed (Appendix A). HvTrx-*h*4 has 63 residues fewer than AtTrx-*o*1, the majority of which are present as a localisation signal (Laloi et al., 2001) and only these are removed. HvTrx-*h*4 and AtTrx-*o*1 share just 19.39% identity and HvTrx-*h*4 does not contain the cleavage site sequence (Appendix A). Therefore, the putative truncated variant of HvTrx-*h*4 is unlikely to be from cleavage of an import signal. In support, Juttner et al. (2000) concluded that grass thioredoxin-*h*4 proteins are not preceded by transit peptides.

N-terminal protein sequencing was attempted to confirm the presence of a truncated thioredoxin and the extent of truncation in the purified protein preparations but was unsuccessful (see 4.3.3). Apart from difficulty separating the lower band from the upper thioredoxin-*h*4 protein band, sequencing of the truncated thioredoxin may have been hindered by a blocked N-terminus. It is estimated 40 - 80% of all naturally occurring proteins are N-terminally blocked, in which case sequencing data cannot be obtained through Edman sequencing (Wellner et al., 1990). The blocked N-terminal residue may be an N-acetyl amino acid, a glycosylated amino acid or a pyrrolidone carboxylate group (Fernandez et al., 1998). Previously, a thioredoxin-*f* protein from spinach was reported to have a blocked N-terminal amino acid (Kamo et al., 1989).

The protein band beneath recombinant HvTrx-*h*4 is not seen following expression and purification of other recombinant proteins, including barley thioredoxins-*h*1, -*h*2 and -*h*3, which utilised the same expression vector, *E. coli* strain and procedures. Therefore, it is highly unlikely that the lower band present in HvTrx-*h*4 preparations is due to a problem with the expression vector, inadequate purification, nor a random *E. coli* protein containing successive histidines. Further, many discrete preparations of recombinant HvTrx-*h*4 were generated, ruling out contamination as a source of the low molecular weight protein band. Thus, the absence of the lower band in the other recombinant barley thioredoxin-*h* preparations supports the possibility of a modified HvTrx-*h*4 form being present.

4.4.3 Activity of Recombinant Thioredoxin-*h*4

A significant quantity of purified recombinant thioredoxin-*h*4 in an active conformation was successfully generated (Figure 4.9) despite the presence of modified and dimerised variants. As found in studies by Gautier et al. (1998) and Juttner et al. (2000), the rate of insulin reduction increased as a function of thioredoxin concentration. Therefore, the recombinant thioredoxin-*h*4 used in all protein trapping experiments was active and functioning as required.

The reduction of HvTrx-*h*4 by the NADPH: *E. coli* thioredoxin reductase 1 (NTR1) system is lower than for HvTrx-*h*1 and HvTrx-*h*2 (Appendix A) and NTR1 is not as efficient at reducing HvTrx-*h*4 compared to insulin; 0.4 verses 0.7 Ab_{max} readings respectively (Appendix A and Figure 4.9). However, it is still successful. Juttner et al. (2000) reported that *Lolium perenne* and *Phalaris coerulescens* thioredoxins-*h* from class 4 were also poor substrates for *E. coli* NTR1. Juttner et al. (2000) hypothesised that homologous thioredoxin classes are preferentially reduced by a particular NTR. Whilst this is plausible, it is also possible that thioredoxin-*h* class 4 is in fact reduced by the glutaredoxin system. Gelhaye et al. (2003) and Koh et al. (2008), both demonstrated that PtTrx-*h*4 is effectively reduced by glutathione and glutaredoxin. Given the high degree of identity between HvTrx-*h*4 and PtTrx-*h*4 (Appendix A), reduction of HvTrx-*h*4 by the glutaredoxin system should be considered for future research. Nonetheless, it is imperative to appreciate that the recombinant forms of HvTrx-*h*4 are indeed active (Figure 4.9) and therefore suitable for use in the protein trapping experiments.

4.4.4 Isolation of Proteins Interacting with HvTrx-*h*4: Monocysteinic Thioredoxin-Immobilised Affinity Chromatography

4.4.4.1 Interference from Rubisco

The monocysteinic mutant affinity chromatography method was initially applied to identify potential protein targets in extracts derived from barley leaves. When using leaves, the large quantity of Rubisco was problematic because it dominated the protein extract sample. Therefore, an alternative source of prey proteins containing less Rubisco, barley anthers and stigmas, was used in future experiments. The Rubisco saturation problem was also encountered by Balmer et al. (2004) who stated it to be a source of contamination when applying the affinity chromatography method with leaf material, to search for thiordoxin-*o* targets. I suspect Rubisco was probably problematic for other researchers too. For example, Yamazaki et al. (2004) used dark-grown arapidopsis seedlings as their prey protein source for

studies with *A. thaliana* thioredoxin-*h* studies. This is not an ideal source considering plants are growing under abnormal conditions, so one could assume it was done to avoid Rubisco. Whilst the polyacrylamide gels by Motohashi et al. (2001) show that they trapped a large amount of Rubisco, they were fortunate enough to have isolated several other interacting proteins in high enough concentrations to be identified.

4.4.4.2 Varying Protein Concentrations in Elution Samples

A lower concentration of proteins was eluted from the activated thiol Sepharose resin-only control sample compared to the mutant and wild-type thioredoxin-*h*4 samples. Balmer et al. (2003) also used a resin-only independent control to identify proteins forming a nonspecific heterodisulfide, in their monocysteinic mutant affinity chromatography based study. In this case, thioredoxins-*f* and -*m* with the buried cysteine of the active site disulfides replaced by serine and alanine, respectively, were used to isolate target proteins in spinach chloroplast stroma. They too found the quantity of protein eluted was lower in the resin-only control sample and they identified one protein also found with the mutant thioredoxin-*f* and -*m* columns (phosphoglycerate kinase). Curiously, Balmer et al. (2003) are the only researchers to have employed the monocysteinic trapping method who incorporate a wild-type thioredoxin control in their publication. They deemed the wild-type thioredoxin-*f* control to be necessary, but not a wild-type thioredoxin-*m*, because of the extra free cysteine in the *f*-type thioredoxin which has the capacity to form a heterodimer with some prey proteins (Balmer et al., 2003).

Motohashi et al. (2001) began affinity experiments in spinach with a thioredoxin-*f* mutant but found a greater amount of proteins eluted from the mutant thioredoxin-*m*:resin conjugate, so decided to use only the thioredoxin-*m* for further experiments. Balmer et al. (2003) also collected more proteins using mutant thioredoxin-*m* compared to mutant thioredoxin-*f*, 250 µg and 150 µg respectively. They speculated that the increased recovery with mutant thioredoxin-*m* could reflect its greater stability relative to the -*f* type (Balmer et al., 2003). Potentially, the additional free cysteine present in the thioredoxin-*f* protein is responsible for this phenomenon.

Some may question if the binding of thioredoxin to the resin results in it becoming physiologically inactive. Yamazaki et al. (2004) ruled out this possibility by confirming activity of the wild-type thioredoxin-*h* isoform, which was immobilised to the resin, by the insulin reduction assay. Hence, I am confident that the pool of resin-bound thioredoxin is not rendered inactive by its immobilisation.

4.4.4.3 Potential HvTrx-h4 Target Proteins

As described in 4.3.5, HvTrx-*h*4 was identified in both wild-type and mutant samples. This could be expected considering the resin was so heavily saturated with recombinant HvTrx-*h*4. A small proportion of HvTrx-*h*4 may have been dislodged during elution of trapped proteins. In hindsight, this could have been investigated by using the anti-polyhistidine antibody. It is also likely that some HvTrx-*h*4 homodimers were present (see 4.4.1), possibly between recombinant and endogenous HvTrx-*h*4, which were subsequently eluted. Encouragingly, HvTrx-*h*4 was not detected in the resin-only control samples. Motohashi et al. (2001) also found mutant thioredoxin-*m* released from the resin following the elution. Likewise, Lindahl et al. (2004) who employed a similar method comment that "a large amount of thioredoxin mutant becomes inevitably trapped as nonreactive homodimer during the binding assay".

The proteins identified exclusively in the HvTrx-*h*4 wild-type and mutant samples were profilin 2/4, 14-3-3 and a protein similar to a Group V allergen precursor (Tables 4-2 and 4-3). The fact they were trapped by both forms of HvTrx-*h*4 may indicate they were not interacting with HvTrx-*h*4 exclusively through the active site. Perhaps these proteins really are potential HvTrx-*h*4 targets but are interacting through the extra cysteine present at the N-terminus, or even with the first cysteine in the active site. If true, the interactions must be resolved by means other than *via* the HvTrx-*h*4 active site, *in vivo*. It is unlikely that interactions are occurring at the first cysteine in the active site as one could expect the second cysteine to resolve the bond immediately, assuming the interaction is a redox reaction. In a study with thioredoxin-*f* and -*m*, issues with the extra cysteine in thioredoxin-*f* were suspected and attributed with significantly fewer proteins being trapped by thioredoxin-*f* when compared to thioredoxin-*m* (Balmer et al., 2003). Similarly, Motohashi et al. (2001) found the amount of proteins eluted from the mutant thioreodoxin-*m* resin conjugate was much more than that from the thioredoxin-*f* mutant. An alternative or additional possibility is that these proteins were actually present in the negative control but not abundant enough to detect.

Assuming profilin 2/4, 14-3-3 and the potential group V allergen precursor, identified exclusively in the HvTrx-*h*4 samples, are indeed true targets they may be involved in several possible roles. Profilins constitute a ubiquitous family of cytoskeletal proteins that control actin polymerization in eukaryotic cells (Valenta et al., 1992). They function as actin sequestering proteins (Isenberg et al., 1980) and participate in the phosphoinositide pathway during signal transduction and reassembly of the cytoskeleton (Goldschmidtclermont et al., 1990; Vojtek et al., 1991).The amino acid sequence similarity among profilins is not highly conserved across organisms including fungi, yeast, insects, mammals and plants, yet despite

this the structure is conserved (Federov et al., 1997; Schutt et al., 1993; Vinson et al., 1993). Some members of the profilin family are allergens, prominent in the pollen of trees, weeds and grasses (Valenta et al., 1992). Phl p 11 and Phl p 12 are two such profilin allergens (Asturias et al., 1997; Benitez et al., 2001; Marknell DeWitt et al., 2002; Valenta et al., 1994). Allergens, such as pollen, trigger hypersensitivity reactions of the immune system (allergies) in some people. Thioredoxins and allergens, including profilins, have been linked previously. In a study where the allergenic repertoires of wheat and maize were screened in humans, both thioredoxin and profilin were found to have cross-reactive potential (Weichel et al., 2006). In addition, a profilin was identified as a thioredoxin target by Wong et al. (2004) in wheat endosperm. Yano et al. (2001) documented 3 allergens (Ara -h2, -h3, -h6) as *Chlamydomonas reinhardtii* thiroedoxin-*h* targets in peanut seeds. Therefore, if profilin can be considered as a true HvTrx-*h*4 target, so could the group 5 allergen precursor.

According to Thandavarayan et al. (2008), 14-3-3 protein regulates apoptosis signal regulating kinase 1 (Ask1) signalling in humans. In addition, 14-3-3 protein and thioredoxin are reported to limit Ask1 activity in humans by guarding the C-terminal and N-terminal of Ask1 kinase, respectively (Li et al., 2005). Interestingly, Ask1 activation is regulated *via* oxidative stress (Goldman et al., 2004). Treatment with an antioxidant enhanced the interaction of 14-3-3 protein and thioredoxin with Ask1 in human breast cancer cells (Kuo et al., 2007). Considering the results from these studies, it may be reasoned that thioredoxin-*h*4 and 14-3-3 work together in plants in response to oxidative stress.

4.4.4.4 Contaminating Proteins

The majority of proteins that were isolated and identified appear to be interacting with the resin rather than specifically with the thioreodoxin-*h*4, mutant or wild-type (see 4.3.5). It is possible that the level of non-specific adsorption of proteins exceeds the binding of thioredoxin target species thus, resulting in a higher level of 'background proteins' being detected. In addition, it is conceivable that the extra cysteine in the N-terminus is able to substitute for the mutated cysteine and is resolving the sulfide bond binding the interacting protein. In which case the target protein would be released and therefore not detected by this trapping technique. If both these events are occurring, it is not surprising that none of the proteins isolated were unique to the mutant HvTrx-*h*4 sample. Instead, the proteins identified are likely to be originating from interactions with the resin. In support of this interpretation, when Wong et al. (2004) considered the possibility of false positives, they reasoned it was possible to trap a non-target protein with a free, exposed cysteine.

The final attempts made to isolate HvTrx-*h*4 protein targets, using a different series of washes, resulted in no distinct protein bands visible on polyacrylamide gels (see 4.3.5). The lack of proteins eluted from the negative control samples, resin-only and mutant HvTrx-*h*4 iodoactamide treated (cysteines-blocked), indicates that the wash steps were indeed more stringent and the resin and mutant HvTrx-*h*4 were successfully blocked. The iodoacetamide appeared to work as desired considering proteins usually interacting with HvTrx-*h*4 through cysteines should no longer be isolated, due to the cysteines being blocked. The absence of proteins in the mutant and wild-type HvTrx-*h*4 samples might be simply because the washes were too stringent. However, results obtained when using previous protocol versions showed that the buffer compositions were not at fault, as proteins were detected. Therefore, we assume the washes were suitable and there are simply no proteins stably interacting with HvTrx-*h*4, to a detectable degree. This conclusion supports the hypothesis that Cys_4 may cause interference in the affinity chromatography technique and also indicates that target proteins isolated do not interact with HvTrx-*h*4 through the active site. In hindsight, it is clear that a positive control, such as mutated AtTrx-*h*1, would have allowed for more reliable interpretation.

To test the hypothesis, that the N-terminal cysteine is interfering in the stable binding of interacting proteins, future studies could involve mutating Cys_4. An increase in the number of proteins isolated by the resulting HvTrx-*h*4 double mutant would confirm that the Cys_4 is able to substitute for the mutated active site Cys_{58}. Furthermore, it may be possible to determine which of the previously isolated proteins were stably interacting with Cys_4 and not the HvTrx-*h*4 active site.

Should the additional cysteine in HvTrx-*h*4 (Cys_4) be capable of reducing redox interactions, the same would be true for target proteins that contain an additional free cysteine. A target protein with these properties would not be detected as it would be capable of releasing itself from the bond linking it to the thioredoxin. Balmer et al. (2003) also considered this possibility when a known thioredoxin-linked enzyme of the calvin cycle, fructose-1,6-bisphosphatase, was not detected in their affinity chromatography experiments. They concluded the failure could be attributed to the presence of a third cysteine in fructose-1,6-bisphosphatase having the ability to displace the enzyme from the column bound thioredoxin-*f* (Balmer et al., 2003). Consistently, earlier research by Balmer et al. (2001) also failed to identify fructose-1,6-bisphosphatase as a thioredoxin-*f* target.

4.4.4.5 Isolated Proteins Previously Classified as Thioredoxin Targets

Table 4-4 contains the proteins isolated and identified in this study, including those present in control samples, which have previously been assigned as thioredoxin targets by other thioredoxin protein-protein interaction investigations. The key details of each study are outlined in Table 4-5.

Table 4-4: **Proteins identified in this and other studies**. Listed are proteins identified in this study (isolated by the monocysteinic mutant thioredoxin affinity chromatography technique), which have also been identified in other interaction studies. None of these proteins have been confirmed as real targets by other means in any studies. It is necessary to clarify the interaction between thioredoxin and these proteins before concluding they are genuine. Details regarding each study are summarised in Table 4-5

Target Protein Isolated	Other Studies that Isolated Comparable/the Same Target Protein
Peroxiredxoin-2C	Motohashi et al. 2001; Balmer et al. 2003 and 2004; Yamazaki et al. 2004; Wong et al. 2004
Triosephosphate Isomerase	Balmer et al. 2003; Wong et al. 2004; Maeda et al. 2005
Fructose-1,6-Bisphosphate Aldolase	Yamazaki et al. 2004
Elongation Factor 1-β	Balmer et al. 2003 and 2004; Yamazaki et al. 2004; Wong et al. 2004
Profilin	Wong et al. 2004
Tubulin	Wong et al. 2004

Table 4-5: **Summary of studies which isolated a potential thioredoxin target that was also identified in this study.** Several different techniques were used including the monocysteinic mutant thioredoxin affinity chromatography (Affinity) and the thiol-specific probe monobromobiamane technique (mBBr). mBBr involves reduction of the protein extract by the NADP/thioredoxin system and subsequent labelling of the newly generated sulfhydryl (SH) groups with monobromobimane. Proteins are then resolved by 2D gel electrophoresis and the resulting staining patterns are analysed to look for protein shifts (treated versus untreated protein).

Study that Isolated Comparable Protein/s	Thioredoxin Bait	Tissue Source	Method
Motohashi et al. 2001	Trx-*m* $C_{41}S$ mutant, Trx-*m* $C_{37}S/C_{41}S$ mutant	Stroma lysate of spinach chloroplasts	Affinity
Balmer et al. 2003	Wt Trx-*f*, Trx-*f* $C_{49}S$ mutant, Trx-*m* $C_{40}A$ mutant	Stroma from intact spinach chloroplasts	Affinity
Balmer et al. 2004	Trx-*m* $C_{40}A$ mutant, Pt Trx-*h1* $C_{42}S$ mutant	Pea, spinach and potato tuber extracts	Affinity and other
Marx et al. 2003	Trx-*h*	Barley (*cv* Golden Promise) embryos or seedlings, germinated in the dark	mBBr
Yamazaki et al. 2004	HvTrx-*h*1 $C_{43}S$ and $C_{40}S$	Cell lysate of dark grown *A. thaliana* whole tissues	Affinity
Wong et al. 2004	PtTrx-*h*1	Wheat seed endosperm 10 days post anthesis and flour	Affinity and mBBr
Maeda et al. 2005	HvTrx-*h*1 and -*h*2	Barley seed (*cv* Barke) micromalted	Other

Tubulin and elongation factor-1β were found exclusively in the resin-only control in this study whilst Wong et al. (2004) suggests both proteins are probable thioredoxin targets. However, Wong et al. (2004) do not report any controls included in their research. Considering the findings reported here, it is not unreasonable to suspect that had a resin-only control been employed by Wong et al. (2004) it would have contained both tubulin and elongation factor-1β. Interestingly, Balmer et al. (2003; 2004) and Yamazaki et al. (2004) also identified elongation factors as thioredoxin targets, but of the forms -Tu, -g and -EF2. Balmer et al. (2003) included a resin-only control in their experiments and proteins were eluted, although fewer compared to the immobilised thioredoxin samples. They did not discover elongation factor -Tu or -g in this control, nor the triosephosphate isomerase or peroxiredoxin-2C.

Preceding Balmer et al. (2003), Motohashi et al. (2001) also considered peroxiredoxin-2C to be a likely thioredoxin target. However, this protein was discovered in a negative control (see Table 4-2.). Interestingly, Motohashi et al. (2001) used an alternative negative control, an active-site double cysteine mutant, thioredoxin-*m* $Cys_{37}Ser/Cys_{41}Ser$. In their report, it is stated that they were unable to trap any proteins with this thioredoxin-*m* double mutant.

Yamazaki et al. (2004) identified fructose-1,6-bisphosphate adolase as a thioredoxin target and yet it was present in the resin-only negative control reported here (see Table 4-2). Whilst Yamazaki et al. (2004) collected a small amount of protein from their resin-only control they did not analyse the sample further. Their negative control could be considered insufficient as they used only enough resin to provide theoretically equal amounts of exposed SH groups as those present for the thioredoxin mutant. This control is only suitable if all the proteins binding to thioredoxin in the test samples are doing so specifically. Assuming proteins are binding non-specifically, as previously discussed, the amount of resin used for their control may be deficient.

Balmer et al. (2004) do not mention any affinity chromatography controls and used a thioredoxin-*m* and a thioredoxin-*h* to trap mitochondrial derived proteins, which were then inferred to be thioredoxin-*o* targets. Considering thioredoxin types are distinctly different, as highlighted by their classifications into distinct groups, this approach is fraught with opportunities for error, especially regarding interpretation of the results.

4.4.5 Is the Monocysteinic Thioredoxin Affinity Chromatography Robust?

The value of the monocysteinic thioredoxin affinity chromatography technique can be questioned especially when it is applied in a non-targeted manner. Little is known about the temporal and spatial localisation of most plant thioredoxins-*h*. Thus, the tissues providing protein extracts might be unsuitable for trapping interacting proteins. Studies have attempted to isolate chloroplastic targets using cytosolic thioredoxins (Yamazaki et al., 2004) and mitochondrial targets using chloroplastic and cytosolic thioredoxins (Balmer et al. (2004). Exactly why thioredoxin-*o* was not used as bait instead was not explained nor the thioredoxin substitution rationalized. According to Buchanan et al. (2005), the high concentration of thioredoxin immobilised to the sepharose column favours the formation of a heterodisulfide, regardless of enzyme preference. Thus, perhaps substituting thioredoxin types is possible, considering the lack of specificity as previously observed (Motohashi et al., 2001). However, it is probable that this approach results in the capture of proteins which do not truly interact with thioredoxin *in vivo*.

Further consideration must be given to the nature of disulfide bonds. Thioredoxins will reduce target proteins based upon their redox potential and whether disulphide bonds are exposed. Therefore, even if a protein is not usually redox-regulated, in an artificial environment thioredoxin may be able to modify any exposed cysteines and so it will appear to be a target protein. In addition, the long period of incubation with protein extracts (*30 min to 1 h*) may also facilitate the identification of false positives and abundant proteins in the extract may interfere with capture of target proteins that are in lower abundance. With all these considerations in mind, further, vigilant biochemical research is required for each protein isolated, before they can definitively be claimed as thioredoxin targets.

4.4.6 Alternative Approaches

Considering the lack of likely HvTrx-*h*4 targets acquired *via* the monocysteinic thioredoxin affinity chromatography technique, along with the likely reasons for the outcome, to discover HvTrx-*h*4 thioredoxin targets in the future an alternative approach would need to be pursued. Firstly, substitution of the HvTrx-*h*4 Cys_4 residue would be required, in addition to Cys_{55} or Cys_{58}, to prevent it from potentially resolving disulfide interactions forming between the HvTrx-*h*4 active site and target protein. A suite of mutant HvTrx-*h*4 forms containing different $Cys_{4,\ 55\ and\ 58}$ substitution combinations would be most beneficial for interpretation of the results.

The inclusion of an antibody with specific and strong affinity for HvTrx-*h*4 would be advantageous for protein-protein affinity based experiments. Binding the antibody to a matrix would enable the HvTrx-*h*4:target-protein interactions to occur separately and subsequently be precipitated as complexes *via* the matrix bound antibody. This *in vitro* co-immunoprecipitation technique could be exploited further if transgenic plants were generated, containing the mutated forms of HvTrx-*h*4, thereby allowing *in vivo* interactions to be isolated. In such experiments, expression of the mutated HvTrx-*h*4 could be controlled by the endogenous promoter or, if desired, it could be over-expressed constitutively by an alien promoter. A similar approach was employed by Rey et al. (2005) to isolate protein interacting with the CDSP32 from potato (S. *tuberosum*). Antibodies raised against StCDSP32 were immobilised on a gel and incubated with leaf extracts containing protein extracts from plants over-expressing a StCDSP32 Cys_{216}Ser mutant. Following a series of washes, StCDSP32 or StCDSP32 bound to a target protein were eluted and the proteins collected were analysed by immunoblotting (Rey et al., 2005). This experiment was carried out using the Profound$_{TM}$ Co-Immunoprecipitation Kit (Pierce). Importantly, control gels provided in this kit enabled the specificity of the interaction with the gel matrix to be examined. This technique enabled the authors to show that CDSP32 and a known target (BAS1), co-immunocprecipitated.

Yet another approach to identify proteins interacting with HvTrx-*h*4 would be to apply the monobromobiamane (mBBr) based technique. (Gautier et al., 1998; Marx et al., 2003; Wong et al., 2004). The method involves reduction of the protein extract by the NADP/thioredoxin system (e.g. HvTrx-*h*4) and subsequent labelling of the newly generated sulfhydryl (SH) groups with the thiol-specific probe, mBBr. Treated and untreated protein samples are then resolved using 2-dimensional gel electrophoresis and the resulting staining patterns are contrasted to identify protein shifts. The proteins of interested can then be excised from the gel and identified by mass spectrometry. In all future experiments, negative and positive controls are recommended.

4.4.7 Conclusion

The monocysteinic thioredoxin affinity chromatography technique was deemed to be unsuccessful in this study, potentially due to the presence of an extra cysteine in the N-terminus of HvTrx-*h*4. Thus, no proteins were confidently identified to be interacting with HvTrx-*h*4. Consequently, pathways which barley thioredoxin-*h*4 may be regulating, or be involved in, were not elucidated. Finally, the possible presence of a truncated HvTrx-*h*4 variant and the ability for HvTrx-*h*4 to dimerise were discovered.

5 *Thioredoxin-h*4 Gene Expression Analysis

5.1 Introduction

The gene for *Hordeum vulgare* cytosolic thioredoxin class 4 member (*HvTrx-h4*) was previously isolated by Juttner et al. (2000). The mRNA sequence is translated into 131 amino acids which fold into a protein approximately 14 kDa in size (see Chapter 4). The presence of a conserved cysteine at position 4 in the amino acid chain, and three conserved phenylalanines towards the carboxyl end, clearly distinguishes grass *thioredoxin-h4*s from all other grass *thioredoxins*.

Phylogenetic analysis also conducted by Juttner (*data not published*) revealed that *thioredoxin-h4* is likely to represent the most ancient subclass of cytosolic thioredoxins. *Thioredoxin-h4* sequences from diverse species are more similar to one another, than to the other thioredoxin-*h* sequences from the same species. In addition, *thioredoxin-h4*s share the greatest sequence similarity with ancient plant forms such as biophytes and ferns (Juttner, 2003). This implies that thioredoxin-*h*4 evolved early in terrestrial plants and that sequence changes have been largely constrained over a long period of time. Perhaps the high degree of sequence conservation is related to a crucial function of the translated protein. If this is true, the function must be common to higher plants.

Gene expression profiling can assist with identifying the function of a protein. Comparing transcript abundance in differing tissues can provide insight into the spatial and temporal regulation of a gene of interest. To this end, transcript expression analysis of *HvTrx-h1-4,* with a focus on -*h4,* was undertaken using real-time, quantitative, polymerase chain reactions (Q-PCR) and is reported in this chapter. Considering the highly conserved nature of thioredoxin-*h*4s in angiosperms and gymnosperms, barley reproductive tissues were of particular interest as seed production is common and unique to these plant phylogenic classes (Friedman et al., 2004). Accordingly, the reproductive tissues at various developmental stages

were targeted for analysis. The main aim of this research was to identify the specific tissues in which *HvTrx-h4* was highly or differentially expressed and thereby attempt to link processes uniquely occurring in these tissues, to a potential HvTrx-*h*4 function.

Green Fluorescent Protein (GFP), originally isolated from the jellyfish *Aequorea victoria*, can be used as a visual genetic reporter (Shimomura et al., 1962). GFP can be fused to a gene of interest or to the gene's regulatory elements, such as the promoter. Subsequently, it provides a genetic tag for visualisation of the endogenous spatial and temporal expression of the gene, in a living system (Chalfie et al., 1994). GFP is visible following excitation with blue light and no other components are required (Tsien and Prasher, 1998), making it non-destructive and potentially enabling real-time analysis of the gene's response to a change in growing conditions. GFP is an extremely valuable tool as highlighted by the Nobel Prize in Chemistry for 2008, which was awarded to three of the pioneers in GFP discovery and development, namely Osamu Shimomura, Martin Chalfie, and Roger Y. Tsien (*The Royal Swedish Academy of Sciences*). The announcement of this award was accompanied by a review on GFP (Ehrenberg, 2008).

The merits of GFP were exploited in this research in an attempt to reveal the function of HvTrx-*h*4 and the work is presented in this chapter. Isolation and manipulation of the upstream genomic sequence of *HvTrx-h4* was necessary, to enable transformation of barley plants with *HvTrx-h4* promoter:*GFP* reporter constructs, in a study designed to reveal the spatial and temporal expression, and regulation, of *HvTrx-h4*. Of particular interest, due to the increased stress tolerance of tobacco plants over-expressing *PcTrx-h4* (as reported in Chapter 3), was the gene expression and regulation of endogenous *HvTrx-h4* in response to abiotic stresses.

The work presented in this chapter was ultimately undertaken to examine the genetic expression and regulation of *HvTrx-h4*, to gain further insight into the function HvTrx-*h*4.

5.2 Materials and Methods

5.2.1 Chromosomal Mapping of HvTrx-*h*4: Wheat-Barley Disomic and Ditelosomic Addition Line Analysis.

Wheat-barley disomic and ditelosomic chromosome addition lines (Islam et al., 1981) were used to determine the chromosomal location of HvTrx-*h*4. Southern hybridisations were performed (see 2.5.3) on restriction fragment length polymorphism (RFLP) membranes, containing genomic DNA from the wheat-barley chromosome addition lines digested with various restriction enzymes, which were a general laboratory resource. Theses membranes were probed with *HvTrx-h4* cloned and isolated from the pQE-70/HvTrx-*h*4 construct (see 4.2.2).

5.2.2 Plant Material Collection for Analysis of Transcript Expression

Barley florets were harvested from individual plants of various ages and viewed at 4 x magnification with an inverse dissection microscope to determine their development stage. Florets at the stages of pre-meiotic, meiotic (or very close to), immature microspores and mature microspores were harvested. Likewise, anthers and stigmas were harvested from florets at the development stages of 1, 3 and 5 days pre-anthesis. Harvested tissue was immediately snap frozen in liquid nitrogen and stored at -80^{o}C. The mRNA was extracted from each sample (see 2.6.1), DNA removed (see 2.6.2) and cDNA synthesised (see 2.4.3), in preparation for use in quantitative real-time polymerase chain reactions (Q-PCR).

An abscisic acid (ABA) stress (cDNA) series was made by Alexandra Smart (*PhD Student, ACPFG, Australia*) from *H. vulgare* cv Golden Promise. Seedlings were grown in supported hydroponics in growth solution [5 mM NH_4NO_3, 5 mM KNO_3, 2 mM $Ca(NO_3)_2.4H_2O$, 2 mM $MgSO_4.7H_2O$, 0.1 mM KH_2PO_4, 0.5 mM Na_2SiO_3, 0.05 mM NaFe(III)EDTA, 10 mM H_3BO_3, 5 mM $MnCl_2.4H_2O$, 5 mM $ZnSO_4.7H_20$, 0.5 mM $CuSO_4.5H_2O$, 0.1 mM Na_2MoO_3] in the glasshouse. Fourteen day old seedlings were stressed with ABA which was added to the growth solution at a final concentration of 10 μM. Roots and shoots were collected prior to ABA stress (0 h) and 30 min, 1, 2, 4, 8, 12 and 24 h after treatment.

5.2.3 Quantitative Real-Time Polymerase Chain Reaction (Q-PCR) Analysis of Transcript Concentrations

Quantitative real-time PCR experiments were conducted with Dr Neil Shirley (*University of Adelaide*), as described by Burton et al. (2004). For each gene analysed, a primer set was designed to amplify a small fragment (100-250 bp) of the 3' coding region, including the stop codon. Primer pairs specific for *HvTrx-h4* and control genes were designed for barley cv Golden Promise and are shown in Appendix B. HPLC purified PCR products were quantified and diluted to contain 10^9 copies of the PCR product μl^{-1} as outlined by Burton et al. (2004). A dilution series encompassing seven orders of magnitude (10^1 to 10^7) was prepared from this stock solution. Three replicates of these seven standard concentrations and two "no template" controls were included in every Q-PCR experiment to create standard curves linking fluorescence levels to PCR product (transcript) concentrations. For each cDNA, mean transcript levels and standard deviations were calculated from 4 replicates. The cDNA was amplified in a QuantiTect SYBR Green PCR reagent reaction (Qiagen, Valencia, CA) in a RG 2000 Rotor-Gene Real Time Thermal Cycler (Corbett Research, Australia) as outlined by Burton et al. (2004).

Following determination of mRNA transcript levels for the four control genes, a normalisation factor was established and used to account for varying total mRNA quantities in each cDNA sample. The normalisation factor was derived from the geometric mean of expression data for the most stably expressed control genes, using the geNorm program (Vandesompele et al., 2002). The calculated transcript levels of the *HvTrx-h* genes were multiplied by the normalisation factor to reach the 'normalised mRNA copies per µl' values given in section 5.3.2. These values indicate the relative abundance of transcripts with comparison to the control genes.

5.2.4 Genomic Walking: *HvTrx-h4* Promoter and 5′-UTR Isolation and Cloning

Genomic walking was performed to isolate the HvTrx-*h*4 promoter. Four genomic walking libraries were supplied by Dr Klaus Oldach (*ACPFG, University of Adelaide, Australia*). Each consisted of barley cv Atlas46 genomic DNA digested with a different restriction enzyme (EcoRV, DraI, PvuII and StuI) and nucleotide adapters ligated to the resulting fragment ends. A nested PCR approach was employed to amplify the promoter of *HvTrx-h*4 and primer sequences can be found in Appendix B. Briefly, adaptor primer 1 (AP1) was used with a reverse primer specific to *HvTrx-h4* (GWR1) in a standard PCR (see 2.4.2). The resulting product was diluted 50 fold and 1 µl was used in a second PCR with adaptor primer 2 (AP2)

and a nested primer specific to *HvTrx-h4 (*GWR2), 5' to GWR1. Resulting fragments of interest were extracted from the agarose gel in which they were separated (see 2.4.6) and cloned (see 2.4.9). Plasmid DNA was extracted from single colonies cultured in LB (see 2.4.10) and a diagnostic PCR, using primers AP2 and GWR2, was performed to identify plasmids containing 5' upstream region of *HvTrx-h4*. Fragments from desired colonies were sequenced (see 2.4.11) using the primers SP6, T7 and GWF1seq.
To obtain the HvTrx-*h*4 promoter sequence from the barley cultivar Golden Promise, primers GpPF1 and GWR2 were used in a standard PCR (see 2.4.2) and the resulting fragment was cloned and sequenced (see 2.4.9 and 2.4.11).

5.2.5 Databases for Motif Identification

The Plant cis-acting regulatory DNA elements (PLACE 30.0, 469 entries) database was used to analyse the HvTrx-*h*4 promoter and 5′-UTR to identify potentially significant motifs (Higo et al., 1999; Prestridge, 1991). The sequence was analysed against the database following an update on 8th January, 2007 (final update). http:/www.dna.affrc.go.jp/PLACE/index.html

5.2.6 Gateway Vector Construction and Barley Transformation

Two different lengths of the isolated HvTrx-*h*4 promoter and 5′-UTR sequence were amplified to produce two fragments of approximately 2.5 and 2 kb using primer sets 2.5PromTrx4F - HvPromR and 2.5PromTrx4F - HvPromR2, respectively (Appendix B). These fragments were cloned into the Gateway entry vector pCR8/GW/TOPO according to the manufacturer's instructions (Invitrogen). In brief, the TOPO cloning reaction consisted of 2 µl PCR product, 1 µl Salt Solution and 1 µl TOPO Vector/Enzyme in a final volume of 8 µl. The reaction was incubated at room temperature for 40 min, then transformed into DH5α cells *via* heat shock (see 2.4.9). DNA was isolated from several of the resulting spectinomycin resistant colonies (see 2.4.10), screened for those containing the desired inserts *via* restriction mapping with EcoRI (see 2.4.7) and a diagnostic PCR using primers GW1 and HvPromR2 and then finally sequenced with primers GW1 and GW2 to determine the insert orientations (see 2.4.2, 2.4.11 and Appendix B).

It is possible to clone blunt end PCR fragments in the correct orientation, between the *att*L1 and *att*L2 recombination sites present in gateway entry vectors, using Topoisomerase I, which originates from the *Vaccinia* virus (Shuman, 1994). The *attI*L1 and *att*L2 sites subsequently enable site-specific recombination events to occur, analogous to the bacteriophage Lambda system upon which the Gateway technology is based (Landy, 1989). Hence, DNA fragments can be moved from the entry vector to many different destination vectors, containing different

properties and functions, without the need for restriction enzyme digestions and ligations. The entry and destination vectors used in this study were courtesy of Dr. Andrew Jacobs (*ACPFG, University of Adelaide*).

The *HvTrx-h4* fragments were recombined from their entry vector into the Gateway GFP expression destination vector, pMDC107, *via* a Gateway cloning LR reaction (Invitrogen). LR reactions contained approximately 100 ng each of purified entry and destination vectors, 4 µl Tris-EDTA (pH 8), 2 µl of LR Clonase buffer and 2 µl of LR Clonase II enzyme in a final volume of 10 µl. The reaction was incubated at 25^{o}C overnight and then stopped by incubation with 2 µl of proteinase K enzyme (Invitrogen) at 37^{o}C for 20 min. The reaction was used to transform DH5α cells *via* heat shock (see 2.4.9). Plasmids were extracted from resulting colonies (see 2.4.10) and restriction mapped with Pst1 and BamHI enzymes to identify those containing the desired inserts (see 2.4.7). To confirm that the GFP expression vector pMDC107 definitely contained the desired HvTrx-*h*4 promoter ± 5′-UTR insert, sequencing with primers pMDC-RB-SC and GpFwd3 was performed (see 2.4.11 and Appendix B).

The two constructs built, containing GFP to be driven by the *HvTrx-h4* promoter ± 5′-UTR insert, were sent to the Barley Transformation Group (*The University of Adelaide, ACPFG*) to be transformed into *H. vulgare* cv Golden Promise.

5.2.7 Identification of Transgenic Barley Containing the *HvTrx-h4* Promoter*:GFP* Integration and Determination of Copy Number

5.2.7.1 Southern Analysis for T0 Populations

Southern analysis was used to confirm successful transformation of individual T0 barley plants and to determine the number of copies of the transgene present in each plant. Genomic DNA was extracted (see 2.5.1) and digested overnight with 40 units of restriction enzyme in a 20 ul reaction (see 2.5.3). The restriction enzymes used were EcoRV, which cut once within each integration sequence (between left and right borders) in both Trx4PL and Trx4PS constructs, and HindIII, which did not cut at all. Digested DNA was resolved on a 1% agarose gel and transferred to nylon membrane (see 2.5.3.1). Membranes were probed as previously described in section 2.5.3, using a 700 bp purified PCR product of GFP sequence, generated from primers SProbeFwd, SProbeRev and Trx4PL plasmid DNA template (see 2.4.2, 2.4.5, 2.5.6 and Appendix B).

5.2.7.2 PCR Screen for T1 Populations: Identification of Individuals Containing the HvTrx-h4 Promoter:GFP Integration

A diagnostic PCR was executed to identify individuals in the T1 populations that contained the *HvTrx-h4* Promoter:GFP integration. Standard PCR conditions were used (see 2.4.2) with primers GFPfwd and GFPrev (Appendix B), an annealing temperature of 56^{o}C and a 20 fold dilution of neat DNA from resulting from the extraction (see 2.5.1). Products were resolved on a 1% agarose gel and if a single band of 706 bp was present, the plant was scored as positive for containing the desired HvTrx-*h*4 Promoter:GFP introduced genetic information.

5.2.8 GFP Visualisation and Image Capture: Stereo Microscope

Fluorescence emitted by GFP was detected with a Leica MZ FLIII fluorescence stereomicroscope (Leica Microscopie Systemes, Switzerland) fitted with GFP (GFP1) and GFP Plus (GFP2) fluorescence filter sets [GFP1, 425 nm excitation filter (bandwidth of 60 nm) and 480 nm barrier filter; GFP2, 480 nm excitation filter (bandwidth of 40 nm) and 510 nm barrier filter]. Images were captured with a Leica DC 300F digital camera.

5.2.9 Stress and Hormone Challenges for *HvTrx-h4* Promoter:GFP Transgenic Barley Lines

Derived from each transgenic line (T0), Trx4PL and Trx4PS, at least four T1 individuals were challenged with the various stresses and hormones. In addition, a minimum of four leaves per plant were examined. Within each experiment, tissues of comparable ages, lengths, widths and thicknesses were used for repetitions, to allow accurate comparisons. For all experiments, each transgenic line was compared to a wild-type control which was treated in the same manner. Initially, tissues at a variety of developmental stages were treated and examined when establishing 'standard' treatment conditions. Following each stress or hormone treatment, the tissues of interest were examined for the presence or absence of GFP.

5.2.9.1 Ultraviolet Light Stress and Translocation Analysis

Transgenic and wild-type barley leaves, approximately 20 cm in length, were detached from several individual plants and exposed to 2 Wm^{-2} of UVB (λ 302 nm) for up to 24 h. Recovery periods, where the leaves were returned to their original light conditions, ranged from 0- 36 h.

To test if the signal resulting in the appearance of GFP was able to migrate/translocate, detached barley leaves approximately 20 cm in length were floated on water and partially covered with alfoil. The leaf was exposed to 8 Wm^{-2} of UVB (λ302 nm) for 3 h with the

aluminium foil blocking UVB penetration to approximately half of the leaf surface. Each leaf was returned to original light conditions for 30 min prior to visualisation of GFP.

5.2.9.2 Wounding Challenge

To see if GFP was expressed in response to wounding, young, fresh leaves approximately 10 cm in length were detached and stabbed with the sharp metal points of fine nosed forceps, cut with sharp metal scissors and torn by hand. In addition, awns were wounded by snapping them in half, by hand or with the edge of fine nosed forceps, after the floret had been detached from the plant. The plant tissues were observed immediately and up to 20 mins following wounding.

5.2.9.3 Methyl Viologen Stress

Upon nightfall, leaves approximately 15 cm in length were detached and the wounded end was placed in water. Droplets (10 µl) of 0.1, 1, 5 and 10 µM methyl viologen (MV) in a background of 0.1% Tween 20 (Merck, Australia) were pipetted onto each leaf and left in the dark until after sunrise. After 12 or 18 h the MV treated sites were examined for the presence of GFP.

5.2.9.4 Hormone Applications

Ethephon (ethylene) (Sigma-Aldrich, Australia) at concentrations of 100µM and 100 mM in a 0.01% tween 20 background (pH 3.5), was applied to the surface of a range of young and older detached leaves. Several discrete droplets of 15 µl were pipetted onto each leaf and incubated at room temperature for 1.5 – 2 h in the dark. The cut end of each leaf was submerged in water for the duration of the treatment.

For treatment with Jasmonic acid (JA) and Abscisic Acid (ABA) (Sigma-Aldrich, Australia), detached young leaves were cut into 4 cm lengths and floated upon the hormone solutions. Each hormone was diluted with methanol to 10 µM, 100 µM and 1 mM concentrations and contained within small weighing boats (~5 mL). At least 4 leaves per line were treated. The leaf sections were incubated in the dark under alfoil for 1, 2, 4 and 14 h. In preparation for future transcript analysis, the treated leaves were snap frozen in liquid nitrogen and stored at -80^{o}C.

5.2.10 Prediction of RNA Secondary Structures: RNAProfile Algorithm

To investigate the likelihood of secondary structures forming in *HvTrx-h4* mRNA, the 5′-UTR region sequence isolated (see 5.2.4) was used to data mine for homologous thiroedoxin-*h*4 5′-UTR sequences available in the NCBI database. These were supplied to Michael Tran (*University of Adelaide*) who performed RNA secondary structure prediction using the RNAProfile algorithm (Pavesi et al., 2004). The RNAProfile program was run with the following parameter settings: region lengths set to 20 (min) and 40 (max) nucleotides, number of iterations set to 24, the default energy threshold and random alignment order.

5.2.11 Glutathionylation

Purified recombinant HvTrx-*h*4 protein (see 4.2.4) was treated with glutathione by Dr Juan Juttner (*ACPFG, University of Adelaide*) and then sent to Dr John Patterson (*ACPFG, University of Melbourne*) for analysis, to determine if HvTrx-*h*4 was the subject of post-translational modifications, specifically glutathionylation. Dr Patterson analysed 2 aliquots of HvTrx-*h*4, one of which had been treated with DTT (control) and the other incubated with glutathione. In addition, an aliquot of each sample was digested with trypsin after treating the unmodified cysteine residues with iodoacetamide (IAA) to add carbamiomethyl groups to the cysteine residues. The intact and digested protein samples were desalted using a C_{18} ZipTip (Millipore, Australia) and analysed by mass spectrometry using a QStar XL ESI-Q-TOF (Applied Biosystems, Australia). The spectra of intact proteins or peptides were collected and the mass of the parent ion was determined using the equation m/z = (mass of protein (Da) + nH^+)/n where n was the number of positive charges.

5.3 Results

5.3.1 Chromosomal Location of the Barley *Thioredoxin-h4* Gene

For chromosome mapping of *HvTrx-h4*, wheat-barley addition plant lines were used. These lines were developed by adding one barley cv *Betzes* chromosome (disomic addition line) or chromosome arm (ditelosomic addition line) into wheat cv *Chinese spring* (Islam et al., 1981). The barley chromosome 1 ditelosomic addition line contains only the short arm of the chromosome (1SH). Southern analysis of the wheat-barley addition lines reveals that *HvTrx-h4* is located on the short arm of barley chromosome 1. The *HvTrx-h4* probe hybridised to restriction fragments present in the *Betzes* barley (HB) and the ditelosomic addition line (CS + 1SH) but not to the *Chinese spring* wheat restriction fragments (Figure 5.1).

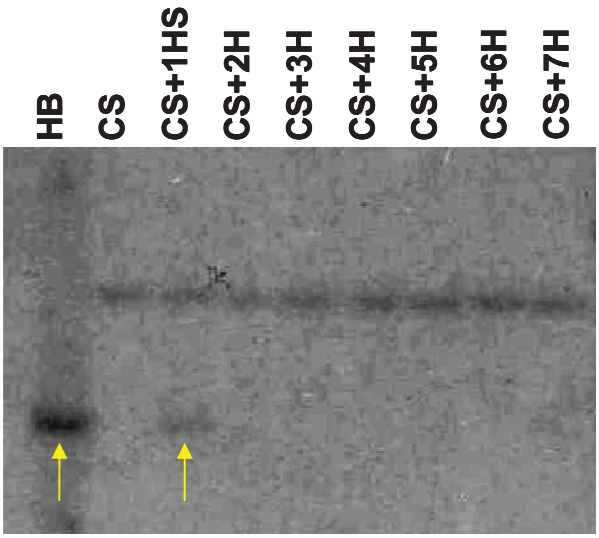

Figure 5.1: **Southern analysis of barley-wheat addition lines reveals that *thioredoxin-h4* is located on the short arm of Chromosome 1.** An *HvTrx-h4* cDNA probe was used to analyse DNA of wheat-barley addition lines derived from barley cv *Betzes* and wheat cv *Chinese spring*, cut with the restriction enzyme BamHI. The probe detected one band in *Betzes* barley (HB) which was also present in the addition line containing the short arm of chromosome 1 (CS + 1SH), as highlighted by the arrows. The band was absent in *Chinese spring* wheat (CS). Lanes labelled CS+2H to CS+7H contain the ditelosomic addition lines with barley chromosomes 2 to 7, to which the *HvTrx-h4* probe does not hybridise.

5.3.2 Transcript Analysis of Barley *Thioredoxin-h* in Reproductive Tissues

In plants, cytosolic thioredoxins are thought to play a role during germination, floral and early seedling development (Bower et al., 1996; Lozano et al., 1996; Shahpiri et al., 2008; Zahid et al., 2008). Considering this and the highly conserved nature of *HvTrx-h4* in angiosperms, the expression of the barley cytosolic thioredoxins in reproductive tissues was of interest. Accordingly, quantitative real-time PCR (Q-PCR) was employed to investigate the temporal and spatial expression of *HvTrx-h*s in barley reproductive tissues at various developmental stages. The transcript levels of all four cytosolic barley thioredoxins were analysed, for each cDNA sample, to ascertain whether *HvTrx-h4* exhibited a unique transcript profile. RNA was extracted from whole florets, anthers and stigmas at various developmental stages. Endosperm cDNA was courtesy of Dr Rachel Burton (*APCFG, University of Adelaide*).

Barley florets were harvested from individual plants of various ages and it was established that florets at development stages of pre-meiotic through to mature microspores were contained in barley head sizes of up to 5 cm (Table 5-1). The florets within a head were at different development stages with the younger ones found in the centre and the more mature florets at either end of the head. With this knowledge, florets at the stages of pre-meiotic, meiotic (or very close to), immature microspores and mature microspores were collected. Anthers and stigmas were harvested from florets at the development stages of 1, 3 and 5 days pre-anthesis.

Table 5-1: **Approximate barley head sizes required for collection of florets at pre-meiotic, meiotic (or very close to), immature microspores and mature microspores development stages.** Florets, anthers and stigmas were viewed under 4 x magnification with an inverse dissection microscope and their development stage was determined.

Stage	*Head Size*
Pre-meiotic	< 1.5 cm
Meiotic	~ 2 cm
Immature microspores	3- 4.5 cm
Mature microspores	5cm (awns just protruding from sheath)

The control genes used to normalise the data were glyceraldehyde-3- phosphate dehydrogenase, α-tubulin, heat shock protein 70, and cyclophilin. These genes were previously established as suitable control genes as their mRNA levels were stably expressed in a wide variety of barley tissue (Burton et al., 2004). The normalisation factor was calculated from the geometric mean of transcript data for the 3 most stably expressed control genes, for each development series (Vandesompele et al., 2002). This enabled comparisons between cDNAs from different tissue samples.

The first development series examined was the florets (Figure 5.2). *HvTrx-h1* and *-h2* have high relative abundance of transcripts and the pattern of transcript expression is the same. *HvTrx-h3* has a similar transcript profile to *–h1* and *–h2*, although the quantity is approximately 5-10 fold lower, depending on the tissue's development stage. *HvTrx-h4* has the lowest abundance of transcript for all floret stages examined, with a minimum of 62, 41 and 8 fold fewer transcripts present compared to *HvTrx-h1*, *-h2* and *-h3* respectively. Furthermore, the transcript profile of *HvTrx-h4* has a distinctly different pattern in comparison to the other thioredoxins-*h* (Figure 5.2A). The quantity of *HvTrx-h4* transcripts steadily increases as the florets mature (Figure 5.2B).

Upon subdivision of floret tissue into anther and stigma constituents it is apparent that the increase in transcript levels seen in the floret development series can be attributed primarily to the male reproductive tissue (Figure 5.3C). The *HvTrx-h4* transcript quantity increased in anther tissue as it matured towards anthesis. Relative to male tissues, the *HvTrx-h4* transcript was less abundant in the female, stigma tissues and remained constant (Figure 5.3C). A similar pattern was found for the *HvTrx-h3* transcript (Figure 5.3B). By contrast, *HvTrx-h2* transcript levels were found to decrease in anther tissues as they matured, whilst the reverse occurs in the stigma tissue (Figure 5.3A).

Surprisingly, the *HvTrx-h2* transcript was recorded as being more abundant in anther and stigma tissues compared to *HvTrx-h1* (Figure 5.3A). The finding contrasts with the transcript levels determined from mRNA extracted from whole florets in which *HvTrx-h1* transcript levels were recorded as the highest of the four thioredoxins studied (Figure 5.2A). Similarly, *HvTrx-h4* transcript is more abundant in the anther/stigma development series relative to *HvTrx-h3* (Figure 5.3), which contradicts the transcript quantification studies employing mRNA extracted from whole floret tissues (Figure 5.2A). A potential explanation for the aforementioned discrepancies is that *HvTrx-h1* and *HvTrx-h3* transcripts are in higher

abundance in the remaining floret components, compared to *HvTrx-h2* and *HvTrx-h4*, respectively.

In the barley developing endosperm tissue series, *HvTrx-h1* had the highest number of transcripts present in all samples, of all the barley cytosolic thioredoxins examined in this study (Figure 5.4A). A peak in *HvTrx-h1* transcript abundance occurred 4 days after pollination and then fell to its lowest 4 days later. The transcript profile patterns of both *HvTrx-h2* and *-h3* mirror that of *HvTrx-h1* (Figure 5.4A and B). However, across all sample time points, the *HvTrx-h2* transcript abundance was, on average, 16.8 fold lower than it was for *HvTrx-h1*, whilst *HvTrx-h3* transcript was 5 fold lower again. The transcript profile for *HvTrx-h4* was different to the other three *HvTrx-h*s (Figure 5.4A and B). A large peak in *HvTrx-h4* transcript abundance was observed 5 days after pollination (Figure 5.4B). This period corresponds to the beginning of cellularisation during barley endosperm morphogenesis (Figure 5.4C). A second peak in *HvTrx-h4* transcript levels, 4 fold lower than the highest transcript peak, was recorded 3 days later (Figure 5.4B). At this time, 8 days after pollination, the cellularisation phase ends and differentiation begins (Figure 5.4C).

The differences in temporal and spatial *HvTrx-h* transcript profiles seen in all the developing tissue series examined, suggests that not all barley cytosolic thioredoxins serve the same function in reproductive tissues. Of all the *HvTrx-h*s examined, *-h4* appears to have the most unique expression profile, particularly in the floret and endosperm tissue series (Figure 5.2 and Figure 5.4).

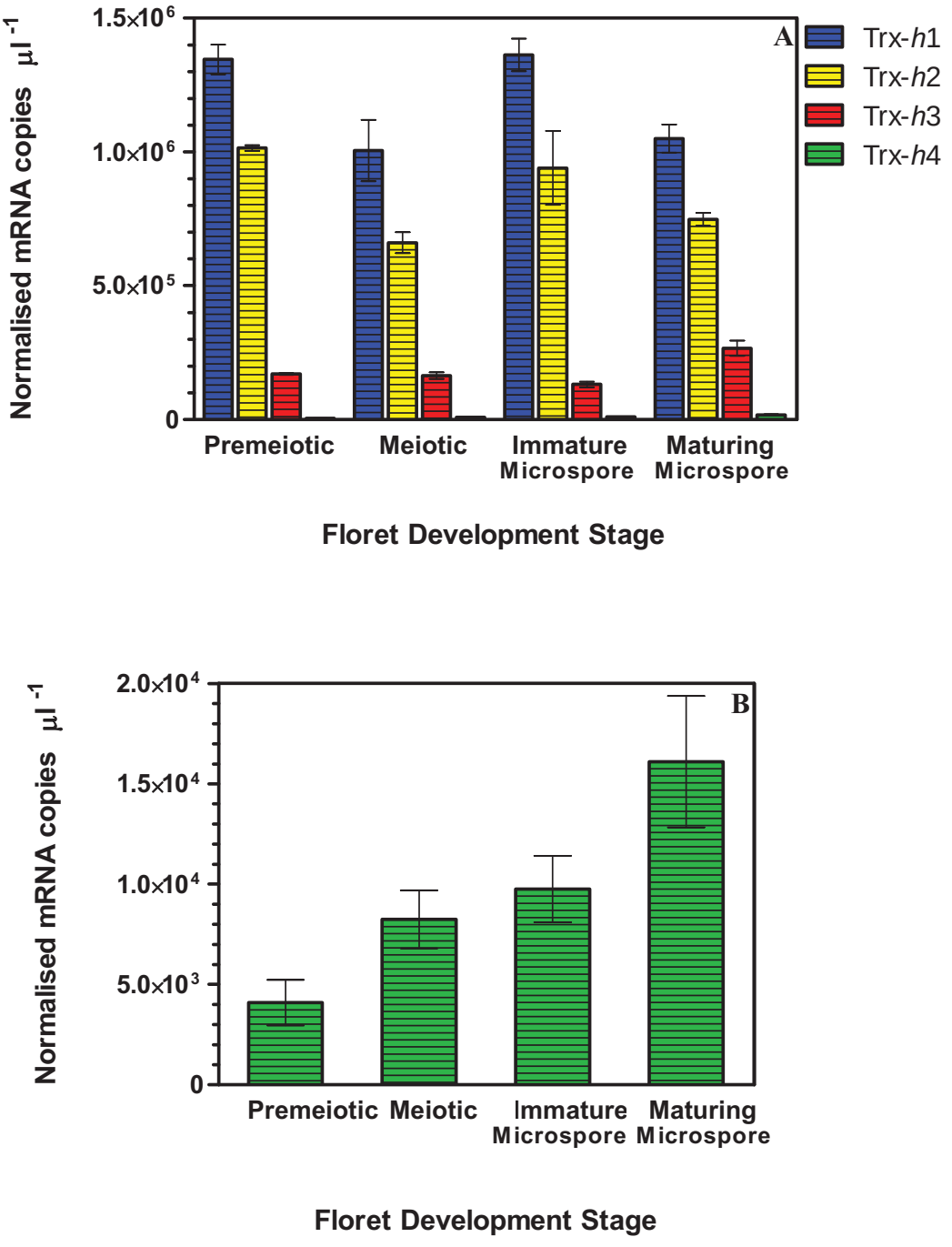

Figure 5.2: **Quantitative-PCR analysis of thioredoxin-*h* transcripts in developing floret tissues of barley plants.** cDNA was synthesised from floret RNA, derived from soil grown *Hordeum vulgare* cv Golden Promise. Q-PCR was performed on cDNA using primers specific to each barley *thioredoxin-h.* Transcript levels are shown as normalised mRNA copies per µl of cDNA template. A) Transcript profile of all four barley cytosolic *thioredoxins*. B) Transcript profile of barley *thioredoxin-h4.*

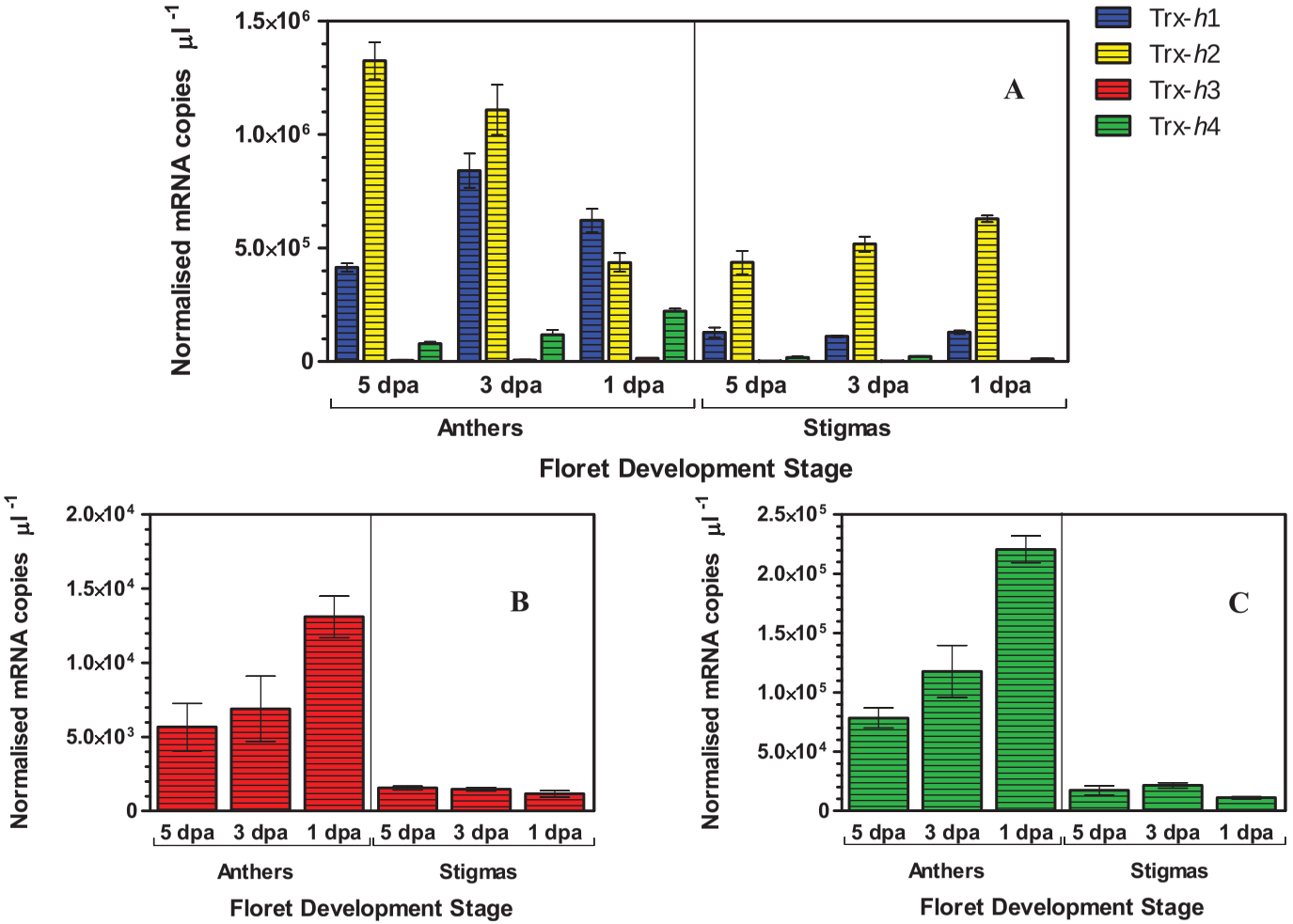

Figure 5.3: **Quantitative-PCR analysis of thioredoxin-*h* transcripts in developing anther and stigma tissues of barley plants.** Anther and stigma tissue, derived from soil grown *H. vulgare*, was isolated at development stages of 1-5 days pre-anthesis (dpa). cDNA was synthesised from the extracted RNA and Q-PCR was performed using primers specific to each barley *thioredoxin-h.* Transcript levels are shown as normalised mRNA copies per µl of cDNA template. A) Transcript profile of all four barley cytosolic *thioredoxins*. B) Transcript profile of barley *thioredoxin-h3*. C) Transcript profile of barley *thioredoxin-h4.*

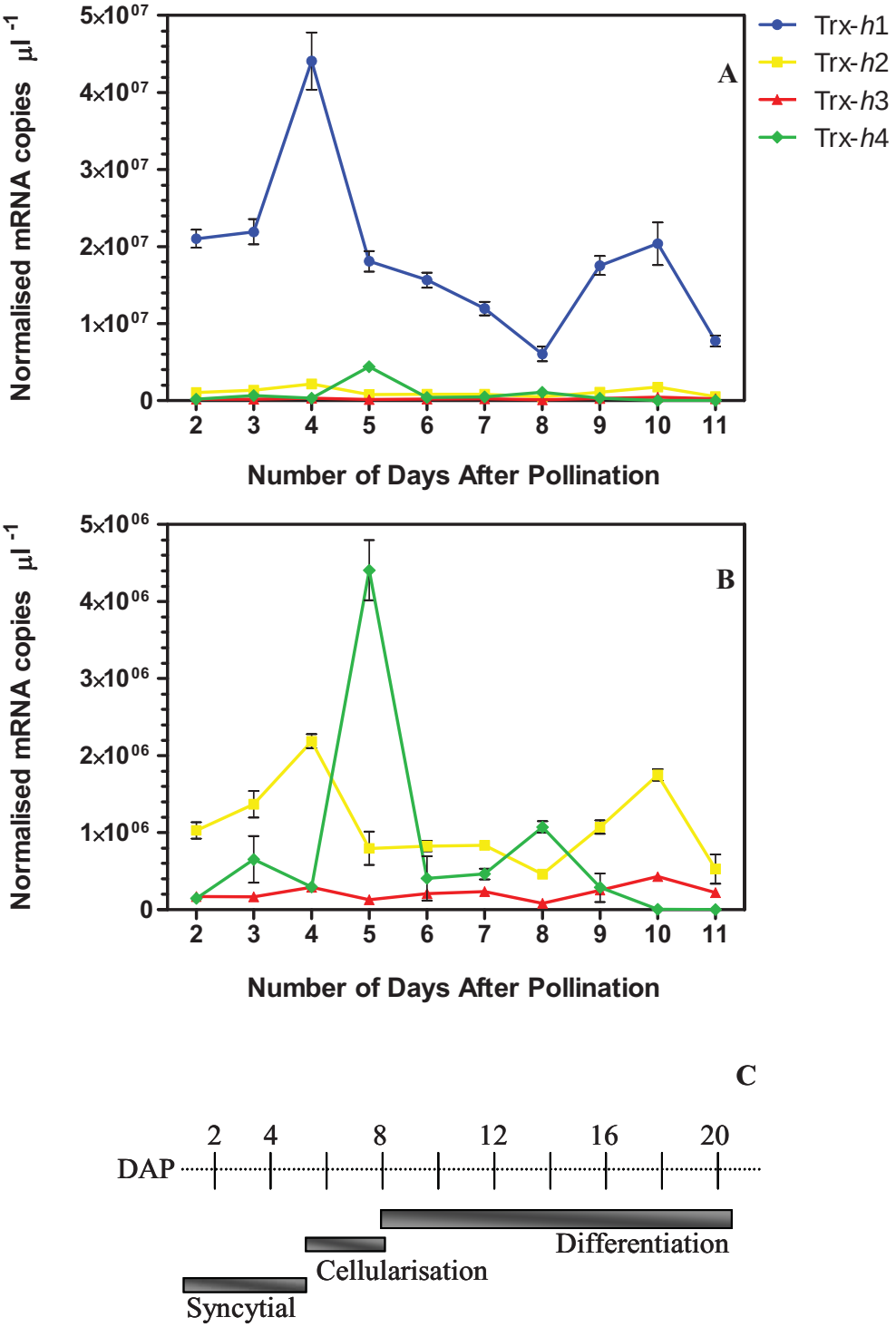

Figure 5.4: **Quantitative-PCR analysis of thioredoxin-*h* transcripts in developing endosperm tissue of barley plants.** cDNA was synthesised from endosperm RNA, collected 2 to 11 days after pollination, derived from soil grown *Hordeum vulgare* cv Golden Promise. Q-PCR was performed on cDNA using primers specific to each barley *thioredoxin-h.* Transcript levels are shown as normalised mRNA copies per µl of cDNA template. A) Transcript profile of all four barley cytosolic *thioredoxins*. B) Transcript profile of barley *thioredoxin-h2, -h3* and *-h4*. C) Stages and timing of the main events of barley endosperm morphogenesis (adapted from Brown et al. (1994)). The time course expressed in days after hand pollination (DAP) for the first three stages of endosperm development is shown.

5.3.3 Analysis of the *HvTrx-h4* Promoter and 5′ Untranslated Region (5′-UTR)

5.3.3.1 Isolation and Cloning of the Sequence 5′ Upstream of HvTrx-h4

To further investigate the spatial and temporal regulation of *HvTrx-h4* expression, isolation and analysis of the *HvTrx-h4* promoter was pursued. To isolate the upstream sequence of *HvTrx-h4*, four *H. vulgare* cv Atlas46 genomic walking libraries (*supplied by Dr Klaus Oldach, ACPFG*) were used as DNA template for a nested PCR approach. Three PCR fragments of approximately 3 kb, 2.5 kb and 600 bp, were isolated. Following cloning of these fragments, plasmids extracted from resulting colonies were subjected to a diagnostic PCR, enabling identification of several plasmids containing the 5′ upstream region of *HvTrx-h4*. The inserts of three plasmids were sequenced, with the result confirming that the *HvTrx-h4* 5′ upstream region had been amplified (Appendix C). Utilising this newly obtained sequence and specifically designed primers, 2556 bp of the 5′ upstream region of *HvTrx-h4* was successfully isolated from the Golden Promise cultivar (Appendix C).

5.3.3.2 Identification of Promoter and 5′-UTR Regions in the Isolated Sequence 5′ Upstream of HvTrx-h4

The isolated sequence was aligned against mRNA sequences of *HvTrx-h4* homologs from *Phalaris coerulescens* (AF159388), *Lolium perenne* (AF159387), *Hordeum bulbosum* (AF159385), *Secale cereale* (AF159386) and *Leymus chinensis* (TA69309_45), derived from Blastn searches of the NCBI and TIGR databases. Alignment with the mRNA sequences began more than 1500 bases into the amplified *HvTrx-h4* cv Golden Promise genomic sequence. After 541 base pairs, the alignment failed (Figure 5.5). In addition, the *HvTrx-h4* non-coding sequence continued 500 bp beyond the start codons (ATG) of the other mRNA sequences. This indicated the presence of an intron in the 5′-UTR genomic sequence of *HvTrxh-4*. The putative intron was removed from the 5′-UTR, which was then re-aligned with the mRNA sequences (Figure 5.6). The predicted *HvTrx-h4* 5′-UTR was split into ‘before intron’ and ‘after intron’ segments and aligned closely, including around the intron splice site. Following this manipulation, the *HvTrx-h4* 5′-UTR now ended at the same place as the mRNA sequences (Figure 5.6).

As shown in Figure 5.7, it was concluded that of the 2556 bp preceding the *HvTrx-h4* start codon, 1515 bp is promoter sequence. The remaining 1041 bp is predicted to be 5′-UTR, within which an intron of 443 bp has been identified. The 5′-UTR sequence 5’ of the intron is 541 bp in length. The 5′-UTR sequence 3’ of the intron is only 57 bp long.

```
Leymus          ------------------------------------------------------------
Secale          ------------------------------------------------------------
Phalaris        ------------------------------------------------------------
H.bulbosum      ------------------------------------------------------------
Lolium          ---------------------------------------------------------AAA
HvUpstream      CAGAAGCTCCACGTCGCCGGATCTCCACCAAGGCAAATACGACCATTTTCCACCAACAGA

Leymus          ---------------------AGGCACGG---CACGAGCCGCGCCAGCCAAGT---GGTG
Secale          ------------------------------------------------------------G
Phalaris        ---------------------CGCACGG---CACGAGCGGCGCCGGCCGGGCCAAGTGG
H.bulbosum      -AAAGCCGTTTCTTTCCGCAGGCGCACGCAAACACCAGCGGCGCCGGCCAACCCAGGTGG
Lolium          AAAAGCCGTTTCTTTCCGCAGGCGCACGCGAACACCAGCGGCGCCGGCCGAGCCAGGTGG
HvUpstream      AAAGGCATTTTCTTTCGGTAGGCGCACACGG-CACGAGCCGCGCCAGCCAAGT---GGCG

Leymus          TGCGACGC-GA--GACGCG------TCACGGGCTC----GCTCACGCCGGCCGGCCGGGA
Secale          TGCGACGC-GA--GACGCG------TCACGGGCCC----GCTCACACCGGCCGGCCGGGA
Phalaris        TGCGACGCCGACCGACGCGGTTAATTCACGGGCTC----GCCCACGCACGCCGGCCGTCC
H.bulbosum      TGCAACCC-CA---ACGCGGTTAATCCACGGGCTC----GCTCACGCACGCACGCCGGCC
Lolium          TGCGACGCCGA----CGCGGTTAATCCACGGGCTC----ACTCACGCACGCACGCCGGCC
HvUpstream      TGCGACGC-GA--GACGCGG------CACGGGCTCTCTCGCTCACGCCGGCCGGCCGGGA

Leymus          G-CGGACGG----GCCGGTCGATCC-ATCCTG---------GTCGTCGGCGTCGTC----
Secale          G-CGGACGGACGGGCCGATCGATCC-ATCCAGCCCCACCGGGTCGTCCCCGTCGTCCCCG
Phalaris        GTCCGACG-------CGGTTAATCC-ACCGCG----------TCGTCGCCGTCGCCGCCG
H.bulbosum      GCCCGCCCGAC--TCCATCCAATCC-CACCGG---------GCCGTCGCCATCGCCGTCG
Lolium          GCCCGCCCGAC--TCCATCCAATCC-CACCGG---------GCCGTCGCCGTCGCCGTCG
HvUpstream      G-CGGACGGC----CCGATCGATCCCATCCAG---------GTCGTCGGCGTCGGC---G

Leymus          --GTCGTCGTCG---CCTCCAGAAGCACGAGCCCAGCATAGCACGGCCGCAGAATATTCC
Secale          TCGTCGTCGTCT---CCTCCAGAAACACGAGCCCAGCATAGCACGGCCGCAGAATATTCC
Phalaris        TCGTCGTCGTCG---CCTCCAGAAACACGAGCCGGCCATAGCACGGCCGCGGAATATTCC
H.bulbosum      TCGTCCTCGTCGTC-CCTCCAAAAACACAAACCGGGCATACCACGGCCGCAAAATATTCC
Lolium          TCGTCCTCGTCGTCGCCTCCAGAAACACGAGCCGGGCATAGCACGGCCGCAGAATATTCC
HvUpstream      TCGTCGTCGTCG---CCTCCAGAAGCACGAGCCCAGCATAGCACGGCCGCAGAATATTCC

Leymus          ACGTCCCTTCCCTT--------TGCG-----------------CCCCAGCAGCAATA--A
Secale          ACGTCCCTTCACTT--------TCCGGCT--------------CCCCAGCAACAATA--A
Phalaris        ACGTCCCTCCCCTCCCCCCTCCTCCGTCCTCATCCACGGGACCCCCCAGCACCACTACAA
H.bulbosum      ACTTCCCTTCCCTTCCACCCTCTCCGTCCTCATCCACGGGAC-CCCCAGCACCAATACAA
Lolium          ACGTCCCTTCCCTTCCACCCTTTCCGTCCTCATCCACGGGAC-CCCCAGCAGCAATACAA
HvUpstream      ACGTCCCTTCCCCTCATCCTCCCCAGG-----------------CCCAGCAGCAATA--A

Leymus          AAAAGCAAGCCAATCCCCCACCCCTCCTCCTCTTCCTCCGATTAATCAA----ACCGCGC
Secale          AAAAGCAAGCCAATCCCCCACCTCT-------TTCCTCCGATTAATCAA----ACCGCGC
Phalaris        AAAAGAAAGAAAACCAATCCTCCTTCCCCCTCCTCCTCCGATTAATCAA----ACCACAC
H.bulbosum      AACAAAAAAACAAATCCTCCTCCTCC----TCCACCTCCGATTAATCAATCAAACCACTC
Lolium          AACAAGAAACCAAATCCTCCTCCTCC----TCCACCTCCGATTAATCAATCGAACCACTC
HvUpstream      AAAAGCAAGCCATTCCCCTCCTCTT---------CCTCCGATTAATCAA----ACCGCGC

Leymus          G--GCGGCGGCGGCGGCG--AGCGTGCGACCTACGACCACCAGACGA--CC--CAACCGA
Secale          G--GCGGCGGCGGCGAC------GTGCGACCTGCGACCACCAGACGA--CC--CAACCGA
Phalaris        GCTGCGGCGGCGCCCAGCGAAGCGAGCAACCTACGACCAGGAGAGGAGACCGTCCACTGA
H.bulbosum      CCTGCGGCGGCGGCAAA------GACCAACCTACAACCACCAAAGGAAACC--CAACCAA
Lolium          GCTGCGGCGGCGGCGAG------GAGCAACCTACGACCAGGAGAGGAGACC--CAACCAA
HvUpstream      G--GCGGCGGCGGCGAG-----CGTGCGACCTGTGACCACCAGACGA--CC--CAACCGA

Leymus          C-------CCACTGACCC----AC-ACCA-CCGGAGA--GCTCTTCCTTTTACGTCAATC
Secale          C-------CCACTGACCC----AC-ACCA-CCGGAGA--GCTCTCCCTTTTACGTTAATC
Phalaris        C-------CCCCACCACC----ACCACCA-CCGGAGACAGCGTTGCCTTGCACGTTAATC
H.bulbosum      GT------CCTCTGACCCC-TCACCACCG-CCGGAGA--GCTCTTCCTTGTACGTTAATC
Lolium          CCACTGGTCGTCTGACCCCCTCACCACCGGCCGGAGA--GCTTTGCCTTCTACGTCAATC
HvUpstream      C-------CCACTGACCCACACCACACCA-CCGGGGA--GCTCTCCCTTTTACGTCAATC

Leymus          AATCGAACCC-AGTTAAAGAACCTCTTAATTGCCCGCCAGGAGATCCGCCAGGCTTATCT
Secale          AATCGAACCC-AGTTAAAGAACCTCTTAATTGCCCGCCAGGAGATCCGCCAGGCTTACCT
Phalaris        CACCCAGCCG-AGTTAAGGAGCCTCTTAATTGCCCG----GAGATCCGCCAGGCTCGTCG
H.bulbosum      AATCCAACCCGAGTTAAGGAACCTCTTAATTGCCCG----GAGATCCGCCAGGCTTACCG
Lolium          AATCCAGCCCGAGTTAAGGGACCTCTTAATTGCCCG----GAGATCCGCCAGGCTTATCG
HvUpstream      AATCGAAACCCAGTTAAAGAACCTCTTAATTGCCCGCCAGGAGATCCGCCAGGCTTATCT
```

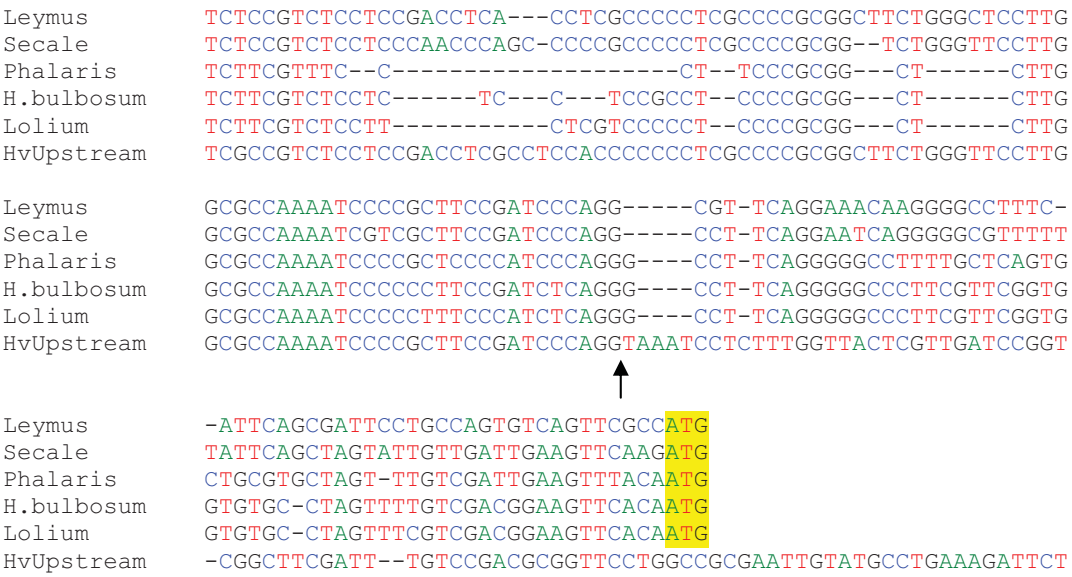

Figure 5.5: **Identification of promoter and 5′-UTR features in the sequence isolated upstream of the *HvTrx-h4* coding sequence.** *HvTrx-h4* genomic sequence isolated by genomic walking was aligned against the mRNA sequences of *Phalaris coerulescens* [AF159388] (Phalaris), *Lolium perenne* [AF159387] (Lolium), *Hordeum bulbosum* [AF159385] (H.bulbosum), *Secale cereale* [AF159386] (Secale) and *Leymus chinensis* [TA69309_45] (Leymus), to identify the most likely 3′end of promoter sequence and start of 5′-UTR sequence. The alignment fails at the site indicated by the arrow. The start codons for the mRNA sequences are highlighted in yellow. Each nucleotide base (A, C, G or T) is coloured alike to assist with visualisation of aligning regions.

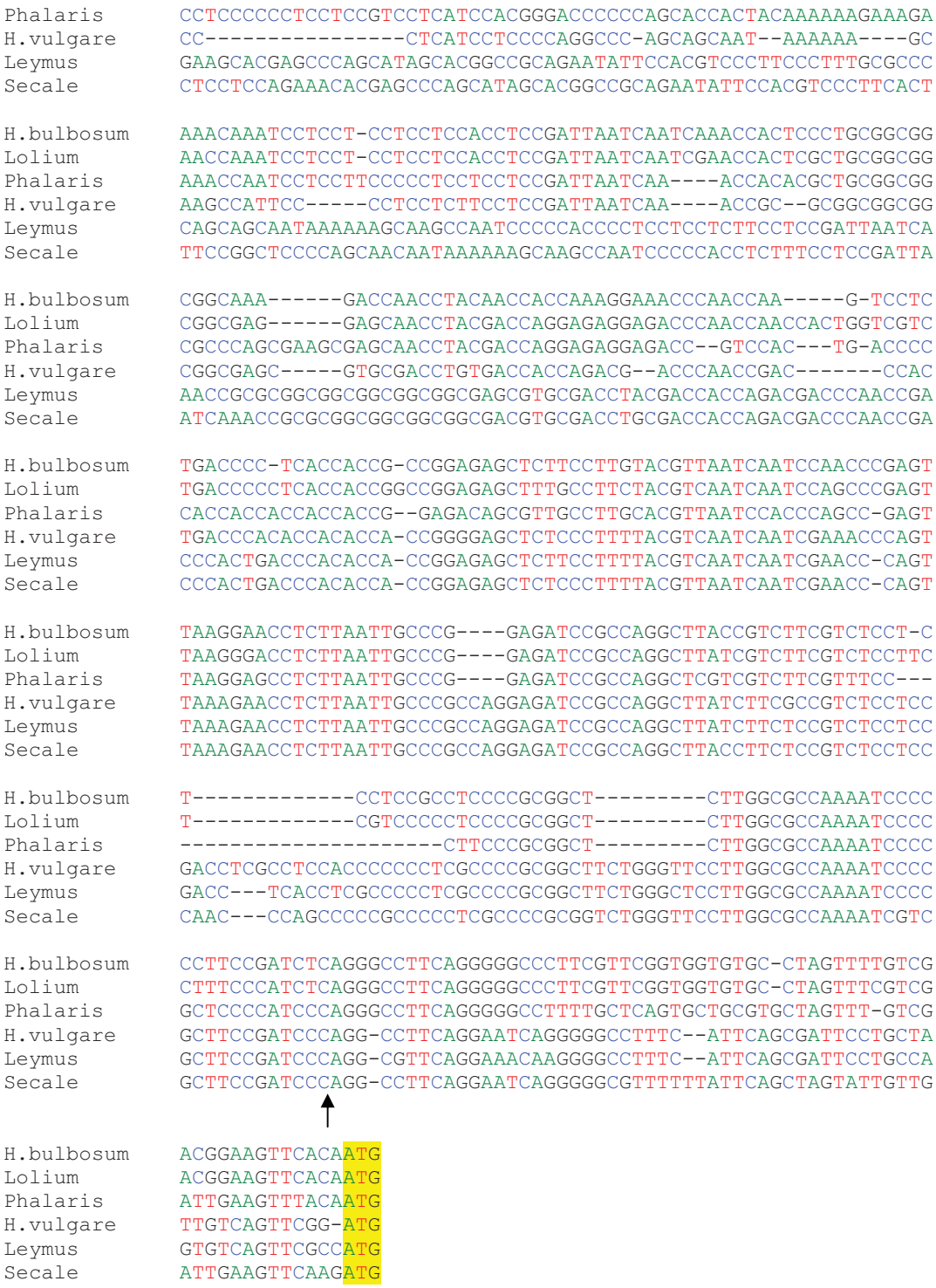

Figure 5.6: ***HvTrx-h4* 5′-UTR.** The predicted 5′-UTR sequence of *HvTrx-h4*, with the putative intron removed, was aligned against the mRNA sequences of *Phalaris coerulescens* [AF159388] (Phalaris), *Lolium perenne* [AF159387] (Lolium), *Hordeum bulbosum* [AF159385] (H.bulbosum), *Secale cereale* [AF159386] (Secale) and *Leymus chinensis* [TA69309_45] (Leymus). The arrow indicates the splice site for the intron (between C and A). The start codons for the mRNA sequences are highlighted in yellow. Each nucleotide base (A, C, G or T) is coloured alike to assist with visualisation of aligning regions.

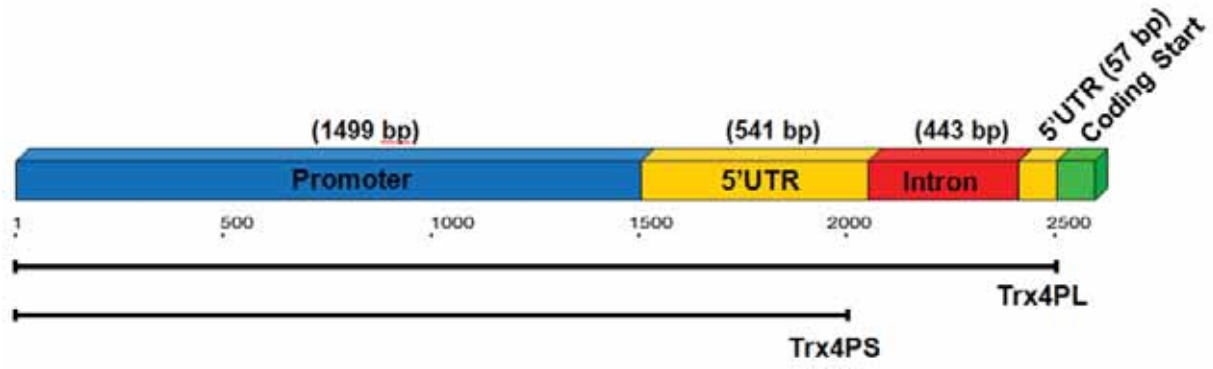

Figure 5.7: **The HvTrx-*h*4 promoter and 5′-UTR were isolated from *Hordeum vulgare* by genomic walking.** A total of 2540 bp preceding the HvTrx-*h*4 start codon was amplified and inserted into GFP expression vectors. The 1st 1499 bp is putative promoter sequence. The remaining 1041 bp is predicted to be a 5′-UTR, in which an intron of 443 bp has been identified. Two fragments differing in length, Trx4PL (2500 bp) and Trx4PS (1932 bp), were amplified from *H. vulgare* cv Golden Promise genomic DNA and inserted into vectors. The shorter fragment, Trx4PS, contains promoter sequence and the 1st 432 bp of 5′-UTR. The longer fragment, Trx4PL, contains the entire promoter and 5′-UTR region that was isolated, including the putative 5′-UTR intron.

5.3.3.3 Motifs Present in the HvTrx-h4 Promoter, 5′-UTR Regions and Intron

The isolated 5′ genomic sequence upstream of HvTrx-*h*4 was scanned by the plant cis-acting regulatory DNA elements (PLACE) database to identify potentially significant motifs. Appendix D contains the full list of motifs identified. Table 5.2 contains some of the motifs that are at least 5 bases in length and were considered perhaps more relevant to thioredoxin in a biological context. There are at least five motifs with functional annotations relating to abscisic acid (Table 5.2). The hormones auxin, jasmonate, salicylic acid and ethylene are also represented. Light responsive elements, an amylase box, endosperm, embryo and seed storage linked motifs were identified as well.

5.3.3.4 Generation of Constructs with Which to Transform Barley

The isolated 5′ upstream region of *HvTrx-h4* was cloned into pMDC107 to drive expression of green fluorescent protein (GFP) (Figure 5.8). The aim was to produce one fragment containing the promoter and 5′-UTR sequence and another truncated version, with just promoter sequence. Unfortunately, the initial sequence alignments and prediction of the 5′-UTR start site was later found to be incorrect and an intron in the 5′-UTR was identified. The error was not detected until after the constructs had been made and the resulting transformed plants were obtained. Therefore, the features in the 2 constructs generated were not as initially intended. Nevertheless, examination of the transformed barley plants was still considered worthwhile as the 5′-UTR intron is not present in one of the constructs (Figure 5.7). The construct containing the shorter fragment (1932 bp), designated Trx4PS, includes the promoter sequence and the 1st 432 bp of 5′-UTR. The construct containing the longer fragment (2540 bp), designated Trx4PL, contains all of the promoter and 5′-UTR region isolated, including the putative 5′-UTR intron. Figure 5.7 depicts a schematic representation of the features present in the two different inserts recombined into the pMDC107 vectors (Figure 5.8).

Table 5-2: **Some of the motifs identified in the HvTrx-*h*4 Promoter, 5′-UTR and Intron regions.** Sequence was screened against the PLACE database. Only 5+ residue motifs were considered. Included is a brief description of the potential or confirmed functions of the motif. The complete list of motifs identified can be found in Appendix D. P = Promoter; 5′B = 5'UTR sequence located before the Intron; I = Putative Intron located within the *HvTrx-h4* 5′-UTR. If the motif was present more than once in a particular sequence feature, the number of times is indicated.

Name	Sequence	Locations	Function Annotation
-10PEHVPSBD	TATTCT	P, 5'B	UVA, Photosystem II
-300CORE	TGTAAAG	I	Endosperm storage
ABRELATERD1	ACGTG	3 x P, 5'B	ABRE-like
ABREOSRAB21	ACGTSSSC	P	Abscisic acid-responsive (ABRE)
AMYBOX1	TAACARA	I	Amylase box
ARFAT	TGTCTC	P	Auxin response factor (ARF)
ASF1MOTIFCAMV	TGACG	P, 5'B, I	Transcriptional activation of genes by auxin and/or salicylic acid
AUXRETGA1GMGH3	TGACGTAA	5'B	Region in Auxin responsive element (AUXRE)
CANBNNAPA	CNAACAC	I	Core of an element in storage protein genes; embryo and endosperm specific transcription of a storage protein gene
CBFHV	RYCGAC	P, 3 x 5'B, I	Binding site of barley CBF (= DRE: dehydration-responsive element)
DPBFCOREDCDC3	ACACNNG	3 x P, I	bZIP transcription factor binding core sequence; bZIP TFs are induced by ABA
EMHVCHORD	TGTAAAGT	I	Endosperm motif, involved in nitrogen response of barley c-hordein promoter
ERELEE4	AWTTCAAA	P	Ethylene responsive element (ERE)
GCCCORE	GCCGCC	P, 3 x 5'B	Core of GCC-box; can function as an ERE; Role in Jasmonate-responsive gene expression
LTRECOREATCOR15	CCGAC	2 x P, 4 x 5'B, 2 x I	Core of low temperature responsive element (LTRE); ABA responsive
RYREPEATBNNAPA	CATGCA	2 x P	Required for seed specific expression; ABA mediated transactivation
RYREPEATLEGUMINBOX	CATGCAY	P	Found in seed storage protein genes
TGACGTVMAMY	TGACGT	5'B	Required for high level expression of alpha-amylase in the cotyledons of germinated seed (of vigna mungo)

A

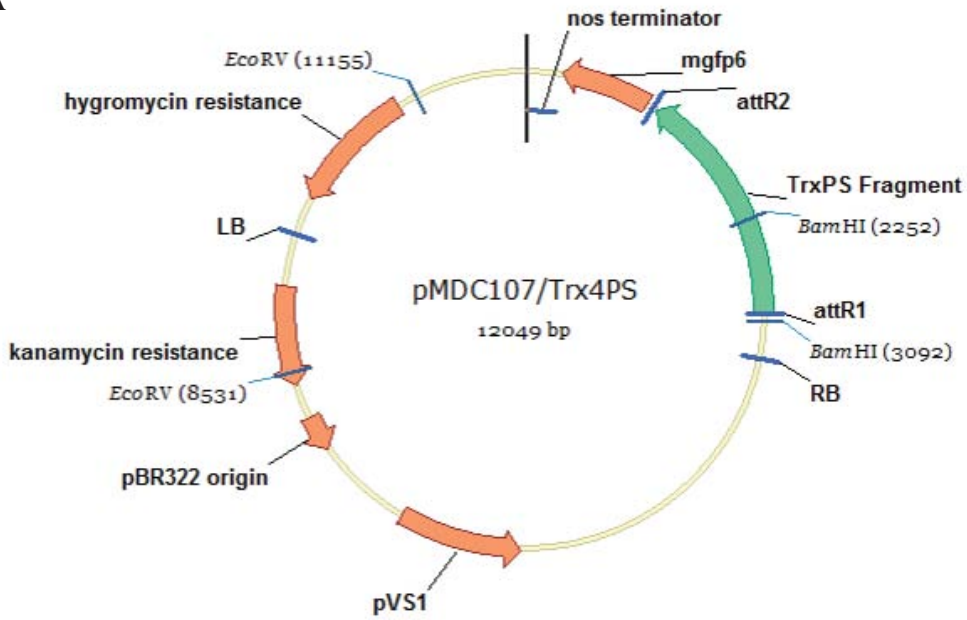

B

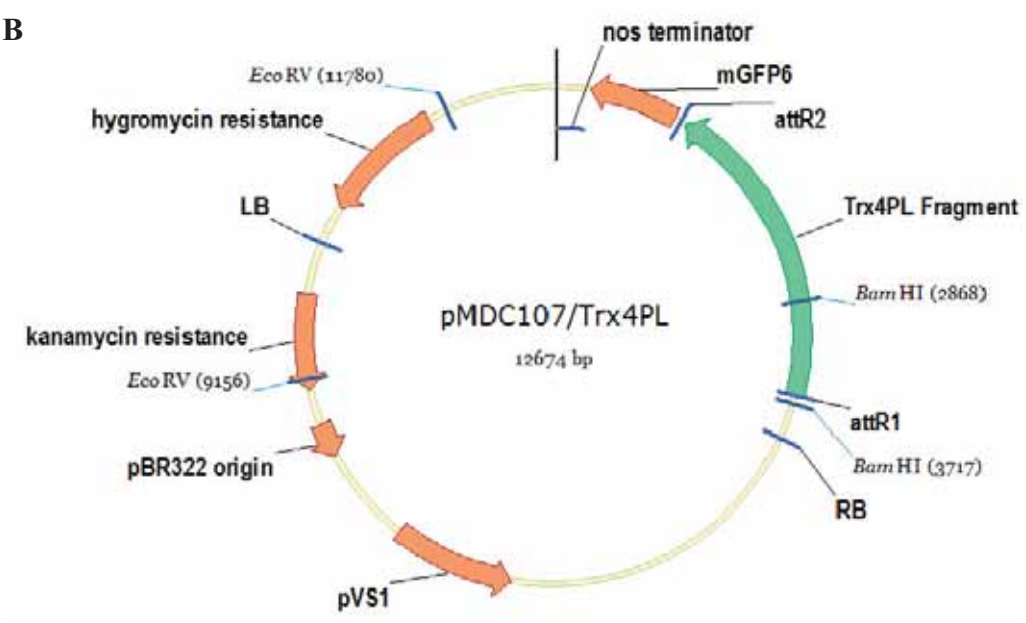

Figure 5.8: **Vector diagram of pMDC107 constructs transformed into *Horddeum vulgare* cv Golden Promise.** Two constructs with the *HvTrx-h4* promoter driving the expression of green fluorescent protein (mgfp6) were built using Gateway® technology. The constructs differ by the length of *HvTrx-h4* 5′-UTR that is included. The restriction sites used in diagnostic PCRs and Southern analysis are indicated. From the right border sequence [RB] the insertion cassette contains: Gateway® recombination sequence attR1; Trx4PS (A) or Trx4PL (B) fragment; Gateway® recombination sequence attR2; green fluorescent protein gene [mGFP6]; bacterial nopaline synthase terminator [nos terminator]; hygromycin resistance gene; left border sequence [LB]. Present in the vector backbone are the kanamycin resistance gene, pBR322 origin of replication and replication protein pVS1 sequence.

5.3.3.5 Confirmation of Successful Transformation of Barley and Determination of the Number of Insertion Events

Ten plants transformed with Trx4PL and five plants transformed with Trx4PS were generated courtesy of the Barley Transformation Group (*The University of Adelaide, ACPFG*). Southern analysis was used to confirm the presence of the insertion cassette and to ascertain the number of copies of the transgene present in each T0 barley plant. Genomic DNA extracted from the transgenic barley plants was digested with a range of restriction endonucleases. Digestion with EcoRV and HindIII was the most complete and resulted in the clearest autoradiographs following Southern hybridisation. EcoRV cuts the insertion cassette sequence once, whilst HindIII does not cut within the insertion cassette. Membranes containing digested DNA were probed with a 700 bp radio-labelled fragment of mGFP6. All ten plants regenerated following transformation with the Trx4PL construct contained the Trx4PL insertion cassette, six of which were single copy insertion events. Of the five plants containing the Trx4PS insertion cassette, two contained single copies of the introduced genetic information (Figure 5.9).

For the next generation of transgenic barley plants (T1), a diagnostic PCR was used to screen the population for the presence of the alien DNA. If positive for the insertion of Trx4PL or Trx4PS, a band of 706 bp was amplified and visible on an ethiduim bromide stained agarose gel. On average, the insertion event was detected in a $1_{negative}$:$3_{positive}$ segregation ratio, as expected according to the Mendelian Inheritance Law.

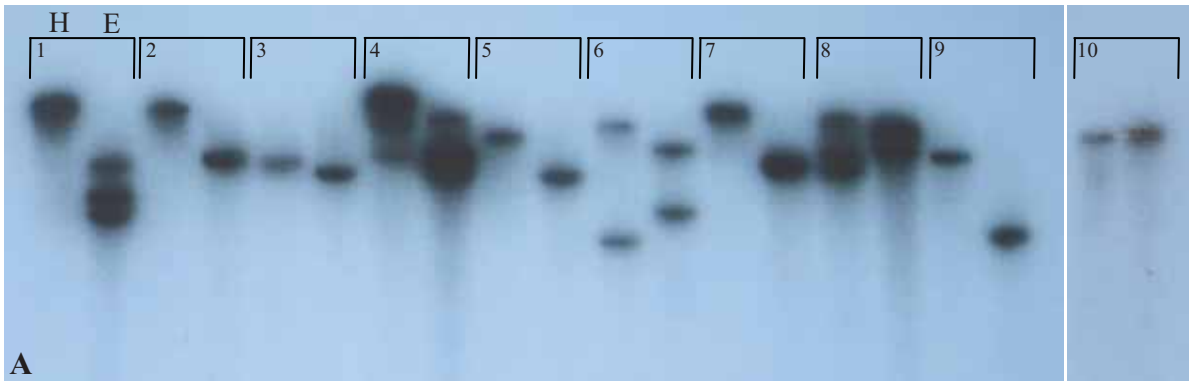

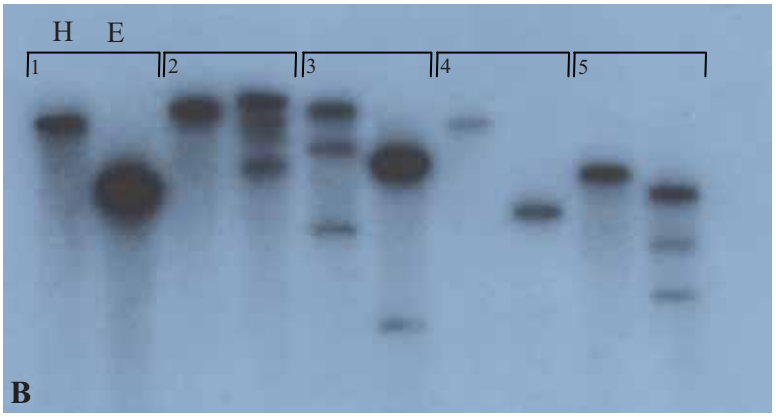

Figure 5.9: **Southern analysis of barley T0 seedlings confirm the presence of TrxPL (A) or TrxPS (B) genetic information and indicate the number of insertion events.** DNA samples from each T0 plant were digested with restriction enzymes HindIII [H] and EcoRV [E] and probed with mGFP6. A) 10 transgenic lines containing TrxPL insertions. B) 5 transgenic lines containing TrxPS insertions.

5.3.4 Analysis of Transgenic Barley

Both transgenic barley lines, containing the Trx4PL or Trx4PS fragment, displayed phenotypes akin to unmodified barley plants, when grown under standard growth conditions. No GFP was seen in any of the T0 or T1 population tissues when viewed under magnification, through a GFP filter. The tissues viewed were: leaves (ranging from 1 week to 2 months of age), stems, awns, florets, anthers, stigmas, endosperm, coleoptiles and young roots (1-3 weeks old). Auto-fluorescence was seen in stigma, pollen and developing seed tissues and attempts to overcome this challenge using quenching chemicals as recommended and supplied by Dr Alex Johnson (*ACPFG, University of Adelaide*) were ineffective. The endosperm at 5 and 8 days after pollination was of particular interest considering the sudden increase in *HvTrx-h4* transcript at these times (see Figure 5.4: Q-PCR). Unfortunately, the level of auto-fluorescence present in wild-type endosperm tissue was highly variable, leading to large discrepancies in the results. Consequently, conclusive interpretation of GFP expression in the transgenic endosperm, based on visual inspection using fluorescence microscopy, was not possible.

5.3.5 Response to Stress and Hormones

As previously discussed in Chapter 3, tobacco plants over-expressing *thioredoxin-h4* showed increase tolerance to several abiotic stresses. Therefore, it was hypothesised that GFP may be produced in the transgenic barley lines following stress with ultraviolet light B (UVB), heat or methyl viologen (MV). It was also considered that HvTrx-*h*4 expression may be hormonally regulated/modulated since the promoter and/or 5′-UTR were predicted to contain abscisic acid (ABA), jasmonic acid (JA) and ethylene response motifs/elements (Table 5-2).

5.3.5.1 Ultraviolet Light Stress Responses

Following exposure to 2 Wm^{-2} of UVB (λ 302 nm), GFP was visible in leaf material from transgenic barley lines containing either the Trx4PL or Trx4PS inserts. Wild-type leaves did not auto-fluoresce. A number of different combinations of UVB stress and recovery times were tested, as outlined in Table 5-3. It was found that following 12 h of UVB stress, a recovery period of at least 18 h was required before GFP was observed (Table 5-3). In very young leaves that were no more than 5 cm in length, 12 h of UVB irradiation alone was enough to elicit GFP expression (Figure 5.10), whilst no GFP was seen in older leaf tissue, for the same treatment. With 12 h of UVB exposure and 24 h of recovery for leaves approximately 20 cm long, GFP was detected only in small patches along the leaf, despite the whole leaf being irradiated (Figure 5.11). The same phenotype was seen when the recovery

period was extended to 30 h. GFP fluorescence was not consistently observed until a recovery time of 36 h was employed (Figure 5.12). No correlation between the individual plant or line and the likelihood of GFP appearing, was obvious. GFP phenotypes were the same for both Trx4PL and Trx4PS lines and results from individual plants within a line were consistent between one another. This observation held true in each irradiation/recovery scenario, suggesting that the absence of part of the 5′-UTR and the intron was not significant for UVB stress response.

Table 5-3: **Transgenic and wild-type barley leaves were exposed to a range of different irradiation and recovery combinations.** Transgenic barley leaves analysed were approximately 20 cm in length unless otherwise stated. Leaves were exposed to 2 Wm^{-2} of UVB (λ302 nm) for the specified duration and recovery was under original growing conditions. Fluorescence emitted by GFP was seen through a Leica MZ FLIII fluorescence stereomicroscope fitted with GFP fluorescence filter sets. Images were captured with a Leica DC 300F digital camera.

UVB Exposure + Recovery Times (h)	GFP Status in Transgenic Barley Leaves
12 + 0	Absent except in several very young leaves ~3 cm long
24 + 0	GFP seen in ~ 75% of leaves
12 + 12	Absent
12 + 18	Absent
12 + 24	Absent except in a couple of small patches, ~1 cm length, on a couple of leaves (not line specific)
12 + 30	Absent except in a couple of small patches, ~1 cm length, on a couple of leaves: not always same line as in 24 h recovery samples
12 + 36	GFP seen in ~ 50% of leaves

Considering the presence of numerous hormonal response elements predicted in the *HvTrx-h4* promoter region, the possibility of hormonal involvement in the expression of GFP in response to stress was considered. In addition, initial experiments revealed that GFP accumulation appeared to be highest along plant vasculature suggesting possible translocation of signal. Therefore, it was questioned whether the signal resulting in GFP expression following UVB stress was mobile and if it could be translocated along the leaf tissue. To test this, one half of leaves approximately 20 cm in length were shielded from the UVB irradiation. Several leaves from at least four individual plants from each transgenic line were analysed in this signal translocation experiment. As evident in Figure 5.13, no migration of the signal occurred. GFP was visible only where UVB contacted the leaf surface directly and it was never seen in the shielded, unstressed leaf tissue (Figure 5.13). Therefore, GFP driven by the *HvTrx-h4* promoter and 5′-UTR was responsive to UVB stress but the signal was not translocated. Both transgenic lines behaved in the same manner.

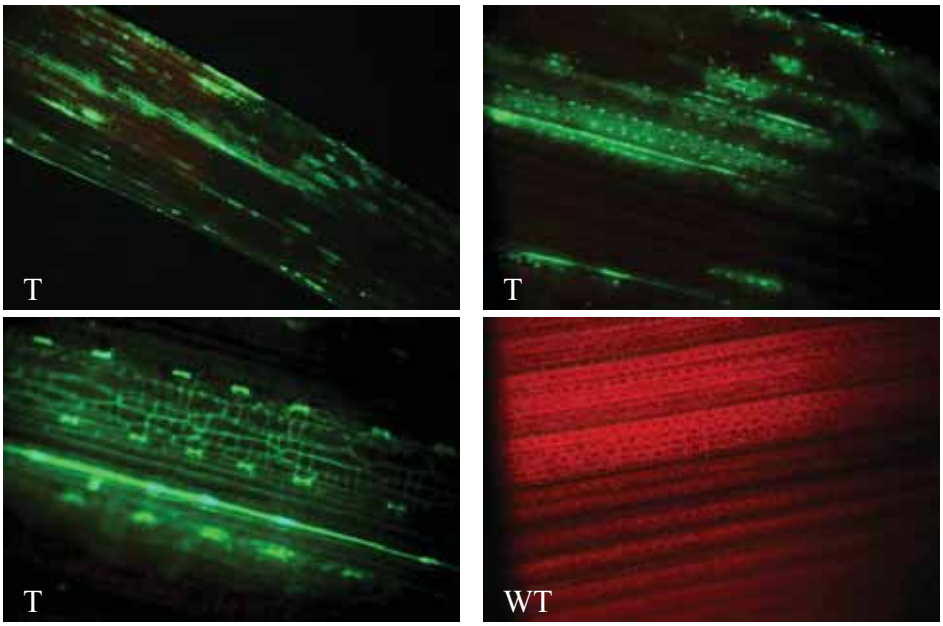

Figure 5.10: **GFP was visible only in very young transgenic barley leaves (T) following 12 h of UVB exposure.** Leaves that were no more than 5 cm in length were irradiated with 2 Wm^{-2} UVB (λ302 nm) and then immediately viewed. The transgenic barley lines contained Trx4PL or Trx4PS inserts (T). Wild-type barley images (WT) show extent of auto-fluorescence. No differences in GFP expression were apparent between the two lines, Trx4PL and Trx4PS. Fluorescence emitted by GFP was seen through a Leica MZ FLIII fluorescence stereomicroscope fitted with GFP fluorescence filter sets. Images were captured with a Leica DC 300F digital camera.

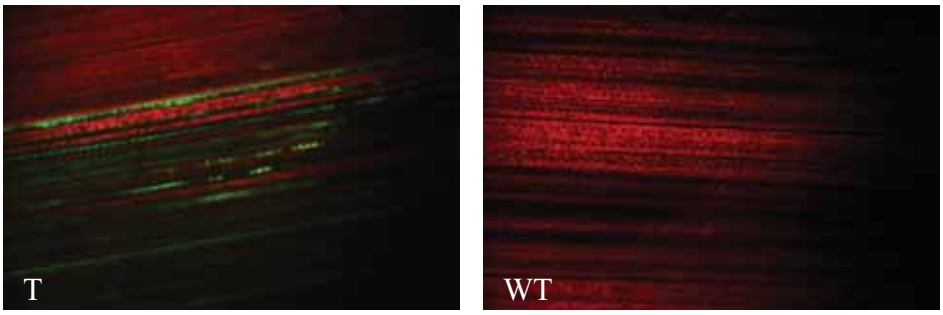

Figure 5.11: **Patches of GFP were visible in transgenic barley leaves (T) after 12 h of UVB exposure and a 24 h recovery period.** The transgenic barley lines (T) contained Trx4PL or Trx4PS inserts. Leaves approximately 20 cm in length were irradiated with 2 Wm^{-2} UVB (λ302 nm). No differences in GFP expression were apparent between the two constructs. Wild-type barley images (WT) show extent of auto-fluorescence. No differences in GFP expression were apparent between the two lines, Trx4PL and Trx4PS. Fluorescence emitted by GFP was seen through a Leica MZ FLIII fluorescence stereomicroscope fitted with GFP fluorescence filter sets. Images were captured with a Leica DC 300F digital camera.

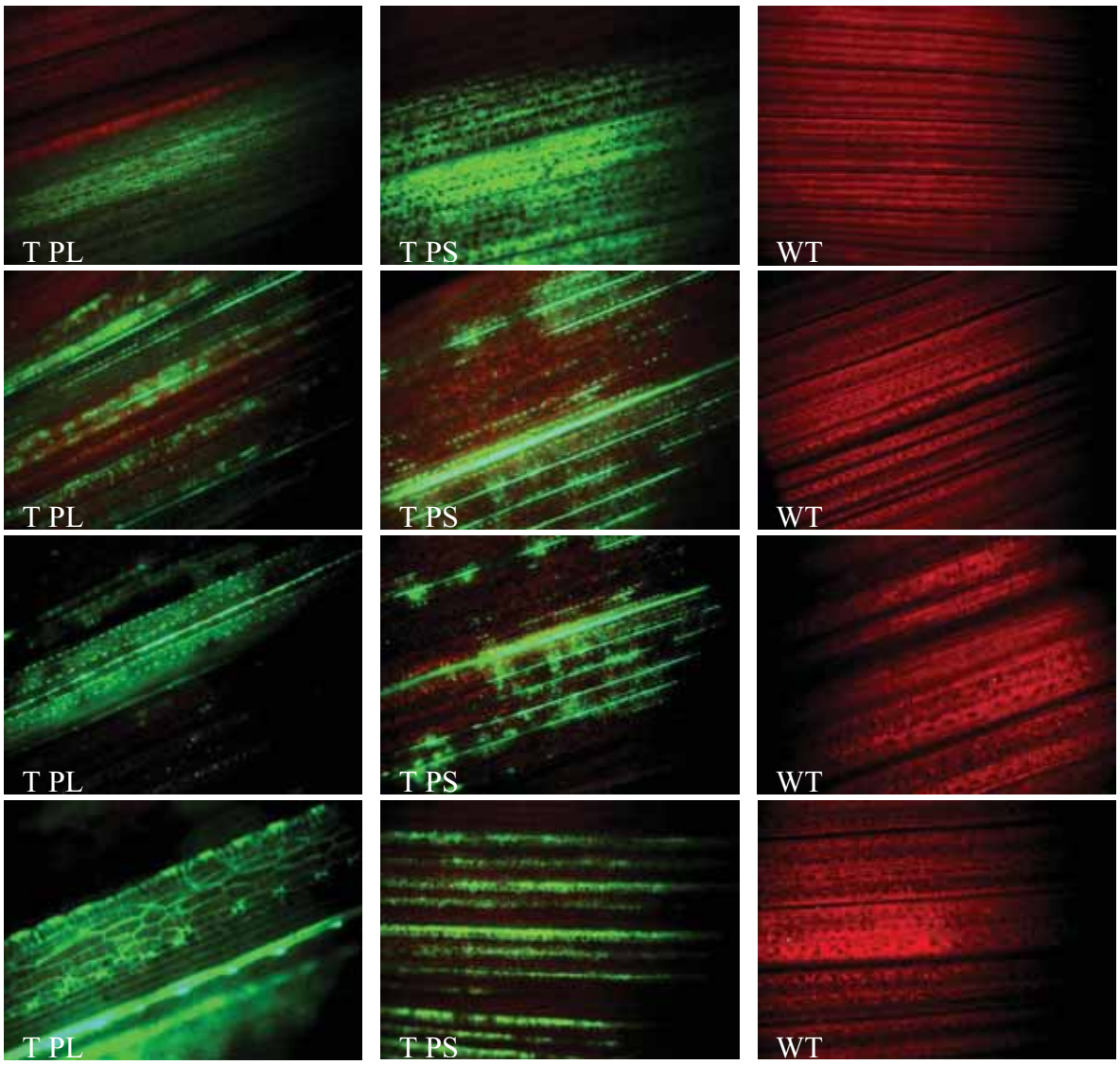

Figure 5.12: **GFP was visible in transgenic barley leaves after 12 h of UV exposure and a 36 h recovery period.** Leaves from transgenic lines containing Trx4PL (PL) or TrxPS (PS) were approximately 20 cm in length and were irradiated with 2 Wm^{-2} UVB (λ302 nm). Wild-type barley images (WT) show extent of auto-fluorescence. No differences in GFP expression were apparent between the two lines, Trx4PL and Trx4PS. All GFP patterns were seen in both transgenic lines. Fluorescence emitted by GFP was seen through a Leica MZ FLIII fluorescence stereomicroscope fitted with GFP fluorescence filter sets. Images were captured with a Leica DC 300F digital camera.

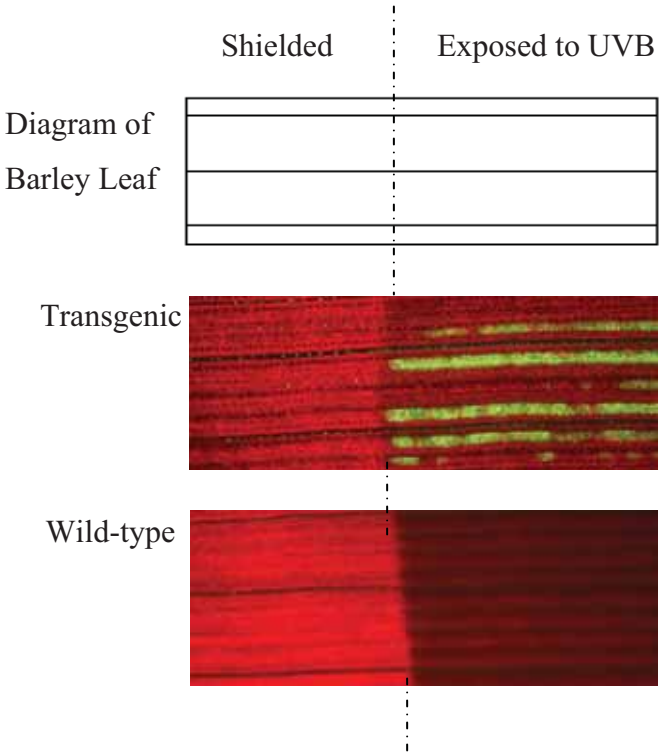

Figure 5.13: **GFP is elicited by UVB stress but the signal is not translocated.** Detached transgenic barley leaves containing Trx4PL or Trx4PS, were floated on water whilst partially covered with aluminium foil and exposed to 8 Wm^{-2} of UVB (λ302 nm). Leaves were returned to their original light conditions for 30 min of recovery. Wild-type barley leaves were treated the same way. Fluorescence emitted by GFP was seen through a Leica MZ FLIII fluorescence stereomicroscope fitted with GFP fluorescence filter sets. Images were captured with a Leica DC 300F digital camera. Both transgenic lines behaved in the same manner.

The behaviour of the endogenous *HvTrx-h4* in the transgenic plants expressing GFP (following UVB stress) was investigated to determine if *GFP* was mimicking *HvTrx-h4* expression. To begin with, RNA was extracted from UVB stressed and unstressed leaf tissue, the DNA was degraded and *HvTrx-h4* and *GFP* transcript expression was assessed by reverse transcriptase (RT)-PCR (see 2.6 and 2.4.4). The gene *CHS2,* which was previously reported to be UV responsive (Christensen et al., 1998), and *18S ribosomal RNA* (*18SrRNA*) transcripts (Kim et al., 2003) were also examined to serve as controls (see Appendix B for primer sequences). The expression of *18SrRNA* indicated consistent template quantities were supplied for the RT-PCR. As expected, *CSH2* transcripts were only present in tissue exposed to UVB (Figure 5.14).

As shown in Figure 5.14, endogenous *HvTrx-h4* transcript is present in all samples, whether UVB irradiated or not and does not appear to increase in response to UVB. *GFP* transcript expression mimics that of *HvTrx-h4* in the transgenic barley lines (Figure 5.14). The RT-PCR results revealed that although GFP protein is not visible in unstressed leaf tissue of either transgenic line (see 5.3.4 also), *GFP* transcript is indeed present (Figure 5.14). Therefore, it appears that UVB can induce translation of the transgene mRNA. This result suggests that the expression of the HvTrx-*h*4 protein is post-transcriptionally regulated.

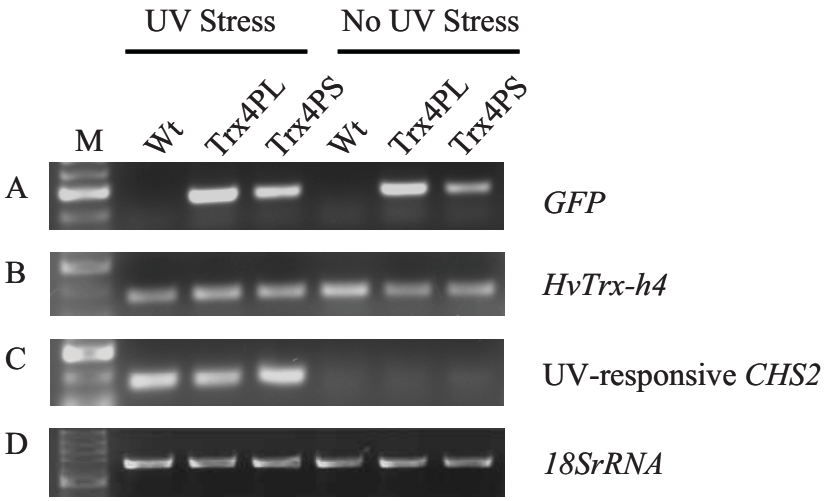

Figure 5.14: **Semi-quantitative RT-PCR analysis shows *GFP* expression mimics that of endogenous *HvTrx-h4* in unstressed and UVB stressed tissue.** RNA was extracted from unstressed and UVB stressed leaf tissue derived from wild-type (Wt) and transgenic barley lines (Trx4PL and Trx4PS). Transcripts were analysed using OneStep RT-PCR with primers specific to the gene of interest. The resulting products were separated and viewed on a 1.4 % agarose gel. A) *GFP* transcript B) Endogenous *HvTrx-h4* transcript C) Transcript of the UV responsive gene *CHS2* D) *18SrRNA* transcript was used as a template/loading control. Marker (M); Wt UVB stressed (lane 1); UVB stressed Trx4PL transgenic line (lane 2); UVB stressed Trx4PS transgenic line (lane 3); Wt unstressed (lane 4); Unstressed Trx4PL transgenic line (lane 5); Unstressed Trx4PS transgenic line (lane 6).

5.3.5.2 Wounding Response

Whilst dissecting tissues to analyse the unstressed phenotype of the transgenic barley lines, it was observed that GFP could often be detected at wounded sites. As shown in Figure 5.15, GFP expression is localised to the wound site of leaves injured with metal tweezers or cut with scissors, as well as at the broken end of awns. A small amount of auto-fluorescence is visible at the wound site of the broken awns as indicated by the wild-type control. However, an increase in green fluorescence intensity is clear in the transgenic awn sample. Once again, no differences in GFP expression are evident between the two different transgenic lines, which contained differing amounts of 5′-UTR sequence. The results indicate that GFP protein is localised to wound sites, when controlled by the *HvTrx-h4* promoter.

Transcript analysis of *HvTrx-h4* and *GFP* were also investigated by RT-PCR in wounded tissue to determine if expression of *GFP* was mimicking that of *HvTrx-h4*. The RT-PCR analysis included the *Ubiquitin* gene as a control to demonstrate the quantity of template RNA supplied from each sample (Figure 5.15). A wound responsive gene, *PWMK1*, served as a positive wounding control (Eckey et al., 2004) . Although *PWMK1* transcripts are present in unwounded tissue, they increase in response to wounding in all three samples, when taking into account the *Ubiquitin* loading control transcript levels seen (Figure 5.16). *HvTrx-h4* transcript is present in all samples, whether wounded or not and the endogenous *HvTrx-h4* transcript does not appear to increase in response to wounding. Importantly, *GFP* transcript expression mimics that of endogenous *HvTrx-h4*, in the transgenic barley lines (Figure 5.16).

The RT-PCR results were consistent with those from the UVB stress experiment. Again, although GFP protein is not visible in the non-wounded leaf tissue of either transgenic line (see 5.3.4 also), *GFP* transcript is in fact present (Figure 5.16). As concluded for UVB, it appears that wounding also induces the translation of the mRNA coding for GFP, which is under the control of *HvTrx-h4* regulatory sequence. This result also supports the previous hypothesis, that a post-transcriptional modification may regulate the expression/translation of HvTrx-h4 protein.

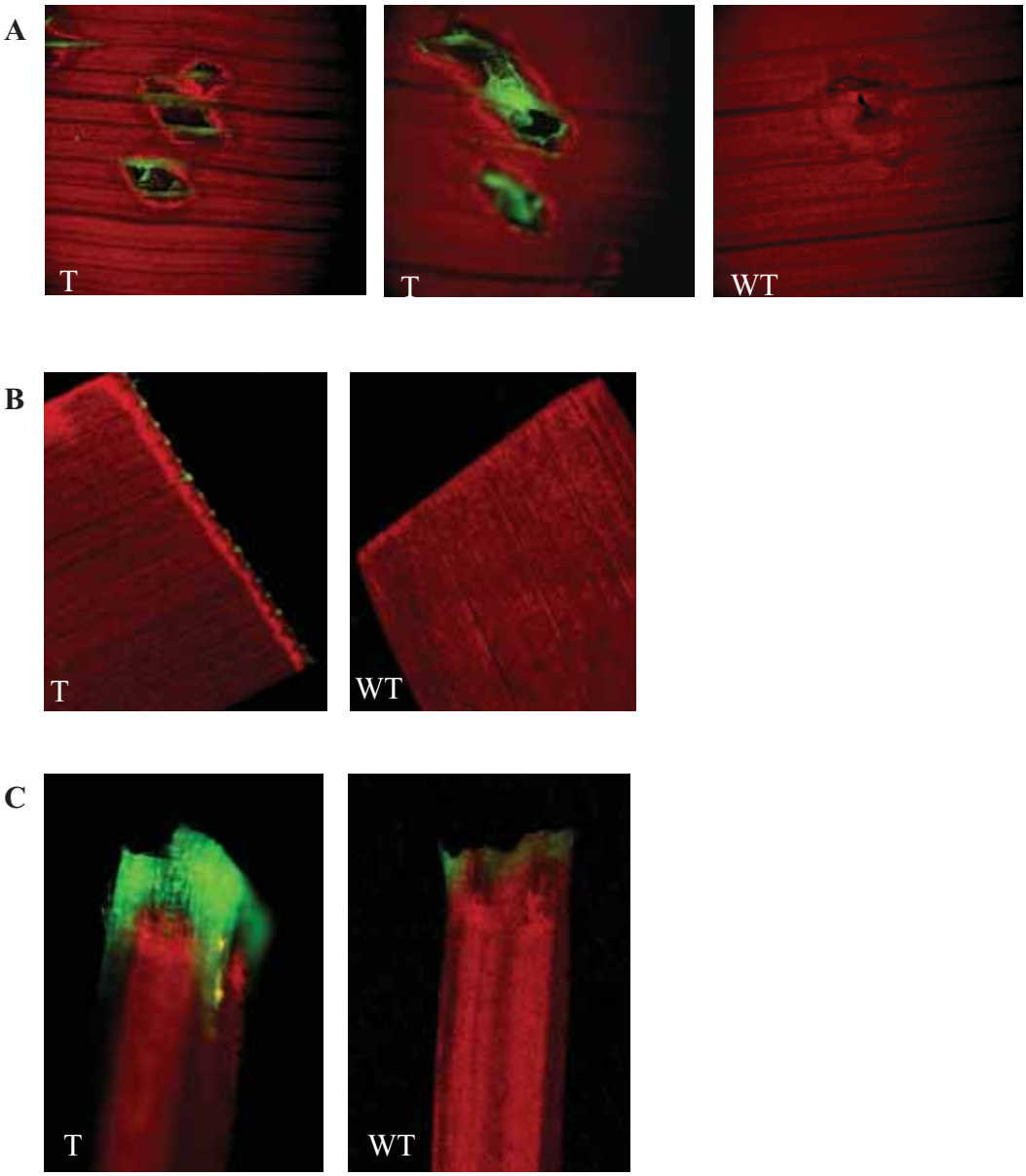

Figure 5.15: **GFP was visible in transgenic barley (T) in response to wounding.** Leaves approximately 20 cm in length from transgenic lines containing Trx4PL (PL) or TrxPS (PS) were injured with the sharp points of metal tweezers (A) and cut with sharp metal scissors (B). Barley awns were broken by hand (C). Wild-type barley images (WT) show extent of auto-fluorescence. No differences in GFP expression were apparent between the two lines, Trx4PL and Trx4PS. Fluorescence emitted by GFP was seen through a Leica MZ FLIII fluorescence stereomicroscope fitted with GFP fluorescence filter sets. Images were captured with a Leica DC 300F digital camera.

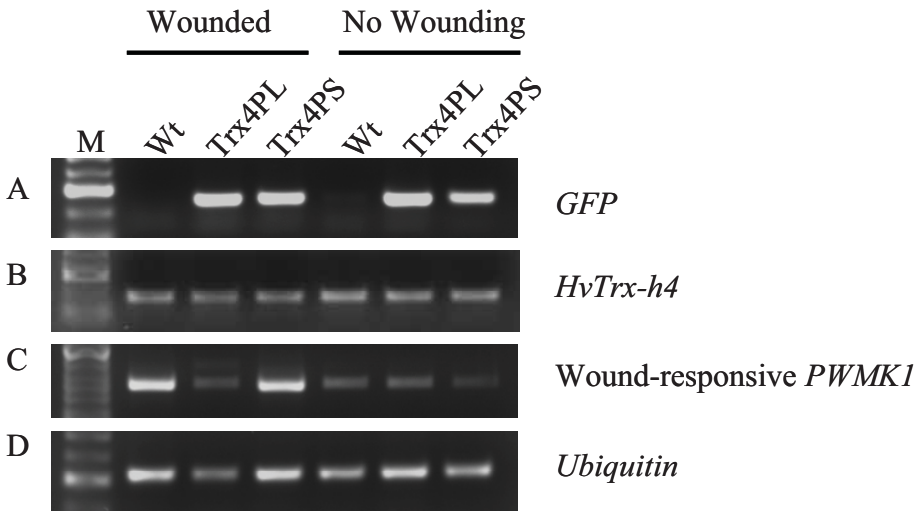

Figure 5.16: **Semi-quantitative RT-PCR analysis shows *GFP* expression mimics that of endogenous *HvTrx-h4* in undamaged and wounded tissue.** RNA was extracted from unwounded and wounded leaf tissue derived from wild-type (Wt) and transgenic barley lines (Trx4PL and Trx4PS). Transcripts were analysed using OneStep RT-PCR with primers specific to the gene of interest. The resulting products were separated and viewed on a 1.4% agarose gel. A) *GFP* transcript B) Endogenous *HvTrx-h4* transcript C) Transcript of the wound responsive gene *PWMK1* D) *Ubiquitin* transcript was used as a template/loading control. Marker (M); Wt UVB stressed (lane 1); UVB stressed Trx4PL transgenic line (lane 2); UVB stressed Trx4PS transgenic line (lane 3); Wt unstressed (lane 4); Unstressed Trx4PL transgenic line (lane 5); Unstressed Trx4PS transgenic line (lane 6).

5.3.5.3 Methyl Viologen Stress Challenge

Tobacco plants over-expressing *thioredoxin-h4* displayed increased tolerance to methyl viologen, as previously reported in Chapter 3. Considering this, it was of interest to see if GFP was visible in the transgenic barley lines following treatment with methyl viologen. Detached barley leaves approximately 15 cm in length were surface treated with 10 µl droplets of methyl viologen at 0, 0.1, 1, 5 and 10 µM concentrations. To maintain leaf turgor, the cut end of each leaf was kept in water throughout the treatment. After 1, 2, 6, 12 and 18 h the treated sites were examined for the presence of GFP. Wild-type barley cv Golden Promise, subjected to the same conditions, was used as a negative control. GFP was never detected in response to any of the methyl viologen treatments, in either transgenic barley line (Figure 5.17). Some auto-fluorescence was present at the treatment sites (Figure 5.17). The results indicate that expression of GFP, when driven by the *HvTrx-h4* promoter and 5′-UTR genetic sequences, is not induced by methyl viologen.

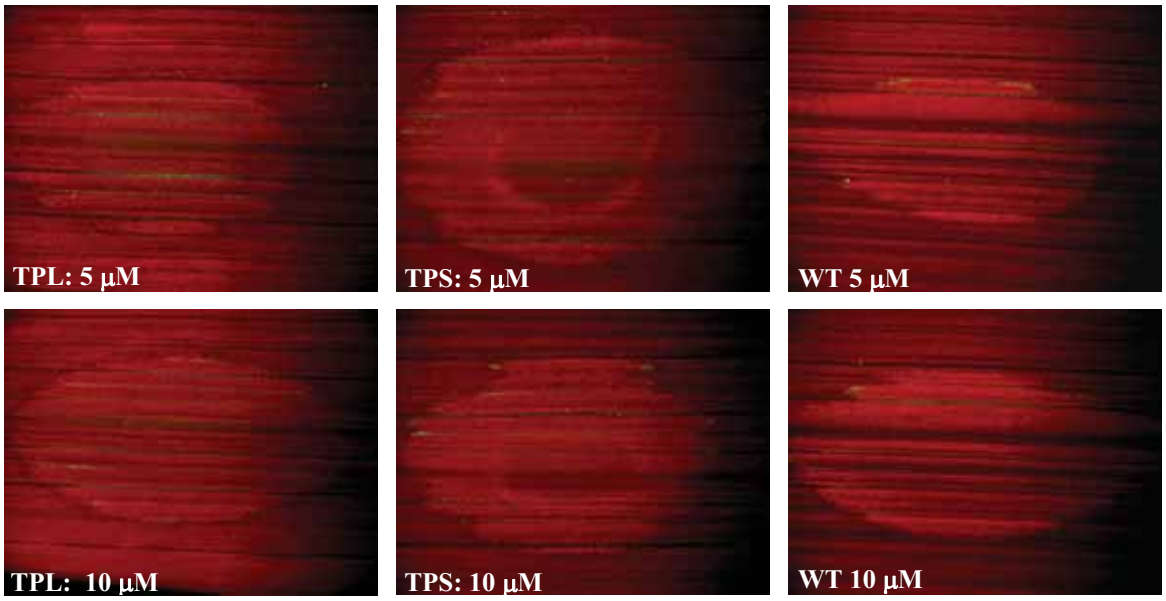

Figure 5.17: **GFP was not visible in transgenic barley leaves following methyl viologen treatment.** Methyl viologen (5 µM and 10 µM) was applied to detached leaves from transgenic barley lines containing Trx4PL (TPL) and Trx4PS (TPS). Twelve hours later, the presence or absence of GFP was assessed. Wild-type barley images (WT) show extent of auto-fluorescence. A Leica MZ FLIII fluorescence stereomicroscope fitted with GFP fluorescence filter sets was used to view the leaves. Images were captured with a Leica DC 300F digital camera.

5.3.5.4 Hormone Treatments: ABA, JA and Ethylene

Reactive oxygen species interact with major signalling pathways including those regulated by abscisic acid (ABA), jasmonic acid (JA) and ethylene (Kotchoni and Gachomo, 2006). Considering this, the presence of GFP in both transgenic lines following wounding and UVB stress, as well as the identification of motifs for these hormones in the promoter and 5′-UTR regions of the *HvTrx-h4* genomic sequence (see 5.3.3.3), the effect of ABA, JA and ethylene upon GFP protein expression in the transgenic barley lines was of interest.

Detached leaves from Trx4PL and Trx4PS transgenic barley lines, approximately 15 cm in length, were surface treated with 15 µl droplets of ethylene at 0, 100µM and 100 mM concentrations. To maintain leaf turgor the cut end of each leaf was kept in water throughout the treatment, which proceeded in the dark. After 1.5 – 2 h of incubation the treated sites were examined for the presence of GFP. Wild-type barley subjected to the same conditions was used as a negative control. GFP was not detected in response to any of the ethylene treatments, in either transgenic barley line (Figure 5.18). The ethylene was considered to have penetrated the leaf surface and entered the cells, as necrotic lesions developed at the droplet sites (Figure 5.18). The results indicate that GFP expression, when driven by the *HvTrx-h4* promoter and 5′-UTR genomic information, is not induced by ethylene.

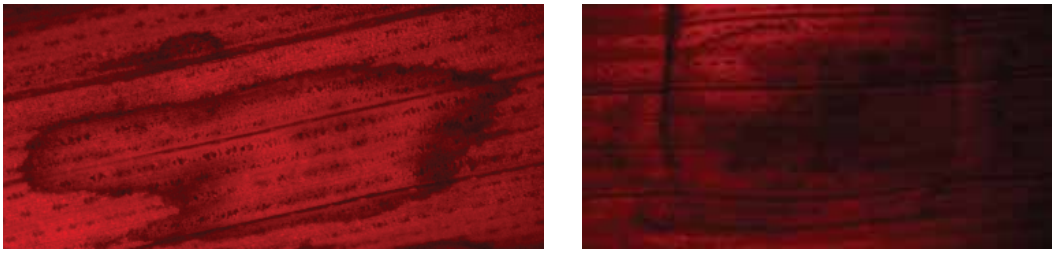

Figure 5.18: **Necrotic lesions are present at the site of ethylene application.** Droplets (15 µl) of ethylene (100 µM) were placed on leaves detached from the transgenic barley lines and absorbed over 1.5 – 2 h. A) Necrotic lesion on leaf following complete absorption of ethylene. B) Necrotic lesion on leaf visible through a partially absorbed ethylene droplet. A Leica MZ FLIII fluorescence stereomicroscope fitted with GFP fluorescence filter sets was used to view the leaves. Images were captured with a Leica DC 300F digital camera.

Leaves from both transgenic barley lines were also exposed to ABA and JA treatments, of 10 μM, 100 μM and 1 mM concentrations. The leaves were detached and 4 cm sections were floated on top of the hormone solutions, with at least one of the cut ends submerged, for 1, 2, 4 and 14 h to allow uptake of the hormone. Wild-type barley subjected to the same conditions was used as a negative control. GFP was not expressed in response to ABA nor JA (*images not shown*). The leaves appeared unaffected by the hormone treatments and so it was considered that the hormones may not have been entering the leaf tissue. To test this, treated samples from several transgenic lines were collected, pooled and RT-PCR was performed using primers designed to amplify genes previously reported to be ABA or JA responsive (Choi et al., 2002; Ortel et al., 1999) (see Appendix B for primer sequences).

Figure 5.19 shows ABA-responsive barley *Dehydrin4* gene expression is switched on in samples treated with ABA, whilst its transcript is not visible in the water treated controls. Therefore, it is clear that ABA did indeed infiltrate the leaf tissue. Similarly, transcript of the JA-responsive barley gene, *JIP23*, is present in all samples treated with JA (Figure 5.20). *JIP23* is not expressed in the untreated controls for wild-type and transgenic line Trx4S. However, *JIP23* transcript is present in the untreated sample derived from the Trx4PL transgenic line. The reason for this is unclear. Repeated RT-PCRs yielded the same result. However, considering the endogenous *HvTrx-h4* promoter and 5′-UTR are still present in the transgenic line, it is unlikely that the alien genetic information is affecting the expression of other genes. Therefore, it was speculated that a stress event inducing *JIP23* expression occurred at the time of sampling. Despite the unexpected appearance of *JIP23* transcript in the Trx4PL transgenic line, we are confident that JA successfully entered the leaf tissues.

The results obtained for all hormone treatments, in conjunction with the previously established presence of GFP transcripts in untreated samples (Figure 5.14 and Figure 5.16), indicate that neither ethylene, ABA nor JA are capable of inducing the translation of GFP. Therefore, it is concluded that translation of *HvTrx-h4* mRNA into protein is not induced by ethylene, ABA nor JA despite the apparent presence of related regulatory elements that were identified in the non-coding *HvTrx-h4* genomic sequence (Table 5.2).

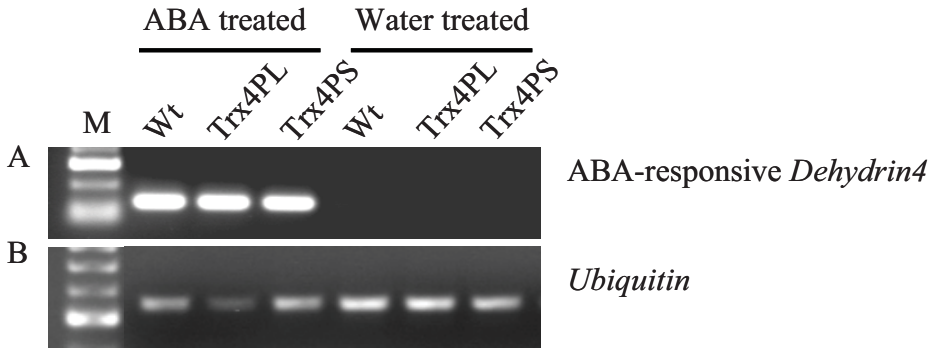

Figure 5.19: **Semi-quantitative RT-PCR analysis of wild-type and transgenic barley lines containing differing *HvTrx-h4* Promoter:*GFP* constructs following treatment with 1 mM abscisic acid (ABA).** RNA was extracted from leaf tissue following ABA or RO water (background control) treatment and transcripts were analysed using OneStep RT-PCR with primers specific to the gene of interest. A) The ABA-responsive gene *Dehydrin4* is expressed in all ABA treated samples. B) Ubiquitin transcript was used as a template loading control. Marker (M); Wt ABA treated (lane 1); ABA treated transgenic line containing Trx4PL (lane 2); ABA treated transgenic line containing Trx4PS (lane 3); Wt RO water treated (lane 4); RO water treated transgenic line containing Trx4PL (lane 5); RO water treated transgenic line containing Trx4PS (lane 6).

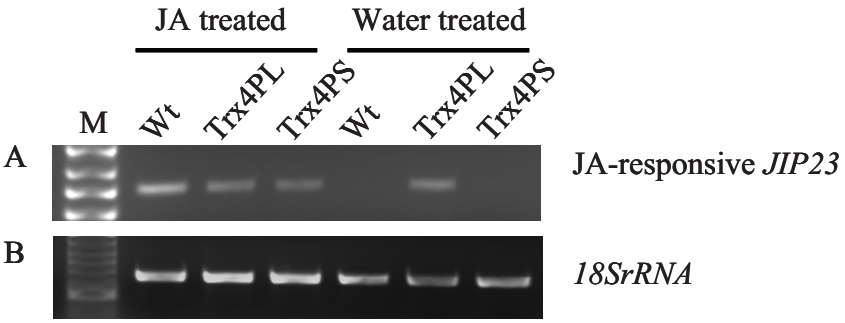

Figure 5.20: **Semi-quantitative RT-PCR analysis of wild-type and transgenic barley lines containing differing *HvTrx-h4* Promoter:*GFP* constructs following treatment with 1 mM jasomonic acid (JA).** RNA was extracted from leaf tissue following JA or RO water (background control) treatment and transcripts were analysed using OneStep RT-PCR with primers specific to the gene of interest. A) The JA-responsive gene *JIP23* is expressed in all JA treated samples as well as the RO water treated transgenic barley line containing construct Trx4PL. JIP23 expression is higher in all JA treated samples compared to their corresponding RO treated samples. B) *18SrRNA* transcript was used as a template loading control. Marker (M); Wt JA treated (lane 1); JA treated transgenic line containing TrxPL (lane 2); JA treated transgenic line containing TrxPS (lane 3); Wt RO water treated (lane 4); RO water treated transgenic line containing TrxPL (lane 5); RO water treated transgenic line containing TrxPS (lane 6).

5.3.5.4.1 ABA Transcript Analysis: Q-PCR:

An ABA stress cDNA series (*developed by Alexandra Smart, PhD student, ACPFG*) was used to examine the transcript profile of *HvTrx-h4* using Q-PCR. This analysis was of interest considering the transcript response of *HvTrx-h4* seen in the transgenic barley RT-PCR analysis (see 5.3.5.4). For the ABA stress series, *H. vulgare* cv Golden Promise plants were grown in hydroponics until 14 days old and then stressed by the addition of ABA into the growth medium, to a final concentration of 10 μM. Plant roots and shoots were collected at 0 to 24 hours after treatment. As shown in Figure 5.21, *HvTrx-h4* transcript increases dramatically 12 hours after the addition of ABA, by more than 2.5 fold, in both roots and shoots.

The next sample was taken 12 h later and the amount of *HvTrx-h4* transcript had decreased (Figure 5.21). In this 24 h sample, *HvTrx-h4* transcripts in the shoot tissue had returned to approximately the same level that was present after only 8 h of ABA stress (Figure 5.21A). For the equivalent sample in root tissue, *HvTrx-h4* transcripts were slightly less abundant than after just 4 h of stress (Figure 5.21B).

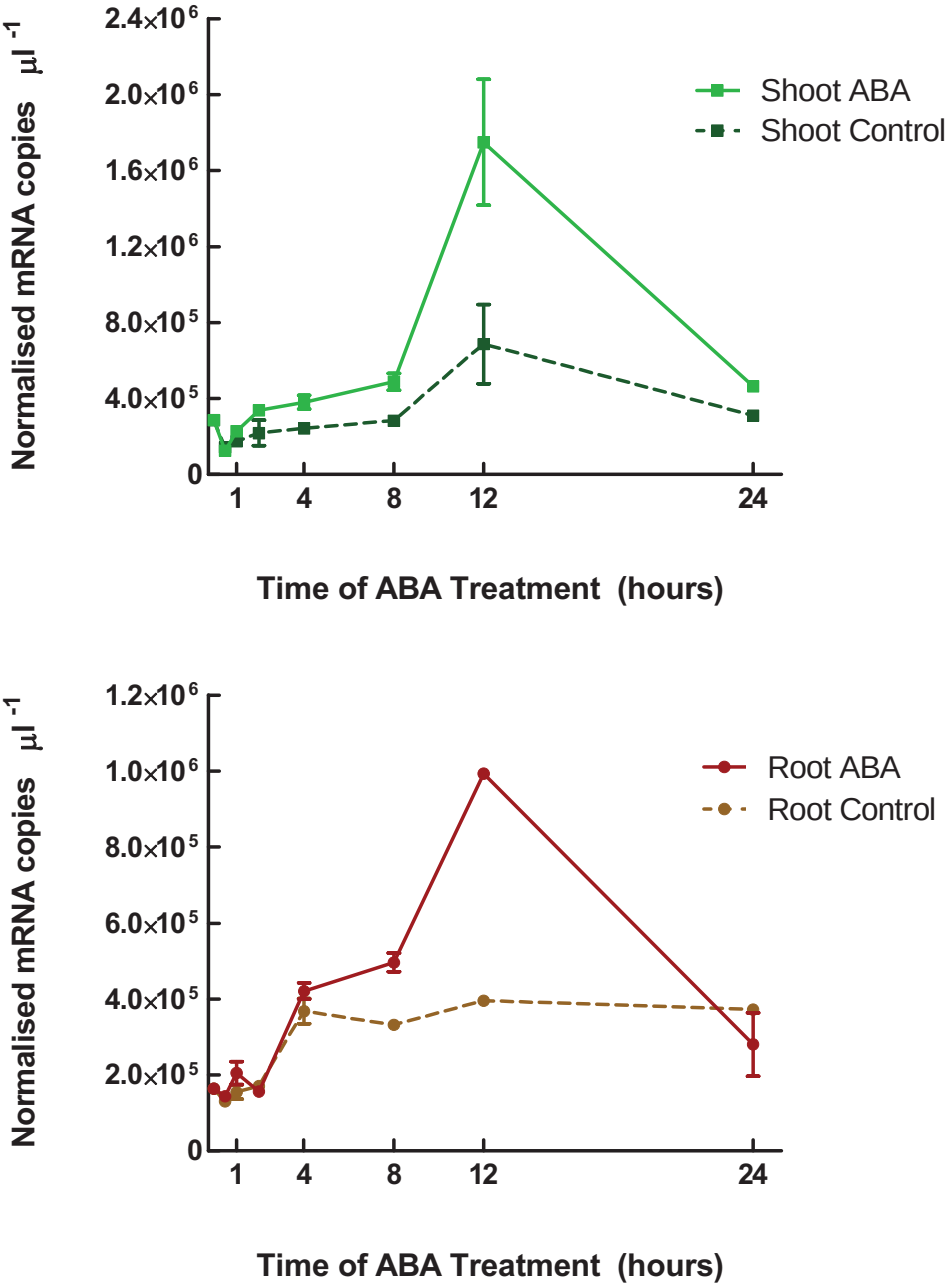

Figure 5.21: **Quantitative-PCR analysis of barley *thioredoxin-h4* transcripts in shoots (A) and roots (B) in response to ABA treatment.** cDNA was synthesised from shoot and root RNA, derived from hydroponically grown 14 day old *H. vulgare* plants that were unstressed (control) or stressed (ABA) by the addition of ABA to the growth solution at a final concentration of 10 µM. Q-PCR was performed on cDNA using primers specific to *HvTrx-h4*. Transcript levels are shown as normalised mRNA copies per µl of cDNA template. Data courtesy of Alexandra Smart, ACPFG, University of Adelaide (*unpublished*).

5.3.6 Examination of Secondary Structures Present in 5′-UTR Sequence

The possibility of post-transcriptional regulation of *HvTrx-h4* was further explored by examining the 5′-UTR sequence for possible secondary structure formations. The mRNA of *HvTrx-h4* was used to identify homologous *thioredoxin-h4* sequences from cereals that were available in the NCBI database. The resulting sequences from wheat, perennial ryegrass, rye, bilbous barley and blue canary grass, along with the *HvTrx-h4* sequence, were supplied to Michael Tran (*PhD student, University of Adelaide*) for secondary structure prediction analysis using RNAProfile. It was concluded that 5 of the 7 sequences were likely to contain secondary structures, given their resulting 'positive fitness' scores (Figure 5.22). *HvTrx-h4* is predicted to contain a 22 nucleotide stem-loop with an internal loop (bulge), located near the 5′ end of the 5′-UTR (Figure 5.22). Notably, the motif is located in a conserved block, when the 5′-UTRs are aligned (Figure 5.23). Furthermore, the motif falls just before the intron which was identified in the *HvTrx-h4* sequence (see 5.3.3.3).

```
>Hv_trx4 5′UTR
tCGGCGtCGgcgtCGtCGTCGt
.((((((.((....)).)))))).        (E: -8.200 Fitness: 2.129)
>Sc_trx4 5′UTR
cAGGaGAtCCgccaGGcTTaCCTt
.(((.((.((....)).)).))).       (E: -4.300 Fitness: 2.264)
>Lp_trx4 5′UTR
cCGGaGAtCCgccaGGcTTaTCGt
.(((.((.((....)).)).))).       (E: -3.200 Fitness: 3.372)
>Hb_trx4 5′UTR
cCGGaGAtCCgccaGGcTTaCCGt
.(((.((.((....)).)).))).       (E: -5.600 Fitness: 3.196)
>Ta_trx4 5′UTR
tCGGCGtCGtcgtCGtCGTCGc
.((((((.((....)).))))).        (E: -8.300 Fitness: 0.697)
>seq_D15071.1
aCGGCTcCCtcccGGcAGTgCGg
.((((((.((....)).))).)).       (E: -4.500 Fitness: -1.807)
>Pc_trx4 5′UTR
cAGGGCCTtcaggGGGCCTTt
.(((((((.....)))))))).         (E: -9.700 Fitness: -143.953)
```

Figure 5.22: **Highest scoring motifs predicted by RNAProfile on the *Trx-h4* 5′-UTR dataset with their respective energy and fitness value.** The dataset consists of sequences from common barley (*Hordeum vulgare*: Hv_trx4), wheat (*Triticum aestivum:* Ta_trx4), perennial ryegrass (*Lolium perenne:* Lp_trx4), rye (*Secale cereale:* Sc_trx4), bulbous barley (*Hordeum bulbosum:* Hb_trx4), blue canary grass (*Phalaris coerulescens:* Pc_trx4). Output includes one contaminating (outlier) control sequence (Iron responsive element 5′-UTR: seq_D15071.1).

Figure 5.23: **CLUSTALW alignment of cereal *thioredoxin-h4* 5′-UTRs.** The multiple alignment consists of sequences (approximately the first 225 nucleotides) from common barley (*Hordeum vulgare*, Hv4_5UTR), blue canary grass (*Phalaris coerulescens*, Pc4_5UTR), bulbous barley (*Hordeum bulbosum,* Hb4_5UTR), rye (*Secale cereale,* Sc4_5UTR), perennial ryegrass (*Lolium perenne,* Lp4_5UTR) and wheat (*Triticum aestivum,* Ta4_5UTR). Location of predicted (RNAProfile) secondary structure for HvTrx-*h*4, a stem-loop with one internal bulge, is highlighted in yellow. The * indicates locations of 100% alignment of the 6 sequences.

5.3.7 Investigation of HvTrx-*h* Post-Translational Modifications: Glutathionylation

Green fluorescent protein was not detected in the unstressed transgenic barley plants, despite the presence of GFP transcript (see 5.3.4-5). Furthermore, the HvTrx-*h*4 protein during Western analysis of transgenic tobacco (Chapter 3) appeared to be slightly larger than the recombinant his-tagged HvTrx-*h*4 positive control that was expressed in a bacterial system (see 4.3.1). These observations raise the question of whether post-translational modifications of HvTrx-*h*4 occur.

Of the four cytosolic thioredoxins, HvTrx-*h*1 and -*h*4 contain an additional, non-active site, N-terminal cysteine residue. These were considered potential targets for glutathionylation. To determine if HvTrx-*h*4 was the subject of post-translational modifications, specifically glutathionylation, purified recombinant HvTrx-*h*1 and -*h*4 proteins (see 4.2.4) were treated with glutathione by Dr Juan Juttner (*ACPFG, University of Adelaide*). Control samples were then treated with DTT to dislodge potential glutathione interactions. Next, Dr John Patterson (*ACPFG, University of Melbourne*) used mass spectrometry to determine the mass of each parent ion from the spectra of intact proteins. The parent ion masses were equivalent for both treated (13,945 Da) and untreated (13,944 Da) HvTrx-*h*1 proteins (Figure 5.24). Hence, HvTrx-*h*1 is not glutathionylated. However, the theoretical mass of HvTrx-*h*1 is 12,753 Da as predicted by ExPASy pI/Mw predictor software, which is 1,191 Da less than the parental mass observed. This may indicate an alternative post-translational modification occurs for HvTrx-*h*1. For HvTrx-*h*4 the parental mass differed between control and treated samples, being 15,696 Da and 16,002 Da, respectively (Figure 5.25). This is an increase of 306 Da, which is equivalent to the expected mass of a glutathione residue (305 Da). Therefore, it appears that HvTrx-*h*4 is glutathionylated *in vitro*. As seen for HvTrx-*h*1, the theoretical mass and recorded parental mass of HvTrx-*h*4 differ. The increase in mass observed, of 1234 Da, indicates that a second post-translational modification may occur for HvTrx-*h*4.

The iodoacetamide treated, trypsin digested HvTrx-*h*1 and -*h*4 peptides identified by mass spectrometry were identical in both control and treated samples. This indicates that none of these residues were modified (Figure 5.26). Also, the active-site cysteine residues in HvTrx-*h*4 (Figure 5.26) were found to be carbamidomethylated, so are unlikely to be glutathionylated (*Dr Patterson, pers. comm.*). In conclusion, HvTrx-*h*4 can be glutathionylated *in vitro* but probably not at the active-site cysteines, and it is expected that another post-translational modification of HvTrx-*h*4 can occur.

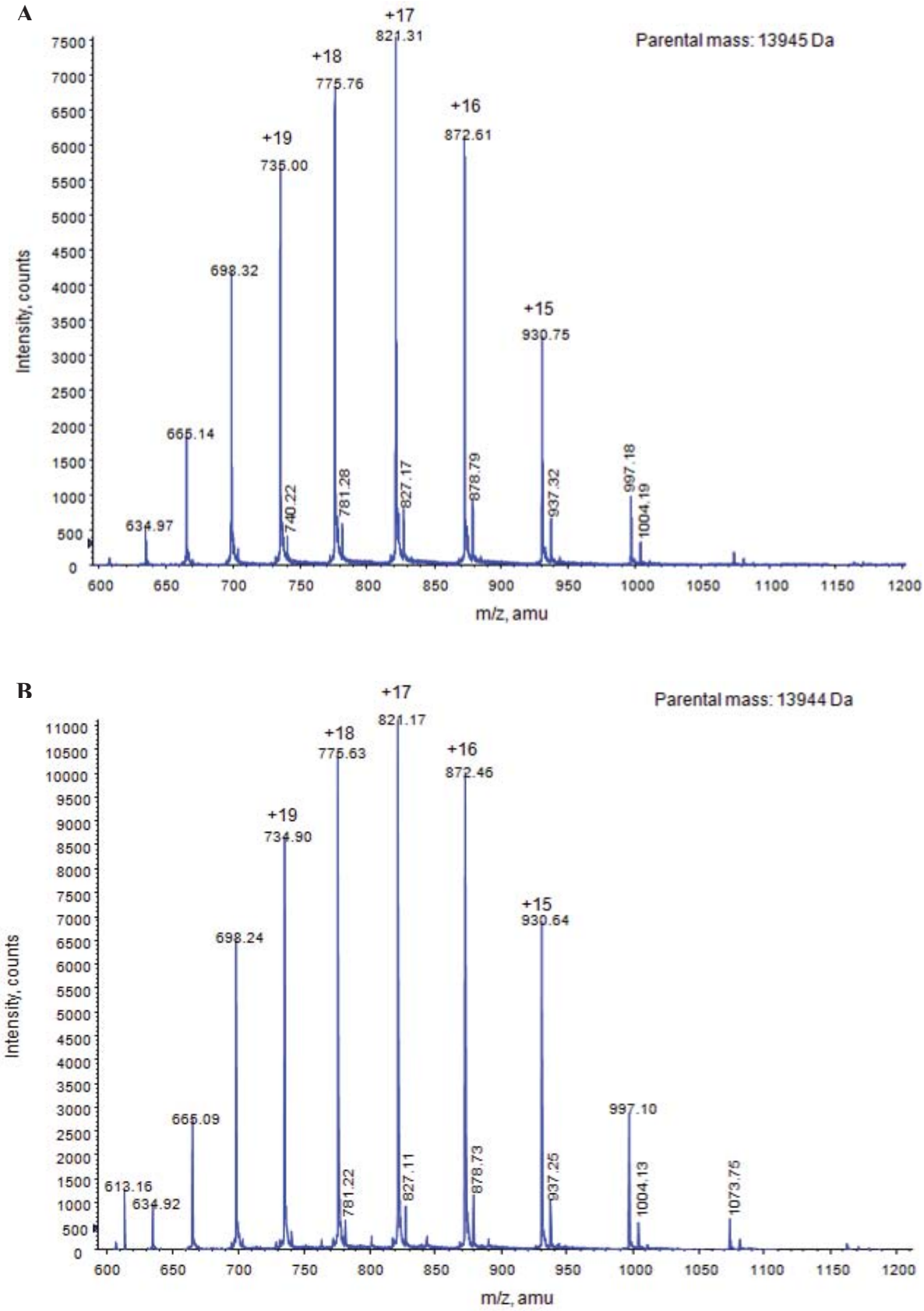

Figure 5.24: **Spectra were used to calculate the parental mass of HvTrx-*h*1.** Control (A) and glutathione treated (B) HvTrx-*h*1 samples were analysed by mass spectrometry. There was no change in parental mass.

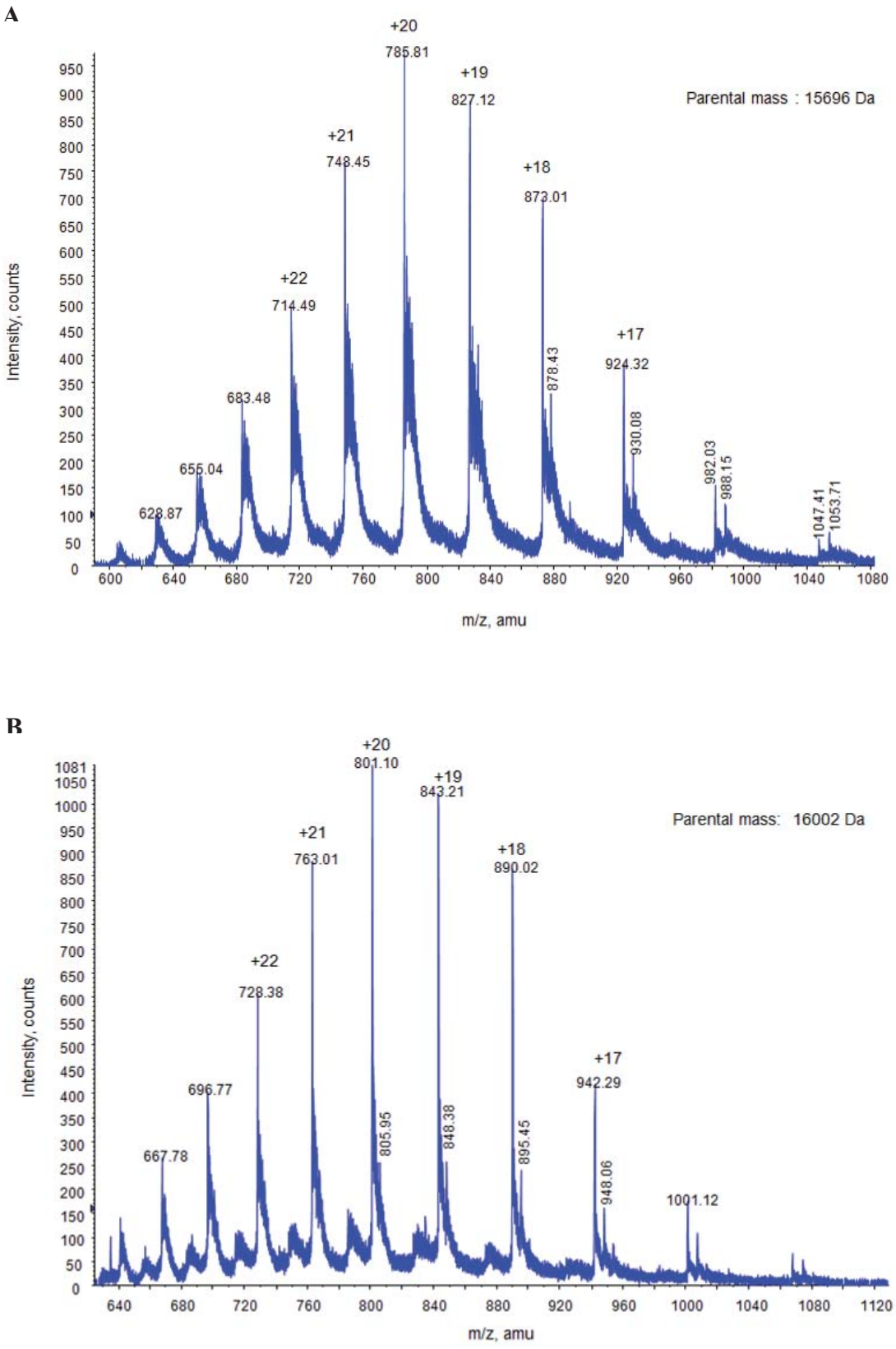

Figure 5.25: **Spectra were used to calculate the parental mass of HvTrx-*h*4.** Control (A) and glutathione treated (B) HvTrx-*h*4 samples were analysed by mass spectrometry. There was an increase of 306 Da in the parental mass of the glutathione treated HvTrx-*h*4 sample.

>HvTrx-*h*1

MAAEEGAVIA**C**HTKQEFDTHMANGKDTGKLVIIDFTAS**WCGPC**R
VIAPVFAEYAKKFPGAIFLKVDVDELK**DVAEAYNVEAMPTFLFIK**
DGEKVDSVVGGRKDDIHTKIVALMGSAST

>HvTrx-*h*4

MGG**C**VGKGRGVVEEKLDFKGGNVHVITTKEDWDQKIEEANKDGK
IVVANFSASWCGPC**RVIAPVYAEMSK**TYPQLMFLTIDVDDLMDFSST
WDIR**ATPTFFFLK**NGQQIDKLVGANKPELEKKVQALGDGS

Figure 5.26: **Amino acid sequence features of HvTrx-*h*1 and HvTrx-*h*4. The N-terminal, conserved cysteine is highlighted in red.** The conserved, thioredoxin active-site motif is highlighted in green. The peptides identified following protein digestion with trypsin and mass spectrometry are underlined.

5.4 Discussion

5.4.1 *Thioredoxin-h* Transcript Analysis in Barley Reproductive Tissues

Transcript analysis by Q-PCR revealed that *HvTrx-h4* mRNA in barley reproductive tissues was present in lower abundance compared to the other three cytosolic thioredoxins. Also, the pattern of expression seen as the tissues matured was distinctly different. This suggests that *HvTrx-h4* has a unique role in these tissues. The change in *HvTrx-h4* mRNA expression in barley anthers may indicate that HvTrx-*h*4 is involved in the anther maturation process. However, considering the results from the GFP transgenic tobacco plants that showed *HvTrx-h4* transcript expression does not necessarily correlate with protein expression, transcript levels may not be a good indicator of when or where the HvTrx-*h*4 protein is functioning.

A large spike in *HvTrx-h4* transcript was seen in barley endosperm 5 days after pollination. This coincides with cessation of the syncytial phase and initiation of cellularisation during barley endosperm morphogenesis (Brown et al., 1994). Perhaps HvTrx-*h*4 is acting in a signalling capacity. Considering the secondary spike in HvTrx-*h*4 transcript occurs as cellularisation ends, it could be speculated that HvTrx-*h*4 is in some way linked to the cellularisation process. Regardless, HvTrx-*h*4 appears to be involved in the process of endosperm development. Supporting this theory is the presence of at least three different endosperm-specific elements in the non-coding region upstream of *HvTrx-h4*. Perhaps of significance is the fact that all 3 putative motifs identified were located in the intron region of the 5′-UTR sequence (see Table 5-2).

The question of HvTrx-*h*4 function remains. The Q-PCR data presented in section 5.3.2 points towards the involvement of HvTrx-*h*4 in specific tissue developmental processes, linked to plant reproduction. In addition, the Q-PCR analyses show the transcript profile of each *HvTrx-h* to be different, indicating that cytosolic thioredoxins are not functionally redundant. Instead, each is likely to have its own specific role. A unique *HvTrx-h4* pattern of expression in reproductive tissues is not surprising considering the high sequence conservation of this class of thioredoxin-*h* in angiosperms and gymnosperms, unlike the other cytosolic thioredoxin class members (Juttner, 2003). Further investigation into functional redundancy of the cytosolic thioredoxins could be achieved using a suite of transgenic barley lines with various combinations of silenced thioredoxins-*h*.

5.4.2 Multiple Levels of *HvTrx-h4* Regulation: Evidence of Post-Transcriptional Regulation

The regulation of HvTrx-*h*4 was examined by isolation of its promoter and 5′-UTR genetic information and subsequent tagging with green fluorescent protein (GFP). Two lines of transgenic barley plants were generated, differing by the amount of HvTrx-*h*4 genetic information controlling GFP expression; all promoter and 5′-UTR sequence, including the 5′UTR intron, that was isolated (Trx4PL) and all promoter but only the 1st 432 bp of 5′UTR sequence. These transgenic barley plants enabled visualisation of the temporal and spatial expression of GFP, representing HvTrx-*h*4. Considering grass thioredoxin-*h*4 transcript had previously been detected in most plant tissues, including leaves (Juttner, 2003), it was surprising that no GFP protein was visible in healthy, unstressed barley plants (5.3.4). However, GFP transcript was detected in leaf tissues despite the absence of GFP fluorescence in both transgenic lines (5.3.5). This indicates that post-transcriptional modifications of the transcribed RNA are necessary before translation of GFP is achieved. The genetic information for GFP does not require additional elements for synthesis of the protein so, if GFP mRNA is translated, the protein should be visible (provided it is present above the detection limits) (Tsien and Prasher, 1998). Considering this and that the *GFP* transcript mimicked that of HvTrx-*h*4, it is assumed that GFP is representing HvTrx-*h*4 accurately.

Post-transcriptional regulation concerns the management of protein synthesis events through the control of RNA translation. Regulation of protein synthesis is essential for coordinated assembly and localisation of proteins that are required by a cell at a given time. In all organisms, regulation of mRNA translation allows fine modulation of the level of protein synthesized from its corresponding mRNA. Consequently, post-transcriptional regulation assists with the adaption and response of a cell to changes in its environment.

Several different mechanisms of post-transcriptional regulation of nuclear genes have been discovered, occurring at the stages of messenger RNA (mRNA) processing (capping, splicing, and polyadenylation), stability, silencing, localisation and translation (Floris et al., 2009). In plants, translation regulation involving untranslated region (UTR) elements has been identified (Floris et al., 2009; Kawaguchi and Bailey-Serres, 2005). Recently, post-transcriptional control *via* compartmentalisation of mRNAs within the cytoplasm of tomato cell cultures has also been investigated (Anderson and Kedersha, 2009; Marx, 2005; Weber et al., 2008).

5.4.2.1 Post-transcriptional Regulation of Thioredoxins

Post-transcriptional regulation of thioredoxins has been described previously. A RNA binding protein, heterogenous ribonucleoprotein A18 (hnRNP A18), was shown to bind the 3′-UTR of thioredoxin in human carcinoma cells, resulting in post-transcriptional regulation (Yang et al., 2006). No evidence that HvTrx-*h*4 could be similarly regulated, *via* the 3′-UTR, was obtained in this thesis. The HvTrx-*h*4 3′-UTR was not present in the GFP expression constructs inserted into the transgenic barley plants. Therefore, it is clear that the post-transcriptional regulation of HvTrx-*h*4 observed cannot be attributed to the influence of the HvTrx-*h*4 3′-UTR.

A study using *Rhodobacter sphaeroides*, a free-living facultatively phototrophic bacterium, also concluded that a thioredoxin (RsTrxA) was post-transcriptional regulated. The thioredoxin mRNA transcript greatly increased after the bacterium culture was exposed to the compounds methyl viologen (paraquot) or tertiary-butylhydroperoxide, both free radicals inducers. However, the protein levels increased only slightly (Li et al., 2003). This implies that post-transcriptional processes were important in determining the amount of thioredoxin protein synthesised. In comparison, the results in Figure 5.17 show no GFP expression in response to methyl viologen, hence no observable change in HvTrx-*h*4 protein expression occurred. GFP was not observed in any of the transgenic barley plants before or after treatment with methyl viologen. The mRNA transcripts of HvTrx-*h*4 or GFP were not assessed following methyl viologen treatment so comparison with *RsTrxA* is not possible.

Plant thioredoxins and post-transcriptional regulation have been linked previously. In potato (*Solanum tuberosum*) a chloroplastic drought-induced stress protein (CDSP32) is considered to be a novel type of plant thioredoxin, as it consists of two distinctive thioredoxin components with only one redox active disulphide centre in the C-terminal domain (Rey et al., 1998). Transcription of CDSP32 has not always correlated with protein abundance and hence, CDSP32 is believed to be post-transcriptionally regulated (Broin et al., 2003; Broin et al., 2000; Broin and Rey, 2003). Firstly, there were no clear differences in CDSP32 mRNA levels in leaves of varying maturity from wild-type and transgenic plants over-expressing CDSP32. However, in both plant lines, protein abundance was highest in young leaves and decreased as the leaf matured (Broin et al., 2003). Secondly, the transgenic plants showed no change in CDSP32 transcript levels, compared to control plants, when subjected to water deficit stress. Yet, variations in CDSP32 protein abundance were apparent (Broin et al., 2003; Broin et al., 2000; Broin and Rey, 2003). Thirdly, despite a constitutively active promoter

driving CDSP32 expression in the transgenic plants, no CDSP32 protein was detected in flowers and less was present in stems, tubers and roots compared to leaves (Broin et al., 2003). In summary, post-transcriptional regulation of CDSP32 mRNA occurs differentially in a variety of plant tissues and during leaf development, under normal growth conditions. In addition, the post-transcriptional regulation is altered in response to environmental stress, namely water deficiency.

Unlike CDSP32, HvTrx-*h*4 protein, as inferred from the presence/absence of GFP in the transgenic barley lines, does not appear to be present in leaf tissue, independent of age or maturity level. Nor was it confirmed to be present in any other tissues, under normal growth conditions. The transgenic barley plants were not subjected to water deficit stress due to previous results indicating over-expression of thioredoxin-*h*4 did not confer protection for this condition (see Chapter 3). CDSP32 is localised to the chloroplast whereas HvTrx-*h*4 is cytosolic. In addition, CDSP32 is structurally quite different to HvTrx-*h*4. Considering this, it is likely that CDSP32 and HvTrx-*h*4 participate in different processes. Therefore it is not surprising that the post-transcriptional control appears to differ for each protein, assuming GFP accurately represents HvTrx-*h*4 expression. It would be interesting to investigate the response of CDSP32 regulation to UVB stress to determine if CDSP32 translation is induced, as was seen for GFP controlled by the HvTrx-*h*4 promoter, as CDSP32 is speculated to play a role in protecting or regenerating proteins inactivated by oxidative stress (Rey et al., 1998).

Chloroplastic and cytosolic thioredoxins of germinating pea (*Pisum sativum*) have been examined and are thought to be post-transcriptionally regulated (Montrichard et al., 2003; Pagano et al., 2000). Under light-stress conditions, high levels of chloroplastic thioredoxin transcripts (types-*f* and -*m*) were detected in the middle and basal leaves of pea plants. However, this did not correlate with protein abundance. Instead, high-light conditions resulted in a lower concentration of chloroplastic thioredoxin proteins, than was detected in unstressed plants, despite the corresponding mRNA transcript levels being substantially higher in the light-stressed plants. It was speculated that rapid degradation of thioredoxin protein by light-induced factors may be partially responsible, but it was also concluded that post-transcriptional regulation of thioredoxin protein translation appeared to contribute (Pagano et al., 2000). The decrease in chloroplastic pea thioredoxin protein following high-light stress is in contrast to the induced expression of GFP, as regulated by the HvTrx-*h*4 promoter, following UVB stress. Previously, pea plants exposed to UVB radiation showed increased tolerance to subsequent high-light exposure and it was speculated that the UVB pre-treatment resulted in increased antioxidant capacity (Bolink et al., 2001). Hence, it would be interesting

to investigate the response of HvTrx-*h*4 translation to high-light considering the UVB-induced translation of HvTrx-*h*4, as inferred from the observed expression of GFP.

More recently, two pea cytosolic thioredoxins, -*h*3 and -*h*4, were studied and a distinct lack of positive correlation between mRNA transcript levels and subsequent protein expression was observed. Notably in cotyledons, PsTrx-*h*4 mRNA transcripts were abundant but the protein was not detected (Montrichard et al., 2003). This finding corresponds with that for HvTrx-*h*4 in leaf tissues, where transcript was detected but the GFP tag was not visible. Montrichard et al. (2003) also concluded that post-transcriptional regulation was responsible for the lack of correlation between mRNA and protein abundances but like Pagano et al. (2000), did not speculate as to the type of post-transcriptional regulation mechanism.

5.4.2.2 Mechanisms of Thioredoxin Post-transcriptional Regulation

The mechanism of post-transcriptional regulation of HvTrx-*h*4 may involve the formation of a secondary structure within the mRNA in the form of a stem-loop with one-internal loop (bulge) (see 5.3.6). This motif lies within the HvTrx-*h*4 5′-UTR, approximately 145 nucleotides after the predicted promoter end and consequently, is present in both transgenic barley lines. Therefore, it is not surprising that the two lines behaved in the same manner assuming that post-transcriptional control is indeed due to a mRNA secondary structure at this location. It is certainly regrettable that the 5′-UTR length was initially incorrectly identified as it resulted in the generation of one transgenic line containing 430 bp of 5′-UTR, when the original intention was to completely remove the 5′-UTR. Had the HvTrx-*h*4 5′-UTR been absent, as desired, and GFP protein detected in unstressed tissues of this transgenic line, the involvement of the 5′-UTR in post-transcriptional regulation of HvTrx-*h*4 would have been evident. Consequently, more support for the validity of the speculated mRNA secondary structure formation would also have been provided. Analysis of a barley transgenic line with only the promoter driving GFP expression is a sensible future experiment to assess the impact of the HvTrx-*h*4 5′-UTR on HvTrx-*h*4 protein expression. To support conclusions made about HvTrx-*h*4 regulation, which are inferred from GFP visualisation, Western analysis of HvTrx-*h*4 protein expression is also recommended.

It is worthwhile noting that the two transgenic barley lines generated did differ from each other, in HvTrx-*h*4 regulatory genomic sequence lengths. Considering the differences and the fact that GFP expression was alike, it can be deduced that the 5′-UTR intron, 109 nucleotides preceding and 57 nucleotides following the intron, do not contribute to post-transcriptional regulation of HvTrx-*h*4.

Even if HvTrx-*h*4 post-transcriptional regulation is attributed to the conserved 5′UTR motif, the precise mechanism of control provided by the resulting mRNA secondary structure is not certain without further research. However, internal bulges of stem-loops have previously been shown to facilitate attachment to RNA-binding proteins (Ke et al., 1998). The iron responsive protein is the best characterised RNA-binding protein and it has been found to regulate mRNA translation by binding to the iron responsive element. Consequently, mRNA entry to the 40S ribosomal subunit is blocked, thereby impeding downstream translation (Proudhon et al., 1996). It is plausible that the Hv*Trx-h4* 5′-UTR motif may function similarly.

Post-transcriptional regulation of thioredoxins through 5′-UTR elements has not been previously reported. To date, the regulation mechanisms of plant thioredoxins reported to be post-transcriptionally controlled have not been speculated or investigated (Broin et al., 2003; Li et al., 2003). The best characterised potential mechanism for thioredoxin post-transcriptional regulation was reported by Lottin et al. (2002). In the study, a human gene designated H19 was demonstrated to up-regulate the level of thioredoxin protein synthesised, post-transcriptionally. Human cells transfected with H19 had highly elevated levels of thioredoxin protein despite no change in mRNA levels. The H19 gene is believed to be a structured RNA that acts as a riboregulator (Brannan et al., 1990; Juan et al., 2000). It is transcribed, spliced, polyadenylated and transported to the cytoplasm but not translated (Brannan et al., 1990). H19 has been linked with polyribosomes (Li et al., 1998) and therefore, it was speculated that H19 increased translation of thioredoxin by enhancing association of the thioredoxin mRNA with polyribosomes (Lottin et al., 2002). Considering this, it could be hypothesised that the HvTrx-*h*4 5′-UTR secondary structure is resolved by the binding of a protein or structured RNA such as H19, allowing entry to the 40S ribosomal subunit and subsequent translation. However, this hypothesis is highly speculative and detailed experiments would be essential to test this theory.

5.4.2.3 Post-Transcriptional Regulation and Stress Conditions

Post-transcriptional regulation is emerging as a key element in how plants respond to abiotic stress. It is commonly argued that post-transcriptional regulation is likely to be important for stress responses as it facilitates faster adaptation in the proteome compared to transcriptional regulation (Floris et al., 2009). Accordingly, differential translation of mRNA has been observed following changes in environmental conditions including salt stress, water deficit, oxygen deprivation, heavy metal exposure, heat stress, sucrose starvation and pathogen infection (review: (Floris et al., 2009; Lemaire et al., 1999). As recently reviewed by Floris et al. (2009), translational control of plant mRNAs is often achieved through control elements

located within the 3′ and 5′ untranslated regions, particularly in response to environmental stresses. This supports the hypothesis that HvTrx-*h*4 post-transcriptional regulation is conferred by the formation of a secondary structure, located in the 5′-UTR of HvTrx-*h*4. Additionally, UVB stress and wounding, which both generate reactive oxygen species that are common to environmental stresses, induced the expression of HvTrx-*h*4 protein. However, treatment with methyl viologen, which also generates reactive oxygen species, did not cause HvTrx-*h*4 translation and is therefore a source of confusion, especially when also considering that over-expression of thioredoxin-*h*4 in tobacco conferred tolerance to methyl viologen (see Chapter 3). Considering the results presented earlier in Chapter 3, further investigation into heat stress is recommended for future research. Over-expression of thioredoxin-*h*4 in tobacco resulted in increased heat stress tolerance and therefore it would be interesting to see if HvTrx-*h*4 translation is induced.

Translation of HvTrx-*h*4 mRNA in response to wounding but not in response to hormone treatments, particularly JA, was unexpected. Although the potential involvement of ABA in plant wounding responses is controversial, JA and ethylene are well documented to play a role (Birkenmeier and Ryan, 1998; Koo et al., 2009; Lorenzo and Solano, 2005; Lulai et al., 2008). Also, ABA, JA and ethylene have all been reported as oxidative stress signalling components (Bari and Jones, 2009; Gao et al., 2008; Lee et al., 1996; Ortel et al., 1999). In addition, ABA, JA and ethylene responsive motifs were identified in the HvTrx-*h*4 regulatory sequence. However, the putative motifs identified were all located in the promoter sequence and therefore would not be transcribed into mRNA, which is where the post-transcriptional regulation mechanism is predicted to be located. It could be speculated that if these predicted motifs are functional a change in HvTrx-*h*4 transcript would occur. Indeed, HvTrx-*h*4 transcripts in wild-type barley plants treated hydroponically with ABA were found to increase in root and shoot tissues compared to untreated controls (see Figure 5.21). Why the transcript would increase if the protein is not synthesised is puzzling. It may be that the HvTrx-*h*4 transcript response to ABA detected is an artefact caused by the abnormally high concentration of ABA (10 μM) used for the treatment. Despite this and considering the spike in *HvTrx-h4* transcript after 12 h of ABA treatment, protein might have been translated at the 12h time point. To examine this, the hydroponic experiment would need to be repeated using the transgenic GFP barley plants. Finally, it is possible that hormone induced changes in post-transcriptional regulation are spatially dependent and might be revealed in future investigations using non-leaf tissues. To fully test this hypothesis, the challenge of auto-fluorescence which unfortunately occurred in anther, stigma and endosperm tissues would

need to be overcome. One option is to use an alternative tag to GFP, such as red fluorescence protein (RFP). Alternatively, protein from these tissues could be harvested and probed with a GFP specific antibody.

5.4.3 Multiple Levels of HvTrx-*h*4 Regulation: Evidence of Post-Translational Regulation

The cytosolic thioredoxin system has been shown to act in a post-translational regulatory role by reducing protein targets (Meyer et al., 2008; Montrichard et al., 2003). In this thesis of work, results suggest that HvTrx-*h*4 is itself the subject of a redox-based post-translational modification. It was found that HvTrx-*h*4 was glutathionylated *in vitro*, most probably at the N-terminal cysteine (amino acid position 4) that is highly conserved across grass species. Experimental investigation of this aspect of thioredoxins could not be explored extensively during the project duration. In the next section the likely under-pinning reasons for, and implications of, glutathionylation of thioredoxins is discussed. Future experimentation for HvTrx-*h*4 is also identified.

Glutathionylation is the formation of a mixed disulfide between glutathione and the free thiol (sulfhydryl) of a protein (Rouhier et al., 2008a). This form of post-translational modification is reversible but the exact mechanism by which glutathione interacts with proteins *in vivo*, is only partially understood (Haendeler, 2006). Glutathionylation allows modulation of protein activity and can also protect proteins from irreversible oxidation (Rouhier et al., 2008a). The glutathionylation process commonly occurs following an increase in cellular reactive oxygen species (ROS) and/or oxidized glutathione (Gallogly and Mieyal, 2007; Rouhier et al., 2008a).

Glutathionylation has chiefly been identified and studied in mammalian systems and the discovery of thioredoxin as a subject of glutathionylation is relatively recent (Haendeler, 2006). In 2002, a human thioredoxin (HsTrx-1), which is ubiquitously expressed in mammalian cells (Holmgren, 1989), was shown to be glutathionylated under oxidative stress conditions (Casagrande et al., 2002). The occurrence of glutathionylation in plants was first reported in *Arabidopsis* (Dixon et al., 2000) whilst glutathionylation of a plant thioredoxin was later discovered in poplar (Gelhaye et al., 2004).

If HvTrx-*h*4 is regulated post-translationally by glutathionylation *in planta*, the reason why is intriguing. A number of explanations are feasible. It is possible that glutathionylation might be used to alter the activity of HvTrx-*h*4, acting as an ‘on/off switch’ for protein function.

Considering the results of others, from studies with human thioredoxin (HsTrx-1) and several plant thioredoxins (Casagrande et al., 2002; Gelhaye et al., 2004; Michelet et al., 2005), it is likely that the activity of HvTrx-*h*4 is reduced following glutathionylation. Firstly, the enzymatic activity of HsTrx-1 was shown to be decreased as a consequence of glutathionylation (Casagrande et al., 2002). Secondly, a mitochondria-associated poplar thioredoxin (PtTrx-*h*2) incubated with glutathione disulfide, *in vitro*, resulted in a glutathionylated form. As a direct result, the redox potential of PtTrx-*h*2 was markedly increased from –290 to –225 mV following and it was concluded that glutathionylation was able to modulate the enzymatic activity of PtTrx-*h*2 (Gelhaye et al., 2004). Thirdly, Michelet et al. (2005) studied chloroplastic thioredoxins from *A. thaliana* and *C. reinhardtii* and identified that glutathionylation of the *f*-type thioredoxin occurred, also resulting in a reduction of enzymatic activity. Specifically, the ability of thioredoxin-*f* to activate target enzymes, NADP-malate dehydrogenase and GAPDH, was decreased when glutathionylated. This was attributed to thioredoxin-*f* no longer being as effectively reduced by ferredoxin-thioredoxin reductase, when in the glutathionylated form.

The site of glutathionylation was located at a C-terminal cysteine separate to the active-site cysteines, for both AtTrx-*f* and HsTrx-1 (amino acid positions 60 and 72 respectively) (Casagrande et al., 2002; Michelet et al., 2005). In AtTrx-*f*, this cysteine is highly conserved across plant species (Lemaire et al., 2007) and it has been speculated that the status of this cysteine plays a key role in modulating the efficiency of *f*-type thioredoxin (Michelet et al., 2005). Hence, the same could be speculated for HvTrx-*h*4 also.

Glutathionylation of thioredoxin has been detected under conditions of oxidative stress (Casagrande et al., 2002; Michelet et al., 2005). Thus, these thioredoxins may be glutathionylated as a protective mechanism to prevent the occurrence of other oxidation or modification processes which may deactivate thioredoxin activity permanently. HvTrx-*h*4 is likely to be involved in key processes induced during plant oxidative stress events, considering its presence in UVB stressed tissues (see 5.3.5.1) and its apparent ability to reduce deleterious effects of oxidative stress in tobacco (see Chapter 3). Therefore, the need for HvTrx-*h*4 to be protected under oxidative stress conditions is likely and the reversible nature of glutathionylation is ideal. Reversible modification of a protein through a covalent interaction, as is the case for glutathionylation, enables a fast response to changing conditions (Lillo, 2008; Storey, 2004) in comparison to complete resynthesis. The activity status can be reversed when the oxidative danger decreases and the need for resynthesis of the protein can be avoided, thereby leaving cellular components and machinery available for synthesis of key

enzymes that have been damaged during the stress event (Storey, 2004). If HvTrx-*h*4 activates and/or regulates proteins required for oxidative stress tolerance and free radical scavenging processes, its function may be significant enough for even a small amount of protection, as conferred through glutathionylation, to be highly advantageous for cellular survival at times of extreme stress. Additionally, despite glutathionylation and a subsequent decrease in activity, AtTrx-*f* retained the capacity to reduce targets and therefore still has some functional ability (Michelet et al., 2005). If merit is given to this conjecture, the function of HvTrx-*h*4 linked to the additional cysteine, which is highly conserved and possibly shielded from irreversible oxidative modifications, is all the more intriguing.

Other reasons for glutathionylation are also possible and these may stand alone or be additional. The event of glutathionylation may indicate a signalling capacity for HvTrx-*h*4 since oxido-reduction of protein thiols is considered a regulatory mechanism (Niwa, 2007). Glutathionylation has previously been shown to regulate signal transduction of redox-driven cascades (Fratelli et al., 2005; Rouhier et al., 2008b). It has been hypothesised that glutathionylation provides a reversible way to store glutathione during oxidative stress. Crosstalk between a thioredoxin system and glutathione, in plants under oxidative stress conditions, may signal the redox status of the cell (Haendeler, 2006; Michelet et al., 2006; Rouhier et al., 2008b). Accordingly, glutathionylation of proteins increases under oxidative stress conditions (Gilbert, 1984; Rouhier et al., 2008b).

An alternative reason for glutathionylation of HvTrx-*h*4 may be again linked to function. HvTrx-*h*4 could participate in more than one process and do so in different capacities. Glutathionylation may provide a 'switch' to regulate the specific function of HvTrx-*h*4 at a particular time, in a particular cellular or tissue location and/or in response to a particular environmental condition. This may be achieved by alteration of HvTrx-*h*4 affinity for its interacting proteins. Casagrande et al. (2002) considered this idea, stating that despite the reduction in HsTrx-1 enzymatic activity following glutathionylation, a more subtle effect on other activities of the proteins, including altering its affinity for target proteins or initiation of alternative functions was possible (Casagrande et al., 2002).

Michelet et al. (2005) studied nine *A. thaliana* and five *C. reinhardtii* chloroplastic thioredoxins (-*m* and -*f* types) and found that only the *f*-type were glutathionylated. Thus, it was concluded that this post-translational modification is probably a general feature of thioredoxins-*f* (Michelet et al., 2005). Also, Koh et al. (2008) studied cytosolic thioredoxins in poplar and found only PtTrx-*h*4 to be glutathionylated, not PtTrx-*h*1 nor -*h*3. The common

link between these glutathionylated thioredoxins is that each has an additional, conserved cysteine which is separate to the active-site. These results suggest that the capacity for glutathionylation is related to the additional cysteine and it introduces a degree of specificity between thioredoxin types and within type classes.

The study by Koh et al. (2008) centred upon the redox system responsible for reduction of a poplar thioredoxin, PtTrx-*h*4, which is orthologous to HvTrx-*h*4 (see Appendix A). It was concluded that PtTrx-*h*4 is reduced by glutathione and glutaredoxin instead of NADPH:thioredoxin reductase (NTR) (Koh et al., 2008). Unlike HvTrx-*h*4, NTR was not effective at regenerating PtTrx-*h*4 (see Appendix A). However, the effectiveness of reduction by NTR was lower for HvTrx-*h*4 compared to HvTrx-*h*1, -*h*2 and -*h*3 and the NTRs used in each study were not identical (Koh et al., 2008). Considering these results, HvTrx-*h*4 may actually be regulated by the glutaredoxin system and a modified activity assay, using glutatredoxin instead of NTR, could confirm this in the future. It was speculated by Koh et al. (2008) that glutathionylation PtTrx-*h*4 was transient and part of a four-step disulfide cascade mechanism converting PtTrx-*h*4 to its active reduced form. In light of this report, it is possible that glutathionylation of HvTrx-*h*4 serves the same purpose, and is linked to the reduction and subsequent regeneration of HvTrx-*h*4 activity.

Like HvTrx-h4, PtTrx-*h*4 also contains a highly conserved N-terminal cysteine at amino acid position 4 and this is the location of a glutathionylation event (Koh et al., 2008). Hence, it is highly likely that the glutathionylation site for HvTrx-*h*4 would also be at the Cys_4 residue. This could be confirmed in the future through tryptic digestion of glutathionylated and control HvTrx-*h*4 protein (no glutathione treatment and Cys_4Ser mutated form) and analysis of the fragments by mass spectrometry.

Considering the findings from previous reports just discussed, it is highly likely that HvTrx-*h*4 is glutathionylated *in planta*. Validation of HvTrx-*h*4 glutathionylation *in vivo* is a worthy topic for future research and is highly recommended. I suggest using an experimental approach centred upon intracellular radiolabelling of GSH *in planta*, which is akin to that developed by Thomas et al. (1995) for use in a mammalian system to document protein mixed disulfide formation in cells under oxidative stress conditions. This technique is established as a specific method for identification of protein glytathionylation formation intracellularly. It was used to ascertain that GRX is the main catalyst of de-glutathionylation in mammalian cells (Jung and Thomas 1996). The experiment involves radiolabelling of cell-permeable precursors of GSH (^{35}S-labeled □-cysteine or -methionine) to radiolabel the intracellular GSH

pool. The cell lysate could then be analysed by two-dimensional electrophoresis. Spots in the resulting autoradiographic protein map, which correspond to thioredoxin-h4's molecular weight, could be excised and identified by mass spectrometry. The transgenic tobacco plants expressing thiroedxoin-h4 protein in higher abundance relative to wild-type plants (Chapter 3) would be an ideal plant material source as the likelihood of thioredoxin-h4 detection would probably be increased. Also, the cells could be pre-treated with cycloheximide to inhibit protein synthesis, to prevent incorporation of the intracellular radiolabel into newly synthesized proteins.

5.4.4 Conclusion

It was shown that *HvTrx-h4* has a unique expression profile in reproductive tissues, relative to the other cytosolic *thioredoxins* in barley. The 5'upstream genomic sequence of *HvTrx-h4* was isolated and used to drive expression of GFP in transgenic barley. This lead to the discovery that *HvTrx-h4* is regulated post-transcriptionally, possibly *via* the formation of a secondary structure in the mRNA. At the post-translational level, we discovered that HvTrx-*h*4 can be glutathionylated *in vitro*. *HvTrx-h4* appears to be a highly regulated thioredoxin and further investigations in these areas may assist in revealing the pathway(s) in which grass thioredoxins-*h*4 operate.

6 Conclusions

6.1 Relevance and Focus

Plants are at the mercy of environmental conditions because of their immobilised nature. Thus, common changes in the environment are a regular cause of stress for plants. For example, abiotic stresses such as water-deficit, extreme temperatures and varying light intensities alter the redox state of plant cells, which often leads to oxidative stress. The ability for an individual plant to respond and adapt to these redox changes are essential for its continued survival. Indeed, plant cells generally have a remarkable ability to cope with oxidative stress, a property largely attributed to a tight control of redox homeostasis. Thioredoxin driven disulfide-dithiol exchanges certainly play a significant role in the maintenance of cellular redox homeostasis. Additionally, it is emerging that plant thioredoxins are key participants within the plant antioxidant network. There is evidence for the involvement of plant thioredoxins-*h* in response to, and protection against, oxidative stress.

This thesis centres upon characterisation of plant cytosolic thioredoxins with a focus on their potential role(s) during oxidative stress events. Specifically, increased understanding of the subclass 4 member of thioredoxin-*h* in cereals was pursued. Additional knowledge and understanding of oxidative stress tolerance mechanisms in plants may ultimately facilitate the development of crop plants that possess increased tolerance to environmental stresses. To this end, information gained from characterisation of grass thioredoxin-*h*4, both here and in the future, is expected to be useful for the establishment of how cereal plants may be more effectively modified.

6.2 Key Discoveries

In the work presented here, characterisation of grass thioredoxin-*h*4 was undertaken using a considerable variety of molecular and protein biochemistry based tools. A large part of the research initially focussed upon identifying HvTrx-*h*4 protein targets as well as examining a potential link between thioredoxin-*h*4 and oxidative stress. Genetically modified tobacco and barley plants were successfully exploited to gain new insight into the latter objective and subsequent investigations progressed to increase the understanding of HvTrx-*h*4 regulation.

6.2.1 HvTrx-*h*4 is Regulated at Multiple Stages

A key finding presented in this thesis is the discovery that HvTrx-*h*4 is highly regulated, at both post-transcriptional and post-translational levels. It was also evident that the state of HvTrx-*h*4 regulation is affected by specific stress events. Comparative analysis of HvTrx-*h*4 gene and protein expression, before and after stress events, indicates post-transcriptional modification of HvTrx-*h*4 occurs. In transgenic barley, UVB irradiation and wounding events induced expression of GFP, which was controlled by the *HvTrx-h4* promoter and 5′UTR genetic information. Although *HvTrx-h4* transcript was detected prior to these stresses, and appeared to remain unchanged throughout the experiment, GFP was only observed subsequently. This indicates post-transcriptional regulation of *HvTrx-h4* mRNA transpired in response to the UVB and wounding stresses. Further investigations led to the hypothesis that the mechanism of post-transcriptional regulation of HvTrx-*h*4 may involve formation of a secondary structure within the mRNA (Chapter 5).

For UVB stress, it was established that the signal leading to HvTrx-*h*4 protein synthesis is not translocated but localised to the point of irradiation (Chapter 5). Interestingly, UV irradiation of mammalian cells elicits the activation of transcription factors, including activation of nuclear factor-κB (NF-κB), which is regulated by a thioredoxin. It has been shown that UVB irradiation induces translocation of the thioredoxin from the cytoplasm into the nucleus, where it was found to directly associate with NF-κB p50 (Hirota et al., 1999). Furthermore, it was concluded that thioredoxin played dual and opposing roles in the regulation of NF-κB. In the cytoplasm, it interfered with signals to IκB kinases and blocked IκB degradation. Whilst in the nucleus, the thioredoxin enhanced NF-κB transcriptional activity by enhancing its ability to bind DNA (Hirota et al., 1999). Didier et al. (2001) also demonstrated that thioredoxin translocates from the cytoplasm to the nucleus, in UVA irradiated human skin fibroblasts. Considering these reports, the possibility of plant thioredoxin-*h*4 being translocated into the nucleus to regulate transcription factors is worth considering. To pursue this idea, a comparison of the sub-cellular location of HvTrx-*h*4 in wounded versus unstressed plants is an appealing initial experiment for the future.

Considering GFP was not translated in response to methyl viologen, the post-transcriptional regulation of thioredoxin-*h*4 must not be directly related to the production of ROS. Similarly, GFP translation was not directly influenced by the hormones JA, ABA and ethylene, although the wounding response, in which these hormones are known to play crucial roles, did induce GFP expression. Therefore, the suspected translation of HvTrx-*h*4 in response to wounding

must not be directly mediated by JA, ABA or ethylene. Supporting this hypothesis are findings by Titarenko et al. (1997), which showed that wound signals can be transmitted by a JA independent pathway in *A. thaliana*. This pathway was preferentially responsible for the activation of genes in the vicinity of the wound site (Titarenko et al., 1997). In addition, another study using GUS as a reporter for Ribonuclease LE activity in tomato plants, found GUS could be detected upon wounding but not after treatment with JA (Gross et al., 2004). These authors also concluded that a localised, wound-inducible, JA-independent signalling pathway exists, and is responsible for local gene activation (of Ribonuclease LE). Considering these studies and the fact that GFP was localised to the wound site, it is reasonable to suggest that following wounding, a JA-independent signal is triggered that results in translation of thioredoxin-*h*4. Determining what this signal is could be an interesting area for further investigations and may provide some answers regarding the apparent specificity of thioredoxin-*h*4 regulation relative to the nature of the eliciting stress.

A second level of HvTrx-*h*4 regulation, through a redox-based post-translational modification, was discovered *in vivo*. Data presented suggests that HvTrx-*h*4 is most probably glutathionylated at the N-terminal cysteine (Cys_4) (Chapter 5) and may also be glycosylated, since a highly conserved NFS motif was identified within the protein sequence (Chapter 3). Glutathionylation is thought to be involved in redox signalling mechanisms to facilitate the detection of deleterious conditions in cells and trigger suitable responses (Gao et al., 2009; Giustarini et al., 2004). In addition, glutathionylation appears to participate in regulating several signal transduction cascades, such as the NF-κB pathway in mammals (Reynaert et al., 2006; Shelton et al., 2007; Kil et al., 2008). Therefore, it could be speculated that HvTrx-*h*4 may function in a signalling capacity. Confirmation that thioredoxin-*h*4 is glutathionylated *in planta*, the requirements eliciting glutathionylation, and the physiological impact, are certainly worthy topics for future research.

Other forms of post-translational modifications have been linked to thioredoxins previously. The reported post-translational modifications of a human thioredoxin (Trx1), including glutathionylation, thiol-oxidation, and S-nitrosylation, are the focus of a review by Haendeler et al. (2006). Specifically, their contribution towards Trx1 functional regulation is discussed. The main biological functions of Trx1 are reported to include anti-oxidative, anti-apoptotic, and pro-proliferative properties. More recently, Hashemy and Holmgren (2008) found Trx1 to be the subject of S-nitrosylation following treatment with S-nitrosoglutathione. It was reported that this S-nitrosylation was critically dependent upon the redox state of Trx1. Furthermore, Trx1 activity was shown to be reversible inhibited by H_2O_2 treatment as well as

S-nitrosylation. The authors state that the physiological importance of these modifications is relatively unknown. However, they do suggest that Trx1 may be involved in cell signalling through temporal control of reduction, to confer oxidative signals in thiol redox control. This study aligns with our findings implicating the involvement of grass thioredoxin-*h*4 in oxidative stress responses. Therefore the possibility of grass thioredoxin-*h*4 functioning in a signalling capacity should be considered. It is highly likely that further understanding of these areas of thioredoxin-*h*4 regulation could assist with revealing the pathway(s) in which grass thioredoxins-*h*4 operate.

6.2.2 Monocysteinic Thioredoxin Affinity Chromatography Technique is Problematic

Identification of HvTrx-*h*4 protein interactions was problematic, most likely because of the additional cysteine present in the N-terminus. Although a mutant form of HvTrx-*h*4 was successfully engineered, expressed, purified and immobilised, no HvTrx-*h*4 target proteins were confidently established. Clearly, alternative approaches to those pursued in this study are required to identify protein interactions with grass thioredoxins-*h*4. In addition, findings such as the large number of isolated proteins that were common to both wild-type and mutant HvTrx-*h*4 'baits', also highlight the need for caution when using the monocysteinic thioredoxin affinity chromatography technique. Results obtained must be carefully analysed and interactions confirmed through alternative means.

The discovery of multiple levels of regulation acting upon thioredoxin-*h*4 expression highlights the need for careful selection of 'prey' protein sources in future protein interaction experiments. Given thioredoxin-*h*4 protein expression is induced by UVB, proteins derived from barley leaves stressed with UVB may be an ideal source. Although some grass thioredoxin-*h*4 targets may be present in unstressed tissues, others may also be induced by a UVB stress event and would therefore be more abundant, hence more likely to be isolated from UVB irradiated leaves.

6.2.3 Functional Redundancy within the Barley Thioredoxin-*h* Family is Unlikely

Characterisation of the barley cytosolic thioredoxins in reproductive tissues reveals that within the family of barley thioredoxins-*h* functional redundancy is not likely. QPCR showed unique transcript expression profiles for each *HvTrx-h* gene in the reproductive tissues examined; florets, anthers, stigmas and developing endosperm (Chapter 5). However, tobacco plants with *thioredoxin-h4* silenced were viable and furthermore, did not display increased sensitivity to oxidative stress (Chapter 3). This suggests that compensation for the loss of *thioredoxin-h4* occurred, possibly by another thioredoxin or even a glutaredoxin. Even so, the

differential regulation seen for each *HvTrx-h* member indicates that a degree of functional specificity is present within this class of thioredoxins.

In regards to *HvTrx-h4* characterisation, the QPCR analysis indicated that *HvTrx-h4* may be involved in a tissue developmental process linked to plant reproduction. Transcript expression of *HvTrx-h4* increased in maturing barley florets and the location of up-regulation was further refined to anther tissue. Additionally, spikes in *HvTrx-h4* transcription were detected in developing endosperm, at 5 and 8 days after pollination. These events can be correlated with the commencement and cessation of the cellularisation process within developing barley endosperm (Brown et al., 1994). Hence, HvTrx-*h*4 may be acting in a signalling capacity during this time. Further investigations into this hypothesis are necessary considering results from the GFP-reporter transgenic barley plants, which showed *HvTrx-h4* transcript expression does not necessarily correlate with its protein expression. Transcript levels may therefore not be a good indicator of when or where the HvTrx-*h*4 protein is active. Additional analysis of HvTrx-*h*4 protein expression is required before functional conclusions can be made, including in regards to potential HvTrx-*h*4 roles in grass reproductive tissues. Accordingly, techniques such as Western analysis and immunohistochemistry are recommended for future investigations.

6.2.4 Increased Thioredoxin-*h*4 Expression Confers Tolerance to Specific Oxidative Stresses

Multiple lines of evidence acquired during this study suggest a place for grass thioredoxins-*h*4 in the plant oxidative stress response. Firstly, constitutive over-expression of *PcTrx-h4* in tobacco resulted in increased tolerance to UVB irradiation, heat stress and methyl viologen application (Chapter 3). Secondly, protein translation of HvTrx-*h*4 appeared to be induced by UV irradiation and wounding events. This conclusion was extrapolated from analysis of genetically modified barley, where GFP was coupled to the *HvTrx-h4* promoter plus 5′UTR and used as a reporter gene/protein (Chapter 5). In addition, results obtained indicate that the source of oxidative stress is significant in relation to eliciting a response by thioredoxin-*h*4. For example, whilst over-expression of *PcTrx-h4* provided tolerance to extreme heat, no influence during water-deficit stress was detected. Upon demonstrating a correlation between *thioredoxin-h4* over-expression and oxidative stress tolerance in tobacco, potential mechanisms of this tolerance were investigated. Results showed that the tolerance mechanism does not involve scavenging of reactive oxygen species, neither directly nor indirectly. This

finding is consistent with the observed tolerance selectivity in regards to differing oxidative stress inducing events.

Although tolerance to topical application of methyl viologen occurred in transgenic tobacco plants over-expressing *PcTrx-h4*, HvTrx-*h*4 protein translation was not induced by a similar treatment in the transgenic barley (as inferred from a lack of visible GFP). Considering this discrepancy, the possibility that the stress tolerances observed exist due to an artificial function, ensuing from excessive and unnatural levels of forced thioredoxin-*h*4 expression, is raised. However, it may be argued that the genetically modified tobacco's increased tolerance to UVB stress (Chapter 3) is not derived from an induced, artificial function, because translation of GFP (driven by *HvTrx-h4* genetic information) occurred in barley in direct response to UVB irradiation (Chapter 5). Although RT-PCR showed no alteration in *HvTrx-h4* (nor *GFP*) transcript levels in response to UVB stress in barley, GFP was subsequently visible. Furthermore, the majority of the thioredoxin-*h*4 protein expressed in the transgenic tobacco plants was not controlled by the endogenous promoter or 5'UTR regulatory information. Consequently, the apparent post-transcriptional regulatory steps required (Chapter 5) were bypassed. This is likely to result in a faster response to the UVB stress event in the transgenic plants, compared to the wild-types where alterations in regulatory signals and protein synthesis must first occur. Hence, over-expression of *PcTrx-h4* would most likely result in an increased UVB tolerance phenotype, such as the one observed.

6.3 Future Focus and Further Recommendations

Within the discussion sections of this thesis a number of areas have been recommended and highlighted as worthy of future investigation. A crucial topic for pursuit, which I believe is essential for continued valuable investigations of HvTrx-*h*4, is to ascertain the system responsible for regeneration/reduction of HvTrx-*h*4. Recently, a report was published that focussed upon a poplar thioredoxin-*h*, designated PtTrx-*h*4. This paper is significant, and the data must be considered for future investigations of HvTrx-*h*4, because HvTrx-*h*4 is the barley homologue of PtTrx-*h*4 (Appendix A).

PtTrx-*h*4 was found to be regenerated by a glutathione/glutaredoxin reducing system and not by the typical NADPH/thioredoxin reductase (NTR) reducing system (Koh et al., 2008). We found that HvTrx-*h*4 can be reduced by *E. coli* NTR1 but is a poor substrate, especially compared to HvTrx-*h*2 (Appendix A). More recently, recombinant barley NTR2 was purified and preliminary activity studies initiated. According to Dr Juan Juttner, HvTrx-*h*4 appeared to be a poor substrate for the barley NTR2 as well (*pers. comm.*). These observations are

consistent with the PtTrx-*h*4 results and suggest that HvTrx-*h*4 may also be reduced by glutaredoxin; an hypothesis certainly worth investigating further. Koh et al. (2008) proposed a four-step disulfide cascade mechanism for glutaredoxin-dependent PtTrx-*h*4 catalysis and this could be investigated for the barley thioredoxin-*h*4. However, simply replicating Koh's experiments in barley may be unnecessary. Demonstration that HvTrx-*h*4 is regenerated by the glutathione/glutaredoxin reducing system may be sufficient to enable accurate extrapolation from the poplar data acquired by Koh et al. (2008). Instead, extension of the knowledge would be more beneficial and thus, perhaps future collaboration is merited.

In addition, Koh et al. (2008) proposed that transient glutathionylation of Cys_4 was responsible for conversion of PtTrx-*h*4 to its active, reduced form. In conjunction with our data demonstrating *in vitro* that HvTrx-*h*4 is glutathionylated, further investigations along this line of research for HvTrx-*h*4 is justified.

A study by Marty et al. (2009) also demonstrates a link between thioredoxin and glutaredoxin systems. Similar to that seen in our thioredoxin-*h*4 silenced tobacco plants, *A. thaliana* NADPH-dependent glutathione reductase (GR1) deletion mutants did not display an altered phenotype, even when subjected to stress inducing conditions. Therefore, it was speculated that functional redundancy is present in this pathway. In support, the deletion of both NADPH-dependent thioredoxin reductase A and GR1 resulted in a pollen lethal phenotype. Thus, along with biochemical and genetic assays, the authors were able to establish that the NADPH-dependent thioredoxin system can function as a backup system for GR1. Considering this report, it remains plausible that functional redundancy does not occur within the barley thioredoxin-*h* family but rather, a cross-over of function occurs between thioredoxin-*h*4 and the glutaredoxin system. Thus, this is another area of research that can be pursued for thioredoxin-*h*4, which is likely to yield interesting results.

The finding that HvTrx-*h*4 appears to be regulated by UV and wounding raises the question as to whether HvTrx-*h*4 might be located within a biochemical pathway common to both of these stresses. Studies in tomato have revealed that signal transduction associated with both of these stresses converges upon a common mitogen-activated protein kinase (MAPK) cascade (Holley et al., 2003; Kandoth et al., 2007). It is well-documented in mammals that thioredoxin can act as a negative regulator of the mammalian apoptosis stimulating kinase 1 (ASK1), a serine-threonine kinase of the MAPK family (Saitoh et al., 1998). Also, protein microarray experiments in *A. thaliana* indicate that thioredoxin-*m* is a potential substrate for AtMPK3 and AtMPK6 (Feilner et al., 2005). Moreover, a study in rice reported that a thioredoxin-*h*

(OsTrx23) was a potential negative regulator of two stress-related MAPKs, OsMPK3 and OsMPK6 (Xie et al., 2009). Considering these reports, it is tempting to hypothesise that thioredoxin-*h*4 may function as a regulator of MAPKs in the plant cellular stress response.

6.4 Final Remarks

The research presented in this thesis demonstrates progress towards characterisation of grass cytosolic thioredoxins. Findings reveal that thioredoxin-*h*4 is potentially regulated at three levels, and this need for such tight control is certainly intriguing. Coupled with the discovery of thioredoxin-*h*4's involvement in oxidative stress responses, it is tempting to speculate that thioredoxin-*h*4 function is linked to a signalling role. Conjectures of this nature require future investigations, and accordingly, several lines of research have been recommended. Whilst the role(s) of grass thioredoxin-*h*4 remains elusive, the new discoveries strengthen our key hypotheses and support the notion that the subclass 4 members of cytosolic thioredoxins have a significant and remarkable function.

Appendix A – Supplementary Figures

```
                  10        20        30        40        50        60
                   |         |         |         |         |         |
HvTrx-h4    MGGCVGKG---RGVVEEKLDFKGGNVHVITTKEDWDQKIEEANKDGKIVVANFSASWCGP
PcTrx-h4    MGGCVGKD---RGIVEDKLDFKGGNVHVITTKEDWDQKIAEANKDGKIVVANFSASWCGP
AtTrx-h9    MGSCVSKG-KGDDDSVHNVEFSGGNVHLITTKESWDDKLAEADRDGKIVVANFSATWCGP
PtTrx-h4    MGLCLAKRNHDADDDEPHIELAGGNVHLITTKERWDQKLSEASRDGKIVLANFSARWCGP
            ** *  *               ***** ***** ** *  **  ***** ***** ****

                  70        80        90       100       110       120
                   |         |         |         |         |         |
HvTrx-h4    CRVIAPVYAEMSKTYPQLMFLTIDVDDLMDFSSTWDIRATPTFFFLKNGQQIDKLVGANK
PcTrx-h4    CRVIAPVYAEMSKTYPQLMFLTIDVDDLVDFSSTWDIRATPTFFFLKNGQQIDKLVGANK
AtTrx-h9    CKIVAPFFIELSEKHSSLMFLLVDVDELSDFSSSWDIKATPTFFFLKNGQQIGKLVGANK
PtTrx-h4    CKQIAPYYIELSENYPSLMFLVIDVDELSDFSASWEIKATPTFFFLRDGQQVDKLVGANK
            *   **   * *     ****  *** * ***  * * ********  ***  *******

                 130       140
                   |         |
HvTrx-h4    PELEKKVQALGDGS-------
PcTrx-h4    PELEKKVQALGDGS-------
AtTrx-h9    PELQKKVTSIIDSVPESPQRP
PtTrx-h4    PELHKKITAILDSLPPSDK--
            *** **     *
```

Figure A1: *Hordeum vulgare* thioredoxin-*h*4 (HvTrx-*h*4: 131 residues) and *Phalaris coerulescens* thioredoxin-*h*4 (PcTrx-*h*4: 131 residues) share 96% amino acid identity. HvTrx-*h*4 and *Arabidopsis thaliana* thioredoxin-*h*4 (AtTrx-*h*4: 140 residues) share 65% amino acid identity. HvTrx-*h*4 and *Populus trichocarpa* thioredoxin-*h*4 (PtTrx-*h*4: 139 residues) share 61% amino acid identity. Stars indicate amino acid match in all four sequences.

```
                   10        20        30        40        50        60
                    |         |         |         |         |         |
AtTrx-01      MKGNWSIVRKVLHRQFSTLRSSTPSSRLSTSIRPLVLAPNSISSLIARNSLFTASNIGPS
HvTrx-h4      ----------------------------------------MGGCVGKG----RGVVEEK

                   70        80        90       100       110       120
                    |         |         |         |         |         |
AtTrx-01      IDFNFSNTSLPHRRSLCSEAGGENGVVLVKSEEEFINAMSKAQDGSLPSVFYFTAAWCGP
HvTrx-h4      LDFKGGN-----------------VHVITTKEDWDQKIEEANKDGKIVVANFSASWCGP
               **   *                 *      *        *       *  * * ****

                  130       140       150       160       170       180
                    |         |         |         |         |         |
AtTrx-01      CRFISPVIVELSKQYPDVTTYKVDIDEGGISNTISKLNITAVPTLHFFKGGSKKGEVVGA
HvTrx-h4      CRVIAPVYAEMSKTYPQLMFLTIDVDD--LMDFSSTWDIRATPTFFFLKNGQQIDKLVGA
              ** * **  * ** **       * *        *   * * **  * * *      ***

                  190
                    |
AtTrx-01      DVTKLKNLMEQLYK--
HvTrx-h4      NKPELEKKVQALGDGS
                  *      *
```

Figure A2: *Hordeum vulgare* thioredoxin-*h*4 (HvTrx-*h*4: 131 residues) and *Arabidopsis thaliana* thioredoxin-*o*1 (AtTrx-*o*1: 194 residues) share 19.4% amino acid identity. The N-terminal cleavage site for AtTrx-*o*1 is highlighted in yellow. Stars indicate amino acid match.

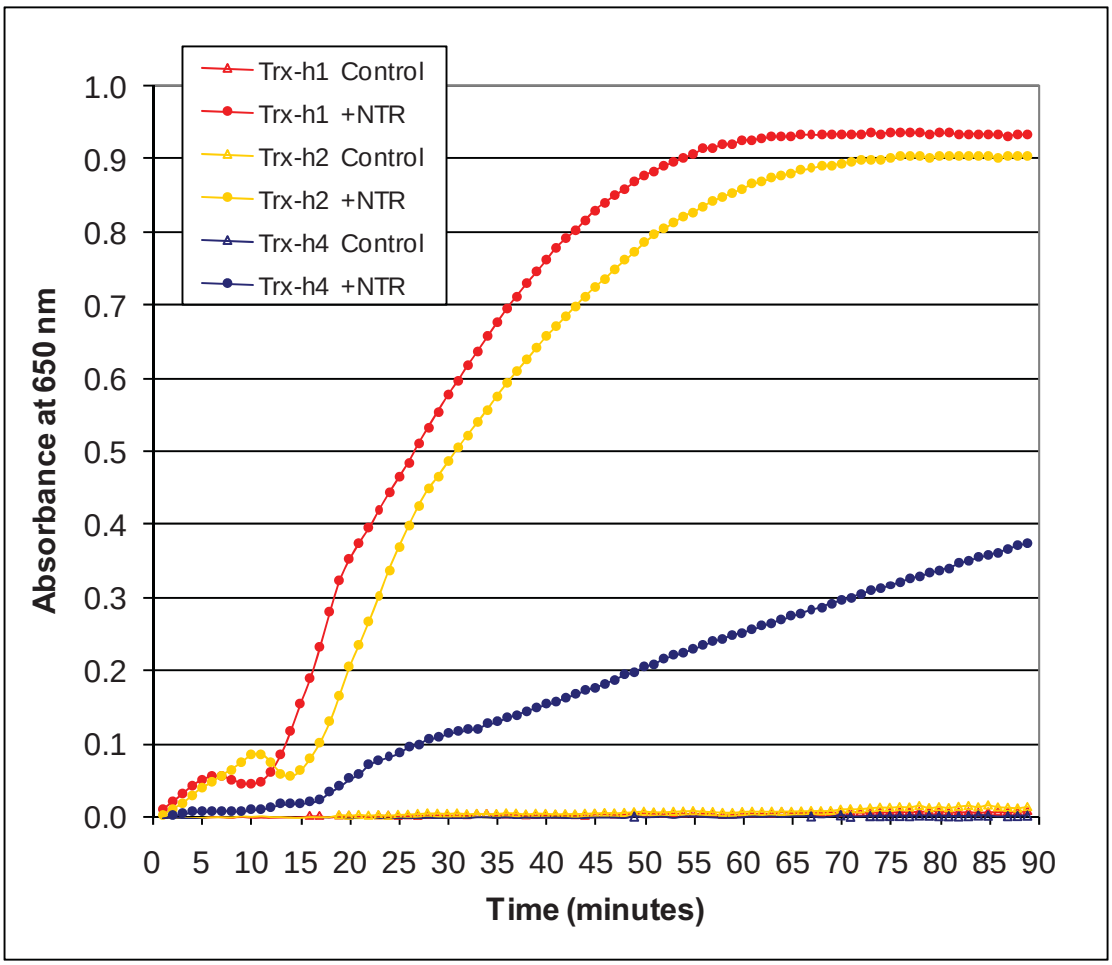

Figure A3: Activity of HvTrx-*h*1, -*h*2 and -*h*4 in the presence of the NADPH:*E.coli* thioredoxin reductase (NTR) system. The reduction of Nbs_2 by HvTrx-*h* in combination with *E. coli* NTR1 was initiated by the addition of NTR1. Nbs_2 reduction was determined spectrophotometrically at 412 nm and recorded every 30 sec for 90 min. All components in the absence of NTR served as a control. Data courtesy of Dr Juan Juttner *(unpublished)*

Appendix B - Primers

Primer Name	Nucleotide Sequence (5′ – 3′)
For Mutation of *HvTrx-h4*	
Hv4E70F	TAAGCATGCGCGGGGGCTGTGTGGGCAAG
Hv4MutF	GGTGTGGGCCATCCCGTGTCATTGCAC
Hv4MutR	GTGCAATGACACGGCATGGCCCACACC
Hv4E70R	TAAAGATCTACTGCCATCACCAAGAGC
For *HvTrx-h4* Promoter and 5'UTR Isolation/Cloning	
AP1	GTAATACGACTCACTATAGGGC
AP2	ACTATAGGGCACGCGTGGT
GWR1	CTTCTTCAATCTTCTGGTCCCAGTCCTC
GWR2	CATGCCGAACTGACAATAGC
SP6	ATTTAGGTGACACTATAG
T7	TAATACGACTCACTATAGGG
GWF1seq	TCCCCTACCGCATCTCATCC
GpPF1	CGGGGATGACTTTAGCTTGAGG
For Gateway Vector Construction	
2.5PromTrx4F	GGGATGACTTTAGCTTGAGGA
HvPromR	CCGAACTGACAATAGCAGGAAT
HvPromR2	GGCGGGCAATTAAGAGGTT
GW1 (fwd)	GTTGCAACAAATTGATGAGCAATGC
GW2 (rev)	GTTGCAACAAATTGATGAGCAATTA
pMDC-RB-SC	GTTGGTCAAGTCCTGGTCGT
For Southern Analysis	
SProbeFwd	CTGGAGTTGTCCCAATTCTTG
SProbeRev	TGGTGGTGGTGGTGTTTGTA
For Barley T1 PCR Screen	
GFPfwd	CTGGAGTTGTCCCAATTCTTG
GFPrev	TGGTGGTGGTGGTGGTGTTTGTA

For Q-PCR

GAPDHfwd	GTGAGGCTGGTGCTGATTACG
GAPDHrev	TGGTGCAGCTAGCATTTGAGAC
HSP70fwd	CGACCAGGGCAACCGCACCAC
HSP70rev	ACGGTGTTGATGGGGTTCATG
TubulinFwd	AGTGTCCTGTCCACCCACTC
TubulinRev	AGCATGAAGTGGATCCTTGG
CyclophilinFwd	CCTGTCGTGTCGTCGGTCTAAA
CyclophilinRev	ACGCAGATCCAGCAGCCTAAAG
HvTrx-h1Fwd	TGCCGACCTTCCTGTTTATCA
HvTrx-h1Rev	CAACCGGTGCATATCTTAAGT
HvTrx-h2Fwd	GGCCATGCCAACGTTCCTGTTCAT
HvTrx-h2Rev	TGAGCGGCAATTTTATTTAG
HvTrx-h3Fwd	GGAGGTTGCAAAGACATTCC
HvTrx-h3Rev	CGGAAACCTGGCACTACAAT
HvTrx-h4Fwd	CCGCGCAACCCCGACGTTCTTCTT
HvTrx-h4Rev	CATGGAGGTACAGATATATA

For RT-PCR

HvPWMK1FwD	GGTGCATCGAACGACAGTAA
HvPWMK1Rev	TCAACAGCGAAACAGGACAG
HvUbiFwd	CTCGCCGACTACAACATCC
HvUbiRev	GGTAAAAGAGCAGAGCAAAC
HvGFPfwd	TGGAGTTGTCCCAATTCTTGTTGA
HvGFPrev	AGATGGTCCTCTCCTGCACGTATC
HvCHS2Fwd	CAACTGGAGAAGGCAAGGAC
HvCHS2Rev	TTTGTGGGCCGCTTATTTTA
HvDhy4Fwd	CATGAGGGACGAGCACCAGACT
HvDhy4Rev	GATCTTCTCCTTGATGCCCTTCT
Hv18Sfwd	CTGCCAGTAGTCATATGCTTGTCT
Hv18Srev	CCCCGTGTCAGGATTGG
HvJIP23Fwd	AATGGCCTCAGGAGTGTTTG
HvJIP23Rev	TTCATGGTAGTGCCTTCACC

Appendix C – *HvTrx-h4* Promoter Sequence

The consensus sequence 5′ Upstream of *HvTrx-h4* cv Atlas46 derived from alignment of sequences from three plasmids.

ACTATAGGGCACGCGTGGTCGACGGCCCGGGTTGGTATCGGCGGGGATGACTTTAGCTTG
AGGAGTTCATGTATTCACTATGTGTTAATGCTTTGCTTCAGTTCTGCATTAAAAGGAGCGC
CTTAATTACCCTTAGTTTCCATTAGGACAAAATATGTCATGCAAATTCTTATTGCAAGCAC
GTATACTATACATGGAATACATGTCAACATATAGTTAATGAATTGAAACTACTGTATGTC
GCTCTAGGTTGTGACTACACTTTTATACTATTTCCTTTGCTCCATTTACTATTACTCTGCGA
GTTACAATTCTACTACTAGTGAAGTTACTATCACCGTTACTTTGCTATCATTGCTATCATA
TTCATTGTGCTATTCATAAATTGATGCAAGGAAGAGATTCTCACATATGGTTGAATTGAC
AACTCAACTTTTAAGGCTTACAAATATTCTTTCTCTCCCCTTGTATCGAATCAATAAATTT
GGGTGAAATACTATCATCGAAGACTATTGCGATCCCTTATACATGTGGGTCGTCAGTTGG
TCGGTCATCTACGCGTGTCTTCGAATCCGGCGCACTGGAGGATTTGTGCCCCGTTCCATCT
CCTTGGGCTCACGGACGTCCTTGCCAACCCGGTCCCAGTGACCCGCATCCGCGTTCCCTCC
ATATCTCGGCTCGCTCTGTCCTTCGGCCACTGTCACATCCCCTACCGCATCTCATCCTCCT
AGTCACCCAGCATATGTGCCCCAATTTGTCCCTCCACCGCTCTGTTGCTTGCACGTCTAGT
AGTGCATGTTGCCTCTCGACGCGCGTGGATCCCCTTCCCGCGGTCGTGGCTCCGACCTATG
CMCGACTTCCTCTTCSCTAACYCATGCNTTTGATGGCTTGGTATTGCTCGAACTCTGTCCA
GGACAAAATCCCTGCATACTATGATGGCASCAGCGACMCYCGCGGGTGTCGTCCCCTYCT
TGGTGGCGCTATCACAACGGTTATCTGGCCCCTCTTGAAGCATCAKGGGAMCNACGCCYA
KKTCCGAYTTTCCGGATCGAACGACGATGGCGTCTCGACGTAGTACTCCTTCGTGAAGGT
TGTGTCTTGGTTGCTCGCGACGTCCCAGGGTCTTGATGTGAAGATGTTGGTCGTGGTGTTG
TTAGTCTTGGCTTACTTCGTAGGATGGCGAGTTTAGCTGTGTTTTTCTCTTGTTTGAGTCGA
GCATCGTATATCTCTTTGCTCCGGACATTATGTTGATGCATCTTGTTTCCGTATCTTGTATT
GTATCTCGTCTTGTACTCTAACTTTTCTTGTCAATGAAATGATACGCAGACTTTGCATATT
CGCAGAAAAAGAAAAAGAAAAACACATTTTGAAATTTGTATAGCCACAAGGCAGACGGC
GGCGGGGTAGTCTCCGTGCCAGTAGTCTACCGGAGGTTGTCTCAAAAAAAAAAGTAGTCC
ACCGGAGGTCCGGTCCGGTCCGGAGCAACACAGAAGCTCCACGTCGCCGGATCTCCACC
AAGGCAGAATASGACCATTTTCCACCAGCAGAAAGGGCATTTTCTTTCGGTAGGCGCACA
CGGCACGAGCCGCGCCAGCCAAGTGGCGTGCGACGCGAGACGCGGCACGGGCTCTCTCG
YTCACGCCGGCCGGCCGGGAGCGGACGGCCCGATCGGATCCCATCCAGGTCGTCGGCGT
YGGSGTCGTCGTCGTCGCCTCCAGAAGCACGAGCCCAGCATAGCACGGCCGCAGAATATT
CCACGTCCCTTCCCCTCATCCTCCCCAGGCCCAGCAGCAAWAAAAAAGCAAGCCATTCCC
CTCCNTCTTCCTCCGATTAATCAAWCCGCGCGGCGGCGGCGGCGAGCGTGCGACCTGCGA
CMMCCARACGACCCAACCGACYCACTGAYCMAMACMACAYCACCGGGGRGMGTACTC
CCTTTTACGTCAATCAATCGAAACCCAGTTAAAGAACCTCTTAATTGCCCGCCAGGAGAT
CCGCCAGGCTTATCTTCGCCGTCTCCTCCGACCTCGCCTCCACCCCCCCTCGCCCCGCGGC
TTCTGGGTTCCTTGGCGCCAAAATCCCCGCTTCCGATCCCAGGTAAATCCTCTTTGGTTAC
TCGTTGATCCGGTCGGCTTCGATTTGTCCGACGCGGTTCCTGGCCGCGAATTGTATGCCTG
AAAGATTCTTCTTCGTGGATTCTTGATCCGCGAGGGAGCGGACACAACTGGATTTTTGTGT
GTGCTTTTAGTTTACCAGGTTCAGGTTCTTGTCCGGTTCATGATAATGGAAGAATTCCTTC
CTTAAAACTGCAAAGAGATGTAGCTCTAGTTCCTCGCACCCAGTTGGGATGTGTTGGGGA
GAAAAATACTCCCCTTCCCGGGCCAACTGACGACAAGTTATCTGTTAGGAGTACTTTACA
TCATGGAGTATATAATACCTTACCGAAATTACTGTTCCCGCAACGTCTCCATATTTTTTCT
AGTGTTATTACAGACACAGTTTCCTTCTGATAGACCRTGACATGGYTTACTGTTGTTTAGG
CCTTCAGGAATCAGGGGGCCTTTCATTCAGCGATTCCTGCTATTGTCAGTTCGGC(ATG)

The consensus sequence 5′ Upstream of *HvTrx-h4* cv Golden Promise derived from alignment of sequences from three plasmids.

CGGGGATGACTTTAGCTTGAGGAGTTCATGTATTCACTATGTGTTAATGCTTTGTTTCAGT
TCTGCATTAAAAGGAGCGCCTTAATTACCCTTAGTTTTCATTAGGACAAAATATGTCATGC
AAATTCTTATTGCAAGCACGTATACTATACATGGAATACATGTCAACATATAGTTAATGA
ATTGAAACTACTGTATGTCGCTCTAGGTTGTGACTACACTTTTATACTATTTCCTTTGCTCC
ATTTACTATTACTCTGCGAGTTACAATTCTACTACTAGTGAAGTTACTATCACCGTTACTT
TGCTATCATTGCTATCATATTCATTGTGCTATTCATAAATTGATGCAAGGAAGAGATTCTC
ACATATGGTTGAATTGACAACTCAACTTTTAAGGCTTACAAATATTCTTTCTCTCCCCTTG
TATCGAATCAATAAATTTGGGTGAAATACTATCATCGAAGACTATTGCGATCCCTTATAC
ATGTGGGTCGTCAGTTGGTCGGTCATCTACGCGTGTCTTCGAATCCGGCGCACTGGAGGA
TTTGTGCCCCGTTCCATCTCCTTGGGCTCACGGACGTCCTTGCCAACCCGGTCCCAGTGAC
CCGCATCCGCGTTCCCTCCATATCTCGGCTCGCTCTGTCCTTCGGCCACTGTCACATCCCC
TACCGCATCTCATCCTCCTAGTCACCCACAATATGTGCCCCATTTGTCCCTCCACCGCTCT
GTTGCTTGCACGTCTAGTAGTGCATGTTGCCTCTCGACGCGCGTGGATCCCCTTCCCGCGG
TCGTGGCTCCGACCTATGCACGACTTCCTCTTCGCTAACTCATGCTTTGATGGCTTGGTAT
TGCTCGAACTCTGTCCAGGACAAAATCCCTGCATACTATGATGGCAGCAGCGACACTCGC
GGGTGTCGTCCCCTTCTTGGTGGCGCTATCACAACGGTTATCTGGCCCCTCTTGAAGCATC
ATGGGAAACCCTASGTCCGATTTTCCGGATCGAACGACGATGGCGTCTCGACGTAGTACT
CCTTCGTGAAGGTTGTGTCTTGSTTGCTCGCGACGTCCCAGGRTCTTGATGTGAAGATGTT
GGTCGTGGTGTTGTTAGTCTTGGCTTACTTCGTAGGATGGCGAGTYTRGYTKTTSTTGTTG
ATCATCGATTGTCNTTCCGAGTSTGAGCACTCGTWTCGAATCTSTTTGCTCCTGGACATTA
TGTTGATGCATCTTGTTTCCGTATCTTGTATTGTATCTCGTCTTGTACTCTAACTTTTCTTGT
CAATGAAATGATACGCAGACTTTGCATATTCGCAGAAAAAGAAAAAGAAAAACACATTT
TGAAATTTGTATAGCCACAAGGCAGACGGCGGCGGGGTAGTCTCCGTGCCAGTAGTCTAC
CGGAGGTTGTCTCAAAAAAAAAAAGTAGTCCACCGGAGGTCCGGTCCGGTCCGGAGCAA
CACAGAAGCTCCACGTCGCCGGATCTCCACCAAGGCAAATACGACCATTTTCCACCAACA
GAAAAGGCATTTTCTTTCGGTAGGCGCACACGGCACGAGCCGCGCCAGCCAAGTGGCGT
GCGACGCGAGACGCGGCACGGGCTCTCTCGCTCACGCCGGCCGGCCGGGAGCGGACGGC
CCGATCGATCCCATCCAGGTCGTCGGCGTCGGCGTCGTCGTCGTCGCCTCCAGAAGCACG
AGCCCAGCATAGCACGGCCGCAGAATATTCCACGTCCCTTCCCCTCATCCTCCCCAGGCC
CAGCAGCAATAAAAAAGCAAGCCATTCCCCTCCTCTTCCTCCGATTAATCAAACCGCGCG
GCGGCGGCGGCGAGCGTGCGACCTGTGACCACCAGACGACCCAACCGACCCACTGACCC
ACACCACACCACCGGGGAGCTCTCCCTTTTACGTCAATCAATCGAAACCCAGTTAAAGAA
CCTCTTAATTGCCCGCCAGGAGATCCGCCAGGCTTATCTTCGCCGTCTCCTCCGACCTCGC
CTCCACCCCCCCTCGCCCCGCGGCTTCTGGGTTCCTTGGCGCCAAAATCCCCGCTTCCGAT
CCCAGGTAAATCCTCTTTGGTTACTCGTTGATCCGGTCGGCTTCGATTTGTCCGACGCGGT
TCCTGGCCGCGAATTGTATGCCTGAAAGATTCTTCTTCGTGGATTCTTGATCCGCGAGGGA
GCGGACACAACTGGATTTTTGTGTGTGCTTTTGGTTTACCAGGTTCAGGTTCTTGTCCGGT
TCATGATAATGGAAGAATTCCTTCCTTAAAACTGCAAAGAGATGTAGCTCTAGTTCCTCG
CACCCAGTTGGGATGTGTTGGGGAGAAAAATACTCTCCTTCCCGGGCCAACTGACGACAA
GTTATCTGTTAGGAGTACTTTACATCATGGAGTATATAATACCTTACCGAAATTACTGTTC
CCGCAACGTCTCCATATTTTTTCTAGTGTTATTACAGACACAGTTTCCTTCTGATAGACCA
TGACATGGTTTACTGTTGTTTAGGCCTTCAGGAATCAGGGGGCCTTTCATTCAGCGATTCC
TGCTATTGTCAGTTCGGC(ATG)

Appendix D – Motifs Present in the *HvTrx-h4* Promoter, 5′-UTR Regions and Intron

The complete list of motifs identified in the isolated 5′ genomic sequence upstream of *HvTrx-h4*, when scanned by the plant cis-acting regulatory DNA elements (PLACE) database.

Name	Sequence	Locations
10PEHVPSBD	TATTCT	838(+); 2129(-)
-300CORE	TGTAAAG	177 (+)
-300ELEMENT	TGHAAARK	177 (+); 1255 (+)
ABRELATERD1	ACGTG	830 (+) 1087 (+) 1800 (+) 2400 (+)
ABREOSRAB21	ACGTSSSC	1083 (-)
ABRERATCAL	MACGYGB	1922 (+) 1768 (+) 2021 (+)
ACGTCBOX	GACGTC	1473 (+/-)1958 (+/-)
AMYBOX1	TAACARA	190 (+)
ANAERO1CONSENSUS	AAACAAA	2486 (+)
ANAERO2CONSENSUS	AGCAGC	798 (-) 1640 (-)
ARFAT	TGTCTC	1149 (-)
ARR1AT	NGATT	18 sites
ASF1MOTIFCAMV	TGACG	650 (+) 2043 (+) 205 (-)
AUXRETGA1GMGH3	TGACGTAA	650 (+)
B2GMAUX28	CTTGTCGTCA	200 (+)
BIHD1OS	TGTCA	7 sites
BS1EGCCR	AGCGGG	510 (+)
CANBNNAPA	CNAACAC	240 (+)
CAREOSREP1	CAACTC	2154 (-)
CATATGGMSAUR	CATATG	2170 (+/-)
CBFHV	RYCGAC	2033 (+) 463 (+) 892 (+) 898 (+) 696 (-)
CEREGLUBOX2PSLEGA	TGAAAACT	2442 (+)
CGACGOSAMY3	CGACG	13 sites
CGCGBOXAT	VCGCGB	22 sites
DPBFCOREDCDC3	ACACNNG	111 (+) 1625 (+) 2020 (+) 1632 (-)
DRE2COREZMRAB17	ACCGAC	2033 (+) 696 (-)
DRECRTCOREAT	RCCGAC	2033 (+) 463 (+) 892 (+) 898 (+) 696 (-)
E2FCONSENSUS	WTTSSCSS	429 (+) 519 (+) 611 (-)
EBOXBNNAPA	CANNTG	16 sites
EECCRCAH1	GANTTNC	492 (+) 300 (-) 1545 (-) 1724 (-) 2275 (-)
EMHVCHORD	TGTAAAGT	177 (+)
ERELEE4	AWTTCAAA	1216 (+)
GARE1OSREP1	TAACAGA	190 (+)
GCCCORE	GCCGCC	734 (+) 737 (+) 740 (+) 1189 (+)
GT1CONSENSUS	GRWAAW	16 sites
GT1GMSCAM4	GAAAAA	117 (+) 1389 (+) 231 (-) 1229 (-) 1235 (-) 1241 (-)
HEXMOTIFTAH3H4	ACGTCA	650 (-)
IBOX	GATAAG	588 (+)
IBOXCORE	GATAA	195 (+) 588 (+)1589 (+) 312 (-)
INRNTPSADB	YTCANTYY	2355 (+) 2480 (-)
INTRONLOWER	TGCAGG	1658 (+)
LTRE1HVBLT49	CCGAAA	1023 (+) 149 (-)
LTRECOREATCOR15	CCGAC	8 sites
MARTBOX	TTWTWTTWTT	1138 (+) 1139 (+)

MYB1AT	WAACCA	68 (+) 345 (+) 481 (+) 631 (+)
MYB2CONSENSUSAT	YAACKG	7 sites
MYBCORE	CNGTTR	13 sites
MYBCOREATCYCB1	AACGG	1983 (+) 2242 (+) 1594 (-)
MYBPZM	CCWACC	1019 (+) 699 (-) 1870 (-) 1948 (-)
MYCATERD1	CATGTG	2051 (-)
MYCATRD22	CACATG	2051 (+)
MYCCONSENSUSAT	CANNTG	16 sites
NODCON1GM (=OSE1ROOTNODULE)	AAAGAT	413 (-)
NODCON2GM	CTCTT	9 sites
NTBBF1ARROLB	ACTTTA	179 (-) 2529 (-)
OCTAMERMOTIFTAH3H4	CGCGGATC	387 (+)
OSE2ROOTNODULE	CTCTT	9 sites
P1BS	GNATATNC	835 (+/-) 1250 (+/-)
PALBOXAPC	CCGTCC	926 (+)
POLASIG1	AATAAA	792 (-) 2101 (-)
POLLEN1LELAT52	AGAAA	10 sites
PREATPRODH	ACTCAT	1709 (-)
PRECONSCRHSP70A	SCGAYNRN^{15}HD	464 (+) 878 (+)
PROLAMINBOXOSGLUB1	TGCAAAG	1255 (+) 282 (-)
PYRIMIDINEBOXOSRAMY1A	CCTTTT	1036 (+) 2468 (+) 656 (-)
RAV1AAT	CAACA	10 sites
REALPHALGLHCB21	AACCAA	346 (+) 482 (+) 1485 (+)
RHERPATEXPA7	KCACGW	6 sites
ROOTMOTIFTAPOX1	ATATT	9 sites
RYREPEATBNNAPA	CATGCA	1787 (+) 2420 (-)
RYREPEATLEGUMINBOX	CATGCAY	1787 (+)
SEBFCONSSTPR10A	YTGTCWC	1149 (-) 1880 (-)
SEF3MOTIFGM	AACCCA	532 (+) 635 (-)
SEF4MOTIFGM7S	RTTTTTR	361 (-)
SITEIIATCYTC	TGGGCY	803 (+) 859 (+) 1968 (-)
SORLIP1AT	GCCAC	5 sites
SORLIP2AT	GGGCC	5 sites
SP8BFIBSP8BIB	TACTATT	2289 (-) 2310 (-)
SURECOREATSULTR11	GAGAC	6 sites
TAAAGSTKST1	TAAAG	179 (+) 2529 (+) 628 (-)
TATABOX4	TATATAA	162 (-)
TBOXATGAPB	ACTTTG	1257 (-) 2236 (-)
TGACGTVMAMY	TGACGT	650 (+)
TGTCACACMCUCUMISIN	TGTCACA	1879 (-)
TRANSINITDICOTS	AMNAUGGC	1526 (-)
TRANSINITMONOCOTS	RMNAUGGC	1526 (-)
UP2ATMSD	AAACCCTA	1557 (-)
WBOXATNPR1	TTGAC	649 (+) 1278 (+) 2375 (+) 2159 (-)
WBOXHVISO1	TGACT	1850 (+) 2326 (-) 2532 (-)
WBOXNTCHN48	CTGACY	687 (-)
WBOXNTERF3	TGACY	7 sites

References

Alkhalfioui, F., Renard, M., Frendo, P., Keichinger, C., Meyer, Y., Gelhaye, E., Hirasawa, M., Knaff, D.B., Ritzenthaler, C., and Montrichard, F. (2008) A novel type of thioredoxin dedicated to symbiosis in legumes. Plant Physiology, 148(1), 424-435.

Altschul, S., Gish, W., Miller, W., Myers, E., and Lipman, D. (1990) Basic local alignment search tool. Journal of Molecular Biology, 215, 403-410.

Anderson, M.D., Prasad, T.K., and Stewart, C.R. (1995) Changes in isozyme profiles of catalase, peroxidase and glutathione-reductase during acclimation to chilling in mesocotyls of maize seedlings. Plant Physiology, 109(4), 1247-1257.

Anderson, P., and Kedersha, N. (2009) RNA granules: post-transcriptional and epigenetic modulators of gene expression. Nature Reviews Molecular Cell Biology, 10(6), 430-436.

Apel, K., and Hirt, H. (2004) Reactive oxygen species: Metabolism, oxidative stress and signal transduction. Annual Review of Plant Biology, 55, 373-399.

Arner, E.S.J., and Holmgren, A. (2000) Physiological functions of thioredoxin and thioredoxin reductase. European Journal of Biochemistry, 267(20), 6102-6109.

Arora, A., Sairam, R.K., and Srivastava, G.C. (2002) Oxidative stress and antioxidative system in plants. Current Science, 82(10), 1227-1238.

Asada, K. (1994) Causes of photo-oxidative stress and amelioration of defence systems in plants. Boca Raton, FL: CRC Press, pp.77-104.

Asada, K. (2006) Production and scavenging of reactive oxygen species in chloroplasts and their functions. Plant Physiology, 141(2), 391-396.

Asada, K., and Takahashi, M. (1987) Production and scavenging of active oxygen in photosynthesis. Amsterdam: Elsevier, pp.227-287.

Aslund, F., and Beckwith, J. (1999) The thioredoxin superfamily: Redundancy, specificity, and gray-area genomics. Journal of Bacteriology, 181(5), 1375-1379.

Asturias, J.A., Arilla, M.C., Bartolome, B., Martinez, J., Martinez, A., and Palacios, R. (1997) Sequence polymorphism and structural analysis of timothy grass pollen profilin allergen (Phl p 11). Biochimica Et Biophysica Acta-Gene Structure and Expression, 1352(3), 253-257.

Balachandran, S., Xiang, Y., Schobert, C., Thompson, G., and Lucas, W. (1997) Phloem sap proteins from *Curcurbita maxima* and *Ricinus communis* have the capacity to traffic cell to cell through plasmadesmata. PNAS, 14150-14155.

Balmer, Y., and Buchanan, B.B. (2002) Yet another plant thioredoxin. Trends in Plant Science, 7(5), 191-193.

Balmer, Y., Koller, A., del Val, G., Manieri, W., Schurmann, P., and Buchanan, B.B. (2003) Proteomics gives insight into the regulatory function of chloroplast thioredoxins. PNAS, 100(1), 370-375.

Balmer, Y., Vensel, W.H., Tanaka, C.K., Hurkman, W.J., Gelhaye, E., Rouhier, N., Jacquot, J.P., Manieri, W., Schuurmann, P., Droux, M., and Buchanan, B.B. (2004) Thioredoxin links redox to the regulation of fundamental processes of plant mitochondria. PNAS, 101(8), 2642-2647.

Banerjee, A.K., Mandal, A., Chanda, D., and Chakraborti, S. (2003) Oxidant, antioxidant and physical exercise. Molecular and Cellular Biochemistry, 253(1-2), 307-312.

Banze, M., and Follmann, H. (2000) Organelle -specific NADPH thioredoxin reductase in plant mitochondria. Journal of Plant Physiology, 156, 126-129.

Bar-Noy, S., Gorlatov, S.N., and Stadtman, T.C. (2001) Overexpression of wild type and SeCys/Cys mutant of human thioredoxin reductase in *E-coli*: The role of selenocysteine in the catalytic activity. Free Radical Biology and Medicine, 30(1), 51-61.

Bari, R., and Jones, J. (2009) Role of plant hormones in plant defence responses. Plant Molecular Biology, 69(4), 473-488.

Barr, H.D., and Weatherley, P.E. (1962) A re-examination of the relative turgidity technique for estimating water deficit in leaves. Australian Journal of Biological Science, 15, 413-428.

Bartels, D. (2001) Targeting detoxification pathways: An efficient approach to obtain plants with multiple stress tolerance? Trends in Plant Science, 6(7), 284-286.

Bauer, C.E., Elsen, S., and Bird, T.H. (1999) Mechanisms for redox control of gene expression. Annual Review of Microbiology, 53, 495-523.

Baumann, U., and Juttner, J. (2002) Plant thioredoxins: the multiplicity conundrum. Cellular and Molecular Life Sciences, 59(6), 1042-1057.

Benitez, D., Garcia-Ortega, P., Picado, C., Mila, J., Vives, J., Martinez, J., and Vilella, R. (2001) Specific immune response to *Phleum pratense* plant profilin in atopic patients and control subjects. Allergol Immunopathol (Madr), 29(1), 9-15.

Berndt, C., Lillig, C.H., and Holmgren, A. (2008) Thioredoxins and glutaredoxins as facilitators of protein folding. Biochimica Et Biophysica Acta-Molecular Cell Research, 1783(4), 641-650.

Besse, I., Wong, J., Kobrehel, K., and Buchanan, B. (1996) Thiocalsin- a thioredoxin-linked, substrate-specific protease dependent on calcium. PNAS, 93, 3169-3175.

Biguet, C., Wakasugi, N., Mishal, Z., Holmgren, A., Chouaib, S., Tursz, T., and Wakasugi, H. (1994) Thioredoxin increases the proliferation of human B-cell lines through a protein kinase C-dependent mechanism. Journal of Biological Chemistry, 269, 28865-28870.

Birkenmeier, G.F., and Ryan, C.A. (1998) Wound signaling in tomato plants - Evidence that ABA is not a primary signal for defense gene activation. Plant Physiology, 117(2), 687-693.

Blokhina, O., Virolainen, E., and Fagerstedt, K.V. (2003) Antioxidants, oxidative damage and oxygen deprivation stress: a review. Annals of Botany, 91(2), 179-194.

Blum, H., Beier, H., and Gross, H.J. (1987) Improved silver staining of plant-proteins, RNA and DNA in polyacrylamide gels. Electrophoresis, 8(2), 93-99.

Bolink, E.M., van Schalkwijk, I., Posthumus, F., and van Hasselt, P.R. (2001) Growth under UV-B radiation increases tolerance to high-light stress in pea and bean plants. Plant Ecology, 154(1-2), 147-+.

Bolwell, G.P. (1999) Role of active oxygen species and NO in plant defence responses. Current Opinion in Plant Biology, 2(4), 287-294.

Bower, M.S., Matias, D.D., FernandesCarvalho, E., Mazzurco, M., Gu, T.S., Rothstein, S.J., and Goring, D.R. (1996) Two members of the thioredoxin-h family interact with the kinase domain of a *Brassica* S locus receptor kinase. Plant Cell, 8(9), 1641-1650.

Bradford, M.M. (1976) A rapid and sensitive method for the quantitation of microgram quantities of protein utilizing the principle of protein-dye binding. Analytical Biochemistry, 72, 248-254.

Brandes, H.K., Larimer, F.W., and Hartman, F.C. (1996b) The molecular pathway for the regulation of phosphoribulokinase by thioredoxin f. Journal of Biological Chemistry, 271(7), 3333-3335.

Brannan, C.I., Dees, E.C., Ingram, R.S., and Tilghman, S.M. (1990) The product of the H19 gene may function as an RNA. Molecular and Cellular Biology, 10(1), 28-36.

Brisson, L.F., Tenhaken, R., and Lamb, C. (1994) Function of oxidative cross-linking of cell-wall structural proteins in plant-disease resistance. Plant Cell, 6(12), 1703-1712.

Broin, M., Besse, I., and Rey, P. (2003) Evidence for post-translational control in the expression of a gene encoding a plastidic thioredoxin during leaf development in *Solanum tuberosum* plants. Plant Physiology and Biochemistry, 41(4), 303-308.

Broin, M., Cuine, S., Peltier, G., and Rey, P. (2000) Involvement of CDSP 32, a drought-induced thioredoxin, in the response to oxidative stress in potato plants. Febs Letters, 467(2-3), 245-248.

Broin, M., and Rey, P. (2003) Potato plants lacking the CDSP32 plastidic thioredoxin exhibit overoxidation of the BAS1 2-cysteine peroxiredoxin and increased lipid peroxidation in thylakoids under photooxidative stress. Plant Physiology, 132(3), 1335-1343.

Brown, I., Trethowan, J., Kerry, M., Mansfield, J., and Bolwell, G.P. (1998) Localization of components of the oxidative cross-linking of glycoproteins and of callose synthesis in papillae formed during the interaction between non-pathogenic strains of Xanthomonas campestris and French bean mesophyll cells. Plant Journal, 15(3), 333-343.

Brown, R.C., Lemmon, B.E., and Olsen, O.A. (1994) Endosperm development in barley - Microtubule involvement in the morphogenetic pathway. Plant Cell, 6(9), 1241-1252.

Buchanan, B. (1991) Regulation of CO_2 assimilation in oxygenic photosynthesis: the ferredoxin/thioredoxin system. Archives of Biochemistry and Biophysics, 288, 1-9.

Buchanan, B.B., Adamidi, C., Lozano, R.M., Yee, B.C., Momma, M., Kobrehel, K., and Ermel, R. (1997) Thioredoxin-linked mitigation of allergic responses to wheat. PNAS, 94(10), 5372-5377.

Buchanan, B.B., and Balmer, Y. (2005) Redox regulation: A broadening horizon. Annual Review of Plant Biology, 56, 187-220.

Buchanan, B.B., Schurmann, P., Decottignies, P., and Lozano, R.M. (1994) Thioredoxin - A multifunctional regulatory protein with a bright future in technology and medicine. Archives of Biochemistry and Biophysics, 314(2), 257-260.

Buechner, N., Schroeder, P., Jakob, S., Kunze, K., Maresch, T., Calles, C., Krutmann, J., and Haendeler, J. (2008) Changes of MMP-1 and collagen type I alpha 1 by UVA, UVB and IRA are differentially regulated by Trx-1. Experimental Gerontology, 43(7), 633-637.

Burton, R.A., Shirley, N.J., King, B.J., Harvey, A.J., and Fincher, G.B. (2004) The CesA gene family of barley. Quantitative analysis of transcripts reveals two groups of co-expressed genes. Plant Physiology, 134(1), 224-236.

Cabrillac, D., Cock, J.M., Dumas, C., and Gaude, T. (2001) The S-locus receptor kinase is inhibited by thioredoxins and activated by pollen coat proteins. Nature, 410(6825), 220-223.

Cain, P., Hall, M., Schroder, W.P., Kieselbach, T., and Robinson, C. (2009) A novel extended family of stromal thioredoxins. Plant Molecular Biology, 70(3), 273-281.

Carmel-Harel, O., and Storz, G. (2000) Roles of the glutathione- and thioredoxin-dependent reduction systems in the *Escherichia coli* and *Saccharomyces cerevisiae* responses to oxidative stress. Annual Review of Microbiology, 54, 439-461.

Carvalho, A.P., Fernandes, P.A., and Ramos, M.J. (2006a) Similarities and differences in the thioredoxin superfamily. Progress in Biophysics and Molecular Biology, 91(3), 229-248.

Casagrande, S., Bonetto, V., Fratelli, M., Gianazza, E., Eberini, I., Massignan, T., Salmona, M., Chang, G., Holmgren, A., and Ghezzi, P. (2002) Glutathionylation of human thioredoxin: A possible crosstalk between the glutathione and thioredoxin systems. PNAS, 99(15), 9745-9749.

Casselman, A., Vrebalov , J., Conner, J., Singhal, A., Giovannoni, J., Nassrallah, M., and Nassrallah, J. (2000) Determining the physical limits of the *Brassica* S locus by recombinational analysis. Plant Cell, 12, 23-33.

Chae, H., Robinson, K., Poole, L., Church, G., Storz, G., and Rhee, S. (1994) Cloning and sequencing of a thiol-specific antioxidant from mammalian brain. PNAS, 91, 7017-7021.

Chalfie, M., Tu, Y., Euskirchen, G., Ward, W.W., and Prasher, D.C. (1994) Green Fluorescent Protein as a marker for gene-expression. Science, 263(5148), 802-805.

Cheeseman, J.M. (2006) Hydrogen peroxide concentrations in leaves under natural conditions. Journal of Experimental Botany, 57(10), 2435-2444.

Chen, G.X., and Asada, K. (1989) Ascorbate peroxidase in tea leaves - Occurrence of 2 isozymes and the differences in their enzymatic and molecular-properties. Plant and Cell Physiology, 30(7), 987-998.

Cho, M.J., Wong, L.H., Marx, C., Jiang, W., Lemaux, P.G., and Buchanan, B.B. (1999) Overexpression of thioredoxin h leads to enhanced activity of starch debranching enzyme (pullulanase) in barley grain. PNAS, 96(25), 14641-14646.

Choi, D.W., Rodriguez, E.M., and Close, T.J. (2002) Barley Cbf3 gene identification, expression pattern, and map location. Plant Physiology, 129(4), 1781-1787.

Christensen, A.B., Gregersen, P.L., Schroder, J., and Collinge, D.B. (1998) A chalcone synthase with an unusual substrate preference is expressed in barley leaves in response to UV light and pathogen attack. Plant Molecular Biology, 37(5), 849-857.

Clemente., T. (2006) Nicotiana (*Nicotiana tobaccum, Nicotiana benthamiana*). Methods in Molecular Biology, 343, 143-154.

Cock, J. (2000) A receptor kinase and the self-incompatibility response in *Brassica*. New York: Academic Press.

Collin, V., Issakidis-Bourguet, E., Marchand, C., Hirasawa, M., Lancelin, J.M., Knaff, D.B., and Miginiac-Maslow, M. (2003) The Arabidopsis plastidial thioredoxins - New functions and new insights into specificity. Journal of Biological Chemistry, 278(26), 23747-23752.

Conklin, P.L., Williams, E.H., and Last, R.L. (1996) Environmental stress sensitivity of an ascorbic acid-deficient *Arabidopsis* mutant. PNAS, 93(18), 9970-9974.

Coudevylle, N., Thureau, A., Hemmerlin, C., Gelhaye, E., Jacquot, J.P., and Cung, M.T. (2005) Solution structure of a natural CPPC active site variant, the reduced form of thioredoxin h1 from poplar. Biochemistry, 44(6), 2001-2008.

Dalton, T.D., Shertzer, H.G., and Puga, A. (1999) Regulation of gene expression by reactive oxygen. Annual Review of Pharmacology and Toxicology, 39, 67-101.

Das, K.C., and Das, C.K. (2000) Thioredoxin, a singlet oxygen quencher and hydroxyl radical scavenger: Redox independent functions. Biochemical and Biophysical Research Communications, 277(2), 443-447.

Davletova, S., Rizhsky, L., Liang, H.J., Zhong, S.Q., Oliver, D.J., Coutu, J., Shulaev, V., Schlauch, K., and Mittler, R. (2005) Cytosolic ascorbate peroxidase 1 is a central component of the reactive oxygen gene network of *Arabidopsis*. Plant Cell, 17(1), 268-281.

De Pinto, M.C., and De Gara, L. (2004) Changes in the ascorbate metabolism of apoplastic and symplastic spaces are associated with cell differentiation. Journal of Experimental Botany, 55(408), 2559-2569.

Del Rio, L.A., Sandalio, L.M., Corpas, F.J., Palma, J.M., and Barroso, J.B. (2006) Reactive oxygen species and reactive nitrogen species in peroxisomes. Production, scavenging, and role in cell signaling. Plant Physiology, 141(2), 330-335.

Del Val, G., Maurer, F., Stutz, E., and Schurmann, P. (1999) Modification of the reactivity of spinach chloroplast thioredoxin f by site-directed mutagenesis. Plant Science, 149(2), 183-190.

Delaunay, A., Pflieger, D., Barrault, M.B., Vinh, J., and Toledano, M.B. (2002) A thiol peroxidase is an H_2O_2 receptor and redox-transducer in gene activation. Cell, 111(4), 471-481.

Delledonne, M., Zeier, J., Marocco, A., and Lamb, C. (2001) Signal interactions between nitric oxide and reactive oxygen intermediates in the plant hypersensitive disease resistance response. PNAS, 98(23), 13454-13459.

DeLong, J.M., Prange, R.K., Hodges, D.M., Forney, C.F., Bishop, M.C., and Quilliam, M. (2002) Using a modified FOX assay for detection of lipid hydroperoxides in plant tissue. Journal of Agricultural and Food Chemistry, 50, 248-254.

Dhindsa, R.S., Plumb-Dhindsa, P., and Thorpe, T.A. (1981) Leaf senescence: Correlated with increased levels of membrane permeability and lipid peroxidation, and decreased levels of superoxide dismutase and catalase. Journal of Experimental Botany, 32(1), 93-101.

Dietz, K.J. (2003) Plant peroxiredoxins. Annual Review of Plant Biology, 54, 93-107.

Dixon, D.P., Cole, D.J., and Edwards, R. (2000) Characterisation of a zeta class glutathione transferase from *Arabidopsis thaliana* with a putative role in tyrosine catabolism. Archives of Biochemistry and Biophysics, 384(2), 407-412.

Doke, N., and Ohashi, Y. (1988) Involvement of an O-2-generating system in the induction of necrotic lesions on tobacco-leaves infected with tobacco mosaic-Virus. Physiological and Molecular Plant Pathology, 32(1), 163-175.

Dos Santos, C.V., and Rey, P. (2006) Plant thioredoxins are key actors in the oxidative stress response. Trends in Plant Science, 11(7), 329-334.

Eckey, C., Korell, M., Leib, K., Biedenkopf, D., Jansen, C., Langen, G., and Kogel, K.H. (2004) Identification of powdery mildew-induced barley genes by cDNA-AFLP: Functional assessment of an early expressed MAP kinase. Plant Molecular Biology, 55(1), 1-15.

Ehrenberg, M. (2008) The green fluorescent protein: discovery, expression and development. In scientific background on the Nobel Prize in Chemistry 2008: The Royal Swedish Academy of Sciences, Information Department, Stockholm, Sweden.

Eklund, H., Gleason, F.K., and Holmgren, A. (1991) Structural and functional relations among thioredoxins of different species. Proteins-structure function and genetics, 11(1), 13-28.

Fagard, M., and Vaucheret, H. (2000) (Trans)gene silencing in plants: How many mechanisms? Annual Review of Plant Physiology and Plant Molecular Biology, 51, 167-194.

Federov, A.A., Ball, T., Mahoney, N.M., Valenta, R., and Almo, S.C. (1997) The molecular basis for allergen cross-reactivity: Crystal structure and IgE-epitope mapping of birch pollen profilin. Structure, 5(1), 33-45.

Fernandez, J., Gharahdaghi, F., and Mische, S.M. (1998) Routine identification of proteins from sodium dodecyl sulfate-polyacrylamide gel electrophoresis (SDS-PAGE) gels or polyvinyl difluoride membranes using matrix assisted laser desorption/ionization time of flight mass spectrometry (MALDI-TOF-MS). Electrophoresis, 19(6), 1036-1045.

Fischer, R., and Turner, N. (1978) Plant productivity in the arid and semiarid zones. Annual Review of Plant Physiology and Plant Molecular Biology, 29, 277-317.

Fisher, D., Wu, Y., and Ku, M. (1992) Turnover of soluble proteins in the wheat sieve tube. Physiologia Plantarum, 100, 1433-1441.

Florencio, F., Yee, B., Johnson, T., and Buchanan, B. (1988) An NADP/thioredoxin system in leaves. Purification and characterization of NADP-thioredoxin reductase and thioredoxin h from spinach. Archives of Biochemistry and Biophysics, 266, 496-507.

Floris, M., Mahgoub, H., Lanet, E., Robaglia, C., and Menand, B. (2009) Post-transcriptional regulation of gene expression in plants during abiotic stress. International Journal of Molecular Sciences, 10(7), 3168-3185.

Foyer, C., and Noctor, G. (2009) Redox regulation in photosynthetic organisms: Signaling, acclimation and practical Implications. Antioxidants and Redox Signaling, 11(4), 861-905.

Foyer, C.H., Lelandais, M., Edwards, E.A., and Mullineaux, P.M. (1991) Active oxygen, oxidative stress and plant metabolism: Current topics in plant physiology. Rockville: American Society of Plant Physiologists, pp.131-144.

Foyer, C.H., Lelandais, M., and Kunert, K.J. (1994b) Photooxidative stress in plants. Physiologia Plantarum, 92(4), 696-717.

Foyer, C.H., and Noctor, G. (2003) Redox sensing and signalling associated with reactive oxygen in chloroplasts, peroxisomes and mitochondria. Physiologia Plantarum, 119(3), 355-364.

Foyer, C.H., and Noctor, G. (2005a) Oxidant and antioxidant signalling in plants: a re-evaluation of the concept of oxidative stress in a physiological context. Plant Cell and Environment, 28(8), 1056-1071.

Foyer, C.H., and Noctor, G. (2005b) Redox homeostasis and antioxidant signaling: A metabolic interface between stress perception and physiological responses. Plant Cell, 17(7), 1866-1875.

Fratelli, M., Goodwin, L.O., Orom, U.A., Lombardi, S., Tonelli, R., Mengozzi, M., and Ghezzi, P. (2005) Gene expression profiling reveals a signaling role of glutathione in redox regulation. PNAS, 102(39), 13998-14003.

Friedman, W.E., Moore, R.C., and Purugganan, M.D. (2004) The evolution of plant development. American Journal of Botany, 91(10), 1726-1741.

Funasaka, Y., and Ichihashi, M. (1997) The effect of ultraviolet B induced adult T cell leukemia-derived factor/thioredoxin (ADF/TRX) on survival and growth of human melanocytes. Pigment Cell Research, 10, 68-73.

Gallogly, M.M., and Mieyal, J.J. (2007) Mechanisms of reversible protein glutathionylation in redox signaling and oxidative stress. Current Opinion in Pharmacology, 7(4), 381-391.

Gao, S.M., Zhang, H.W., Tian, Y., Li, F., Zhang, Z.J., Lu, X.Y., Chen, X.L., and Huang, R.F. (2008) Expression of TERF1 in rice regulates expression of stress-responsive genes and enhances tolerance to drought and high-salinity. Plant Cell Reports, 27(11), 1787-1795.

Gasdaska, J., Berggren, M., and Powis, G. (1995) Cell growth stimulation by the redox protein thioredoxin occurs by a novel helper mechanism. Cell Growth and Differentiation, 6(12), 1643-1650.

Gautier, M.F., Lullien-Pellerin, V., De Lamotte-Guery, F., Guirao, A., and Joudrier, P. (1998) Characterization of wheat thioredoxin h cDNA and production of an active *Triticum aestivum* protein in *Escherichia coli.* European Journal of Biochemistry, 252(2), 314-324.

Gechev, T.S., Van Breusegem, F., Stone, J.M., Denev, I., and Laloi, C. (2006) Reactive oxygen species as signals that modulate plant stress responses and programmed cell death. Bioessays, 28(11), 1091-1101.

Gelhaye, E., Rouhier, N., Gerard, J., Jolivet, Y., Gualberto, J., Navrot, N., Ohlsson, P.I., Wingsle, G., Hirasawa, M., Knaff, D.B., Wang, H.M., Dizengremel, P., Meyer, Y., and Jacquot, J.P. (2004a) A specific form of thioredoxin h occurs in plant mitochondria and regulates the alternative oxidase. PNAS, 101(40), 14545-14550.

Gelhaye, E., Rouhier, N., and Jacquot, J.P. (2003a) Evidence for a subgroup of thioredoxin h that requires GSH/Grx for its reduction. Febs Letters, 555(3), 443-448.

Gilbert, H.F. (1984) Redox control of enzyme-activities by thiol disulfide exchange. Methods in Enzymology, 107, 330-351.

Girotti, A.W. (2001) Photosensitized oxidation of membrane lipids: reaction pathways, cytotoxic effects, and cytoprotective mechanisms. Journal of Photochemistry and Photobiology B-Biology, 63(1-3), 103-113.

Gitler, C., Zarmi, B., Kalef, E., Meller, R., Zor, U., and Goldman, R. (2002) Calcium-dependent oxidation of thioredoxin during cellular growth initiation. Biochemical and Biophysical Research Communications, 290, 624-628.

Giustarini, D., Rossi, R., Milzani, A., Colombo, R., and Dalle-Donne, I. (2004) S-glutathionylation: from redox regulation of protein functions to human diseases. Journal of Cellular and Molecular Medicine, 8(2), 201-212.

Goldman, E.H., Chen, L., and Fu, H. (2004) Activation of apoptosis signal-regulating kinase 1 by reactive oxygen species through dephosphorylation at serine 967 and 14-3-3 dissociation. Journal of Biological Chemistry, 279(11), 10442-10449.

Goldschmidtclermont, P.J., Machesky, L.M., Baldassare, J.J., and Pollard, T.D. (1990) The actin-binding protein profilin binds to PIP2 and inhibits its hydrolysis by phospholipase-c. Science, 247(4950), 1575-1578.

Goring, D., Glavin, T., Schafer, U., and Rothstein, S. (1993) An S receptor kinase gene in self-compatible *Brassica napus* has a 1-bp deletion. Plant Cell, 5, 531-539.

Grant, J.J., and Loake, G.J. (2000) Role of reactive oxygen intermediates and cognate redox signaling in disease resistance. Plant Physiology, 124(1), 21-29.

Grippo, J., Holmgren, A., and Pratt, W. (1985) Proof that the endogenous, heat-stable glucocorticoid receptoractivating factor is thioredoxin. Journal of Biological Chemistry, 260, 93-97.

Gromer, S., Urig, S., and Becker, K. (2004) The thioredoxin system - From science to clinic. Medicinal Research Reviews, 24(1), 40-89.

Gross, N., Wasternack, C., and Kock, M. (2004) Wound-induced RNaseLE expression is jasmonate and systemin independent and occurs only locally in tomato (*Lycopersicon esculentum* cv. Lukullus). Phytochemistry, 65(10), 1343-1350.

Guo, H.X., Yin, J., Ren, J.P., Wang, Z.Y., and Chen, H.L. (2007) Changes in proteins within germinating seeds of transgenic wheat with an antisense construct directed against the thioredoxin. Journal of Plant Phyisology and Molecular Biology (Zhi Wu Sheng Li Yu Fen Zi Sheng Wu Xue Xue Bao), 33(1), 18-24.

Guzzo, J., Jobin, M.P., Delmas, F., Fortier, L.C., Garmyn, D., Tourdot-Marechal, R., Lee, B., and Divies, C. (2000) Regulation of stress response in *Oenococcus oeni* as a function of environmental changes and growth phase. International Journal of Food Microbiology, 55(1-3), 27-31.

Haberlein, I., Wolf, M., Mohr, L., and Follmann, H. (1995) Differentiation of six distinct thioredoxins in seeds of the soybean. Journal of Plant Physiology, 146(4), 385-392.

Haendeler, J. (2006) Thioredoxin-1 and posttranslational modifications. Antioxidants and Redox Signaling, 8(9-10), 1723-1728.

Haffani, Y.Z., Gaude, T., Cock, J.M., and Goring, D.R. (2004) Antisense suppression of thioredoxin h mRNA in *Brassica napus* cv. Westar pistils causes a low level constitutive pollen rejection response. Plant Molecular Biology, 55(5), 619-630.

Hajheidari, M., Eivazi, A., Buchanan, B.B., Wong, J.H., Majidi, I., and Salekdeh, G.H. (2007) Proteomics uncovers a role for redox in drought tolerance in wheat. Journal of Proteome Research, 6(4), 1451-1460.

Halliwell, B., and Gutteridge, J. (2002) Free radicals in biology and medicine: Oxford, UK:Oxford University Press.

Hartel, H., Haseloff, R.F., Ebert, B., and Rank, B. (1992) Free-radical formation in chloroplasts - methyl viologen action. Journal of Photochemistry and Photobiology B-Biology, 12(4), 375-387.

Hartley, D.P., Kolaja, K.L., Reichard, J., and Petersen, D.R. (1999) 4-Hydroxynonenal and malondialdehyde hepatic protein adducts in rats treated with carbon tetrachloride: immunochemical detection and lobular localization. Toxicology and Applied Pharmacology, 161, 23-33.

Hashemy, S.I., and Holmgren, A. (2008) Regulation of the catalytic activity and structure of human thioredoxin 1 via oxidation and S-nitrosylation of cysteine residues. Journal of Biological Chemistry, 283(32), 21890-21898.

Heath, R.L., and Packer, L. (1968) Photoperoxidation in isolated chloroplasts. I. Kinetics and stoichiometry of fatty acid peroxidation. Archives of Biochemistry and Biophysics, 125(1), 189-198.

Hideg, E., Nagy, T., Oberschall, A., Dudits, D., and Vass, I. (2003) Detoxification function of aldose/aldehyde reductase during drought and ultraviolet-B (280-320 nm) stresses. Plant Cell and Environment, 26, 513-522.

Hidema, J., and Kumagai, T. (2006) Sensitivity of rice to ultraviolet-B radiation. Annals of Botany, 97(6), 933-942.

Higo, K., Ugawa, Y., Iwamoto, M., and Korenaga, T. (1999) Plant cis-acting regulatory DNA elements (PLACE) database: 1999. Nucleic Acids Research, 27(1), 297-300.

Hirota, K., Murata, M., Sachi, Y., Nakamura, H., Takeuchi, J., Mori, K., and Yodoi, J. (1999) Distinct roles of thioredoxin in the cytoplasm and in the nucleus - A two-step mechanism of

redox regulation of transcription factor NF-κB. Journal of Biological Chemistry, 274(39), 27891-27897.

Hisabori, T., Hara, S., Fujii, T., Yamazaki, D., Hosoya-Matsuda, N., and Motohashi, K. (2005) Thioredoxin affinity chromatography: a useful method for further understanding the thioredoxin network. Journal of Experimental Botany, 56(416), 1463-1468.

Hisabori, T., Motohashi, K., Hosoya-Matsuda, N., Ueoka-Nakanishi, H., and Romano, P.G.N. (2007) Towards a functional dissection of thioredoxin networks in plant cells. Photochemistry and Photobiology, 83(1), 145-151.

Holley, S.R., Yalamanchili, R.D., Moura, D.S., Ryan, C.A., and Stratmann, J.W. (2003) Convergence of signaling pathways induced by systemin, oligosaccharide elicitors, and ultraviolet-B radiation at the level of mitogen-activated protein kinases in *Lycopersicon peruvianum* suspension-cultured cells. Plant Physiology, 132(4), 1728-1738.

Holmgren, A. (1979b) Thioredoxin catalyzes the reduction of insulin disulfides by dithiothreitol and dihydrolipoamide. Journal of Biological Chemistry, 254(19), 9627-9632.

Holmgren, A. (1985) Thioredoxin. Annual Review of Biochemistry, 54, 237-271.

Holmgren, A. (1989) Thioredoxin and Glutaredoxin Systems. Journal of Biological Chemistry, 264(24), 13963-13966.

Huber, H., E., Russel, M., Model, P., and Richardson, C., C. (1986) Interaction of mutant thioredoxins of *Escherichia coli* with the gene 5 protein of phage T7. The redox capacity of thioredoxin is not required for stimulation of DNA polymerase activity. Journal of Biological Chemistry, 261, 15006-15012.

Isenberg, G., Aebi, U., and Pollard, T.D. (1980) An actin-binding protein from *Acanthamoeba* regulates actin filament polymerization and interactions. Nature, 288(5790), 455-459.

Ishiwatari, Y., Fujiwara, T., McFarland, K., Nemoto, K., Hayashi, H., and Chino, M. (1998) Rice phloem thioredoxin h has the capacity to mediate its own cell-to-cell transport through plasmodesmata. Planta, 205, 12-22.

Ishiwatari, Y., Honda, C., Kawashima, I., Nakamura, S., Hirano, H., Mori, S., Fujiwara, T., Hayashi, H., and Chino, M. (1995) Thioredoxin h is one of the major proteins in rice phloem sap. Planta, 195(3), 456-463.

Ishiwatari, Y., Nemoto, K., Chino, M., and Hayashi, H. (2000) In situ hybridisation study of the rice phloem thioredoxin h mRNA accumulation: possible involvement in the differentiation of vascular tissues. Plant Physiology, 109, 90-96.

Islam, A., Shepherd, K.W., and Sparrow, D.H.B. (1981) Isolation and characterization of euplasmic wheat-barley chromosome addition lines. Heredity, 46(APR), 161-&.

Issakidis-Bourguet, E., Mouaheb, N., Meyer, Y., and Miginiac-Maslow, M. (2001) Heterologous complementation of yeast reveals a new putative function for chloroplast m-type thioredoxin. Plant Journal, 25(2), 127-135.

Jacquot, J., Vidal, J., and Gadal, P. (1976) Identification of a protein factor involved in dithiothreitol activation of NADP malate dehydrogenase from french bean leaves. Febs Letters, 71, 223-227.

Jacquot, J., Vidal, J., Gadal, P., and Schurmann, P. (1978) Evidence for the existence of several enzyme-specific thioredoxins in plants. Febs Letters, 96, 243-246.

Jacquot, J.P., Lancelin, J.M., and Meyer, Y. (1997) Tansley review no 94 - Thioredoxins: Structure and function in plant cells. New Phytologist, 136(4), 543-570.

Jiao, J., Yee, B., Wong, J., Kobrehel, K., and Buchanan, B. (1993) Thioredoxin-linked changes in regulatory properties of barley α-amylase/subtilisin inhibitor protein. Plant Physiology and Biochemistry, 31, 799-804.

Job, C., Rajjou, L., Lovigny, Y., Belghazi, M., and Job, D. (2005) Patterns of protein oxidation in *Arabidopsis* seeds and during germination. Plant Physiology, 138, 790-802.

Johansson, E., Olsson, O., and Nystrom, T. (2004) Progression and specificity of protein oxidation in the life cycle of *Arabidopsis thaliana*. Journal of Biological Chemistry, 279, 22204-22208

Johnson, T., Cao, R., Kung, J., and Buchanan, B. (1987) Thioredoxin and NADP-thioredoxin reductase from cultured carrot cells. Planta, 171, 321-331.

Juan, V., Crain, C., and Wilson, C. (2000) Evidence for evolutionarily conserved secondary structure in the H19 tumor suppressor RNA. Nucleic Acids Research, 28(5), 1221-1227.

Jung, C.H., and Thomas, J.A. (1996) S-glutathiolated hepatocyte proteins and insulin disulfides as substrates for reduction by glutaredoxin, thioredoxin, protein disulfide isomerase, and glutathione. Archives of Biochemistry and Biophysics, 335(1), 61-72.

Juttner, J. (2003) An analysis of thioredoxins h in the Grasses. PhD Thesis. University of Adelaide, Waite Agricultural Research Institute.

Juttner, J., Olde, D., Langridge, P., and Baumann, U. (2000) Cloning and expression of a distinct subclass of plant thioredoxins. European Journal of Biochemistry, 267(24), 7109-7117.

Kamo, M., Tsugita, A., Wiessner, C., Wedel, N., Bartling, D., Herrmann, R.G., Aguilar, F., Gardetsalvi, L., and Schurmann, P. (1989) Primary structure of spinach-chlorplast thioredoxi-f - protein sequencing and analysis of complete cDNA clones for spinach-chloroplast thioredoxin-f. European Journal of Biochemistry, 182(2), 315-322.

Kandoth, P.K., Ranf, S., Pancholi, S.S., Jayanty, S., Walla, M.D., Miller, W., Howe, G.A., Lincoln, D.E., and Stratmann, J.W. (2007) Tomato MAPKs LeMPK1, LeMPK2, and LeMPK3 function in the systemi n-mediated defense response against herbivorous insects. PNAS, 104(29), 12205-12210.

Kang, S.W., Chae, H.Z., Seo, M.S., Kim, K., Baines, I.C., and Rhee, S.G. (1998) Mammalian peroxiredoxin isoforms can reduce hydrogen peroxide generated in response to growth factors and tumor necrosis factor-alpha. Journal of Biological Chemistry, 273, 6297-6302.

Kawaguchi, R., and Bailey-Serres, J. (2005) mRNA sequence features that contribute to translational regulation in *Arabidopsis*. Nucleic Acids Research, 33(3), 955-965.

Ke, Y.H., Wu, J.Y., Leibold, E.A., Walden, W.E., and Theil, E.C. (1998) Loops and bulge/loops in iron-responsive element isoforms influence iron regulatory protein binding - Fine-tuning of mRNA regulation? Journal of Biological Chemistry, 273(37), 23637-23640.

Keller, R.J., Halmes, N.C., Hinson, J.A., and Pumford, N.R. (1993) Immunochemical detection of oxidized proteins. Chemical Research in Toxicology, 6(4), 430-433.

Keryer, E., Collin, V., Lavergne, D., Lemaire, S., and Issakidis-Bourguet, E. (2004) Characterization of *Arabidopsis* mutants for the variable subunit of ferredoxin:thioredoxin reductase. Photosynthesis Research, 79(3), 265-274.

Kil, I.S., Kim, S.Y., and Park, J.W. (2008) Glutathionylation regulates I kappa B. Biochemical and Biophysical Research Communications, 373(1), 169-173.

Kim, B.R., Nam, H.Y., Kim, S.U., Kim, S.I., and Chang, Y.J. (2003a) Normalization of reverse transcription quantitative-PCR with housekeeping genes in rice. Biotechnology Letters, 25(21), 1869-1872.

Klessig, D.F., Durner, J., Noad, R., Navarre, D.A., Wendehenne, D., Kumar, D., Zhou, J.M., Shah, J., Zhang, S.Q., Kachroo, P., Trifa, Y., Pontier, D., Lam, E., and Silva, H. (2000) Nitric oxide and salicylic acid signaling in plant defense. PNAS, 97(16), 8849.

Klotz, L.O. (2002) Oxidant-induced signaling: Effects of peroxynitrite and singlet oxygen. Biological Chemistry, 383(3-4), 443-456.

Kobrehel, K., Wong, J., Balogh, A., Kiss, F., Yee, B., and Buchanan, B. (1992) Specific reduction of wheat storage proteins by thioredoxin h. Plant Physiology, 99, 919-924.

Kocsy, G., Kobrehel, K., Szalai, G., Duviau, M.P., Buzas, Z., and Galiba, G. (2004) Abiotic stress-induced changes in glutathione and thioredoxin h levels in maize. Environmental and Experimental Botany, 52(2), 101-112.

Koh, C.S., Navrot, N., Didierjean, C., Rouhier, N., Hirasawa, M., Knaff, D.B., Wingsle, G., Samian, R., Jacquot, J.P., Corbier, C., and Gelhaye, E. (2008) An atypical catalytic mechanism involving three cysteines of thioredoxin. Journal of Biological Chemistry, 283(34), 23062-23072.

Koharyova, M., and Kollarova, M. (2008) Oxidative stress and thioredoxin system. General Physiology and Biophysics, 27(2), 71-84.

thioredoxins - completion of the thioredoxin profile of higher plants. Journal of Plant Physiology, 149, 317-321.

Koo, A.J.K., Gao, X.L., Jones, A.D., and Howe, G.A. (2009) A rapid wound signal activates the systemic synthesis of bioactive jasmonates in *Arabidopsis*. Plant Journal, 59(6), 974-986.

Kotchoni, S.O., and Gachomo, E.W. (2006) The reactive oxygen species network pathways: an essential prerequisite for perception of pathogen attack and the acquired disease resistance in plants. Journal of Biosciences, 31(3), 389-404.

Kuo, P.L., Chen, C.Y., and Hsu, Y.L. (2007) Isoobtusilactone a induces cell cycle arrest and apoptosis through reactive oxygen species/apoptosis signal-regulating kinase 1 signaling pathway in human breast cancer cells. Cancer Research, 67(15), 7406-7420.

Laloi, C., Mestres-Ortega, D., Marco, Y., Meyer, Y., and Reichheld, J.P. (2004) The *Arabidopsis* cytosolic thioredoxin h5 gene induction by oxidative stress and its W-box-mediated response to pathogen elicitor. Plant Physiology, 134(3), 1006-1016.

Laloi, C., Rayapuram, N., Chartier, Y., Grienenberger, J.M., Bonnard, G., and Meyer, Y. (2001) Identification and characterization of a mitochondrial thioredoxin system in plants. PNAS, 98(24), 14144-14149.

Lamanda, A., Zahn, A., Roder, D., and Langen, H. (2004) Improved Ruthenium II tris (bathophenantroline disulfonate) staining and destaining protocol for a better signal-to-background ratio and improved baseline resolution. Proteomics, 4(3), 599-608.

Lamb, C., and Dixon, R.A. (1997) The oxidative burst in plant disease resistance. Annual Review of Plant Physiology and Plant Molecular Biology, 48, 251-275.

Landy, A. (1989) Dynamic, structural, and regulatroy aspects of Lambda site-specific recombination. Annual Review of Biochemistry, 58, 913-949.

Laurent, T.C., Moore, E.C., and Reichard, P. (1964) Enzymatic synthesis of deeoxyribonucleotides. IV. Isolation and characterization of thioredoxin, the hydrogen donor from *Echerichia coli* B. Journal of Biological Chemistry(239), 3436-3444.

Lee, Y.S., Choi, Y.B., Suh, S., Lee, J., Assmann, S.M., Joe, C.O., Kelleher, J.F., and Crain, R.C. (1996) Abscisic acid-induced phosphoinositide turnover in guard cell protoplasts of *Vicia faba*. Plant Physiology, 110(3), 987-996.

Lemaire, S., Keryer, E., Stein, M., Schepens, I., Issakidis-Bourguet, E., Gerard-Hirne, C., Miginiac-Maslow, M., and Jacquot, J.P. (1999) Heavy-metal regulation of thioredoxin gene expression in *Chlamydomonas reinhardtii*. Plant Physiology, 120(3), 773-778.

Lemaire, S., Richardson, J., Goyer, A., Keryer, E., Lancelin, J., Makhatadze, G., and Jacquot, J. (2000) Primary structure determinants of the pH and temperature dependent aggregation of thioredoxin. Biochimica et Biophysica Acta, 1476, 311-323.

Lemaire, S.D., Michelet, L., Zaffagnini, M., Massot, V., and Issakidis-Bourguet, E. (2007) Thioredoxins in chloroplasts. Current Genetics, 51(6), 343-365.

Levin, R. (1990) Determination of carbonyl content in oxidatively modified proteins. Methods in Enzymology, 186, 464-478.

Levine, R.L., Williams, J.A., Stadtman, E.R., and Shacter, E. (1994) Carbonyl assays for determination of oxidatively modified proteins. Oxygen Radicals in Biological Systems, Pt C, 233, 346-357.

Li, K., Hartig, E., and Klug, G. (2003a) Thioredoxin 2 is involved in oxidative stress defence and redox-dependent expression of photosynthesis genes in *Rhodobacter capsulatus*. Microbiology-Sgm, 149, 419-430.

Li, K.Y., Pasternak, C., and Klug, G. (2003b) Expression of the trxA gene for thioredoxin 1 in *Rhodobacter sphaeroides* during oxidative stress. Archives of Microbiology, 180(6), 484-489.

Li, X.H., Zhang, R., Luo, D.H., Park, S.J., Wang, Q., Kim, Y., and Min, W. (2005) Tumor necrosis factor alpha-induced desumoylation and cytoplasmic translocation of homeodomain-interacting protein kinase 1 are critical for apoptosis signal-regulating kinase 1-JNK/p38 activation. Journal of Biological Chemistry, 280(15), 15061-15070.

Li, Y.M., Franklin, G., Cui, H.M., Svensson, K., He, X.B., Adam, G., Ohlsson, R., and Pfeifer, S. (1998) The H19 transcript is associated with polysomes and may regulate IGF2 expression in trans. Journal of Biological Chemistry, 273(43), 28247-28252.

Lillo, C. (2008) Signalling cascades integrating light-enhanced nitrate metabolism. Biochemical Journal, 415, 11-19.

Lindahl, M., and Florencio, F.J. (2004) Systematic screening of reactive cysteine proteomes. Proteomics, 4(2), 448-450.

Lorenzo, O., and Solano, R. (2005) Molecular players regulating the jasmonate signalling network. Current Opinion in Plant Biology, 8(5), 532-540.

Lottin, S., Vercoutter-Edouart, A.S., Adriaenssens, E., Czeszak, X., Lemoine, J., Roudbaraki, M., Coll, J., Hondermarck, H., Dugimont, T., and Curgy, J.J. (2002) Thioredoxin post-transcriptional regulation by H19 provides a new function to mRNA-like non-coding RNA. Oncogene, 21(10), 1625-1631.

Lozano, R.M., Wong, J.H., Yee, B.C., Peters, A., Kobrehel, K., and Buchanan, B.B. (1996) New evidence for a role for thioredoxin h in germination and seedling development. Planta, 200(1), 100-106.

Lulai, E.C., Suttle, J.C., and Pederson, S.M. (2008) Regulatory involvement of abscisic acid in potato tuber wound-healing. Journal of Experimental Botany, 59(6), 1175-1186.

Maeda, K., Finnie, C., and Svensson, B. (2004) Cy5 maleimide labelling for sensitive detection of free thiols in native protein extracts: identification of seed proteins targeted by barley thioredoxin h isoforms. Biochemical Journal, 378, 497-507.

Maeda, K., Hagglund, P., Finnie, C., Svensson, B., and Henriksen, A. (2008) Crystal structures of barley thioredoxin h isoforms HvTrxh1 and HvTrxh2 reveal features involved in protein recognition and possibly in discriminating the isoform specificity. Protein Science, 17(6), 1015-1024.

Malhotra, J.D., and Kaufman, R.J. (2007b) Endoplasmic reticulum stress and oxidative stress: A vicious cycle or a double-edged sword? Antioxidants and Redox Signaling, 9, 2277-2293.

Marchand, C., Le Marechal, P., Meyer, Y., Miginiac-Maslow, M., Issakidis-Bourguet, E., and Decottignies, P. (2004) New targets of *Arabidopsis* thioredoxins revealed by proteomic analysis. Proteomics, 4(9), 2696-2706.

Marcus, F., Chamberlain, S., Chu, C., Masiarz, F., Shin, S., Yee, B., and Buchanan, B. (1991) Plant thioredoxin h: an animal-like thioredoxin occurring in multiple cell compartments. Archives of Biochemistry and Biophysics, 287(1), 195-198.

Marknell DeWitt, A., Niederberger, V., Lehtonen, P., Spitzauer, S., Sperr, W.R., Valent, P., Valenta, R., and Lidholm, J. (2002) Molecular and immunological characterization of a novel timothy grass (*Phleum pratense*) pollen allergen, Phl p 11. Clinical and Experimental Allergy, 32(9), 1329-1340.

Marti, M.C., Olmos, E., Calvete, J.J., Diaz, I., Barranco-Medina, S., Whelan, J., Lazaro, J.J., Sevilla, F., and Jimenez, A. (2009) Mitochondrial and nuclear localization of a novel pea thioredoxin: Identification of its mitochondrial target proteins. Plant Physiology, 150(2), 646-657.

Martinez-Sanchez, G., Giuliani, A., Perez-Davison, G., and Leon-Fernandez, O.S. (2005) Oxidized proteins and their contribution to redox homeostasis. Redox Report, 10(4), 175-185.

Marx, C., Wong, J.H., and Buchanan, B.B. (2003) Thioredoxin and germinating barley: targets and protein redox changes. Planta, 216(3), 454-460.

Marx, J. (2005) Molecular biology - P-bodies mark the spot for controlling protein production. Science, 310(5749), 764-765.

Matsui, M., Oshima, M., Oshima, H., Takaku, K., Maruyama, T., Yodoi, J., and Taketo, M. (1996) Early embryonic lethality caused by targeted disruption of the mouse thioredoxin gene. Developmental Biology, 178, 179-185.

Matthews, J., Wakasugi, N., Virelizier, J., Yodoi, J., and Hay, R. (1992) Thioredoxin regulates the DNA binding activity of NF-κB by reduction of a disulphide bond involving cysteine 62. Nucleic Acids Research, 20, 3821-3830.

Maxwell, D.P., Wang, Y., and McIntosh, L. (1999) The alternative oxidase lowers mitochondrial reactive oxygen production in plant cells. PNAS, 96(14), 8271-8276.

Mazzurco, M., Sulaman, W., Elina, H., Cock, J.M., and Goring, D.R. (2001) Further analysis of the interactions between the *Brassica* S receptor kinase and three interacting proteins (ARC1, THL1 and THL2) in the yeast two-hybrid system. Plant Molecular Biology, 45(3), 365-376.

McLusky, S.R., Bennett, M.H., Beale, M.H., Lewis, M.J., Gaskin, P., and Mansfield, J.W. (1999) Cell wall alterations and localized accumulation of feruloyl-3 '-methoxytyramine in onion epidermis at sites of attempted penetration by *Botrytis allii* are associated with actin polarisation, peroxidase activity and suppression of flavonoid biosynthesis. Plant Journal, 17(5), 523-534.

Mellersh, D.G., Foulds, I.V., Higgins, V.J., and Heath, M.C. (2002) H_2O_2 plays different roles in determining penetration failure in three diverse plant-fungal interactions. Plant Journal, 29(3), 257-268.

Mestres-Ortega, D., and Meyer, Y. (1999) The *Arabidopsis thaliana* genome encodes at least four thioredoxins mand a new prokaryotic-like thioredoxin. Gene, 240, 307-331.

Meyer, Y., Reichheld, J.P., and Vignols, F. (2005) Thioredoxins in *Arabidopsis* and other plants. Photosynthesis Research, 86(3), 419-433.

Meyer, Y., Siala, W., Bashandy, T., Riondet, C., Vignols, F., and Reichheld, J.P. (2008) Glutaredoxins and thioredoxins in plants. Biochimica Et Biophysica Acta-Molecular Cell Research, 1783(4), 589-600.

Meyer, Y., Verdoucq, L., and Vignols, F. (1999) Plant thioredoxins and glutaredoxins: Identity and putative roles. Trends in Plant Science, 4(10), 388-394.

Michelet, L., Zaffagnini, M., Marchand, C., Collin, V., Decottignies, P., Tsan, P., Lancelin, J.M., Trost, P., Miginiac-Maslow, M., Noctor, G., and Lemaire, S.D. (2005) Glutathionylation of chloroplast thioredoxin f is a redox signaling mechanism in plants. PNAS, 102(45), 16478-16483.

Michelet, L., Zaffagnini, M., Massot, V., Keryer, E., Vanacker, H., Miginiac-Maslow, M., Issakidis-Bourguet, E., and Lemaire, S.D. (2006) Thioredoxins, glutaredoxins, and glutathionylation: new crosstalks to explore. Photosynthesis Research, 89(2-3), 225-245.

Miller, G., Shulaev, V., and Mittler, R. (2008) Reactive oxygen signaling and abiotic stress. Physiologia Plantarum, 133(3), 481-489.

Mitsui, A., Hamuro, J., Nakamura, H., Kondo, N., Hirabayashi, Y., Ishizaki-Koizumi, S., Hirakawa, T., Inoue, T., and Yodoi, J. (2002) Overexpression of human thioredoxin in transgenic mice controls oxidative stress and life span. Antioxidants and Redox Signaling, 4(4), 693-696.

Mittard, V., Blackledge, M., Stein, M., Jacquot, J., Marion, D., and Lancelin, J. (1997) NMR solution structure of an oxidised thioredoxin h from the eukaryotic green alga *Chlamydomonas reinhardtii*. European Journal of Biochemistry, 243.

Mittler, R. (2002) Oxidative stress, antioxidants and stress tolerance. Trends in Plant Science, 7(9), 405-410.

Mittler, R. (2006) Abiotic stress, the field environment and stress combination. Trends in Plant Science, 11(1), 15-19.

Mittler, R., Herr, E.H., Orvar, B.L., van Camp, W., Willekens, H., Inze, D., and Ellis, B.E. (1999) Transgenic tobacco plants with reduced capability to detoxify reactive oxygen intermediates are hyperresponsive to pathogen infection. PNAS, 96(24), 14165-14170.

Mittler, R., Vanderauwera, S., Gollery, M., and Van Breusegem, F. (2004) Reactive oxygen gene network of plants. Trends in Plant Science, 9(10), 490-498.

Moller, I.M., Jensen, P.E., and Hansson, A. (2007) Oxidative modifications to cellular components in plants. Annual Review of Plant Biology, 58, 459-481.

Moller, I.M., and Kristensen, B.K. (2004) Protein oxidation in plant mitochondria as a stress indicator. Photochemical and Photobiological Sciences, 3(8), 730-735.

Montrichard, F., Alkhalfioui, F., Yano, H., Vensel, W.H., Hurkman, W.J., and Buchanan, B.B. (2009) Thioredoxin targets in plants: The first 30 years. Journal of Proteomics, 72(3), 452-474.

Montrichard, F., Renard, M., Alkhalfioui, F., Duval, F.D., and Macherel, D. (2003) Identification and differential expression of two thioredoxin h isoforms in germinating seeds from pea. Plant Physiology, 132(3), 1707-1715.

Morimyo, M. (1988) Isolation and Characterization of methyl viologen-sensitive mutants of *Escherichia coli* K-12. Journal of Bacteriology, 170(5), 2136-2142.

Motohashi, K., Kondoh, A., Stumpp, M.T., and Hisabori, T. (2001) Comprehensive survey of proteins targeted by chloroplast thioredoxin. PNAS, 98(20), 11224-11229.

Mouaheb, N., Thomas, D., Verdoucq, L., Monfort, P., and Meyer, Y. (1998) *In vivo* functional discrimination between plant thioredoxins by heterologous expression in the yeast *Saccharomyces cerevisiae*. PNAS, 95(6), 3312-3317.

Muller, E. (1991) Thioredoxin deficiency in yeast prolongs S phase and shortens the G1 interval of the cell cycle. Journal of Biological Chemistry, 266(14), 9194-9202.

Mullineaux, P., and Karpinski, S. (2002) Signal transduction in response to excess light: getting out of the chloroplast. Current Opinion in Plant Biology, 5(1), 43-48.

Nassrallah, J., Rundle, S., and Nassrallah, M. (1994) Genetic evidence for the requirement of the *Brassica* S-locus receptor kinase gene in the self-incompatibility response. Plant Journal, 5, 373-384.

Natera, S.H.A., Ford, K.L., Cassin, A.M., Patterson, J.H., Newbigin, E.J., and Bacic, A. (2008) Analysis of the *Oryza sativa* plasma membrane proteome using combined protein and peptide fractionation approaches in conjunction with mass spectrometry. Journal of Proteome Research, 7(3), 1159-1187.

Neill, S., Desikan, R., and Hancock, J. (2002) Hydrogen peroxide signalling. Current Opinion in Plant Biology, 5(5), 388-395.

Netto, L.E.S. (2001) Oxidative stress response in sugarcane. Genetics and Molecular Biology, 24(1-4), 93-102.

Newman, G.W., Balcewiczsablinska, M.K., Guarnaccia, J.R., Remold, H.G., and Silberstein, D.S. (1994) Opposing regulatory effects of thioredoxin and eosinphil cytotoxicity-enhancing factor on the development of human-immunodeficiency -virus-1. Journal of Experimental Medicine, 180(1), 359-363.

Nishinaka, Y., Masutani, H., Nakamura, H., and Yodoi, J. (2001) Regulatory roles of thioredoxin in oxidative stress-induced cellular responses. Redox Report, 6(5), 289-295.

Niwa, T. (2007) Protein glutathionylation and oxidative stress. Journal of Chromatography B-Analytical Technologies in the Biomedical and Life Sciences, 855(1), 59-65.

Nonn, L., Williams, R., Erickson, R., and Powis, G. (2003) The absence of mitochondrial thioredoxin 2 causes massive apoptosis, exencephaly, and early embryonic lethality in homozygous mice. . Molecular and Cellular Biology, 23, 916-922.

Nordberg, J., and Arner, E. (2001) Reactive oxygen species, antioxidants and the mammalian thioredoxin systems. Free Radical Biology and Medicine, 31, 1287-1312.

Orozco-Cardenas, M., and Ryan, C.A. (1999) Hydrogen peroxide is generated systemically in plant leaves by wounding and systemin *via* the octadecanoid pathway. PNAS, 96(11), 6553-6557.

Ortel, B., Atzorn, R., Hause, B., Feussner, I., Miersch, O., and Wasternack, C. (1999) Jasmonate-induced gene expression of barley (*Hordeum vulgare*) leaves - the link between jasmonate and abscisic acid. Plant Growth Regulation, 29(1-2), 113-122.

Pagano, E.A., Chueca, A., Hermoso, R., Lazaro, J.J., and Lopez-Gorge, J. (2000) Ontogenic changes of thioredoxins f and m, and of their targets fructose-1,6-bisphosphatase and NAD(P)-malate dehydrogenase, of pea plants grown under light stress conditions. New Phytologist, 145(1), 21-28.

Park, S.K., Jung, Y.J., Lee, J.R., Lee, Y.M., Jang, H.H., Lee, S.S., Park, J.H., Kim, S.Y., Moon, J.C., Lee, S.Y., Chae, H.B., Shin, M.R., Jung, J.H., Kim, M.G., Kim, W.Y., Yun, D.J., Lee, K.O., and Lee, S.Y. (2009) Heat-shock and redox-dependent functional switching of an h-type *Arabidopsis* thioredoxin from a disulfide reductase to a molecular chaperone. Plant Physiology, 150(2), 552-561.

Parthasarathy, M. (1975) Sieve element structure. In Encycolpedia of plant physiology (M. Zimmermann, and J. Milburn, eds), Springer: Berlin, pp 3-38.

Passioura, J. (1996) Drought and drought tolerance. Plant Growth Regulation, 20(2), 79-83.

Passioura, J. (2007) The drought environment: physical, biological and agricultural perspectives. Journal of Experimental Botany, 58(2), 113-117.

Pekkari, K., Avila-Carino, H., Gurunath, R., Bengtsson, A., Scheynius, A., and Holmgren, A. (2003) Truncated thioredoxin (Trx80) exerts unique mitogenic cytokine effects *via* a mechanism independent of thiol oxido-reductase activity. Febs Letters, 539(1-3), 143-148.

Perkins, D.N., Pappin, D.J.C., Creasy, D.M., and Cottrell, J.S. (1999) Probability-based protein identification by searching sequence databases using mass spectrometry data. Electrophoresis, 20(18), 3551-3567.

Pitzschke, A., Forzani, C., and Hirt, H. (2006) Reactive oxygen species signaling in plants. Antioxidants and Redox Signaling, 8(9-10), 1757-1764.

Polidoros, A.N., Mylona, P.V., and Scandalios, J.G. (2001) Transgenic tobacco plants expressing the maize Cat2 gene have altered catalase levels that affect plant-pathogen interactions and resistance to oxidative stress. Transgenic Research, 10(6), 555-569.

Polle, A., Chakrabarti, K., Schurmann, W., and Rennenberg, H. (1990) Composition and properties of hydrogen-peroxide decomposing systems in extracellular and total extracts from needles of Norway Spruce (*Picea-Abies* L, Karst). Plant Physiology, 94(1), 312-319.

Pospisil, P., Arato, A., Krieger-Liszkay, A., and Rutherford, A.W. (2004) Hydroxyl radical generation by photosystem II. Biochemistry, 43(21), 6783-6792.

Potters, G., Horemans, N., Bellone, S., Caubergs, R.J., Trost, P., Guisez, Y., and Asard, H. (2004) Dehydroascorbate influences the plant cell cycle through a glutathione-independent reduction mechanism. Plant Physiology, 134(4), 1479-1487.

Prestridge, D.S. (1991) Signal Scan - a computer-program that scans DNA-sequences for eukaryotic transcriptional elements. Computer Applications in the Biosciences, 7(2), 203-206.

Prieto-Alamo, M.J., Jurado, J., Gallardo-Madueno, R., Monje-Casas, F., Holmgren, A., and Pueyo, C. (2000) Transcriptional regulation of glutaredoxin and thioredoxin pathways and related enzymes in response to oxidative stress. Journal of Biological Chemistry, 275(18), 13398-13405.

Proudhon, D., Wei, J., Briat, J.F., and Theil, E.C. (1996) Ferritin gene organization: Differences between plants and animals suggest possible kingdom-specific selective constraints. Journal of Molecular Evolution, 42(3), 325-336.

Pulido, P., Cazalis, R., and Cejudo, F.J. (2009) An antioxidant redox system in the nucleus of wheat seed cells suffering oxidative stress. Plant Journal, 57(1), 132-145.

Puntarulo, S., Sanchez, R.A., and Boveris, A. (1988) Hydrogen-peroxide metabolism In soybean embryonic axes at the onset of germination. Plant Physiology, 86(2), 626-630.

Purvis, A.C. (1997) Role of the alternative oxidase in limiting superoxide production by plant mitochondria. Physiologia Plantarum, 100(1), 165-170.

Ramanjulu, S., and Bartels, D. (2002) Drought- and desiccation-induced modulation of gene expression in plants. Plant Cell and Environment, 25(2), 141-151.

Reichheld, J.P., Khafif, M., Riondet, C., Droux, M., Bonnard, G., and Meyer, Y. (2007) Inactivation of thioredoxin reductases reveals a complex interplay between thioredoxin and glutathione pathways in *Arabidopsis* development. Plant Cell, 19(6), 1851-1865.

Reichheld, J.P., Mestres-Ortega, D., Laloi, C., and Meyer, Y. (2002) The multigenic family of thioredoxin h in *Arabidopsis thaliana*: specific expression and stress response. Plant Physiology and Biochemistry, 40(6-8), 685-690.

Rey, P., Cuine, S., Eymery, F., Garin, J., Court, M., Jacquot, J.P., Rouhier, N., and Broin, M. (2005) Analysis of the proteins targeted by CDSP32, a plastidic thioredoxin participating in oxidative stress responses. Plant Journal, 41(1), 31-42.

Rey, P., Pruvot, G., Becuwe, N., Eymery, F., Rumeau, D., and Peltier, G. (1998) A novel thioredoxin-like protein located in the chloroplast is induced by water deficit in *Solanum tuberosum* L. plants. Plant Journal, 13(1), 97-107.

Reynaert, N.L., van der Vliet, A., Guala, A.S., McGovern, T., Hristova, M., Pantano, C., Heintz, N.H., Heim, J., Ho, Y.S., Matthews, D.E., Wouters, E.F.M., and Janssen-Heininger, Y.M.W. (2006) Dynamic redox control of NF-kappa B through glutaredoxin-regulated S-glutathionylation of inhibitory kappa B kinase beta. PNAS, 103(35), 13086-13091.

Reznick, A. (1994) Oxidative damage to proteins: spectrophotometric method for carbonyl assay. Methods in Enzymology, 233, 357-363.

Ritz, D., Patel, H., Doan, B., Zheng, M., Aslund, F., Storz, G., and Beckwith, J. (2000) Thioredoxin 2 is involved in the oxidative stress response in *Escherichia coli*. Journal of Biological Chemistry, 275(4), 2505-2512.

Rivas, S., Rougon-Cardoso, A., Smoker, M., Schauser, L., Yoshioka, H., and Jones, J.D.G. (2004) CITRX thioredoxin interacts with the tomato Cf-9 resistance protein and negatively regulates defence. Embo Journal, 23(10), 2156-2165.

Rizhsky, L., Liang, H.J., Shuman, J., Shulaev, V., Davletova, S., and Mittler, R. (2004b) When defense pathways collide. The response of *Arabidopsis* to a combination of drought and heat stress. Plant Physiology, 134(4), 1683-1696.

Rouhier, N., and Jacquot, J. (2002) Plant peroxiredoxins: alternative hydroperoxide scavenging enzymes. Photosynthesis Research, 74, 259-268.

Rouhier, N., Koh, C.S., Gelhaye, E., Corbier, C., Favier, F., Didiejean, C., and Jacquot, J.P. (2008a) Redox based anti-oxidant systems in plants: Biochemical and structural analyses. Biochimica Et Biophysica Acta-General Subjects, 1780(11), 1249-1260.

Rouhier, N., Lemaire, S.D., and Jacquot, J.P. (2008b) The role of glutathione in photosynthetic organisms: Emerging functions for glutaredoxins and glutathionylation. Annual Review of Plant Biology, 59, 143-166.

Roxas, V.P., Lodhi, S.A., Garrett, D.K., Mahan, J.R., and Allen, R.D. (2000) Stress tolerance in transgenic tobacco seedlings that overexpress glutathione S-transferase/glutathione peroxidase. Plant and Cell Physiology, 41, 1229-1234.

Rozen, S., and Skaletsky, H. (2000) Primer3 on the WWW for general users and for biologist programmers. In Bioinformatics Methods and Protocols: Methods in Molecular Biology. , Totowa, NJ: Humana Press, pp 365-386.

Sahrawy, M., Hecht, V., Lopez-Jaramillo, J., Chueca, A., Chartier, Y., and Meyer, Y. (1996) Intron position as an evolutionary marker of thioredoxins and thioredoxin domains. Journal of Molecular Evolution, 42(4), 422-431.

Saitoh, M., Nishitoh, H., Fujii, M., Takeda, K., Tobiume, K., Sawada, Y., Kawabata, M., Miyazono, K., and Ichijo, H. (1998) Mammalian thioredoxin is a direct inhibitor of apoptosis signal-regulating kinase (ASK) 1. Embo Journal, 17(9), 2596-2606.

Sambrook, J., Fritsch, E.F., and Maniatis, T. (1989) Molecular cloning: a laboratory manual. Cold Spring Harbour, New York, USA.: Cold Spring Harbour Laboratory Pres.

Sarkar, N., Lemaire, S., Wu-Scharf, D., Issakidis-Bourguet, E., and Cerutti, H. (2005) Functional specialization of *Chlamydomonas reinhardtii* cytosolic thioredoxin h1 in the response to alkylation-induced DNA damage. Eukaryotic Cell, 4(2), 262-273.

Scandalios, J.G. (1993) Oxygen stress and superoxide dismutases. Plant Physiology, 101(1), 7-12.

Scharf, C., Riethdorf, S., Ernst, H., Engelmann, S., Volker, U., and Hecker, M. (1998) Thioredoxin is an essential protein induced by multiple stresses in *Bacillus subtilis*. Journal of Bacteriology, 180(7), 1869-1877.

Scheibe, R., and Anderson, L. (1981) Dark modulation of NADP-dependent malate dehydrogenase and glucose-6-phosphate dehydrogenase in the chloroplast. Biochimica Et Biophysica Acta-Gene Structure and Expression, 636, 58-64.

Schenk, H., Klein, M., Erdbrugger, W., Droge, W., and Schulze-Osthoff, K. (1994) Distinct effects of thioredoxin and antioxidants on the activation of transcription factors NF-kappa-B and AP-1. PNAS, 91, 1672-1676.

Schobert, C., Baker, L., Szederkenyi, J., Grossmann, P., and Komer, E. (1998) Identification of immunologically related proteins in sieve-tube exudate collected from monocotyledonous and dicotyledonous plants. Planta, 206, 245-252.

Schürmann, P., and Buchanan, B.B. (2008) The ferredoxin/thioredoxin system of oxygenic photosynthesis. Antioxidants and Redox Signaling, 10(7), 1235-1273.

Schürmann, P., and Jacquot, J.P. (2000) Plant thioredoxin systems revisited. Annual Review of Plant Physiology and Plant Molecular Biology, 51, 371-400.

Schürmann, P., Wolosiuk, R., Breazeale, V., and Buchanan, B. (1976) Two proteins function in the regulation of photosynthetic CO_2 assimilation in chloroplasts. Nature, 263, 257-258.

Schutt, C.E., Myslik, J.C., Rozycki, M.D., Goonesekere, N.C.W., and Lindberg, U. (1993) The structure of crystalline profilin beta-actin. Nature, 365(6449), 810-816.

Serrato, A.J., and Cejudo, F.J. (2003) Type-h thioredoxins accumulate in the nucleus of developing wheat seed tissues suffering oxidative stress. Planta, 217(3), 392-399.

Serrato, A.J., Crespo, J.L., Florencio, F.J., and Cejudo, F.J. (2001) Characterization of two thioredoxins h with predominant localization in the nucleus of aleurone and scutellum cells of germinating wheat seeds. Plant Molecular Biology, 46(3), 361-371.

Serrato, A.J., Perez-Ruiz, J.M., and Cejudo, F.J. (2002) Cloning of thioredoxin h reductase and characterization of the thioredoxin reductase-thioredoxin h system from wheat. Biochemical Journal, 367, 491-497.

Shahpiri, A., Svensson, B., and Finnie, C. (2008) The NADPH-dependent thioredoxin reductase/thioredoxin system in germinating barley seeds: Gene expression, protein profiles, and interactions between isoforms of thioredoxin h and thioredoxin reductase. Plant Physiology, 146(2), 789-799.

Shahpiri, A., Svensson, B., and Finnie, C. (2009) From proteomics to structural studies of cytosolic/mitochondrial-type thioredoxin systems in barley seeds. Molecular Plant, 2(3), 378-389.

Shelton, M.D., Kern, T.S., and Mieyal, J.J. (2007) Glutaredoxin regulates nuclear factor kappa-B and intercellular adhesion molecule in Muller cells - Model of diabetic retinopathy. Journal of Biological Chemistry, 282(17), 12467-12474.

Shimizu, O., Watanabe, J., Naito, S., and Shibata, Y. (2006) Quenching mechanism of Rose Bengal triplet state involved in photosensitization of oxygen in ethylene glycol. Journal of Physical Chemistry A, 110(5), 1735-1739.

Shulaev, V., and Oliver, D.J. (2006) Metabolic and proteomic markers for oxidative stress. New tools for reactive oxygen species research. Plant Physiology, 141(2), 367-372.

Shuman, S. (1994) Novel approach to moecular cloning and polynucleotide synthesis using Vaccinia DNA topoisomerase. Journal of Biological Chemistry, 269, 32678-32684.

Silberstein, D.S., Ali, M.H., Baker, S.L., and David, J.R. (1989) Human eosinophil cytotoxicity-enhancing factor - purifictation, physical characteristics and partial amino acid sequence of an active polypeptide. Journal of Immunology, 143(3), 979-983.

Sjolund, R. (1997) The phloem sieve element: a river runs through it. Plant Cell, 9, 1137-1146.

Southern, E.M. (1975) Detection of specific sequences among DNA fragments separated by gel electrophoresis. Journal of Molecular Biology, 98, 503.

Spector, A., Yan, G.Z., Huang, R.R.C., McDermott, M.J., Gascoyne, P.R.C., and Pigiet, V. (1988) The effect of H_2O_2 upon thioredoxin-enriched lens epithelial-cells. Journal of Biological Chemistry, 263(10), 4984-4990.

Stein, M., Jacquot, J., Jeanette, E., Decottignies, P., Hodges, M., Lancelin, J., Mittard, V., Schmitter, J., and Miginiac-Maslow, M. (1995) *Chlamydomonas reinhardtii* thioredoxins: structure of the genes coding for the chloroplastic m and cytosolic h isoforms; expression in *E.coli* of the recombinant proteins, purification and biochemical properties. Plant Molecular Biology, 28, 487-503.

Storey, K.B. (2004) Adventures in oxygen metabolism. Comparative Biochemistry and Physiology B-Biochemistry and Molecular Biology, 139(3), 359-369.

Sun, Y., and Oberley, L. (1996) Redox regulation of transcriptional activators. Free Radical Biology and Medicine, 21, 335-348.

Suske, G., Wagner, W., and Follmann, H. (1979) NADP-dependent thioredoxin reductase and a new thioredoxin from wheat. Naturforsch, 34c.

Svensson, M.J., and Larsson, J. (2007) Thioredoxin-2 affects lifespan and oxidative stress in *Drosophila*. Hereditas, 144(1), 25-32.

Sweat, T.A., and Wolpert, T.J. (2007) Thioredoxin h5 is required for victorin sensitivity mediated by a CC-NBS-LRR gene in *Arabidopsis*. Plant Cell, 19(2), 673-687.

Szederkenyi, J., Komer, E., and Schobert, C. (1997) Cloning of the cDNA for glutaredoxin, an abundant sieve-tube exudate protein from *Ricinus communis* and characterisation of the glutathione-dependent thiol-reduction system in sieve tubes. Planta, 202, 349-356.

Tada, Y., Spoel, S.H., Pajerowska-Mukhtar, K., Mou, Z.L., Song, J.Q., Wang, C., Zuo, J.R., and Dong, X.N. (2008) Plant immunity requires conformational charges of NPR1 via S-nitrosylation and thioredoxins. Science, 321(5891), 952-956.

Takasaki, T., Hatakeyama, K., Suzuki, G., Watanabe, M., Isogai, A., and Hinata, K. (2000) The S receptor kinase determines self-incompatibility in *Brassica stigma*. Nature, 403, 913-916.

Temple, M.D., Perrone, G.G., and Dawes, I.W. (2005) Complex cellular responses to reactive oxygen species. Trends In Cell Biology, 15(6), 319-326.

Thandavarayan, R.A., Watanabe, K., Ma, M., Veeraveedu, P.T., Gurusamy, N., Palaniyandi, S.S., Zhang, S., Muslin, A.J., Kodama, M., and Aizawa, Y. (2008) 14-3-3 protein regulates Ask1 signaling and protects against diabetic cardiomyopathy. Biochemical Pharmacology, 75(9), 1797-1806.

Thomas, J.A., Poland, B., and Honzatko, R. (1995) Protein sulfhydryls and their role in the antioxidant function of protein S-thiolation. Archives of Biochemistry and Biophysics, 319(1), 1-9.

Thompson, J., Higgins, D., and Gibson, T. (1994) CLUSTALW: improving the sensitivity of progressive multiple sequence alignment through sequence weighting, position, specific gap penalties and weight matrix choice. Nucleic Acids Research, 22, 4673-4680.

Titarenko, E., Rojo, E., Leon, J., and SanchezSerrano, J.J. (1997) Jasmonic acid-dependent and -independent signaling pathways control wound-induced gene activation in *Arabidopsis thaliana*. Plant Physiology, 115(2), 817-826.

Tokunaga, T., Miyahara, K., Tabata, K., and Esaka, M. (2005) Generation and properties of ascorbic acid-overproducing transgenic tobacco cells expressing sense RNA for L-galactono-1,4-lactone dehydrogenase. Planta, 220(6), 854-863.

Torres, M.A., and Dangl, J.L. (2005) Functions of the respiratory burst oxidase in biotic interactions, abiotic stress and development. Current Opinion in Plant Biology, 8(4), 397-403.

Traverso, J.A., Lopez-Jaramillo, J., Serrato, A.J., Ortega-Munoz, M., Aguado-Llera, D., Sahrawy, M., Santoyo-Gonzalez, F., Neira, J., and Chueca, A. (2009) Evidence of non-functional redundancy between two pea h-type thioredoxins by specificity and stability studies. Journal of Plant Phyisology, In Press.

Traverso, J.A., Vignols, F., Cazalis, R., Pulido, A., Sahrawy, M., Cejudo, F.J., Meyer, Y., and Chueca, A. (2007) PsTRXh1 and PsTRXh2 are both pea h-type thioredoxins with antagonistic behavior in redox imbalances. Plant Physiology, 143(1), 300-311.

Tsien, R., and Prasher, D. (1998) Molecular biology and mutation of green fluorescent protein. Green Fluorescent Protein: Properties, applications, and protocols, 97-118.

Tsukamoto, S., Morita, S., Hirano, E., Yokoi, H., Masumura, T., and Tanaka, K. (2005) A novel cis-element that is responsive to oxidative stress regulates three antioxidant defense genes in rice. Plant Physiology, 137(1), 317-327.

Ulm, R., and Nagy, F. (2005) Signalling and gene regulation in response to ultraviolet light. Current Opinion in Plant Biology, 8(5), 477-482.

Valenta, R., Duchene, M., Ebner, C., Valent, P., Sillaber, C., Deviller, P., Ferreira, F., Tejkl, M., Edelmann, H., Kraft, D., and Scheiner, O. (1992) Profilins constitute a novel family of functional-plant pan-allergens Journal of Experimental Medicine, 175(2), 377-385.

Valenta, R., Vrtala, S., Laffer, S., Steinberger, P., Ball, T., Ferreira, F., Scheiner, O., and Kraft, D. (1994) B-cell epitopes of allergens determined by recombinant techniques; use for

diagnosis and therapy of type I allergy. Arb Paul Ehrlich Inst Bundesamt Sera Impfstoffe Frankf A M(87), 235-246.

Vandesompele, J., De Paepe, A., and Speleman, F. (2002) Elimination of primer-dimer artifacts and genomic coamplification using a two-step SYBR green I real time RT-PCR. Analytical Biochemistry, 303(1), 95-98.

Verdoucq, L., Vignols, F., Jacquot, J.P., Chartier, Y., and Meyer, Y. (1999) *In vivo* characterization of a thioredoxin h target protein defines a new peroxiredoxin family. Journal of Biological Chemistry, 274(28), 19714-19722.

Vinson, V.K., Archer, S.J., Lattman, E.E., Pollard, T.D., and Torchia, D.A. (1993) 3-Dimensional solution structure of *acanthamoeba* profilin-1. Journal of Cell Biology, 122(6), 1277-1283.

Vivancos, A.P., Castillo, E.A., Biteau, B., Nicot, C., Ayte, J., Toledano, M.B., and Hidalgo, E. (2005) A cysteine-sulfinic acid in peroxiredoxin regulates H_2O_2-sensing by the antioxidant Pap1 pathway. PNAS, 102(25), 8875-8880.

Vojtek, A., Haarer, B., Field, J., Gerst, J., Pollard, T.D., Brown, S., and Wigler, M. (1991) Evidence for a functional link between profilin and cap in the yeast *saccharomyces-cerevisiae.* Cell, 66(3), 497-505.

Wagner, A.M. (1995) A role for active oxygen species as 2nd messengers in the induction of alternative oxidase gene-expression in *Petunia-hybrida* cells. Febs Letters, 368(2), 339-342.

Wahid, A., Gelani, S., Ashraf, M., and Foolad, M.R. (2007) Heat tolerance in plants: An overview. Environmental and Experimental Botany, 61, 199-223.

Wakasugi, N., Tagaya, Y., Wakasugi, H., Mitsui, A., Maeda, M., Yodoi, J., and Tursz, T. (1990) Adult T-cell leukemia-derived factor/thioredoxin, produced by both human T-lymphotropic virus type I- and Epstein-Barr virustransformed lymphocytes, acts as an autocrine growth factor and synergizes with interleukin 1 and interleukin 2. PNAS, 87, 8282-8286.

Wang, W., Vignani, R., Scali, M., and Cresti, M. (2006b) A universal and rapid protocol for protein extraction from recalcitrant plant tissues for proteomic analysis. Electrophoresis, 27(13), 2782-2786.

Weber, C., Nover, L., and Fauth, M. (2008) Plant stress granules and mRNA processing bodies are distinct from heat stress granules. Plant Journal, 56(4), 517-530.

Weichel, M., Vergoossen, N.J., Bonomi, S., Scibilia, J., Ortolani, C., Ballmer-Weber, B.K., Pastorello, E.A., and Crameri, R. (2006b) Screening the allergenic repertoires of wheat and maize with sera from double-blind, placebo-controlled food challenge positive patients. Allergy, 61(1), 128-135.

Weichsel, A., Gasdaska, J.R., Powis, G., and Montfort, W.R. (1996) Crystal structures of reduced, oxidized, and mutated human thioredoxins: Evidence for a regulatory homodimer. Structure, 4(6), 735-751.

Wellner, D., Panneerselvam, C., and Horecker, B.L. (1990) Sequencing of peptides and proteins with blocked N-terminal amino acids - N-acetylserine or N-acetylthreonine PNAS, 87(5), 1947-1949.

Williamson, B., Tudzynsk, B., Tudzynski, P., and van Kan, J.A.L. (2007) *Botrytis cinerea*: the cause of grey mould disease. Molecular Plant Pathology, 8(5), 561-580.

Wong, J., Kobrehel, K., and Buchanan, B. (1995) Thioredoxin and seed proteins. Methods in Enzymology, 252, 228-240.

Wong, J.H., Cal, N., Balmer, Y., Tanaka, C.K., Vensel, W.H., Hurkman, W.J., and Buchanan, B.B. (2004) Thioredoxin targets of developing wheat seeds identified by complementary proteomic approaches. Phytochemistry, 65(11), 1629-1640.

Wong, J.H., Kim, Y.B., Ren, P.H., Cai, N., Cho, M.J., Hedden, P., Lemaux, P.G., and Buchanan, B.B. (2002) Transgenic barley grain overexpressing thioredoxin shows evidence that the starchy endosperm communicates with the embryo and the aleurone. PNAS, 99(25), 16325-16330.

Wood, Z.A., Poole, L.B., and Karplus, P.A. (2003) Peroxiredoxin evolution and the regulation of hydrogen peroxide signaling. Science, 300(5619), 650-653.

Xie, G.S., Kato, H., Sasaki, K., and Imai, R. (2009) A cold-induced thioredoxin h of rice, OsTrx23, negatively regulates kinase activities of OsMPK3 and OsMPK6 in vitro. Febs Letters, 583(17), 2734-2738.

Yamazaki, D., Motohashi, K., Kasama, T., Hara, Y., and Hisabori, T. (2004) Target proteins of the cytosolic thioredoxins in *Arabidopsis thaliana*. Plant and Cell Physiology, 45(1), 18-27.

Yang, R.Q., Weber, D.J., and Carrier, F. (2006) Post-transcriptional regulation of thioredoxin by the stress inducible heterogenous ribonucleoprotein A18. Nucleic Acids Research, 34(4), 1224-1236.

Yano, H., Wong, J.H., Cho, M.J., and Buchanan, B.B. (2001a) Redox changes accompanying the degradation of seed storage proteins in germinating rice. Plant and Cell Physiology, 42(8), 879-883.

Yokomizo, A., Ono, M., Nanri, H., Makino, Y., Ohga, T., Wada, M., Okamoto, T., Yodoi, J., Kuwano, M., and Kohno, K. (1995) Cellular levels of thioredoxin associated with drug sensitivity to cisplatin, mitomycin C, doxorubicin, and etoposide. Cancer Research, 55, 4293–4296.

Zahid, A., Afoulous, S., and Cazalis, R. (2008) Thioredoxin h system and wheat seed quality. Cereal Chemistry, 85(6), 799-807.

Zeller, T., and Klug, G. (2006) Thioredoxins in bacteria: Functions in oxidative stress response and regulation of thioredoxin genes. Naturwissenschaften, 93(6), 259-266.

Zhang, H., Go, Y.M., and Jones, D.P. (2007) Mitochondrial thioredoxin-2/peroxiredoxin-3 system functions in parallel with mitochondrial GSH system in protection against oxidative stress. Archives of Biochemistry and Biophysics, 465(1), 119-126.

Zhang, N., and Portis, R. (1999) Mechanism of light redulation of Rubisco: a specific role for the larger Rubisco activase isoform involving reductive activation by thioredoxin-f. PNAS, 96, 9438-9443.